University of South Wales
2059477

Bound by Abbey
Bookbinding Co.,
Cardiff, South Wales
Tel:(01222) 395882

A Study and Modelling of the Propagation Effects of Vegetation on Radio Waves at Centimetre-Wavelength Frequencies

Richard Brian Leonard Stephens

A thesis submitted in partial fulfilment of the requirements of the University of Glamorgan for the degree of Doctor of Philosophy

1998

University of Glamorgan

DECLARATION

I declare that this thesis has not been, nor is currently being, submitted for the award of any other degree or similar qualification.

Signed .....

Richard Brian Leonard Stephens

ACKNOWLEGEMENTS

I would like to thank my Director of Studies, Professor Miqdad Al-Nuaimi for his guidance and support throughout the research, my other supervisor Dr. Akram Hammoudeh and also Dr. Christopher Haslett for his help and many useful discussions and suggestions.

I am especially indebted to my colleagues of the radio propagation research group, Dr. Ming Ding, Mr Jürgen Richter, Mr Jean-Pierre Pugliese, Dr. Katherine Compton and Dr. Harmen Sthamer formerly of the software testing group for providing valuable assistance and support throughout the research.

Special thanks go to the Wales Higher Education Funding Council (HEFCW) for sponsorship of the project, under the Development of Research (DevR) initiative.

I would like to thank my wife, Kathryn L. Stephens for her constant support throughout the course of research, her help in showing me the light at the end of the tunnel and for her inspiration and constant understanding. Many thanks also to my parents without whom, I may have given up long ago.

ABSTRACT

With the increase in and more diverse applications of microwave radio communications, the probability of a signal propagating through a medium of vegetation is increased. As a direct result of this demand for microwave communication systems, knowledge is required of the effects of vegetation media on the propagating microwave signal. This enables radio system planners to predict the signal loss more accurately, necessitating a detailed study of the propagation effects of vegetation.

A vegetation depth attenuation model has been developed based on the International Telecommunications Union-Radio Sector model and validated against measurements conducted at two microwave frequencies of 11.2 GHz and 20 GHz. The measurements were conducted on a number of sites of differing geometries at different times of the year to obtain the two extreme states of foliage, in- and out-of-leaf. The trees found at the sites were of a number of indigenous species. A variety of species and environments were employed for the outdoor measurements as it was felt that any variation in the signal, occurring as a direct result of the species, climate, environment etc., would be reduced.

A further study has been conducted in an anechoic chamber, the purpose being to investigate the depolarising effect of vegetation, to characterise and to ascertain how and to what extent the polarisation of the incident signal is changed as it passes through the vegetation without the effects of climate, location and environment affecting the resultant signal.

To enable larger quantities of data to be obtained, collated and subsequently analysed and also to remove any scope for error during the collection of results, two data acquisition programs were written for the two main environments in which the measurements were to be undertaken, that is to say, outdoor and indoor (anechoic chamber) environments.

In seeking to provide a model for the prediction of attenuation a radio wave will suffer as it is propagated through a body of vegetation, several models have been examined in turn and their relative merits discussed together with their applicability to the study. After examining the possible models available, the thesis provides a model which enables the prediction of additional attenuation a radiowave signal will suffer as a function of path length (depth) of the vegetation medium and frequency. The model can be recommended for use in the 10 - 30 GHz band.

The study on the depolarisation of signals by vegetation has shown that the components of a vegetation medium e.g. tree trunks, branches and leaves, can cause considerable changes in the polarisation of the incident signal as it propagates through a volume of vegetation. The work presented in this thesis contains new measured results of the polarisation state of the radio wave as it emerges from a vegetation specimen. These results obtained in an anechoic chamber under controlled conditions have demonstrated that additional effects, other than attenuation by absorption and scatter need to be considered in order to characterise and subsequently model the overall effect of vegetation in the radio path of propagating signals.

TABLE OF CONTENTS

Chapter 3 Experimental Work

Chapter 4 Vegetation Attenuation Measurements

LIST OF SYMBOLS AND ABBREVIATIONS

a	constant (dimensionless)
A_m	maximum attenuation (dB)
AR	Axial Ratio ($-1 \leq AR \geq +1$)
b	constant (dimensionless)
B_{Rx}	beamwidth of receive antenna (°)
B_{Tx}	beamwidth of transmit antenna (°)
c	constant (dimensionless)
CCIR	International Radio Consultative Committee
COST	European Collaboration in the Field of Science and Technology
d	vegetation depth (m)
d_m	maximum vegetation depth (m)
D	characteristic of antenna (m)
DRO	dielectric resonator oscillator
E	electrical field intensity (Vm^{-1})
E_{RMS}	RMS error (dB)
f	frequency (Hz)
$f(\theta)$	forward lobe of scatter function (dimensionless)
G_{LNB}	gain of LNB (dB)
G_{Rx}	gain of receive antenna (dBi)
G_{Tx}	gain of transmit antenna (dBi)
ITU-R	International Telecommunications Union Radio Sector committee
k	constant / offset to final attenuation rate (dB)
k′	constant
l_1, l_2, l_3	magnitude response of antenna (volts)
L	attenuation (dB)
L_{Cable}	cable loss (dB)
L_{fs}	freespace loss (dB)
L_{fsdiff}	difference in freespace loss (dB)
LNB	Low Noise Block
Log Amp	Logarithmic Amplifier

OMT	Ortho-Mode Transducer
P	received power (dBm)
P_0	freespace signal power (dB)
P_{Free}	freespace received signal strength (dBm)
P_{Norm}	normalised received signal strength (dBf)
P_{Meas}	received signal strength (dBm)
P_{Rx}	received power (dBm)
P_{Tx}	transmitted power (dBm)
$p(\theta)$	scatter pattern (dimensionless)
q	weighting factor (dimensionless)
R	far field distance (m)
R, R_0	initial attenuation rate (dB/m)
R_∞	final attenuation rate (dB/m)
R_1, R_2	relative power ratio (power ratio)
r_1	transmitter to vegetation distance (m)
r_2	receiver to vegetation distance (m)
W	illumination width (m)
α	ratio of forward scattered power to total scattered power (dimensionless)
α	angle of latitude (°)
β_s	beamwidth of forward lobe (°)
β	angle of longitude (°)
λ	wavelength (m)
θ	angular difference between polarisation states (°)
τ	tilt angle ($-90° \leq \tau \geq +90°$)
ω	width of vegetation (m)

LIST OF FIGURES

LIST OF TABLES

1. Introduction

1.1 Background

In the past and still today microwave point-to-point links have their antennas placed on the top of buildings or towers so that the link is clear of any obstructions that would be in the path were the transmitter and receiver to be positioned at a lower height. With the increase in the number of microwave links, mobile and satellite communications, it is highly probable that a microwave signal has to propagate through a vegetation medium e.g. a group of trees, to get to the receiving terminal of the microwave radio system. This is particularly observed in urban and suburban environments. Vegetation media has a number of effects on the propagation of a signal at microwave frequencies, most significantly resulting in the loss of signal strength. As the use of signals at microwave and higher frequencies for communication becomes increasingly more widespread, and their applications more and more diverse, higher geographical diversity of radio links become necessary. This leads to increased risks of mutual co-channel interference which requires better understanding and assessment of the effects of obstacles such as vegetation in the radio path.

The increase in the number of applications as well as in the geographical diversity of radio links and the utilisation of higher frequencies creates a need to understand and quantify the effects of vegetated media on radiowave signals at higher frequencies. To permit accurate predictions of the amount of signal loss that may be experienced due to the effects that occur within the vegetation, knowledge has to be acquired about the processes by which such effects occur. An approach that provides the greatest insight into these processes is that of measurements. Measurements may be designed and developed to extract general or specific information about the different processes allowing the development of prediction models. Measurements provide an insight into how vegetation can cause adverse effects on the propagation of the signal. The acknowledgement of the prime role of measurements in this project has guided the investigation.

The information of how vegetation affects the propagating signal gained from this research is aimed at engineers involved in the process of planning and the co-ordination of radio systems. Recognising that radio communication systems transcend national boundaries and the need for planning procedures to be applicable internationally, planning procedures and prediction models should be standardised and agreed internationally. This is carried out by the International Telecommunications Union (ITU-R) Radio-Sector committee. Throughout the research collaborative work has been carried out with a number of organisations in the UK and Europe under the auspices of COST 235 [1996]. Results were disseminated via COST 235 and UK Study Group 3 which in turn contributes to the ITU-R.

1.2 Objectives

The overall aim of the research is to provide more accurate prediction of the effects of vegetation on microwave propagation in vegetation media than is possible with the limited models available. Specific objectives of the project are the investigation of the following effects that vegetation media have on signal propagation, using both analysis and measurements.

- Seasonal variations, resulting in both foliated and defoliated states.
- Attenuation caused by the vegetation under the two states of foliage.
- Scatter of the signal as it propagates within the vegetation.
- Depolarisation of the incident signal as it propagates through the media.
- Frequency dependency resulting from the varying size of scattering elements, e.g. leaf size in relation to the wavelength.

Primarily, the research has concentrated on the experimental side as measurements were recognised as providing an insight into the behaviour of the signal propagating in a medium of vegetation. The frequency dependency has been

investigated by using two different frequencies - 11.2 GHz and 20 GHz in the measurement programme.

1.3 Effect of Vegetation on Radio Waves

Vegetation has a number of significant effects upon radio waves in the microwave and millimetre wave bands. They include; absorption, scattering and depolarisation. Each of the three forms will affect the signal magnitude and phase differently. The effect on the signal magnitude caused by the above processes is very much dependant upon the species of the tree and on the physical characteristics of each individual tree. There are other factors which will also affect the magnitude of the effect on the propagating signal such as the moisture content of the leaves and branches and the speed of wind movement. However these factors exercise their influence by varying the position and electrical properties of the scattering elements. Due to the complexities involved in these processes they were not investigated, although some quantification of wind effects were estimated.

1.4 Vegetation Attenuation

Hitherto it has not been necessary to consider the effect vegetation has on the propagating microwave signal as the signal has rarely, if at all, needed to pass through vegetation. Presently however, with the increase in the use of and geographical density of terrestrial as well as satellite communications, particularly in urban and suburban areas, planned links will be more likely to be affected by a medium of vegetation. E.g. single trees, a line of trees, hedge or woods in the radio path.

Attenuation of the propagating signal through a vegetation medium is clearly very important in the design of radio links where vegetation forms part of the radio path. The attenuation of the signal depends on the physical extent of the medium and the attributes of the trees in the medium. Prediction of the attenuation of the

signal is clearly complicated by the process of absorption and scatter caused by the randomly located and orientated branches and leaves, their relative size and density. For example coniferous trees with needle type leaves are expected to exercise different effects compared to those of broad deciduous leaves. Prediction models will be difficult to develop based mainly on analytical considerations. Measurements on the other hand can aid considerably in the development of empirical models applicable to generalised classes of medium, e.g. deciduous and coniferous, in-leaf and out-of-leaf. Briefly parameters affecting propagation are :

- The shape and size of the leaves/needles in relation to the wavelength of the signal being transmitted.
- The orientation of each component of the trees' structure that affects the signal as it propagates through the tree.
- Scattering caused by all of the components of the tree that are larger than the wavelength of the transmission.
- The water content of the tree, which in turn means the time of day and also the time of year.

Previous modelling work [Al-Nuaimi, 1993a], [Stephens, 1995], [Seville, 1995] has demonstrated that trees arranged in a line or plantation behave differently from single trees in the radio path. Investigation of the effects of a single tree were carried out in order to provide an insight of the variability of tree type and structure and also to obtain other information, e.g. signal depolarisation.

There are many models available in the published literature for predicting the attenuation of a signal versus vegetation depth which will be discussed in Chapter 2.

1.5 Single Tree Investigations

Each body of vegetation is made up of individual trees and, by gaining a better understanding of how a single tree interacts with a propagating signal, a

greater knowledge of how vegetation as a whole affects radio waves can be obtained. It is recognised that the propagation of radio waves through vegetation is, in its very nature, complex and by investigating how a wave propagates through a single tree, an insight is provided into the understanding of this highly complex process.

Investigating the effect that a single tree has upon a propagating signal is an important part of the research, as it enables detailed investigation of how the different species of vegetation affect the signal. Radio paths involving single trees can more easily be manipulated allowing individual effects to be more readily identified.

The effect of single trees has been investigated by examining the attenuation, additional to that of free space, a tree presents as a function of its angle of rotation about a central point. Also examined in detail is how the attenuation presented at a particular angle relates to the amount of change in the polarisation of the incident signal caused by the components of the tree e.g. branches and leaves.

1.6 Definitions

Listed below are the definitions used within this thesis.

1. Where ever the word attenuation or loss is used this is taken to mean the additional attenuation to that which would be experienced in propagating through free space caused by vegetation present in the radio path unless otherwise stated.
2. Depolarisation means there has been a change of the incident wave from one recognisable polarisation to another recognisable polarisation.
3. Partial polarisation is where the measured wave is of no definite polarisation but has some recognisable components of a particular polarisation (explained in greater detail in Chapter 6).

1.7 Summary of the Thesis

In Chapter2, adverse effects, such as attenuation and scatter, suffered by a signal propagating through vegetation are discussed in conjunction with the manner in which these adverse effects are caused by the vegetation.

A number of models used for the prediction of the attenuation suffered by a propagating signal as it passes through a body of vegetation are examined. These are mainly empirical models where the parameters are determined from experimental data. Using as a starting point the model recommended by the International Telecommunications Union (ITU). A deterministic model [Hammoudeh *et al*, 1996] which is based upon the radiative energy transfer theory is also discussed. A brief overview of other attenuation prediction models that are available in the literature have also been presented and discussed.

Chapter 3 describes in detail the various measurement systems at 11.2 GHz and 20 GHz that have been used throughout the measurement programme. Descriptions of the different equipment utilised during measurements and their respective calibration are presented. Some of the equipment used created restrictions on how and what measurements could be conducted and this is discussed. The development of the software used to automate the process of acquiring data in the two different environments, that is, outdoor and indoor environments, is presented. To enable meaningful measurements to be conducted there are certain criteria which must be considered when selecting sites for performing measurements and these are presented and discussed.

Chapter 4 presents the sites at which experimental measurements were conducted at, as well as the method employed to facilitate the acquisition of relevant measurement data. The results that were obtained from the different sites and an initial analysis of the measurement data are both presented here. To verify the validity of a prediction model, measured results are used by comparing them with predicted results. A significant portion of the work in this thesis consisted of

experimental measurements and these provided results against which, validation of the prediction models were carried out.

Chapter 5 compares and contrasts a number of prediction models used in vegetation attenuation modelling. The models are individually introduced and their relative fit to the experimental results are presented in tabular form, this data is also shown in graphical form for each measurement site and at each frequency employed. The relative fit is defined by the use of RMS errors and the degree of each models relative fit to the measured data is presented. This is complemented by figures comparing modelled and measured results which are mainly presented at the end of the chapter.

Chapter 6 addresses signal depolarisation and how vegetation causes this. Also shown is how the measurement method for measuring the polarisation state of a propagating wave was developed to enable accurate and therefore meaningful results to be obtained about the depolarisation caused by vegetation. A number of possible methods for measuring the polarisation of a propagating electromagnetic wave are presented, of which one was selected. In an attempt to reduce the experimentation time an alternative method - the Knittel method [Knittel, 1967] was implemented. In the course of the depolarisation studies, the change in polarisation state that a wave propagating through a single tree undergoes was investigated for a number of different specimens of trees.

Discussion of the depolarisation studies and results are presented in chapter 7. An investigation into the relationship between depth of vegetation and signal depolarisation of the propagating wave was performed and the results presented. Partially polarised waves have been experienced and the reason for these are explained. To provide further understanding for the increasing depolarisation of the wave propagating through a specimen of vegetation, measurements were performed on a tree constructed of metal rods whose structure was designed to simulate the effects encountered in a real tree.

2. Literature Review

2.1 Introduction

When a radiowave signal in the frequency band of 10 - 20 GHz propagates through a volume of vegetation it experiences significant attenuation and depolarisation. The effects of vegetation on the magnitude of the signal is an extremely important factor in radio system planning. In the first part of the chapter vegetation attenuation is discussed.

A number of models for predicting the attenuation caused by a volume of vegetation as a function of the depth of vegetation are presented. Depth of vegetation is defined as the path length of signal propagation on which vegetation is present. A brief history of each model is given and reference is also made to other models that are available in the published literature.

In the latter section of the chapter the available published literature on the depolarisation caused by vegetation is reviewed and briefly discussed.

2.2 Effects of Vegetation ou RadioWave Propagation

Radio waves, particularly those with frequencies above 1 GHz experience attenuation, scatter and depolarisation when they propagate through a medium of vegetation. Investigation of attenuation is necessary because it effects the radio path loss experienced by the transmitted signal and this information is required in the planning of radio systems. Here attenuation is taken to mean the attenuation which is experienced in addition to free space attenuation as a result of the signal propagating through the vegetation medium.

The signal loss due to attenuation is created by the various components that make up the trees structure especially the leaves. This is because branches and leaves have finite complex permittivities largely influenced by their water content. It has been shown that a greater loss of signal is suffered when a body of vegetation is

in-leaf compared to when a body of vegetation is not-in-leaf [Schwering et al, 1988], [Stephens and Al-Nuaimi, 1995]. The attenuation is caused by the water content of the tree absorbing a portion of the power of the propagating signal. The portion absorbed is greater for a higher water content, which in turns means that the amount of attenuation due to absorption varies according to the seasons and the prevailing climate and weather. Generally speaking the water content of a tree is higher during the summer months. The actual time of year that the water content is at its highest is very much dependent upon the tree species and is related to the actual internal structure of the tree [Gates, 1991]. The water content of the leaves also varies with the time of day and is at its highest between the middle of the night and close to dawn. The lowest water content is seen in the early afternoon when a portion of the water has moved out of the leaves by transpiration and into the air.

Scattering of the propagating field occurs when the radiowave strikes an object that is larger than the wavelength of the radio wave. All scatterers are larger in dimension than the wavelength of the frequency being transmitted. In the case of a tree, the scatterers are the components that form the complete tree, that is to say, the leaves, twigs, branches and trunk. As can be seen, these components cause attenuation by absorption due to the water content as well as signal loss by scattering the incident field.

Further signal loss is caused by the depolarisation of the radio wave. Depolarisation of the incident field on a tree is caused by the orientation of the trees' components having currents induced by this incident field. These currents cause re-radiated fields in accordance with the random orientations of the trees' components resulting in an overall change in the polarisation of the incident wave.

As a microwave signal propagates through a forest of trees, the signal is subjected to an initial high rate of attenuation at small depths and, as the depth of vegetation increases the rate of attenuation is reduced considerably [Weissberger, 1981], [Al-Nuaimi and Hammoudeh, 1993]. At small depths of vegetation, the coherent

wave is being reduced by absorption and scatter which results in a high attenuation rate. As the depth increases, the incoherent wave caused by the forward scattering of the propagating wave becomes the dominant wave being received. Thus, there is a much reduced rate of attenuation as the signal is primarily propagating through the vegetation by scattering and with this mode of propagation there is relatively less signal loss.

2.3 Vegetation Attenuation Prediction - Theoretical Methods

Within this section a number of models, found within the published literature, for predicting the transmitted signal attenuation due to vegetation are presented. These prediction models include one which may be referred to as the International Telecommunications Union Radio sector (ITU-R) model. Models which are derivatives of the ITU-R model. Two other models included are a model developed at Rutherford Appleton Laboratory (RAL) which initially started as the Maximum Attenuation Rate (MAR) model and a model based on the Radiative Energy Transfer theory (RET).

2.3.1 The ITU-R model and its Derivatives

These models are empirical and from the published literature it has been found that the ITU-R model has been optimised for different dimensions and types of forests. These derivatives of the original ITU-R model are presented in the following sections. The basic format of the ITU-R model is simple and that makes it particularly useful for providing a quick and general estimate of the amount of attenuation caused by a specified medium of vegetation.

2.3.1.1 The ITU-R Model

The ITU-R model [CCIR, 1986] is an empirical model based on the modified exponential decay model [Weissberger, 1981]. The ITU-R model is applicable where either the transmitter or receiver is sufficiently close to a formation of trees so that the signal is predominately propagating through the

trees. An additional criteria of this model is that the body of trees must be less than 400 metres deep. Under these assumptions the attenuation caused by the trees can be modelled using the equation :

$$L \approx 0.2f^{0.3}d^{0.6} \quad dB \qquad 2.1$$

where: L is the attenuation due to the trees in dB,
f is the frequency in MHz and
d is the vegetation depth in metres.

This prediction model is stated as applicable at frequencies in the range of 200 MHz to 95 GHz even though it was based on measurements performed up to a frequency of approximately 10 GHz.

2.3.1.2 Derivatives of the ITU-R Model

The ITU-R model has been utilised by different authors [Seville and Craig, 1995], [Al-Nuaimi and Hammoudeh, 1993] where the 0.2 and 0.6 constants of Equation 2.1 have been adjusted to obtain the best fit to their measured data. The various forms of the ITU-R model are presented in the following sections.

2.3.1.2.1 A Derivative of the ITU-R Model (MITU-R)

In this derivative of the ITU-R model, the model was placed into the form of Equation 2.2 by Al-Nuaimi and Hammoudeh [1993].

$$L = k'd^{x} \quad dB \,[1] \qquad 2.2$$

where: L is the attenuation in dB generated by the vegetation media,
k' and x are constants and
d is the depth of vegetation in metres.

[1] The frequency dependency of the ITU-R model ($0.2f^{0.3}$) has been replaced by the constant k'.

In the literature referenced above, measurements were carried out on an in-leaf apple orchard and a wood of conifers. Values for k' and x were determined by optimising Equation 2.2 against the measured data. This provided the values shown in Table 2-1.

Table 2-1 Values for Constants of Equation 2.2.

Measurement site	k'	x
Orchard in Leaf	11.55	0.414
Conifer wood	7.53	0.394

Al-Nuaimi and Hammoudeh carried out further measurements on the apple orchard when it was without foliage. It was established that a more accurate fit could be obtained in the out-of-leaf case by the use of Equation 2.3.

$$\begin{aligned} L &= 1.74d \quad \text{dB} \quad d \le 31\,\text{m} \\ L &= 23.76d^{0.23} \quad \text{dB} \quad d > 31\,\text{m} \end{aligned} \qquad 2.3$$

This dual-slope representation of the attenuation curve had previously been presented by Weissberger [1981] in the form of a model known as the Modified Exponential Decay model which is described in the following section.

2.3.1.2.2 Modified Exponential Decay Model (MED)

This model as the name suggests behaves in an exponential manner. The form of the model is shown in Equation 2.4 and is described in the literature [Weissberger, 1981] as being applicable to the prediction of attenuation caused by vegetation for the in-leaf case.

$$\begin{aligned} L &= 1.33f^{0.284}d^{0.588} \quad \text{dB} \quad 14\,\text{m} \le d \le 400\,\text{m} \\ L &= 0.45f^{0.284}d \quad \text{dB} \quad 0\,\text{m} \le d \le 14\,\text{m} \end{aligned} \qquad 2.4$$

The above equation provides a dual slope representation of the signal loss caused by vegetation. The numerical values of Equation 2.4 are based upon measurement data acquired between the frequencies of 230 MHz and 9.5 GHz but is recommended for use up to a frequency of 95 GHz. The MED model was compared to the apple orchard data by Al- Nuaimi and Hammoudeh [1993b] and found to offer a very poor fit. There are two reasons for the poor fit. Firstly and most probably, the MED model was derived from measurements mainly performed at U.H.F and V.H.F frequencies. The second reason is that the orchard is not a true representation of a forest due to the regular planting of the trees which offer a greater density of vegetation per square metre in comparison to a natural forest. Accounting for this, a poor fit was also seen for the depth of a single tree.

2.3.2 A Semi-Empirical Model

As has been shown in the literature [Al-Nuaimi and Hammoudeh, 1993a] [Scherwing, *et al*, 1988] the attenuation caused by an increasing depth of vegetation is more accurately represented by a dual curve. Based on this, researchers at Rutherford Appleton Laboratory (RAL) developed a single model to emulate the behaviour indicated by this dual slope curve [Seville and Craig, 1995] [COST 235, 1996].

The initial model developed was one that was termed the maximum attenuation rate model [Seville and Craig, 1995]. This model, Equation 2.5, produces a dual slope curve where the second curve has a gradient that tends towards zero.

$$L = A_m\left(1 - \exp\left(-\frac{Rd}{A_m}\right)\right) \quad \text{dB} \qquad 2.5$$

where: A_m is the maximum attenuation in dB and

R is the initial gradient, in dB per metre, of the attenuation curve taken from a set of measurement data.

This model can provide a relatively good fit to measurement data that has a final curve that approaches a zero gradient. If the measured attenuation curve does not show a final zero gradient then the model in its present form does not provide a good fit. To account for the possibility of measurement data that does not have this near zero gradient the model was developed into the model known as the Non-Zero Gradient (NZG) model shown in Equation 2.6.

$$L = R_{\infty}d + k\left(1 - \exp\left(-\frac{(R_0 - R_{\infty})}{k}d\right)\right) \quad \text{dB} \qquad 2.6$$

Where: R_0 is the initial attenuation rate in dB/m,

R_{∞} is the final attenuation rate in dB/m and

k is referred to as the offset to the final attenuation rate in dB.

This model provides a final slope, R_{∞}, that is not of a fixed gradient, it can also apply to data with a near zero gradient final slope as the NZG model reduces to the MAR model in this case. This may be shown as follows:

As the attenuation rate decreases at increasing depths of vegetation $R_{\infty} \rightarrow 0$ and Equation 2.6 reduces to:

$$A = k\left(1 - \exp\left(-\frac{R_0 d}{k}\right)\right) \quad \text{dB} \qquad 2.7$$

and as the offset k is determined from the final attenuation rate by:

$$k = A_m - (R_{\infty}d_m) \quad \text{dB} \qquad 2.8$$

where d_m is the maximum vegetation depth.

Due to $R_{\infty} \rightarrow 0$, k becomes :

$$k = A_m \quad \text{dB} \qquad 2.9$$

Thus the NZG model reduces to the MAR model:

$$A = A_m\left(1 - \exp\left(-\frac{R_0 d}{A_m}\right)\right) \quad \text{dB}$$

This model was further developed as measurements were made by researchers at RAL with antennas of different beamwidths. The measured data for the different antennas showed a difference in the received signal levels [COST 235, 1996]. This being due to the antennas of different beamwidths seeing varying illuminated widths of vegetation. In turn, this means that there would be a different number of scattering and absorption elements within the vegetation body seen by the antenna thereby affecting the overall received signal level.

To take this effect into account, the NZG model was developed into the Dual Gradient (DG) model which is also an empirical model [COST 235, 1996]. The area of illumination termed the illumination width, W, is defined as shown in Figure 2-1 and is determined as shown in Equation 2.10. The DG model also considers the effect of the frequency as can be seen in Equation 2.11.

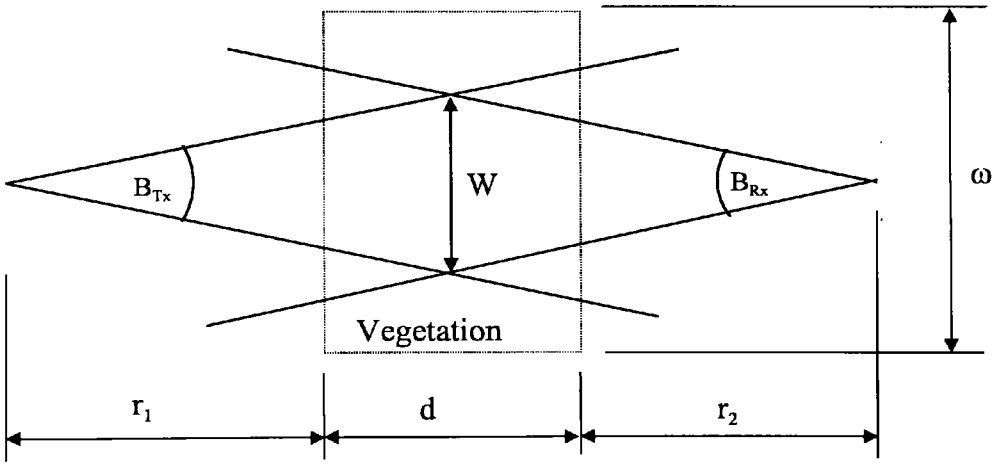

Figure 2-1 Definition of Illumination Width.

$$W = \min\left(\begin{array}{c} \dfrac{(r_1 + d + r_2)\tan(B_{Tx})\tan(B_{Rx})}{\tan(B_{Tx}) + \tan(B_{Rx})} \\ (r_1 + d)\tan(B_{Tx}) \\ (r_2 + d)\tan(B_{Rx}) \\ \omega \end{array}\right) \text{ m} \qquad 2.10$$

$$L = \frac{R_\infty}{f^a W^b} d + \frac{k}{W^c}\left(1 - \exp\left(-\frac{(R_0 - R_\infty)W^c}{k} d\right)\right) \quad \text{dB} \qquad 2.11$$

Where: a, b, c, k, R_0 and R_∞ are constants as shown in Table 2-2 and f is the frequency in GHz.

Table 2-2 Parameter Constants for DG Model.

Constant	With Foliage	Without Foliage
a	0.70	0.64
b	0.81	0.43
c	0.37	0.97
k	68.80	114.70
R_0	16.70	6.59
R_∞	8.77	3.89

The constants presented in Table 2-2 were obtained by the fitting of the model to a number of sets of data obtained from actual measurements past and present [Seville and Craig, 1995] [Al-Nuaimi and Hammoudeh, 1993a] including data acquired during the measurement programme of this research.

2.3.3 Radiative Energy Transfer Theory

The radiative energy transfer theory (transport theory) models the vegetation as a statistically homogenous random medium of scatterers. The theory allows multiple scattering to be taken into account and is therefore well suited to model how vegetation affects the propagating wave [Ishimaru, 1978].

The scatterers are characterised by a scattering function $p(\vec{s}, \vec{s}')$ that has a narrow forward lobe and an omnidirectional background. The unit vectors $\vec{s}$ and $\vec{s}'$

indicate the scatter and incident directions. The forward lobe is assumed to be gaussian and takes the form: [Johnson et al, 1985] [Ulaby et al, 1988]

$$f(\theta) = \left(\frac{2}{\beta_s}\right)^2 e^{-(\theta/\beta_s)^2} \qquad 2.12$$

where: $\theta = \cos^{-1}(\vec{s}, \vec{s}')$ and

β_s is the beamwidth of the forward lobe.

The scattering pattern is represented by the form:

$$p(\theta) = \alpha f(\theta) + (1-\alpha) \qquad 2.13$$

Where: α is the ratio of the forward scattered power to the total scattered power.

The forward lobe and omnidirectional background has been measured at the University of Glamorgan [Hammoudeh et al, 1996] at a frequency of 20 GHz and 62.4 GHz. The forward lobe measured at 20 GHz was found to be most successfully modelled as gaussian. At the higher frequency of 62.4 GHz this forward lobe was also found to be accurately modelled by Equation 2.12 except for a Ficus tree whose foliage started at a higher height from the ground compared to the other specimens of vegetation. This forward lobe was better modelled by Equation 2.14 which is similar to a scatter function presented by Ulaby et al [1988] from measurements at 38 GHz on trees of the same type. One possible reason for this non-gaussian lobe was probably due to there being an insufficient number of scatterers within the cross sectional area of the receive antenna beamwidth illuminating the tree.

$$f(\theta) = \left(2 + 2/\beta^2\right) e^{-|\theta|/\beta_s} \qquad 2.14$$

As well as the vegetation medium being characterised by the scatter function, it is also characterised by the scatter cross-section per unit volume σ_s and the absorption cross-section per unit volume σ_a.

The equation that predicts the attenuation as a function of vegetation depth based on the Radiative Energy Transfer theory is shown below [Hammoudeh et al, 1996]:

$$P = P_o\left[e^{-\sigma_T d} + qe^{-\sigma_T d}\left[\exp(\sigma_s \alpha d) - 1\right]\right] \text{ dB} \qquad 2.15$$

where: P_o is the free space signal power,

d is the vegetation depth,

σ_T is the extinction cross section and is related to σ_A and σ_S,

σ_S is the scatter cross section per unit volume,

α is the ratio of forward scattered power to the total scattered power.

q is a weighting factor related to the scattering pattern $p(\theta)$ and the radiation pattern of the receive antenna.

The values for the two unknowns β_s and α may be found from a measured scattering pattern. The initial part $P = P_o e^{-\sigma_T d}$ of Equation 2.15 may be fitted to the attenuation provided by the depth of one tree where the coherent component is the dominant wave and a value for σ_T may be determined. The scatter cross section per unit volume, σ_S, may been determined by comparing Equation 2.15 with attenuation measurements made with a number of different trees (1, 2 and 3) in the LOS path between the transmitter and receiver, and then finding the mean of the values of σ_S obtained. [Hammoudeh et al, 1996]

Once the parameters for the model have been found, the model provides a good prediction for a vegetation medium that is homogenous. The scattering pattern defined by Equation 2.12 does not apply as well to a medium that is without

leaves, as it is the leaves which form a high proportion of the scattering elements of the vegetation medium. The model therefore provides a better prediction for an in-leaf medium rather than a medium which is in the out-of-leaf state.

2.3.4 Other Prediction Models

There are many more models available that are applicable at lower frequencies than those used within this research. These models have been investigated and they treat the vegetation medium in a number of ways, outlined as follows:

1. as a conducting dielectric slab with a model being available for frequencies in the region of 50 MHz [Sachs and Wyatt, 1968]. The slab models are only applicable up to a frequency of approximately 400 MHz at which point, unless the medium is densely populated, it can no longer be described as being homogenous in relation to the wavelength.
2. as a four layer media with two anisotropic slabs [Lian and Lewin, 1986], where each of the slabs represents the foliage and trunk regions. The vegetation is considered as a body of randomly positioned and orientated canonical scatterers. It is applicable in the UHF (200 - 2000 MHz) region and considers the implication of a lateral wave where the wave travels along the interface of the foliage with the trunk or air region. This is also the case with the next model.
3. a stratified, continuous medium where each stratum could represent the air, the forest and the ground [Seker, 1992]. The stratified forest model takes into account lateral waves. The model is said to be applicable up to a frequency of 2 GHz. For the frequencies used in this investigation the surface of the foliage, be it at the air or trunk interface, is relatively rough in comparison to the wavelength of the frequencies transmitted such that any propagation via lateral waves experienced could be considered as insignificant.

2.4 Literature Review on Depolarisation by Vegetation

Depolarisation is defined within this work as being a change in the polarisation state of a wave from one state to another caused by some medium [Beckmann, 1968], namely, vegetation in this case. This study is concerned with the depolarisation caused by a body of vegetation when a signal has propagated through the vegetation.

The models that are available for predicting depolarisation actually predict the depolarised backscattered signal and not the signal that has been depolarised as a result of passing through a volume of vegetation. The models are used for such things as crop and forest type recognition in the field of remote sensing [Riegger and Wiesbeck, 1986]. The removal of the effect of vegetation on a radar signal has also been investigated so that information from beneath a canopy of vegetation can be obtained. For example, the image of a target [Toups et al, 1996] or the soil moisture content [Mo et al, 1982].

The models available from the current literature do not provide a prediction of the depolarisation that a body of vegetation will provide when it is in the transmission path of a radio wave. Also the purpose of this research was not to necessarily develop a model to predict the depolarisation but to actually investigate and characterise the cause of large nulls seen in attenuation measurement data which will be presented in later chapters. It was therefore the aim of this work to characterise and provide a better understanding of what actually occurs to a signal as it propagates through a medium of vegetation. It is believed to be a difficult task to predict the amount of depolarisation, as there are other factors apart from the shape of the tree(s), which contribute to the amount of depolarisation of the incident signal. The contributors being the actual orientation of branches, twigs, leaves and other components of the tree which are larger than the wavelength of the frequency of the incident wave. External influences, such as the presence and strength of wind, are additional contributors, which may change the orientation of the various components of the trees resulting in variable attenuation and depolarisation of the propagating wave.

The information presented in this study on depolarisation caused by vegetation can help in providing a better insight into the effect vegetation has on microwave signals. With the inclusion of this effect of depolarisation into future models a more accurate prediction of the signal loss caused by vegetation would be available.

2.5 Interim Conclusion

A number of models that enable the prediction of the attenuation that will be experienced by a propagating signal as a function of the depth of vegetation have been presented. These fall into two categories; the empirical models which obtain their parameters from data acquired from measurements performed upon different samples of vegetation, and a deterministic model which has its parameters based upon the physical parameters of the vegetation and is based on the radiative energy transfer theory [Ishimaru, 1978]. This model based on the radiative energy transfer theory is capable of predicting the received signal strength by the combination of the coherent and incoherent waves that propagate through a body of vegetation, but the model does not take into account any signal loss caused by the depolarisation of the propagating wave. If this effect was incorporated, an improved prediction of the signal loss suffered by a wave as it propagates through a vegetation body may result. Other prediction models have also been introduced which are applicable in their current forms at frequencies lower than those used in this study.

There has been much research into the depolarisation by given shapes [Beckmann, 1968] but with vegetation it is not just the shape which has an effect on the radio wave. Published literature has not been found detailing depolarisation caused by vegetation for the line-of-sight mode of propagation though literature has been published where the backscattered signal from vegetation has been used in the field of remote sensing to identify the type of vegetation at a particular location.

3. Experimental Work

3.1 Introduction

The main objective of the initial experimental work was to give better understanding about factors affecting the propagation of microwave signals through vegetation and also to obtain experimental data to which further analyses can be applied. The purpose of the experimental work was also aimed at revealing characteristics of the vegetation under examination which in general has a naturally complex structure.

Experiments during the course of this research programme have been carried out on suitable sites that are in both outdoor and indoor environments. Indoor measurements were conducted in a purpose built anechoic chamber, with suitable outdoor sites being chosen from a survey using Ordnance Survey maps followed by visiting and appraising the sites. Three sites were used, one in South Wales and two others in Oxfordshire. The site in South Wales is a line of Sycamore trees and is shown in Figure 4-14. One of the two sites in Oxfordshire is a triangular shaped copse, referred to as the Mound and is shown in Figure 4-6. The other site consists of a line of Horse Chestnut trees, referred to as Fermi Avenue and is shown in Figure 4-1 with no foliage and in Figure 4-2 with foliated branches. The indoor experiments were performed in an anechoic chamber using different types of small trees, both coniferous and broad leaf types.

Measurements were carried out at two frequencies, 11.2 GHz and 20 GHz. Separate measurement configurations were used for the outdoor and indoor measurements and are described in section 3.2. In the main, linear vertical polarisation transmission has been used.

This chapter will discuss the various items of equipment used in the measurement programme and the link budgets of the various radio links used in the measurements. Along with the calibration of the two systems used, the

development of the measurement software and the criteria for the selection of the measurement sites are also discussed.

3.2 Measurement and Equipment Descriptions

This section details the two measurement systems used in both the indoor and outdoor configurations. There is also a discussion of the link budget of the 11.2 GHz and 20 GHz systems, the different criteria which need to be considered when investigating possible measurement sites and, the other hardware used in conjunction with the microwave systems to obtain the measurement data.

3.2.1 Equipment

Two measurement systems, one operating at 20 GHz and another at 11.2 GHz were used in the experimental investigation. Indoor measurements using the anechoic chamber were made predominately at 20 GHz and these include both attenuation and depolarisation measurements. Outdoor measurements were carried out at both 11.2 GHz and 20 GHz. The 11.2 GHz system evolved from an earlier system specifically configured for outdoor measurements [Ding, 1994], [Haslett, 1993]. The systems described below show that the data acquisition subsystems are different for each of the two measurement environments.

3.2.1.1 The 11.2 GHz System

The transmitter of the 11.2 GHz system is comprised of a signal source of the dielectric resonator oscillator (DRO) type and is rated at a nominal 10 dBm (10mW), with the actual output power from the DRO being measured at 13.5 dBm. The power and frequency of the DRO was found to be stable when the supply voltage was in the range of 11 V to 17 V. For outdoor use the DRO was powered by a 15 V battery pack, made up of twelve 1.2 V, 4 Ah rechargeable nickel-cadmium batteries. For the indoor measurements, power was delivered by a D.C power supply. The output of the DRO was normally coupled to an attenuator followed by a standard gain horn antenna whose gain and beamwidth

are determined by the radio path geometry. The antennas used have gains of 10 dBi, 15 dBi and 20 dBi with respective beamwidths of 60°, 35° and 19°. The attenuator was used to control the power level of the transmitted signal. Figure 3-1 shows a block diagram of the transmitter system.

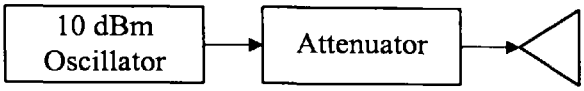

Figure 3-1 Block Diagram of the 11.2 GHz Transmitter.

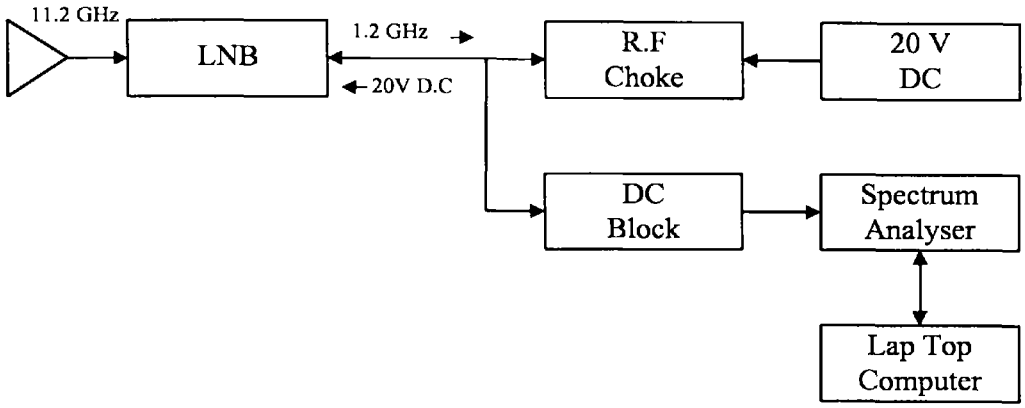

Figure 3-2 Block Diagram of the Outdoor 11.2 GHz Receiver System.

The receiver shown in Figure 3-2 consists primarily of a horn antenna and a low noise block (LNB). The LNB has a gain of 50 dB and is powered by a 20 V DC supply via an R.F choke and the LNB is used to down-convert the received signal to an IF of 1.2 GHz. This is achieved by using the mixer and a 10 GHz local oscillator that is incorporated into the LNB. The output signal of the LNB is limited to 0 dBm since the output saturates just above this point. This results in the LNB being unable to accept a signal greater than -50 dBm. This makes it necessary to control the transmitted signal level, particularly over short distances between the transmitter and receiver, where the power at the input of the LNB could exceed -50 dBm. The output from the IF stage is connected via a D.C block to a spectrum analyser, this being the normal receiver configuration for the outdoor measurements, as shown in Figure 3-2.

For the indoor measurements (see Figure 3-3) a second IF stage giving an IF frequency of 220 MHz is used. The mixer and local oscillator of this stage converts the received signal to the operating frequency of the logarithmic amplifier (log amp). The log amp is used to convert the received signal strength to a DC voltage which is in turn fed to a data acquisition board housed in a personal computer. A type-N coaxial cable that has a loss of 2.5 dB is connected between the LNB and the DC block. The D.C block is required to provide isolation for the spectrum analyser from the 20 V D.C used to power the LNB.

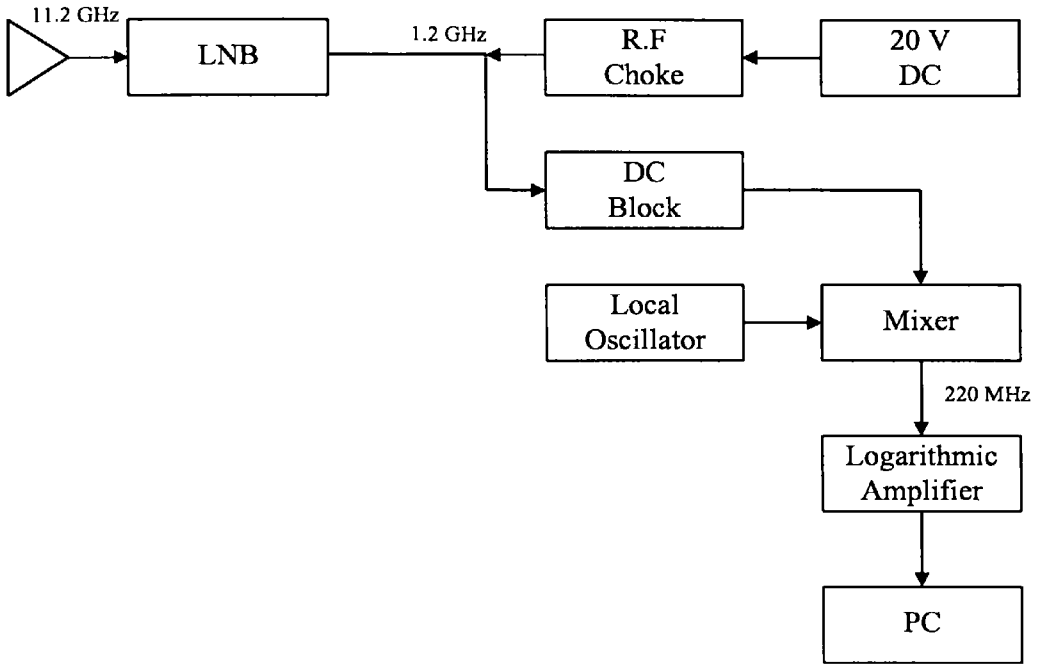

Figure 3-3 Block Diagram of the Indoor 11.2 GHz Receiver System.

3.2.1.2 The 20 GHz system

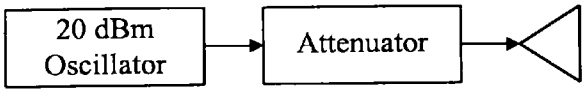

Figure 3-4 Block Diagram of the 20 GHz Transmitter.

The transmitter of the 20 GHz system shown in Figure 3-4 consists of a voltage controlled oscillator rated at a nominal 20 dBm, with the actual transmit

power being measured at 21.2 dBm. The frequency of operation used for all experiments was 20 GHz, although this figure can be varied between 19.89 GHz and 20.05 GHz by applying a voltage in the range 0 V to 20 V to the varactor diode. The frequency of 20GHz used in these experiments being obtained by applying the 7.5 V which powers the oscillator to the varactor input as well. The output of the oscillator is fed to a horn antenna allowing the signal to be radiated. The antennas used have been standard gain antennas of 10 dBi, 15 dBi and 20 dBi which have beamwidths of 60°, 32° and 19° respectively. A lens horn antenna of 19 dBi gain with a beamwidth of 23° was also available for use in the measurement programme.

The receiver comprises a horn antenna which is connected to a mixer. The mixer is used to obtain the required IF and has a local oscillator input which comes from a manually tuneable oscillator. When the tuning is varied, the frequency of the output from the mixer can be adjusted. The output IF most commonly used is 220 MHz, as this is the operating frequency of the log amp most frequently used. This output is coupled to a low noise amplifier. The receiver system has an overall gain of 30 dB. For the outdoor experiments, see Figure 3-5, the receiver is connected via a 10 metre cable having a loss of 2.5 dB to the spectrum analyser.

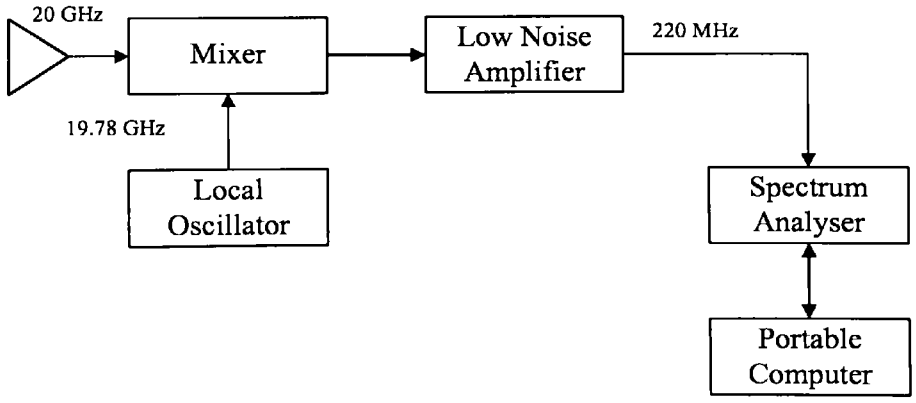

Figure 3-5 Block Diagram of the Outdoor 20 GHz Receiver System.

For the indoor measurements, see Figure 3-6, the receiver is connected to a log amp centred at 220 MHz via a 5 metre cable found to exhibit a loss of 2 dB at this frequency.

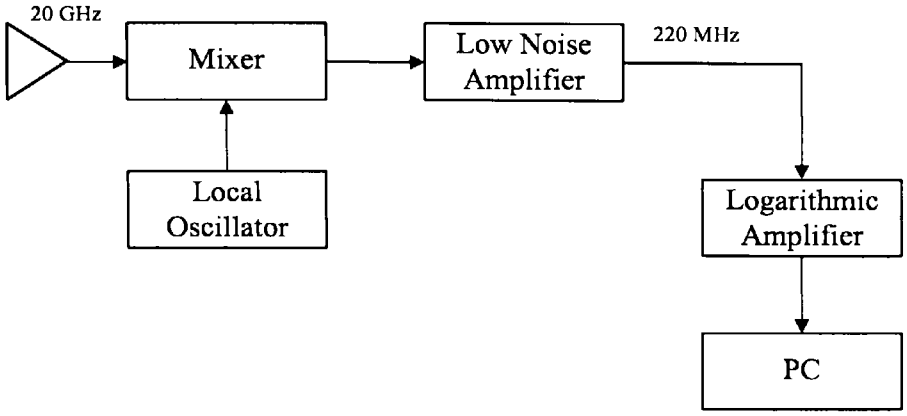

Figure 3-6 Block Diagram of Indoor 20 GHz Receiver System.

3.2.1.3 Dynamic Range

The dynamic range in this case defines the range available for measurement of the signal loss. In this case, the loss is that experienced by the propagating signal due to the vegetation specimen under investigation and present in the radio path. The dynamic range available is dependent upon a number of factors, these being the gain of the transmit and receive antennas, the distance between these antennas, the noise floor of the receiver system, the transmitted power and the gain of the receiver. The dynamic range for each of the microwave systems is detailed in the following sections.

3.2.1.3.1 The 11.2 GHz System Link Budget

For the 11.2 GHz system the noise floor of the receiver when measured with the spectrum analyser was found to be in the region of -80 dBm with a bandwidth of 2MHz. The LNB provides a gain of 50 dB, the transmitter has a transmit power of 13.5 dBm and cable losses amounted to approximately 3.5 dB. Using 20 dBi antennas at both the transmitter and receiver, meant that 180 dB was available for freespace loss and signal loss due to the vegetation. The freespace loss, see Equation 3.1 [Macario, 1991], being 100 dB for a distance of 200 metres between the transmitter and receiver.

$$\text{Freespace loss, } L_{fs} = 20\log(4\pi R/\lambda) \text{ dB} \qquad 3.1$$

where R is the distance between the transmitter and receiver,

and λ is the wavelength of the signal frequency, in the same units as R.

This means that the 11.2 GHz measurement system has a dynamic range of approximately 80 dB available to measure signal loss caused by vegetation when the transmitter and receiver are separated by a distance of 200 metres.

3.2.1.3.2 The 20 GHz System Link Budget

The dynamic range for the 20 GHz system was found in a similar manner. The noise floor of the receiver is -60 dBm using the indoor measuring system and in the region of -85 dBm using the spectrum analyser in the outdoor system. The transmitter provides a signal level of 21.2 dBm and the receiver gives a gain of 30 dB. If 20 dBi antennas are used at both the transmitter and receiver then a dynamic range of 151.2 dB indoors and 176.2 dB outdoors is available to measure the path losses. This is further illustrated in Table 3-1.

Table 3-1 20 GHz System Link Budget.

	Indoor System	Outdoor System
Transmit Power (dBm)	21.2	21.2
Transmit Antenna (dBi)	20	20
Receiver Antenna (dBi)	20	20
Receiver Gain (dB)	30	30
Noise floor of System (dBm)	-60	-85
Max. System Loss (dB)	151.2	176.2

The freespace loss for a distance of 9 metres between the transmitter and receiver is 77 dB. This gives a dynamic range of 70 dB for indoors and 95 dB for outdoors to measure loss due to vegetation. The greater the distance between the

transmitter and receiver, and the smaller the gain of the antennas used, the smaller the available dynamic range available to measure signal loss will be.

3.2.1.4 The Anechoic Chamber

The purpose of the anechoic chamber is to enable experiments to be performed under controlled conditions. The controlled conditions are obtained by the walls and the roof of the chamber being first lined with a metal foil. This foil firstly prevents any outside electromagnetic influence on what is occurring within the chamber and secondly, it improves the performance of the absorption panels which are bonded on top of the foil. The floor is also covered in these absorption panels to prevent any reflections from the floor of the chamber. The operating range of the panels is between 10 GHz and 90 GHz, with each panel measuring a square 24 inches and consisting of 256 pyramid shaped cones. The performance of the walls have been measured and found to give in excess of 40 dB absorption at both 11.2 GHz and 20 GHz. This means that the effect of signals reflecting off the walls of the chamber are negligible in comparison to the direct signal being measured. The chamber offers a usable length of 5.75 metres, a width of 2.5 metres and a height of 2.5 metres.

Housed within the chamber is a high precision two axis turntable. One axis allowing movement in the horizontal plane and the other axis in the vertical axis. Each axis can be moved independently or simultaneously in resolutions as small as 0.01°. This allows for the accurate and automated movement of antennas, vegetation samples or anything else mounted on the turntable. The turntable can be separated to have two axis which can be mounted in any plane and anywhere within the chamber. Each of the axis is controlled by an electronic sub-system called an indexer. The indexer allows each of the axis to be remotely controlled by a computer via a serial link, with the two indexers being mounted in a box placed outside the chamber.

3.2.2 Data Acquisition

Whether an experiment is performed in the anechoic chamber or at a measurement site, the rate at which data can be acquired greatly affects the amount of time an experiment will consume. In the past at the University of Glamorgan (UoG), measurement data was either collected manually from the spectrum analyser which could result in errors, or using a small data logging program [Ding, 1994]. Being able to acquire data consistently over a period of time also allows more accurate description of the received signal level, and also means that any rogue or spurious measurement data caused by a vehicle driving past the experiment site, for instance or any other unwanted influences due to wind movement, could be averaged out.

To allow the automated collection of data, a device was needed that was able to interface with a computer and transfer data to it. This was achieved in two completely different ways for the indoor and outdoor experiments and it is these two methods which are discussed in the following sections.

3.2.2.1 Indoor Environment

For the measurements performed in the anechoic chamber, the device that interfaces with the computer is a data acquisition board (DAQ). The DAQ allows a voltage on any one of its 16 analogue input channels to be measured at a maximum throughput rate of 1 MHz. The data measured by the DAQ is represented by 12 bits. If more than one channel is used to sample the data then the specified sampling (throughput) rate is divided amongst the channels. The DAQ has two input modes; a bipolar mode, -5 V to +5 V and a unipolar mode, 0 V to +5 V. Due to the DAQ requiring a voltage on its input, the log amp introduced above was used to convert the received signal strength into a corresponding voltage level. When the voltage level is sampled by the DAQ a 12 bit binary number that represents the voltage is returned to the computer. This 12 bit number (digital code) is then converted to its corresponding dBm level using two appropriate formulae. The first formula is used to convert the 12 bit number

to a voltage, V, this formula can be one of two formulae depending upon the mode of operation of the DAQ.

For Unipolar mode :

$$V = (\text{digital code})(5)/4096 \quad 3.2$$

For Bipolar mode :

$$V = (\text{digital code}-2048)(5)/2048 \quad 3.3$$

where V is the voltage in volts.

The second formula being the one for the log amp which is used to convert the voltage to a corresponding dBm level.

$$dBm = (V - 2) / 0.025 \quad 3.4$$

Alternatively a program was used which related the raw data provided by the DAQ directly to a corresponding dBm level.

3.2.2.2 Outdoor Environment

For the outdoor measurements the device used to interface with the portable computer is the spectrum analyser. The analyser is equipped with an IEEE bus connector and the portable computer an RS232 port. To enable the two pieces of hardware to be physically connected an RS232 to IEEE converter is employed. This connection provides a bi-directional communication link between the computer and the spectrum analyser, thereby permitting control of the analyser using the computer. The analyser returns the signal strength in dBm and a maximum sample rate of 7 samples per second can be obtained. One of the factors in determining the sample rate is the sweep time of the analyser.

3.2.3 Software Development

During the course of the research, two software programs have been written. One was developed for use when performing measurements in the anechoic chamber allowing control of the DAQ and the two axis turntable housed inside the chamber. The other program was written for use on the portable computer permitting the control and acquisition of data from the spectrum analyser. Both programs automatically collect data which in turn is stored in a format that allows it to be loaded into other software packages for subsequent analysis. The development of these programs enabled the automatic acquisition and pre-processing of large volumes of data.

3.2.3.1 Anechoic Chamber Software

The purpose of writing the anechoic chamber software was to allow completely automated experiments to be performed within the confines of the anechoic chamber, thus reducing the need for human presence in the chamber whilst measurements were in progress. The advantages of this are obvious for the type of measurement undertaken. The program was written to enable straightforward utilisation by the user. The software permits the user to control the two axis high precision turntable, their incremental positioning and the DAQ introduced above.

The program presents the user with two menus. The first menu allows the turntables parameters, acceleration and velocity rates, to be set. The two turntables can be moved either simultaneously or independently. Also available is a function to send the turntable through a sequence; starting and finishing at a specified angle with a particular angular increment, through which the turntable is stepped on its way to the finish angle.

The second menu permits the DAQ to be configured according to the users requirement. The rate of data acquisition and the number of samples can also be specified, along with the name of the file and location where the acquired data will

be stored. The DAQ can be used on its own or in conjunction with either one or both axis of the turntable. If the tables are to be used in conjunction with the DAQ, the software will require the start and finish angles for the turntable along with the incremental step to be used. At each of these steps the software will inform the DAQ to acquire data and place it in the respective file.

3.2.3.2 Outdoor Environment Software

The main objective of the outdoor environment program is to enable the portable computer to communicate with the spectrum analyser which in this case is used to measure the strength of the received signal. The analyser has an IEEE connector which is connected to the lap top computer via an RS232-to-IEEE converter that permits communication in both directions.

As with the anechoic chamber program, this program also has two menus. The more commonly used functions of the analyser are available in the first menu, permitting the user to have remote control of the analyser. There are functions allowing the user to control amongst others the centre frequency, frequency span and resolution bandwidth. The second menu allows data to be collected in three different ways, either by specifying the number of samples to acquire or the period of time over which to acquire data samples. The third method of acquiring data is by the capture of a complete trace from the analyser, this being the trace that is visible on the screen. In the case of experiments which were carried out simultaneously at two frequencies, a function was used that automatically informs the analyser to go to each frequency in turn and to return their respective signal strengths to the computer. This resulted in the speeding up of the process of acquiring the data. The user may also specify the name of the file into which the acquired data should be stored. In a separate file the mean, maximum, minimum and standard deviation of the measured values are stored. A final function permits text to be added to the file in case any notes are to be added.

3.2.4 Calibration of Antennas

All the antennas used in any of the measurements first had their radiation patterns measured in the anechoic chamber in both the horizontal and vertical planes. This operation was performed so that the antennas could be characterised with regards to their radiation pattern and beamwidth. The antenna under investigation was mounted to the centre of the two axis turntable so that the antenna was at the centre of rotation. It was then possible for the antenna to be moved in the vertical and horizontal planes. During these measurements the receiver of the microwave system was placed in the far field region [Jull, 1981] of the transmit antenna. The far field distance R may be estimated from :

$$R = \frac{2D^2}{\lambda} \text{ m} \qquad 3.5$$

where D is a characteristic dimension of the antenna. For example, for a horn antenna D relates to the larger dimension of the rectangular aperture.

Initially the transmit and receive antennas were vertically polarised. The antenna under test was then rotated in the horizontal plane about its vertical axis in incremental steps. At each step of the turntable the received signal strength was measured allowing a plot of the radiation pattern for the H-plane of the antenna to be constructed. The transmit and receive antennas were then aligned for horizontal polarisation. The measurement process was repeated to obtain the E-plane radiation pattern of the antenna under test. [Kraus, 1985]

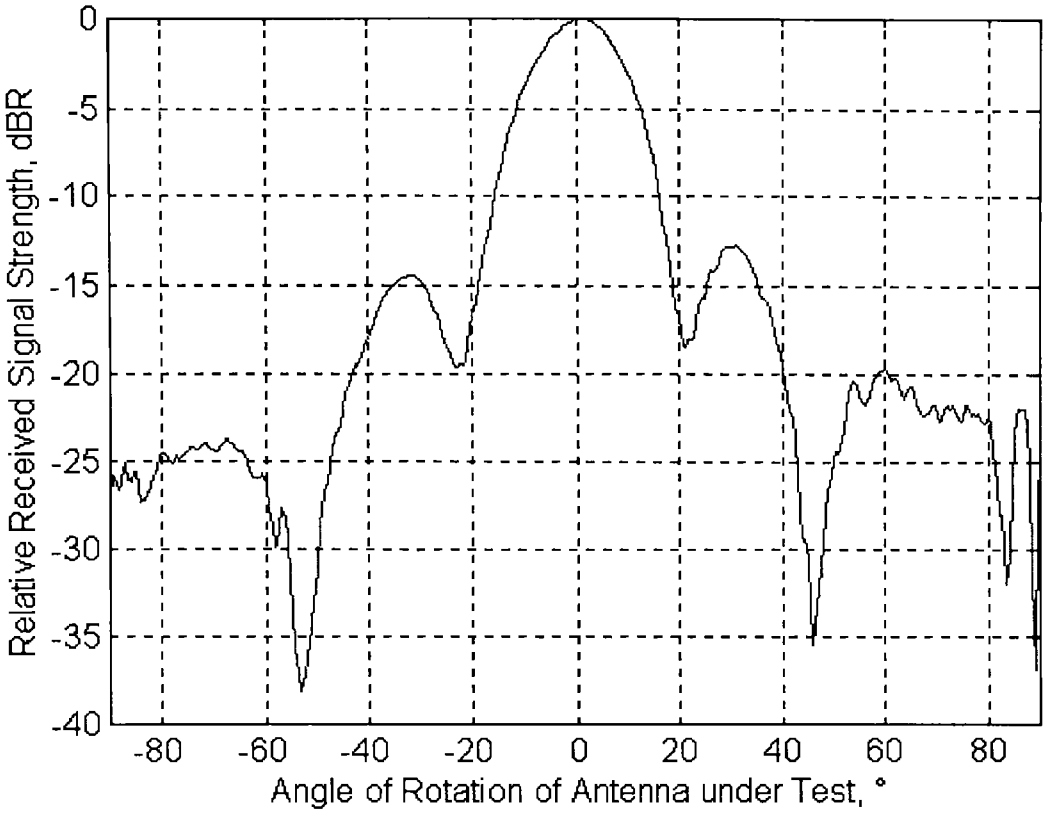

Figure 3-7 Radiation Pattern of 20 dBi Antenna at 20GHz.

3.2.5 Selection Criteria for Experiment Sites

The purpose of the outdoor experimental sites is to permit the experimental investigation of the effects of increasing depths of vegetation on the attenuation and scatter of propagating microwaves. To be able to carry out meaningful experiments some realistic sites were required. Each experiment site includes the vegetation under test, a receiver, a transmitter and a number of other criteria which are explained below.

1. Foreground Clearance

   The potential site has to offer sufficient foreground clearance, so that the transmitter can be placed at a sufficient distance from the vegetation to enable either the vegetation to be in the far field region of the transmit antenna, or at a distance to allow the required width of the vegetation to be illuminated by the 3 dB beamwidth of the transmit antenna. The greater of these two distances is the minimum required foreground clearance.

2. Vegetation

   The vegetation has to be reasonably mature to offer sufficient height, width and in certain cases depth to allow realistic experiments to be performed.

3. Receiver Positioning

   Within the site there has to be space for the receiver to be positioned so that varying depth of vegetation measurements can be performed. Ideally the vegetation should be wedge shaped allowing increasing depth of vegetation measurements to be performed with ease. An acceptable alternative is that there is sufficient space within the vegetation to mount the receiver at various depths, e.g. an appropriate clearance between successive trees in a line of trees.

4. Flatness of Ground

   This criterion is concerned with the flatness of the ground at which the site is located. The site is required to be relatively level or if the ground is sloping that it has a fairly constant gradient. A further criterion is that vehicular access is possible.

5. Obstacles

   This requires that the chosen site is free of obstacles such as a buildings and goal posts, in the vicinity of the site. This is because reflections from such obstacles may significantly affect the measured signal level.

Using the above criteria, various Ordnance Survey maps were examined for the availability of potential sites. Unfortunately, it was necessary in many cases to visit and consequently reject the sites initially chosen from the OS maps because the site did not meet one or more of the required criteria. For example, many orchards chosen because of the regular spacing of the trees, had to be rejected as the trees did not have sufficient height.

Three experiment sites, out of a vast array of potential sites, were selected as they conformed to all of the selection criteria. Two of these were in Oxfordshire and were the result of a collaboration with the Rutherford Appleton Laboratory - one site being a line of Chestnut trees and the other, a triangular shaped copse of Lime and Sycamore trees. One site in South Wales was identified and consisted of a

line of Sycamore trees. Before experiments could be performed at these sites, permission was obtained from the appropriate bodies.

3.3 Interim Conclusion

The two microwave systems at 11.2 GHz and 20 GHz along with the two measurement systems for indoor and outdoor have been introduced and developed in this chapter. Information regarding the anechoic chamber and the equipment therein used to perform experiments in controlled conditions have been presented along with details of their performance. The software used for control of the hardware and the acquisition of data has been developed over a period of time for the two different measurement environments [Appendix A and B]. The criteria used for finding suitable measurement sites along with the three sites that were suitable for vegetation depth measurements have also been introduced.

The next chapter will present the method employed in performing these measurements at each site and the results obtained will also be shown.

4. Vegetation Attenuation Measurements

4.1 Introduction

This chapter presents the three sites that were used to obtain outdoor vegetation attenuation measurements, along with their respective geometries and methods employed in performing the experiments. At two of the sites the 11.2 GHz and 20 GHz systems were used, whereas at the third, only the 11.2 GHz frequency was utilised.

The purpose of performing these experiments was to gain better understanding of the propagating mechanisms that occur within vegetation. The information gained from these experiments can help in quantifying the effects vegetation has on the propagation of radiowaves.

Measurement results from these experiments are presented in this chapter as attenuation due to the vegetation versus vegetation depth for in-leaf and out-of-leaf states. Analysis of the measurement data is given at the end of the chapter.

4.2 Vegetation Depth Attenuation Measurements

In order to characterise the attenuation of radiowaves as a function of the depth of vegetation and frequency, attenuation measurements at the two frequencies were performed at different sites where the geometry enabled results to be obtained at varying depths.

4.2.1 Fermi Avenue

The Fermi Avenue site in Oxfordshire is so named because of the road adjacent to the line of trees on which attenuation measurements were carried out. The trees are of the Horse Chestnut variety with the height of the trees being

approximately 7.5 metres above ground level. The trees are, for the most part, equally spaced with the foliage starting at a height of 2 metres.

4.2.1.1 Measurement Method and Site Geometry

The experiments were performed at 11.2 GHz and 20 GHz with the trees both in-leaf and out-of-leaf in the months of July and March of 1995 respectively. On both occasions the weather had been dry for two days prior to the measurements and there was a slight breeze. The two outdoor measurement systems discussed in Chapter 3 were used in these experiments.

The transmitters fitted to 20 dBi standard gain horn antennas were arranged to give vertically polarised signals and were positioned at a distance of 11 metres from the trunk of the first tree on a pneumatically extendible mast at a height of 4.5 metres. This height was selected as it was equal to the height of the centre of the trees' foliage. The distance of 11 metres was selected so that only the width of the trees would be illuminated by the 19° main lobe beamwidth of the transmit antennas.

The receivers of both systems were equipped with 20 dBi standard gain horn antennas and were vertically polarised. For the out-of-leaf experiment, the receivers were mounted on a tripod which allowed movement in both the horizontal and vertical planes, thus permitting the alignment of the receive antennas to the transmit antennas. The tripod, with receivers and associated measuring hardware were secured on an aerial platform.

Figure 4-1 Fermi Avenue with no Foliage.

The aerial platform and the Fermi avenue site are shown in Figure 4-1, together with the first eleven trees in the line when they were without foliage. The aerial platform can be seen in front of the ninth tree. For the in-leaf measurements, the receivers were mounted on a platform which could be controlled remotely in both azimuth and elevation. The platform was atop a pneumatically extendible mast, up to 9 metres and housed in a van, as can be seen on the left of Figure 4-2 which also shows the trees in leaf. The associated measuring equipment was also housed within the van for the duration of the experiment. The receivers, situated on the aerial platform or on the top of the van, were moved to each midway point between the trees. At each receiver position, the antennas were aligned to the transmit antennas and the received signal strength was recorded for a total of 60 samples at both frequencies. Sixty samples were taken, as this number of samples was found to consistently give approximately the same mean value. Below this number, the mean value was found to be different for each successive batch of samples. More than 60 samples were found to provide the same mean value as that for 60 samples.

Figure 4-2 Fermi Avenue in Leaf.

The total path length, the distance between the transmitters and receivers, and the depth of vegetation each tree presented were measured and recorded. The geometry of this site is shown schematically in Figure 4-3. Initially the receiver at each frequency was positioned in front of the first tree at a distance of 11 metres from the transmitter and a calibration measurement involving freespace propagation was performed.

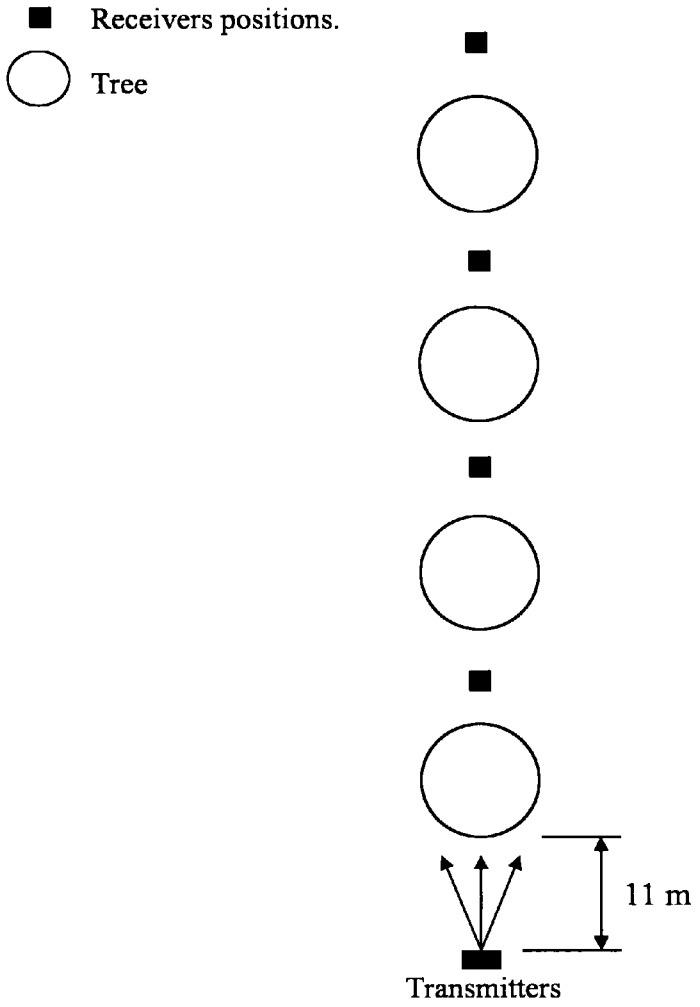

Figure 4-3 Fermi Avenue Measurement Geometry.

4.2.1.2 Fermi Avenue Measurement Results

The data acquired at each receiver position were normalised with respect to the signal level that would have been measured without the vegetation in the path. This signal level is obtained with the help of a calibration measurement performed with the receiver in front of the first tree at a distance of 11 metres from the transmitter. The method of normalisation involves finding the difference in the freespace loss between the distance of the calibration measurement and for each receiver position.

For example at 20 GHz :

$$\text{Freespace loss } (L_{fs}) = 20\log(4\pi R/\lambda) \text{ dB} \qquad 4.1$$

where R is the distance between the transmitter and receiver in metres, and λ is the wavelength, 0.015 metres for a frequency of 20 GHz.

Difference in freespace loss

$$L_{fs_{diff}} = 20\log\left(\frac{d}{d_{CAL}}\right) \text{ dB} \qquad 4.2$$

where d is the distance between the transmitter and receiver in metres and d_{CAL} is 11 metres the calibration measurement distance.

The value obtained from Equation 4.2 is then subtracted from the value obtained for the calibration measurement, thus providing the signal strength that would have been measured with no vegetation in the path.

For example at a distance of 40 metres between the transmitter and receiver:

$L_{fs\,diff} = 11.21$ dB

Calibration measurement at 11 m = 11.33 dBm

$\therefore$ the received signal at 40 m with no vegetation = 0.12 dBm

By normalising with respect to the freespace value using Equation 4.3, a value is obtained that represents the loss experienced due to the vegetation. The units of this normalised data is dBf as it is relative to the freespace level that would have been measured with no vegetation present in the radio path.

$$P_{Norm} = P_{Meas} - P_{Free} \text{ dBf} \qquad 4.3$$

where P_{Norm} is the normalised value, P_{Meas} is the received signal strength with vegetation in the path and P_{Free} is the signal strength that would be measured with no vegetation in the path. In the above example P_{Free} is 0.12 dBm.

The normalised data are shown in Figure 4-4 for the 11.2 GHz measurement and in Figure 4-5 for the 20 GHz measurement. From the sixty samples recorded at each of the receivers positions the maximum, minimum and standard deviation values were found in addition to the mean value. The maximum and minimum values are used to show the fluctuations in the measured data using a vertical line at each measured point. The fluctuations are attributed in the main to the movement of the branches and leaves caused by the prevailing wind.

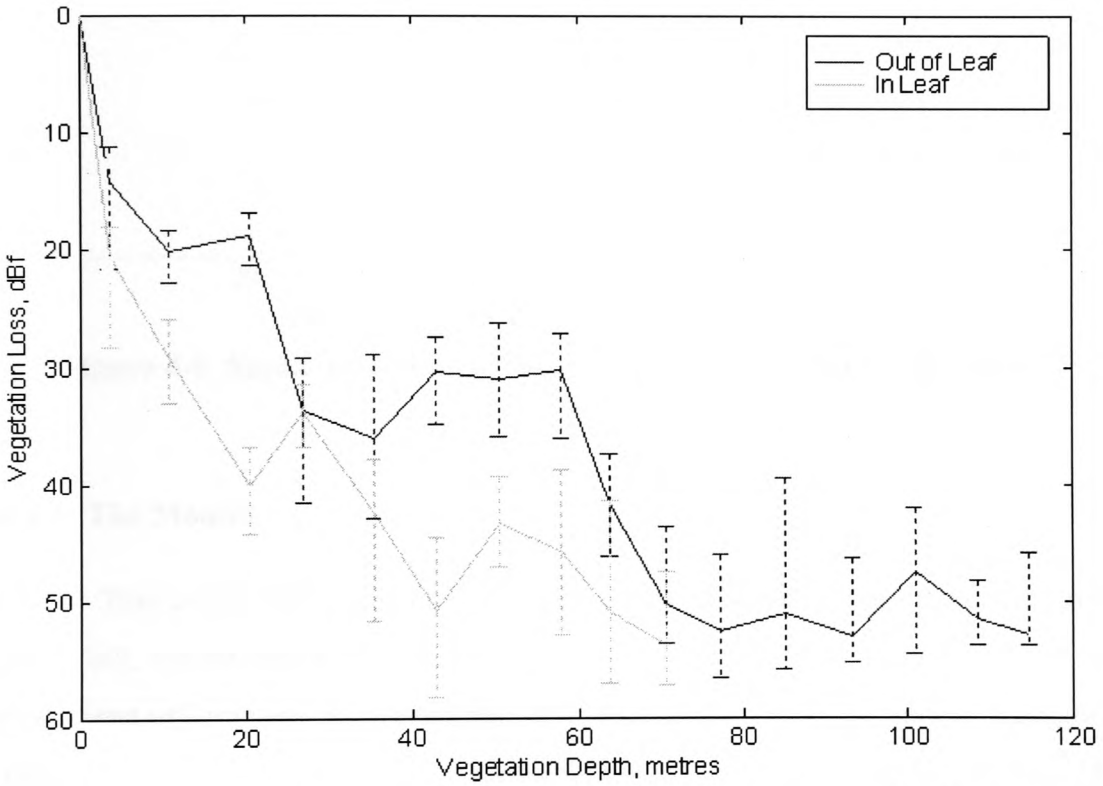

Figure 4-4 Signal Loss due to Vegetation at Fermi Avenue (11.2 GHz).

Contrary to what might be expected the measurement results do not show a smooth curve as the vegetation increases in depth. At particular depths such as just after a depth of 40m on the in-leaf data (Figure 4-4) a trough can be seen. These troughs can also be seen in other vegetation depth figures. The reason for the troughs is explained in detail in Chapter 7.

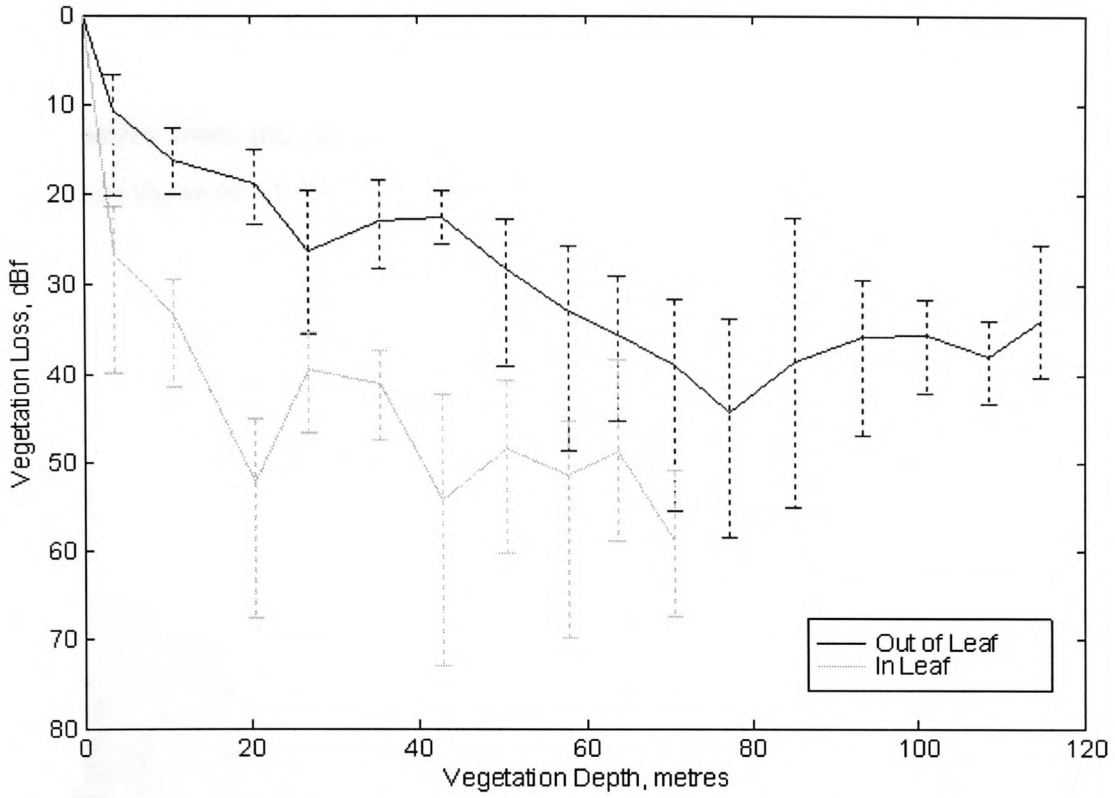

Figure 4-5 Signal Loss due to Vegetation at Fermi Avenue (20 GHz).

4.2.2 The Mound

This site in Oxfordshire is a triangular shaped copse in close proximity to a small hill, whose shape enabled a varied vegetation depth to be obtained. It is comprised of Lime and Sycamore trees that are approximately 10 metres in height. The leaves of the Lime trees are approximately 5 - 10 centimetres long and 18 centimetres long for the Sycamore.

4.2.2.1 Measurement Method and Site Geometry

These experiments were performed at both 11.2 GHz and 20 GHz in the same months as the Fermi Avenue experiments when the trees had foliage and also when there was no foliage. The measurements were completed within a day of the Fermi Avenue experiments in similar weather conditions, that is after two dry days and with a slight breeze.

At both frequencies, signals of linear vertical polarisation were transmitted through 20 dBi standard gain horn antennas. The transmitters were positioned 125 metres from the leading edge of the copse at a height equal to the central height of the trees of the copse.

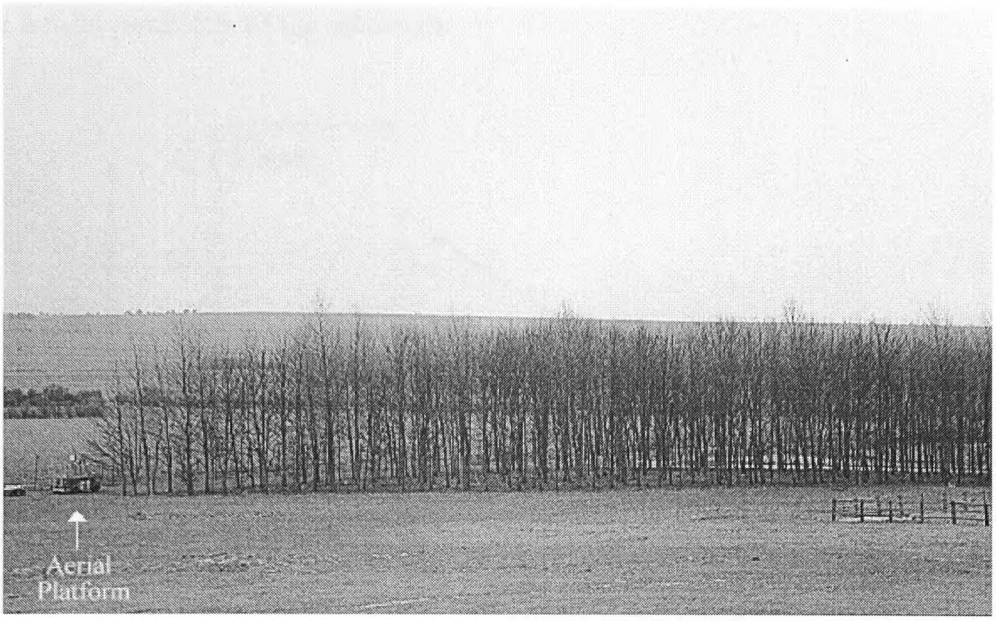

Figure 4-6 The Mound.

Antennas of 20 dBi gain were used on the receivers of both systems and were mounted in an identical configuration to that used for the Fermi Avenue experiments. The copse and the aerial platform to the left of the trees can be seen in Figure 4-6, which also shows that the copse as a vegetation medium is not particularly homogenous. The receivers were moved along the far side of the copse so that there was an increasing depth of vegetation between the transmitters and receiver as shown schematically in Figure 4-7. Each receiver position was equally spaced so that a vegetation depth ranging from 0 to 45.8 metres was realised. An initial measurement was carried out just before the start of the copse with no vegetation in the path to obtain a calibration measurement, subsequently used in the normalisation process. The receivers were fixed at three positions with heights of 3, 5 and 7 metres. At each frequency a set of measurements were taken for each receiver position. Each of the sets of data taken were for each of the heights at which the receivers were placed. Initially the receivers were visually

aligned to the transmit antennas. At every measurement point the receiving antenna was scanned ±10° in the azimuth and elevation to obtain the strongest signal, this being where the transmitter and receivers were aligned. The received signal strength was recorded a total of sixty times using the outdoor measurement system at each receiver position. The process was repeated for each one of the three height positions of the receivers.

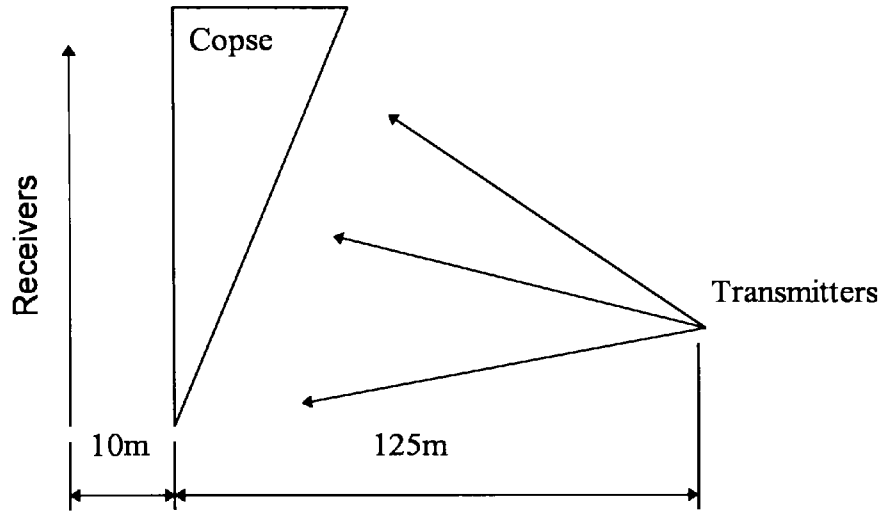

Figure 4-7 Geometry of The Mound.

4.2.2.2 The Mound Measurement Results

Once the measurement data sets had been collected, they were normalised as explained in section 4.2.1.2 (The Fermi Avenue data), with the exception that in this case, the calibration measurement was performed at a distance 125 metres. The normalised data in dBf (relative to freespace) with the receive antennas at a height of 3 metres, for in and out-of-leaf measurements, are shown in Figure 4-8 for 11.2 GHz and in Figure 4-9 for 20 GHz. Figure 4-10 and Figure 4-11 show the in-leaf and out-of-leaf normalised data for the receiver at a height of 5 metres at the frequencies of 11.2 GHz and 20 GHz respectively. The normalised data for the receivers at 7 metres above ground level are shown in Figure 4-12 for 11.2 GHz and Figure 4-13 for 20 GHz. All the figures have vertical lines which represent the fluctuations seen in the measured data. This variability of the measured attenuation is caused mainly by the movement of leaves and branches.

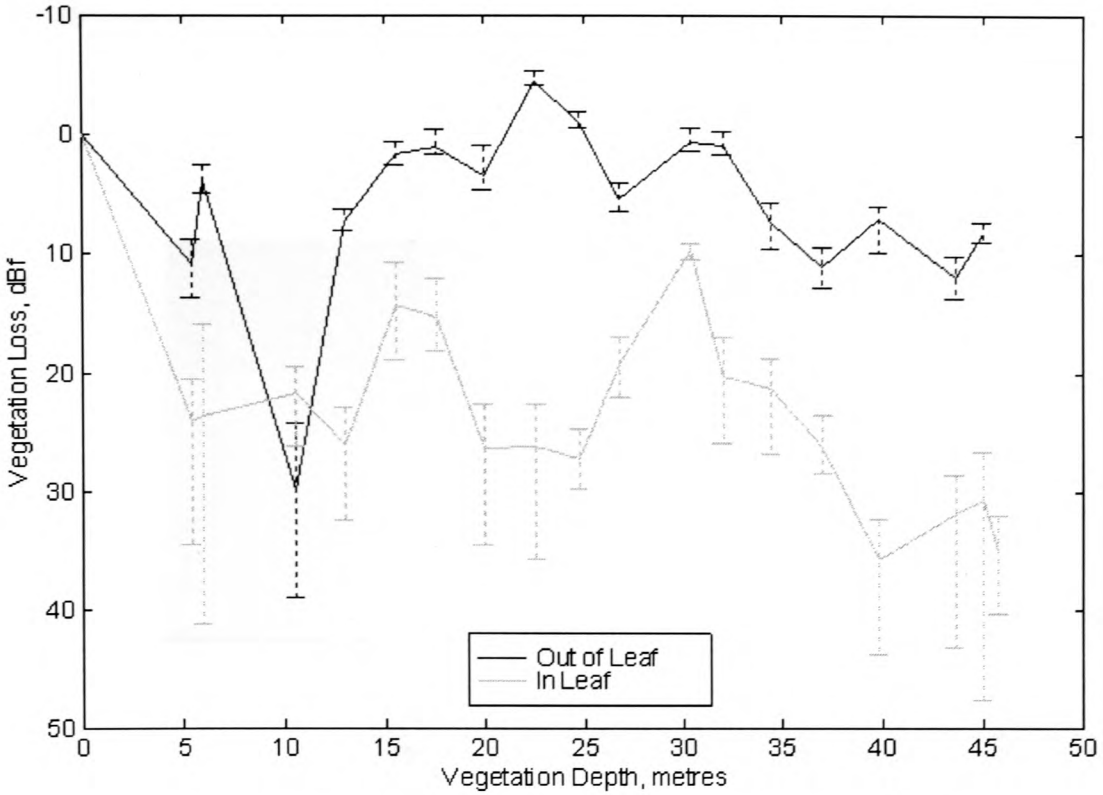

Figure 4-8 Signal Loss at The Mound, Receiver at 3m (Frequency of 11.2 GHz).

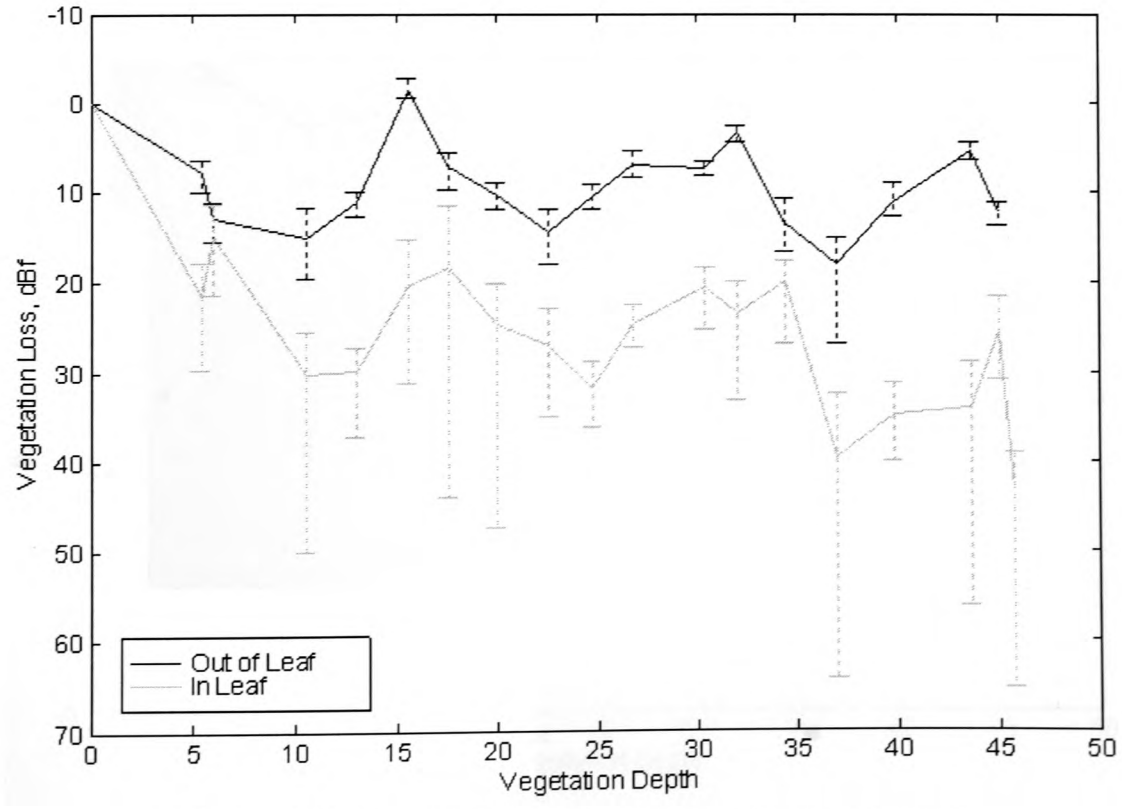

Figure 4-9 Signal Loss at The Mound, Receiver at 3m (Frequency of 20 GHz).

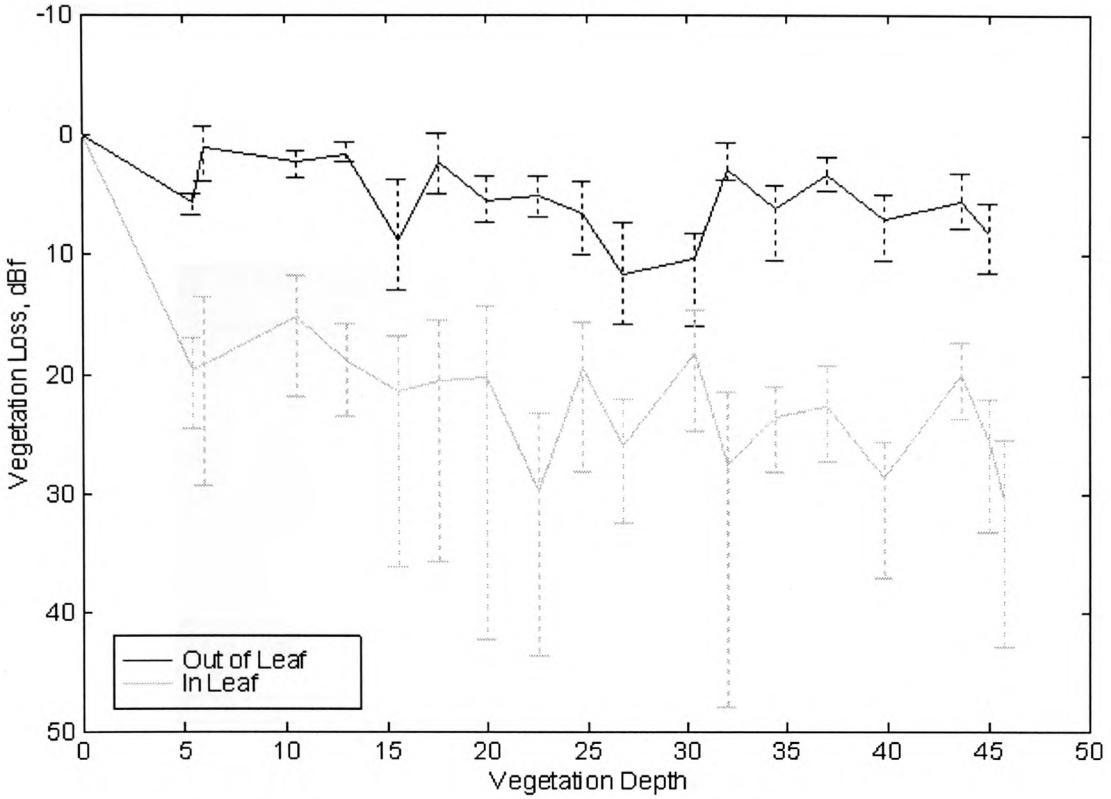

Figure 4-10 Signal Loss at The Mound, Receiver at 5 metres (Frequency of 11.2 GHz).

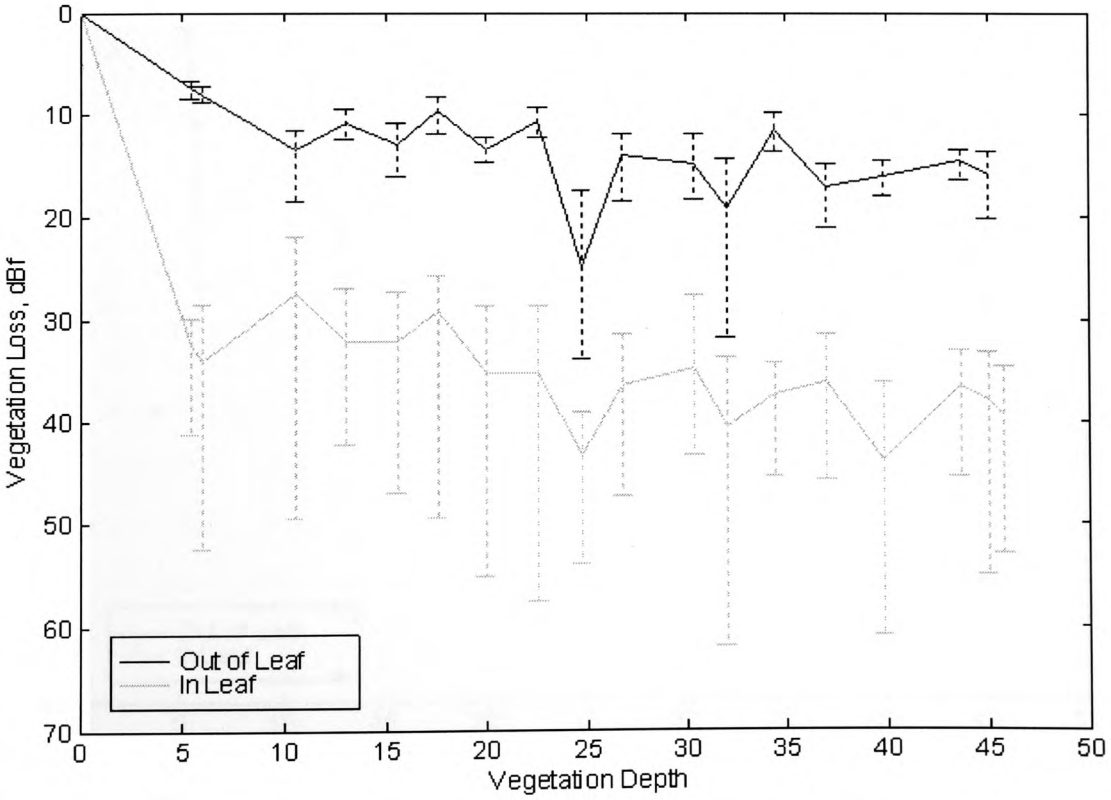

Figure 4-11 Signal Loss at The Mound, Receiver at 5 metres (Frequency of 20 GHz).

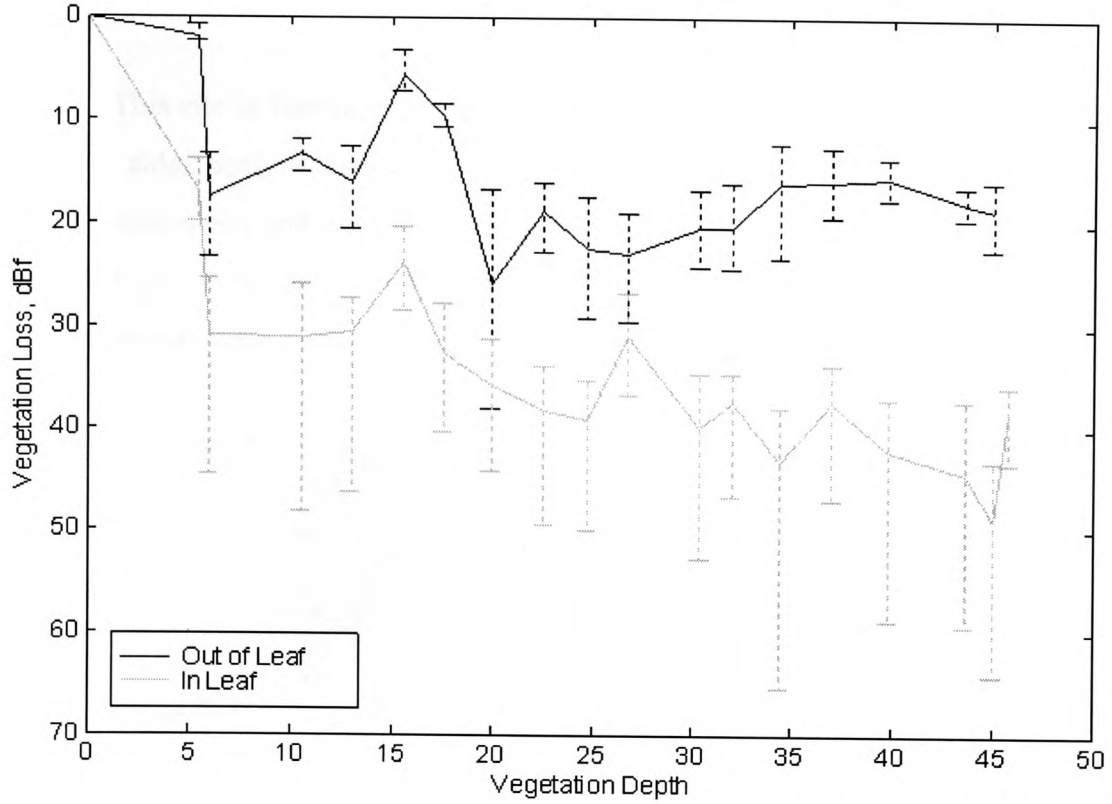

Figure 4-12 Signal Loss at The Mound, Receiver at 7 metres (Frequency of 11.2 GHz).

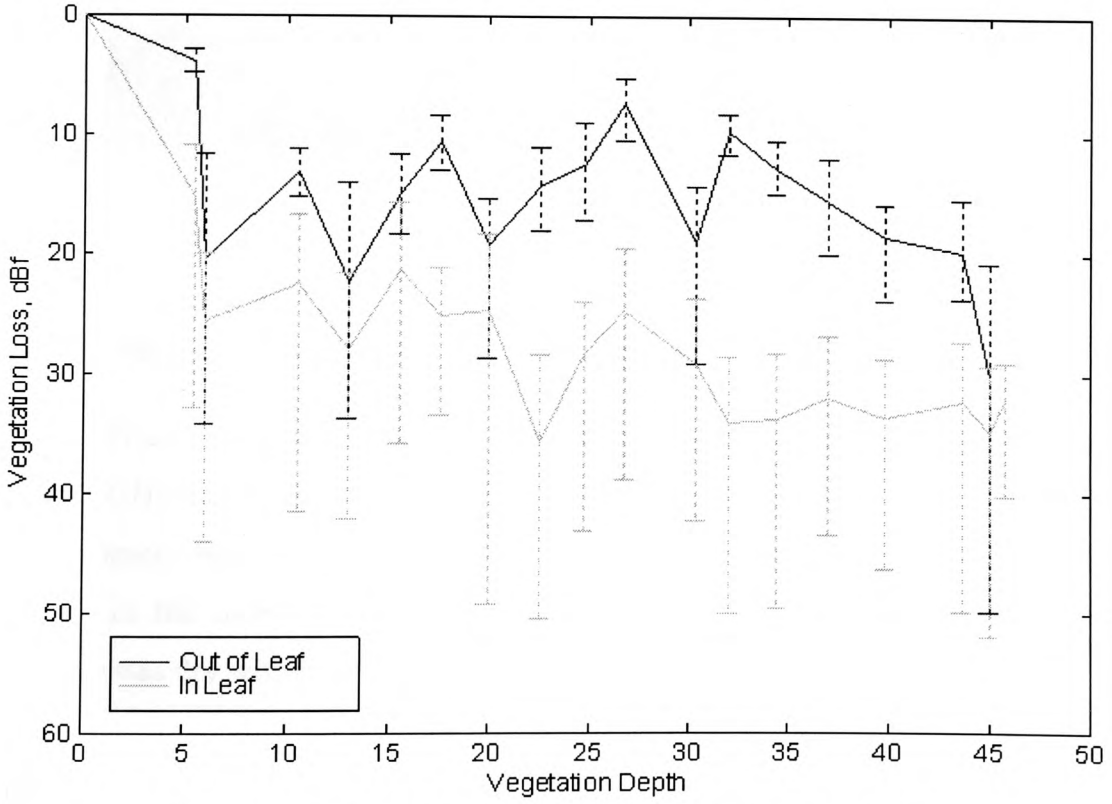

Figure 4-13 Signal Loss at The Mound, Receiver at 7m (Frequency of 20 GHz).

4.2.3 The Ridgeway

This site in Newport, Wales, has a line of Sycamore trees planted along the top of a ridge aptly named as the Ridgeway. Fourteen of the trees were used in the measurements and are approximately 9 metres in height. The site is shown in Figure 4-14. This figure shows the first five trees out of the fourteen upon which measurements were performed.

Figure 4-14 The Ridgeway.

4.2.3.1 Measurement Method and Site Geometry

The attenuation measurements at the Ridgeway site were only carried out at 11.2 GHz due to the 20 GHz system being unavailable. As with the previous experiments, they were carried out when the trees were both with and without foliage in the months of October and December of 1995 respectively. The weather was dry with a slight wind on the day of both experiments.

The transmitter was set up for vertically polarised transmission and a 10 dBi standard gain horn antenna was utilised to illuminate the width of foliage at a distance of 6.5 metres from the trunk of the first tree. This put the first and

successive trees into the far field of the transmitter, with only the width of the trees' vegetation being illuminated by the main beam of the transmit antenna. The transmitter was mounted atop a free standing pneumatically extendible mast at a height of 6 metres and was positioned at the same angle as the slope of the road, approximately 4°, so that the transmitter was angled parallel to the road.

The receiver utilised an antenna of 20 dBi gain and was mounted at the same height on top of a mast similar to that used for the transmitter. The receiver was positioned 7 metres from the trunk of each successive tree in the line in a similar manner to that used at the Fermi Avenue site (see Figure 4-3). At each receiver position, the antenna was aligned to the centre of the foliage which was in line with the transmitter. At each receiver position sixty samples were recorded and stored in a data file as in the previous experiments.

4.2.3.2 The Ridgeway Measurement Results

The measured data were normalised to a signal level that would be received with no vegetation in the path. No calibration measurement was performed at this site due to a limitation of space between the transmitter and the start of the foliage. Instead, the expected received signal with no vegetation in the path was calculated (Equation 4.4) from knowledge of gain and loss factors associated with the 11.2 GHz measurement system.

$$P_{Rx} = P_{Tx} + G_{Tx} + G_{Rx} + G_{LNB} - L_{fs} - L_{Cable} \text{ dBm} \qquad 4.4$$

where P_{Rx} is the received power in dBm, P_{Tx} is the transmitted power in dBm, G_{Tx} is the gain of the transmit antenna, G_{Rx} is the gain of the receive antenna, L_{Cable} is the cable loss.

For example at a distance of 40 meters

$P_{Tx} = 10$ dBm

$G_{Tx} = 10$ dBi

$G_{Rx} = 20$ dBi

G_{LNB} = 50 dB

L_{fs} @ 40 m = 85.5 dB

L_{Cable} = 2.5 dB

$\therefore$ the expected received signal strength, P_{Rx} = 2 dBm

The measured data for each depth of vegetation can then be normalised to a corresponding P_{Rx} value as calculated in Equation 4.3, thus providing the amount of loss experienced due to the vegetation in the path. The normalised data for the in- and out-of-leaf cases are shown in Figure 4-15 with the vertical lines describing the variability seen at each measurement position.

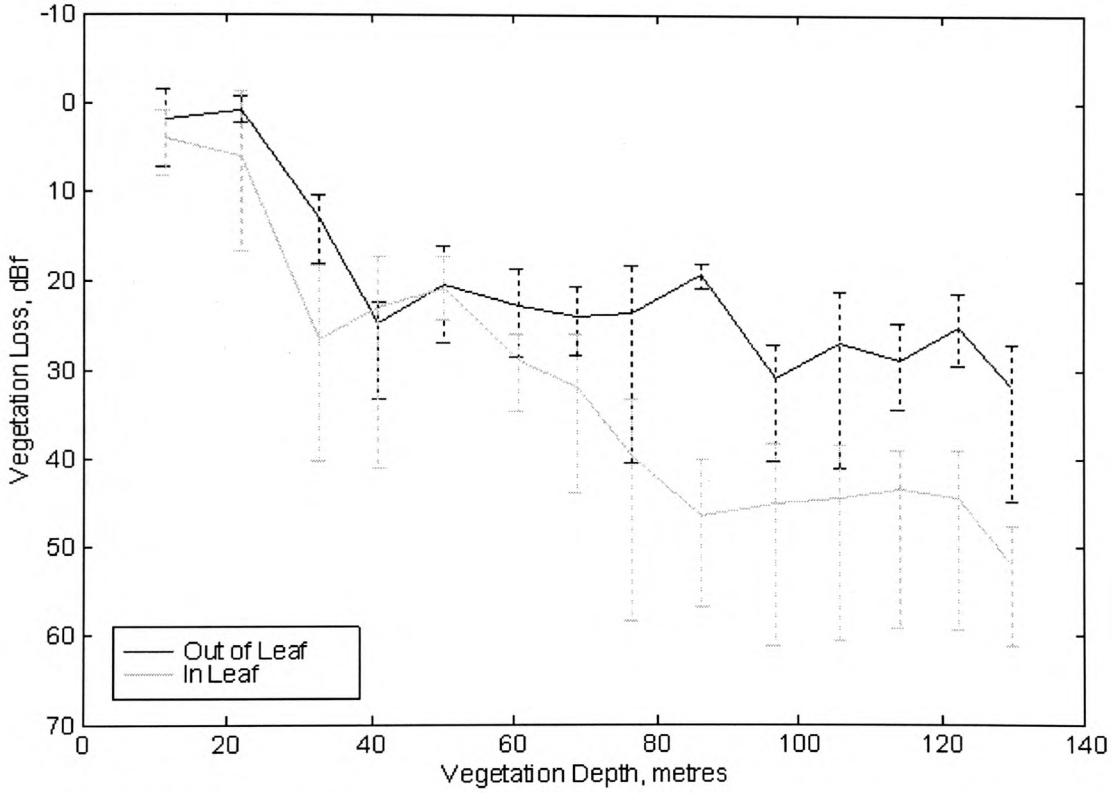

Figure 4-15 Signal Loss at The Ridgeway (Frequency of 11.2 GHz).

4.3 Analysis of Attenuation Measurements

In all the figures showing the loss due to vegetation versus the vegetation depth, it can be seen that in leaf vegetation causes greater attenuation of the propagating signal. This is due to the presence of leaves which, for the case of Lime, Sycamore and Horse Chestnut are all greater in size relative to the

wavelength corresponding to the frequencies used. The wavelengths are 2.67 centimetres at 11.2 GHz and 1.5 centimetres at 20 GHz.

Generally, it can also be seen in these figures that there is an initial high attenuation rate at small depths of vegetation, followed by a smaller attenuation rate as the vegetation depth increases. This is in line with previously obtained results [Al-Nuaimi, 1993]. The initial high attenuation rate is where mainly the coherent propagating wave component is being received. As the vegetation depth increases the received wave changes from being predominately consisting of a coherent wave component to one where the incoherent component becomes dominant. The incoherent wave being generated as the propagating coherent wave becomes scattered by the elements that make up the trees structure. All scatterers are larger in dimension than the wavelength of the propagating wave and as such cause a significant forward scatter of the signal [Ulaby, 1988].

During the experiments when the data acquisition software was set up to acquire sixty samples, the standard deviation corresponding to that depth of vegetation was calculated and stored. The mean of these standard deviations was found for each measurement and are presented in Table 4-1 for Fermi Avenue, Table 4-2 for the Mound and Table 4-3 for the Ridgeway sites.

Table 4-1 Average Standard Deviation for Fermi Avenue.

Fermi Avenue			
11.2 GHz		20 GHz	
No Leaves, dB	In Leaf, dB	No Leaves, dB	In Leaf, dB
1.9735	2.1155	3.0518	3.27

Table 4-2 Average Standard Deviation for the Mound.

	The Mound			
	11.2 GHz		20 GHz	
	No Leaves, dB	In Leaf, dB	No Leaves, dB	In leaf, dB
3 metres	0.6959	2.0026	0.8871	3.0584
5 metres	1.1171	2.7526	1.2065	3.7932
7 metres	1.7788	2.9779	2.1682	3.9047

Table 4-3 Average Standard Deviation for Ridgeway.

Ridgeway, 11.2 GHz	
No Leaves, dB	In Leaf, dB
2.5707	4.2271

From the values in these tables it can readily be seen that the in-leaf data shows a higher variation in the measured data. This of course being due to the presence of leaves which are scatterers. Even if there was exactly the same amount of movement of the vegetation body when in and out-of-leaf, the in leaf experiments would show a greater fluctuation in the measured data and can be attributed to the increased number of scatterers (leaves) and all scatterers collectively changing their relative position due to external influences such as wind movement.

The Mound variability was found to increase with the height of the receivers at both frequencies and when the vegetation was with and without leaves. This is expected as the scatterers are smaller in dimension, namely branches, and are more susceptible to external influences. Also the lack in homogeneity of the medium increases the variability.

It can also be seen from the tables that there is a greater variation in the 20 GHz measurement data than the 11.2 GHz measurements. This is expected as the 20 GHz signal is of a smaller wavelength compared to the 11.2 GHz signal. Therefore the 20 GHz signal will see more scatterers within its propagation path. This in turn means that the smaller elements of the tree that did not have an affect on the 11.2 GHz signal will have an affect on the 20 GHz signal as it propagates

through the vegetation. Due to this increased effect the vegetation has on the 20 GHz signal as it propagates, the more fluctuation will be seen in the received signal level.

To enable a comparison between the attenuation measured at 11.2 GHz and 20 GHz three tables are presented, namely Table 4-4 for Fermi Avenue, Table 4-5 and Table 4-6 for the in-leaf and out-of-leaf Mound data respectively. All three tables present a sample of the attenuation due to vegetation with Table 4-5 and Table 4-6 presenting a sample for the three receive antenna heights of 3m, 5m and 7m used at the Mound. It can be seen from the normalised received signal strength (loss due to vegetation) shown in these tables that the 20 GHz signal as well as having the greater variation is also subjected to a greater amount of attenuation per metre of vegetation compared to the 11.2 GHz data. This is due to the 20 GHz wavelength being smaller than the 11.2 GHz wavelength and hence sees more components of the trees along its propagation path. This means that the 20 GHz signal is subjected to a greater amount of attenuation as demonstrated by the tables. This can also be seen by comparing the attenuation curves presented in the figures.

Table 4-4 A Sample of the Normalised Measurement Values for Fermi Avenue.

	In-Leaf		Out-of-Leaf	
Vegetation Depth (m)	11.2 GHz (dBf)	20 GHz (dBf)	11.2 GHz (dBf)	20 GHz (dBf)
20.4	-40.04	-52.40	-18.76	-18.71
42.9	-50.78	-54.35	-30.43	-22.45
58	-45.85	-51.47	-30.29	-32.86

Table 4-5 A Sample of the Normalised Measurement Values for the Mound (In-Leaf).

	In-Leaf					
	3m		5m		7m	
Vegetation Depth (m)	11.2 GHz	20 GHz	11.2 GHz	20 GHz	11.2 GHz	20 GHz
10.6	-21.71	-30.46	-15.25	-27.41	-31.06	-22.55
24.8	-27.32	-32.05	-19.58	-43.38	-39.19	-28.35
39.8	-35.63	-35.05	-28.61	-43.74	-42.12	-33.71

Table 4-6 A Sample of the Normalised Measurement Values for the Mound (Out-of-Leaf).

	Out-of-Leaf					
	3m		5m		7m	
Vegetation Depth (m)	11.2 GHz	20 GHz	11.2 GHz	20 GHz	11.2 GHz	20 GHz
10.6	-29.94	-2.25	-2.25	-13.37	-13.25	-13.10
24.8	1.10	-6.56	-6.56	-24.75	-22.51	-12.46
39.8	-6.88	-6.94	-6.94	-16.16	-15.49	-18.52

4.4 Single Tree Measurements

The purpose of the single tree measurements was to attempt to characterise the effects of singular vegetation entities on the propagating electromagnetic wave. This examination has taken the form of a number of different types of experiments which will be explained in the following sections.

Single trees are often seen at the side of road and in the middle of fields where they can be present in the path of a microwave link. Trees cause varying amounts of attenuation, scatter and depolarisation of the propagating signal. Measurements were performed on single trees in a park but, owing to external influences, the usefulness of the data was limited. Because of this, all single tree measurements have been performed in the anechoic chamber. Single tree measurements are also useful in investigating the relationship between the physical and radiowave propagation characteristics of the vegetation medium.

4.4.1 360° Attenuation Measurements

These experiments consisted of placing a tree on a turntable and rotating the trees by 360° in 0.1° increments whilst measuring the received signal strength [Ulaby, et al, 1988]. The transmitter and receiver were placed at equal heights and the geometry shown in Figure 4-16 was used.

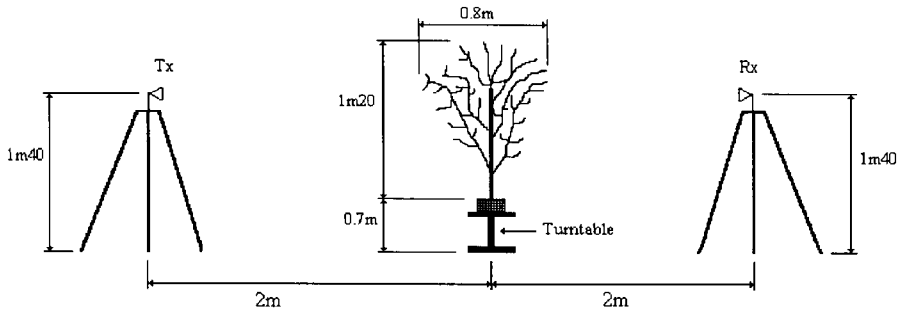

Figure 4-16 360° Attenuation Measurement Geometry.

The distance between the transmitter and start of the foliage places the tree in the far field region of the 20 dBi transmit antenna using the Rayleigh distance far field criterion, $2D^2/\lambda$ [Jull, 1981]. With the transmitter placed at the distance indicated in Figure 4-16, the transmit antenna illuminated an area of 33.5cm diameter. This distance as can be seen is less than the width of the tree. The receiver utilised the same gain antenna as the transmitter and both antennas were vertically polarised. The first of these experiments were carried out on Ficus plants shown in Figure 4-17, which has leaves that are on average 65 mm long and 25 mm across.

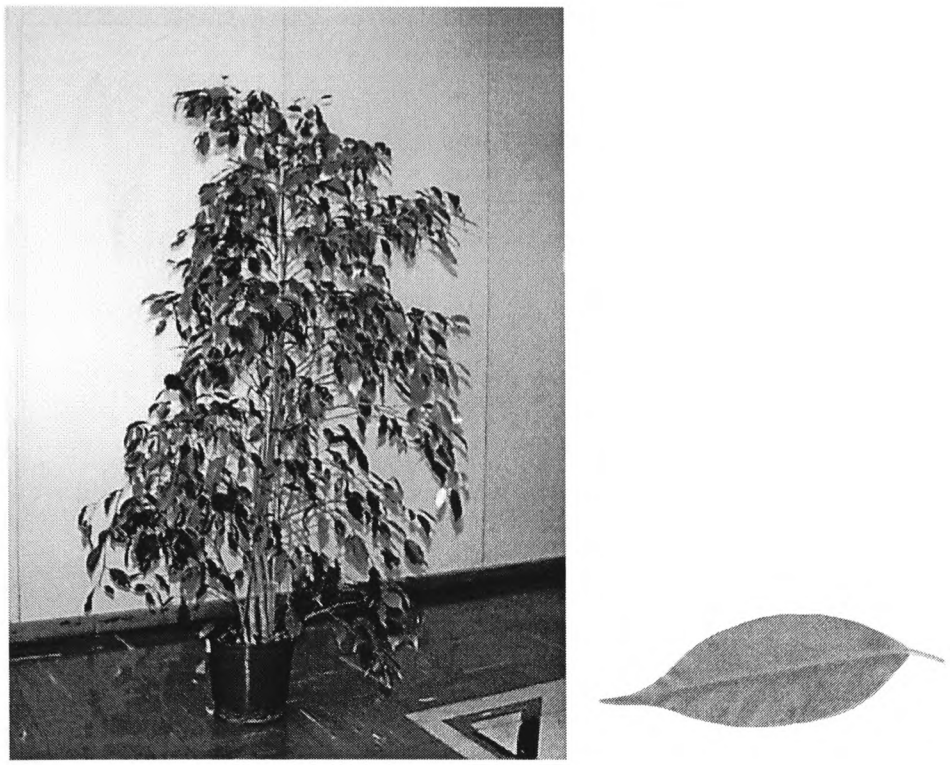

Figure 4-17 Ficus Plant and a Ficus Leaf.

The measured signal strength with the tree in the path was normalised with respect to the measured freespace signal level. This normalised received signal strength was plotted against the rotation angle of the tree (Figure 4-18) and as can be seen, there are large nulls in this data. The reason for these deep nulls, at this stage, was unclear, but could be occurring for a number of reasons such as; a multipath environment occurring within the vegetation body leading in turn to destructive interference, depolarisation of the propagating wave or a combination of the two. These nulls were seen to be similar to those seen in the sixty samples taken when performing the outdoor experiments. These nulls were subjected to investigation to provide further information on the propagation and scatter of the propagating signal and to this end, the following set of experiments were performed.

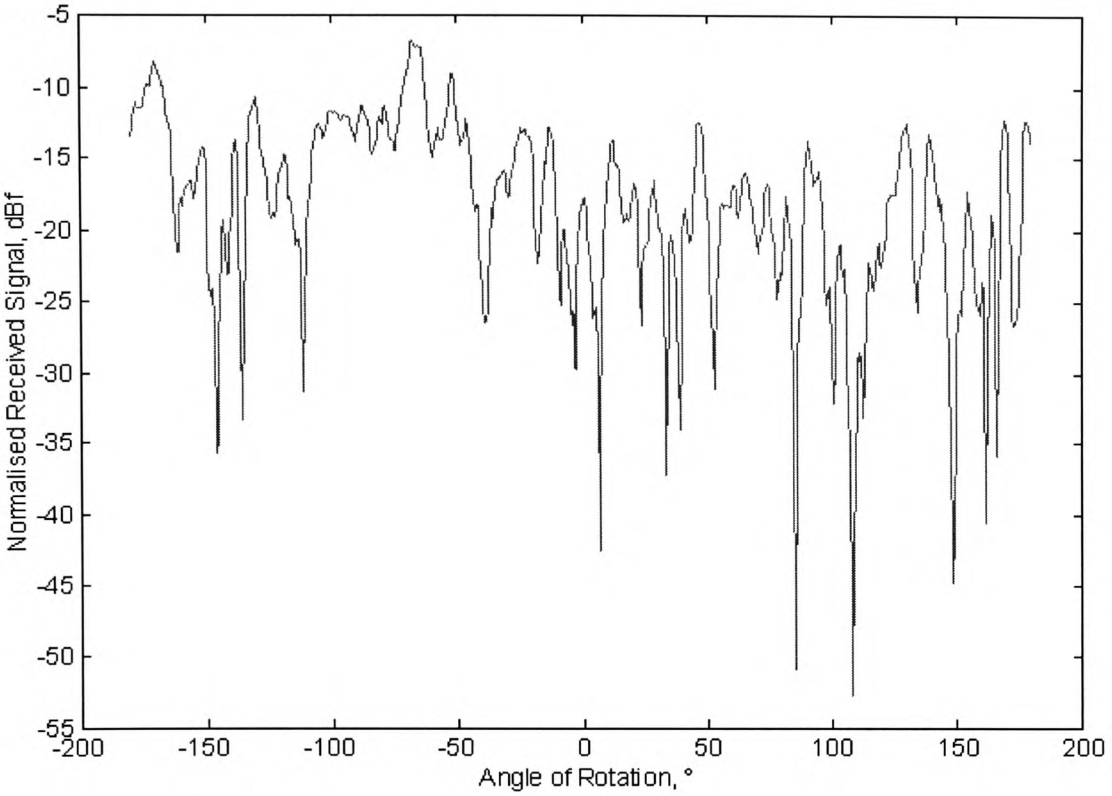

Figure 4-18 Ficus Plant Angular Attenuation Pattern.

4.4.2 Co- and Cross-Polarisation Measurements

For these experiments the same geometry as for the 360° attenuation measurements was utilised, with the only changes being made to the receiver. The tree was first rotated with the receiver vertically polarised to measure the co-polar component, with the receiver then being rotated through 90°, making it horizontally polarised and the tree was rotated again and the cross-polar component was measured.

If the nulls were as a result of depolarisation, an increase above the average cross-polar value would be expected when the co-polar component exhibited a null. What was actually seen was that an increase in the cross-polar component did occur, though this did not exactly coincide with the null in the co-polar component. This possibly being due to the physical rotation of the receive antenna, as upon moving the antenna, it would not be seeing exactly the same

section of foliage. Also with the rotation of the tree the branches and leaves were probably not in the same position for both rotations through 360°.

To overcome this problem, a lens horn antenna of 19 dBi gain with a beamwidth of 23° and a circular waveguide was acquired. The lens horn antenna was coupled to an orthogonal mode transducer (OMT) - the OMT has a circular waveguide inlet and two orthogonal rectangular waveguide outlets. It thereby allowed the co and cross-polar components to be obtained without moving the antenna coupled to the inlet of the OMT. To permit each polarisation to be measured with the single available receiver system, an electronically controlled 2 channel waveguide switch was employed. The switch was controlled by the computer so that the experiment process could be kept fully automated and the measurement time to a reasonable duration. A block diagram of the receiver configuration is shown in Figure 4-19. The receiver system has a cross-polar discrimination equal to or greater than 35dB.

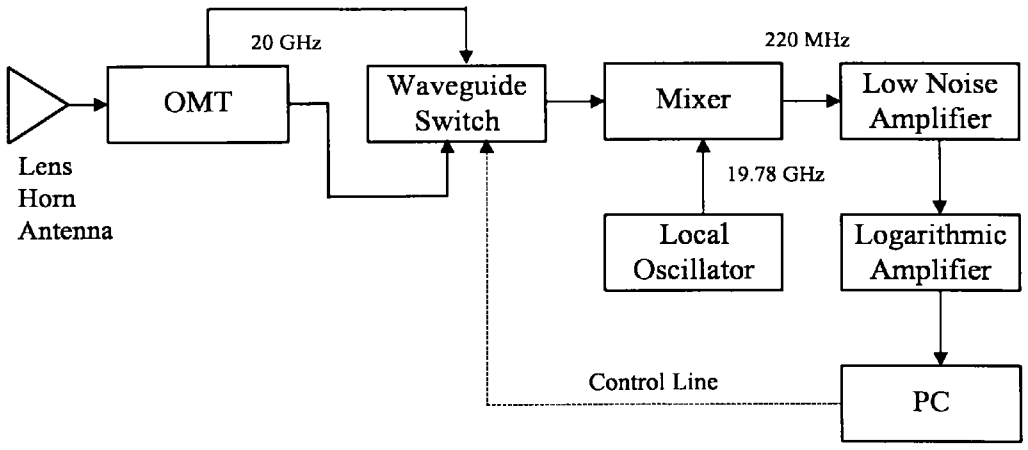

Figure 4-19 Block Diagram of Receiver Configuration.

Using this system measurements were carried out using the set-up of Figure 4-16. The Ficus tree was rotated 360° in 0.5° increments. At each increment of the tree the received co- and cross-polar signal strengths were measured in turn by remotely changing the position of the rotor of the waveguide switch.

The result of this experiment is shown in Figure 4-20 after the measured data had been normalised with respect to the freespace level. Here it can be seen that there is an above average cross-polar value at the angle of rotation that corresponds to the large nulls in the co-polar data. This information points to the received signal being predominately polarised in neither the vertical or horizontal linear planes.

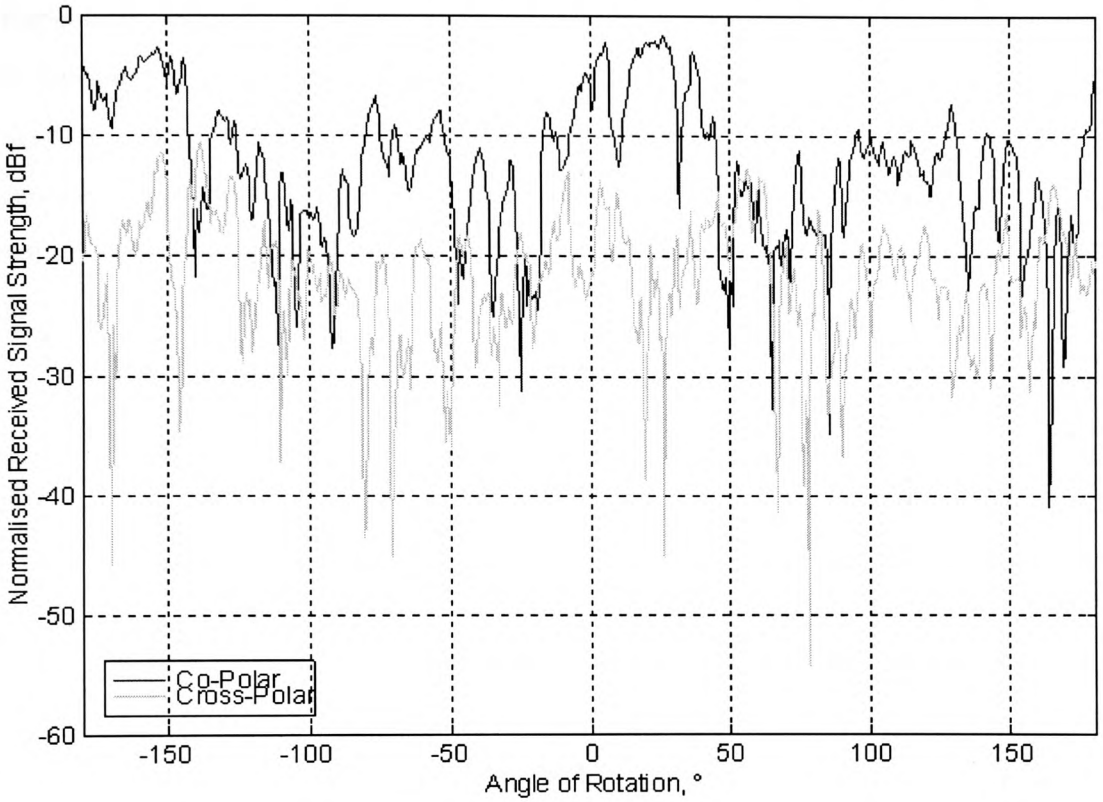

Figure 4-20 V-V and V-H Polarisation.

4.5 Interim Conclusion

The measured data from the out-of-doors experiments has been presented and the application of models to this data will be presented in the next chapter. It has been shown that the in-leaf vegetation gives greater attenuation compared to that from the out-of-leaf case. The attenuation curves can be broken down into two parts - the initial steeper slope of the overall curve, where there is a high attenuation rate, being where the coherent wave is the principal wave being received. The second part of the curve having a much reduced attenuation rate, where the incoherent wave caused mainly by vegetation scattering, represents the dominant portion of the received wave.

Measurements on single trees have been performed and the evolution of these experiments has been outlined. The information gathered from the experiments with the lens horn antenna and the OMT show that the received wave is depolarised significantly being of neither vertical or horizontal linear polarisation. Especially when the cross-polar component is compared to the co-polar component at the angles where there are large nulls in the co-polar data. It can be seen that depolarisation of the incoming wave by elements of the vegetation medium has significant effect on the occurrence of deep nulls in the propagating signal. This information has led to further consideration of the depolarisation due to vegetation which is presented in Chapter 6.

5. Vegetation Attenuation Modelling

5.1 Introduction

In this chapter a number of prediction models previously outlined in Chapter 2 are used to produce predictions for attenuation as a function of vegetation depth. The agreement between predicted and measured data are assessed using root mean square (RMS) error values which are given for the various models presented. This is further discussed in the comparative analysis of the performance of the models in providing an accurate prediction of the attenuation of signals by vegetation at microwave frequencies.

5.2 Models

The prediction models whose results have been compared to the measured data are discussed in the following sections and are referred to as the non-zero gradient model (NZG), the International Telecommunication Union-Radio sector model (ITU-R) and two further models which are derivatives of the ITU-R model. The derivatives of the ITU-R model will be referred to as the modified ITU-R model (MITU-R) [Al-Nuaimi and Hammoudeh, 1993] and the fitted ITU-R model (FITU-R).

5.2.1 International Telecommunications Union-Radio Sector Model (ITU-R)

The ITU-R model [CCIR, 1986] which was developed from measurements performed mainly within the U.H.F frequency band [Weissberger, 1981] has previously been discussed in Chapter 2. This model uses the following equation to predicted the attenuation created by a volume of in-leaf trees.

$$L \approx 0.2f^{0.3}d^{0.6} \quad dB \qquad 5.1$$

where : f is the frequency in MHz and

d is the depth of vegetation in metres.

At the frequencies used in this investigation, this becomes:

$$L \approx 3.28d^{0.6} \text{ dB} \qquad \text{for 11.2 GHz} \qquad 5.2$$

$$L \approx 3.9d^{0.6} \text{ dB} \qquad \text{for 20 GHz} \qquad 5.3$$

This model has been applied to all measured data acquired at the sites discussed in the previous chapter. The agreement between the predicted values and the measured ones can be seen in Figure 5-2 to Figure 5-5 for the Fermi Avenue measurement site, Figure 5-6 to Figure 5-17 for the Mound measurement site and Figure 5-18 to Figure 5-19 for the Ridgeway measurement site. This agreement is assessed by the RMS error, Equation 5.4, which describes the accuracy of the fit between measured and predicted values.

The RMS error, E_{RMS} is defined as:

$$E_{RMS} = \sqrt{\frac{\sum_{i=1}^{N} (E_i)^2}{N}} \text{ dB} \qquad 5.4$$

where: N is the number of measurements

E_i is the error representing the difference between the predicted and the measured value at the i^{th} measurement point.

Table 5-1 presents the relative fit of the ITU-R model to each of the measurement sites as well as to all of the in-leaf and all of the out-of-leaf measurement data acquired at the two frequencies of 11.2 GHz and 20 GHz.

Table 5-1 Relative Fit of ITU-R Model.

	Measurement Site				
	Fermi Avenue	The Mound	The Ridgeway	All in-leaf Data	All out-of-leaf Data
RMS Error (dB)	12.70	20.73	16.85	9.85	15.36

5.2.1.1 The Modified ITU-R Model (MITU-R)

The MITU-R model [Al-Nuaimi and Hammoudeh, 1993] is as the title suggests a modified version of the ITU-R model introduced above. The MITU-R model is expressed in the form:

$$L = k'd^n \quad dB \qquad 5.5$$

where: L is the attenuation caused by the vegetation medium,
d is the depth of vegetation in metres
and k' is a constant.

The variables k' and n were optimised to obtain a best fit to the measured data using the method of least square fit. The measured data being acquired at a frequency of 11.2 GHz and from a site that consisted of an apple orchard in both in-leaf and out-of-leaf conditions. The orchard had an overall depth of approximately 190 metres For the in-leaf case the parameters are shown in Equation 5.6. Whilst for the out-of-leaf data it was found that the attenuation curve measured could not be represented by a single curve of the form $L=k'd^n$, the curve could be more accurately represented by two curves as depicted by Equation 5.7.

In-leaf

$$L = 11.93d^{0.398} \quad dB \qquad 5.6$$

Out-of-leaf

$$\begin{aligned} L &= 1.75d \quad dB \quad d \le 31\,m \\ L &= 28.1d^{0.17} \quad dB \quad d > 31\,m \end{aligned} \qquad 5.7$$

This model has been compared to the measured data that was obtained at a frequency of 11.2 GHz. The agreement between measured and predicted results can be seen in Figure 5-2 and Figure 5-4 for Fermi Avenue, in every even numbered figure from Figure 5-6 to Figure 5-16 for the Mound and in Figure 5-18 and Figure 5-19 for the Ridgeway site. The models relative fit to the measured data is shown in Table 5-2. The table demonstrates the fit of the model to each measurement site which includes the in and out-of-leaf measurements. Also presented is the fit of the model to just all of the out-of-leaf measurement data and separately to all of the in-leaf data.

Table 5-2 Relative Fit of MITU-R Model.

	Measurement Site				
	Fermi Avenue	The Mound	The Ridgeway	All in-leaf Data	All out-of-leaf Data
RMS Error (dB)	12.23	36.43	32.43	19.37	29.66

5.2.1.2 The Fitted ITU-R Model (FITU-R)

The FITU-R model is also an adaptation of the ITU-R model. In this case, the model has been optimised to the data measured (presented in Chapter 4) by adjusting the three numerical values of Equation 5.1. The main benefit of using this formula is that it is possible to obtain a useful prediction of the attenuation without having to define all of the path geometrical parameters for a given volume of vegetation.

Parameters for this model were found which would be relevant for each foliation state of the vegetation body and it is these formulae which are shown in Equation 5.8 and Equation 5.9 respectively.

Foliated state:

$$L = 0.39f^{0.38}d^{0.25} \text{ dB} \qquad 5.8$$

Defoliated state:

$$L = 0.37f^{0.18}d^{0.59} \text{ dB} \qquad 5.9$$

where: L is the signal loss due to the vegetation in dB,
f is the frequency in MHz,
d is the depth of vegetation in metres.

The parameters were obtained by performing optimisation of the formula to all of the in-leaf data acquired at both frequencies of 11.2 GHz and 20 GHz using the least squared error fit approach. The same process was exercised for finding the parameters of the formula for the defoliated case where the optimisation was performed on all of the out-of-leaf data.

Table 5-3 shows the relative fits of Equation 5.8 and Equation 5.9 when applied to the data acquired from the measurements, both in and out-of-leaf. Also shown is the fit of Equation 5.8 to all of the in-leaf data and the fit of Equation 5.9 to all of the out-of-leaf data. The agreement between the measured and predicted values using the FITU-R model can be seen in Figure 5-2 to Figure 5-19 for each of the measurement sites.

Table 5-3 Relative Fit of FITU-R Model.

	Measurement Site				
	Fermi Avenue	The Mound	The Ridgeway	All in-leaf Data	All out-of-leaf Data
RMS Error (dB)	10.85	16.17	9.38	9.42	8.98

5.2.2 The Non-Zero Gradient Model (NZG)

The NZG model was developed at Rutherford Appleton Laboratory (RAL) [Seville and Craig, 1995], [Stephens and Al-Nuaimi, 1995] and postulates a dual slope function that seeks to follow the dual gradient slope of the attenuation curve that previous vegetation modelling and measurements have revealed [Johnson and Schwering, 1985], [Al-Nuaimi and Hammoudeh, 1993]. The initial slope

describes the performance mainly due to the attenuation of the coherent propagating component, whereas the second slope with a much reduced gradient describes performance due to the much weaker, scatter, incoherent component. The NZG model was formulated to take account of both of these components and to yield a good fit with measured results. It takes the form of Equation 2.6.

This model has been fitted to all of the out-of-leaf measurement data acquired at both 11.2 GHz and 20 GHz. It has also been fitted to all of the in-leaf data acquired at both of the frequencies. The values for the three parameters of the NZG model are shown in Table 5-4.

Table 5-4 NZG Model Parameters.

Parameter	In-leaf	Out-of-leaf
R_∞ (dB/m)	0.33	0.24
R_0 (dB/m)	19.82	6.25
k (dB)	37.87	6.45

Shown in Table 5-5 is the relative fit of the NZG model with the fitted parameters to each of the individual measurement sites. Also tabulated are the relative fits to all of the in-leaf data and all of the out-of-leaf data.

Table 5-5 Relative Fit of NZG Model.

	Measurement Site				
	Fermi Avenue	The Mound	The Ridgeway	All in-leaf Data	All out-of-leaf Data
RMS Error (dB)	13.56	15.28	9.81	16.31	12.74

Agreement between predicted values using the NZG model and the measured data can be seen in Figure 5-2 to Figure 5-19 for each of the measurement locations.

5.2.3 The Dual Gradient Model (DG)

The DG model is a development of the NZG model, but differs in that it takes into account parameters of the measurement site geometry. For instance, the model explicitly uses the extent of illumination of the vegetation by the transmit and receive antennas, W, as illustrated in Figure 5-1. W describes the vegetation width being illuminated. Another parameter considered is the frequency of the wave transmitted which unlike the NZG model is explicitly included in the attenuation function.

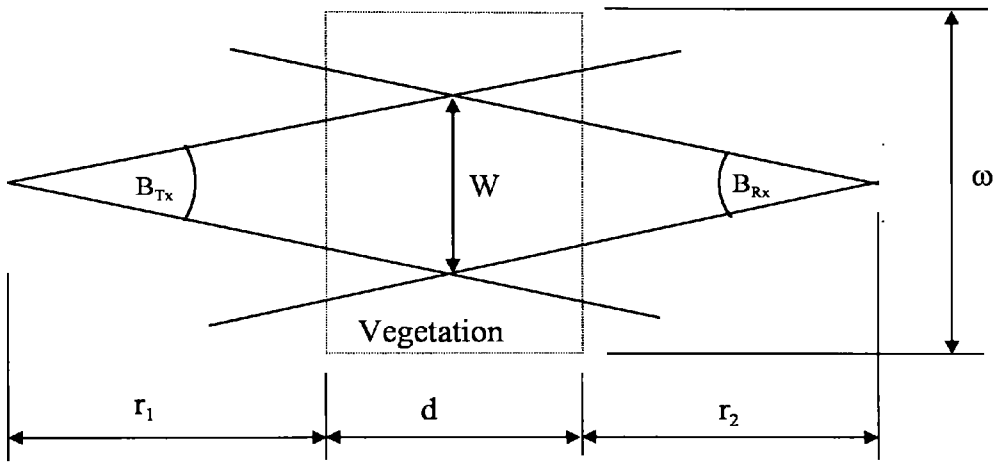

Figure 5-1 Vegetation Measurement Geometry.

The DG model takes the form of:

$$L = \frac{R_\infty}{f^a W^b} d + \frac{k}{W^c}\left(1 - \exp\left(-\frac{(R_0 - R_\infty)W^c}{k} d\right)\right) \qquad 5.10$$

where: a, b, c, k, R_0, R_∞ are constants with values shown in Table 5-6

f is the frequency in GHz and

$$W = \min\begin{pmatrix} \frac{(r_1 + d + r_2)\tan(B_{Tx})\tan(B_{Rx})}{\tan(B_{Tx}) + \tan(B_{Rx})} \\ (r_1 + d)\tan(B_{Tx}) \\ (r_2 + d)\tan(B_{Rx}) \\ \omega \end{pmatrix} \qquad 5.11$$

The variables used to determine the value of the illumination width, W, are related to the geometry of the measurement site as can be seen in Figure 5-1, where B_{Tx} and B_{Rx} are the beamwidths of the transmit and receive antennas respectively. Distances between the transmitter and the vegetation interface, and the receiver and the vegetation interface are represented by r_1 and r_2 respectively.

The parameters for the DG model shown in Table 5-6 were obtained by performing fitting of the model to a database of available experimentally measured data sets. This database includes, amongst others, the data from measurements obtained in this investigation at both 11.2 GHz and 20 GHz from the Fermi and Mound experiment sites, as well as measured data acquired at 38 GHz by researchers at RAL at the same two sites. Other data included was measurement data reported in literature [Schwering et al, 1988] performed at 9.6 GHz, 28.8 GHz and 57.6 GHz At the time of writing this model was not fully tested. However the model has been used to provide predicted results that are shown against measurements in Figure 5-20 and Figure 5-21. The application of this model to the two sites indicated in these two figures has resulted in poor agreement.

Table 5-6 Constants for DG Model.

Parameters	In-leaf	Out-of-leaf
a	0.7	0.64
b	0.81	0.43
c	0.37	0.97
k	68.8	114.7
R_0	16.7	6.59
R_∞	8.77	3.89

5.3 Application of Models to Measurement Data

The ITU-R, MITU-R, FITU-R and the NZG models have been applied to the measurement data. The MITU-R model has only been applied to the data

acquired at a frequency of 11.2 GHz, as this is the only frequency where the model is strictly applicable.

Graphs are given to present predicted results from the above models to show their agreement with the measurement data. This has been done for each of the measurement sites, at the frequencies used in the measurements and also each state of foliation. The vertical lines in all of these figures are included to show the range of variability over which each measurement has varied. This range was determined by noting the maximum and minimum value measured at each depth of vegetation using the system described in Chapter 3.

Figure 5-2 to Figure 5-5 show results for the Fermi Avenue measurement site. Figure 5-2 and Figure 5-3 display the in-leaf measurements at 11.2 GHz and 20 GHz respectively, whereas Figure 5-4 and Figure 5-5 represent results for the defoliated state of the vegetation again at 11.2 GHz and 20 GHz.

The figures relating to the Mound site are presented in Figure 5-6 to Figure 5-17. The twelve figures can be divided into three sets of four figures, Figure 5-6 to Figure 5-9, Figure 5-10 to Figure 5-13 and Figure 5-14 to Figure 5-17. Where each of these three sets corresponds to a different height of the receive antenna; namely 3 m, 5 m and 7 m, used during the measurement programme. Each of the three sets can be further divided into two subsets, where each subset represents the in and out-of-leaf data and contains two figures. Of these two figures one is for the transmitted frequency of 11.2 GHz and the other for that of 20 GHz.

Figure 5-18 and Figure 5-19 give results for the Ridgeway measurement site and show the relative fit of the various models at 11.2 GHz corresponding to the foliated and defoliated states respectively.

5.3.1 Discussion of the Relative Fit of the Models to the Measured Data

The aforementioned models were applied to the measured data acquired at the various experimental sites. The RMS error, Equation 5.4 in dB, was then used to determine the comparative accuracy of the model in predicting the attenuation as a function of vegetation depth for the measurement sites at which data were acquired.

In comparing the predicted results of the four models discussed above and the corresponding measured data shown in Figure 5-2 to Figure 5-19 for the different measurement sites, the RMS error was calculated using Equation 5.4 taking account of the state of foliation and frequency. Table 5-7 shows the RMS errors for each of the models applied to each measurement site. Each model is also applied to all data from both the in-leaf and out-of-leaf states. A smaller value of the E_{RMS} indicates a closer agreement between predictions and measured data for the particular model considered.

With the MITU-R model the RMS error was only calculated against the measurement data from measurements conducted at a frequency of 11.2 GHz. This is due to the parameters of this model being found from experimental data obtained previously at 11.2 GHz on an apple orchard [Al-Nuaimi and Hammoudeh, 1993].

Table 5-7 E_{RMS} Performance of Models.

	Model			
	ITU-R	MITU-R	FITU-R	NZG
Fermi Avenue RMS Error (dB)	12.70	12.23	10.85	13.56
The Mound RMS Error (dB)	20.73	36.43	16.17	15.28
Ridgeway RMS Error (dB)	16.85	32.43	9.38	9.81
RMS Error for all in-leaf (dB)	9.85	19.37	9.42	16.31
RMS Error for all out-of-leaf (dB)	15.36	29.66	8.98	12.74

In comparing the fit of each model to all of the measurement data, it can be seen that the FITU-R model with its fitted parameters offers the best overall fit for both states of foliage. This model also provides, in all but one case, the better fit to each individual site where the RMS error is calculated from all of the data at these measurement sites including both foliage states and both frequencies. In the one case where the FITU-R model offers a slightly poorer fit than the NZG model, this is due to the NZG model offering a better fit to the measurement data collected at a height of 3m where there is mainly trunk in the radio path. At the receiver heights of 5m and 7m the FITU-R model offers a slightly better fit than the NZG model. This indicates that the FITU-R model does not provide as good a fit for the sparse vegetation that exists at a height of 3m in the copse. The fitted parameters, Equation 5.8 and Equation 5.9 provide an all round improved fit to the measured data in comparison to the other prediction models utilised. It provides an improved fit over the MITU-R model whose parameters were found from experimental data acquired at 11.2 GHz, one of the frequencies utilised in this measurement programme. The FITU-R also provides a better fit than the NZG model which models the dual attenuation slope that vegetation presents and whose parameters have also been fitted to this measurement data in the same manner as

the parameters of the FITU-R model. With reference to the figures that depict the fit of the models to the measured data, it can be seen that the FITU-R is the model which most frequently falls within the maximum and minimum values, represented by the vertical line, measured at each value of vegetation depth.

The MITU-R RMS errors are only calculated for where the model is applicable, namely at a frequency of 11.2 GHz. It generally provides the worst fit, even though the other models are applicable over both of the frequencies used in the measurements. The reason for the MITU-R model generally providing the worst fit is due to the fact that the parameters of the model were obtained from an experiment conducted on an apple orchard where the trees were planted much more closely together and more uniformly than any of the other sites, thereby resulting in a greater density of vegetation and thus a higher amount of attenuation. This is visible in the figures that depict the MITU-R model. This points generally to the need for a prediction model to take into account parameters such as the density and homogeneity of the vegetation in relation to the wavelength of the frequency of operation.

The ITU-R model offered a better fit than was expected as the parameters for this model are based on measurements that were performed at lower frequencies. The ITU-R model is not stated as being applicable when the trees are without foliage, even though the model has been applied to this state of foliation. Its prediction of the attenuation for each overall state of foliage was found to be better than the MITU-R model. If the frequency of the wave to be transmitted has a smaller wavelength then the fit of this model would be greatly affected.

The NZG model models the dual slope that vegetation tends to exhibit as can be seen in the figures presented relating to this particular model. The relative fit of this model with its fitted parameters does not provide as good a fit as the FITU-R model when compared to all of the measured data. This could be as a result of the measured data not presenting a clearly defined dual slope. Instead, the NZG

attempts to model a dual slope which in this case, does not offer the best fit to the data acquired.

The DG model which evolved from the NZG model allows the site geometry and the frequency of the wave to be transmitted to be included in the prediction of the attenuation expected from a specified body of vegetation. This model is currently under development [COST 235, 1996], but was initially developed for the purpose of providing an empirical prediction model valid for any vegetation site whose geometry can be defined by providing basic parameters such as vegetation depth, illumination width, and distances from transmit and receive terminals. The models' development was based on all measurement data available including those performed under the present investigation and excluding those measured at the Ridgeway site. The model has not been tested sufficiently and is considered to suffer from a number of shortcomings which may be summarised as follows:

1. In its current form, problems were found in that for certain site geometries, the initial slope of the dual slope attenuation curve shows a decreasing amount of attenuation instead of the expected increase. Similarly the second slope has also shown a decreasing amount of attenuation instead of an increasing amount. This is illustrated in Figure 5-20 where it can be seen that the latter part of the attenuation curve exhibits a negative gradient and in Figure 5-21 where the initial part of the dual slope attenuation curve begins at a lower value than the one at which it ends. These anomalies may be corrected by entering incorrect parameter values for the site geometry. This points to there being a problem with how the site geometry is specified within the model.
2. Curiously, the frequency dependence is seen to be somewhat contrary to those expressed by the ITU-R models. Equation 5.6 and Table 5-6 suggest the loss to be a function of $1/f^{0.7}$ and $1/f^{0.64}$ for in-leaf and out-of-leaf conditions respectively. This inverse relationship with frequency suggests a decreasing attenuation as a function of frequency which is contrary to what is expected from the physical considerations of the processes involved in propagation through a scattering medium such as vegetation.

For the purpose of being able to quickly estimate the attenuation in terms of vegetation depth that a propagating wave will experience, the FITU-R model provides a simple solution in comparison to the NZG or DG models and especially in comparison to a model based on the radiative energy transfer theory [Ulaby, 1988] [Al-Nuaimi and Hammoudeh, 1994]. The FITU-R model also provides a good general estimation of the amount of attenuation that can be expected as a function of frequency and depth of vegetation. It can be recommended for use in the frequency range of 10 GHz to 30 GHz.

5.4 Interim Conclusion

In this chapter a number of prediction models have been discussed and their relative fit to the data measured at the sites shown in Chapter 4 in terms of RMS errors have been presented. The FITU-R model is a derivative of the ITU-R model which was based on measurements performed at lower frequencies than those used in the current measurement programme. It has provided the better all round prediction of the attenuation caused by vegetation versus vegetation depth at the frequencies used in the measurement programme. The numerical parameters for the FITU-R model were found by optimising the formula to all of the in-leaf data acquired at both frequencies and at all sites, and the same was repeated for all of the out-of-leaf data acquired at both frequencies and all sites. By using the measurement data acquired at all of the sites in the optimisation process, any site dependence factors are removed from or significantly weakened in the calculation of the values found for the model. The main advantage of the FITU-R model is its simplicity of use, allowing for a quick and useful prediction of the attenuation due to vegetation as a function of vegetation depth and frequency. The information presented in this chapter and in chapter 4 has been published in paper 6 listed in the 'Contribution to Published Literature' section (page 8-6).

Problems have been found with the DG model when it is used with certain measurement site geometries. The problem manifests itself in the predicted

results where the rate of attenuation appears to be negative at either small or large values of vegetation depth. This behaviour, together with the inverse frequency dependence are currently under investigation.

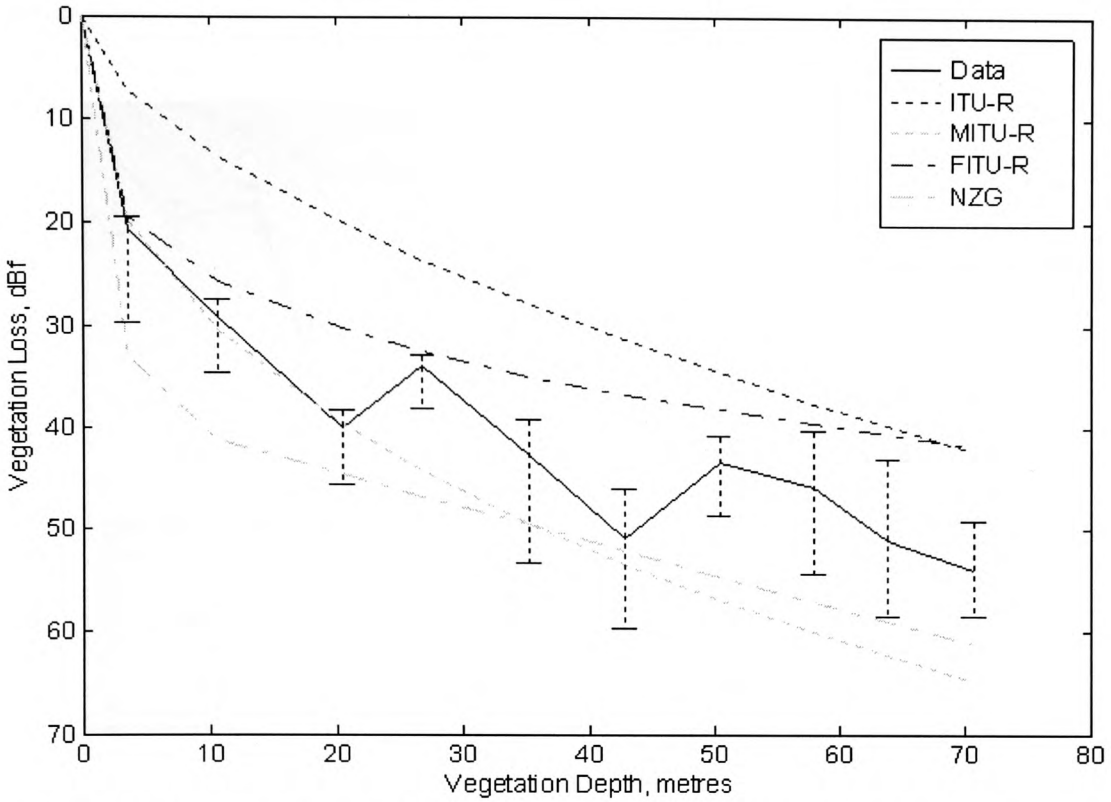

Figure 5-2 Comparison of Modelled and Measured Attenuation in-leaf at 11.2 GHz for Fermi Avenue.

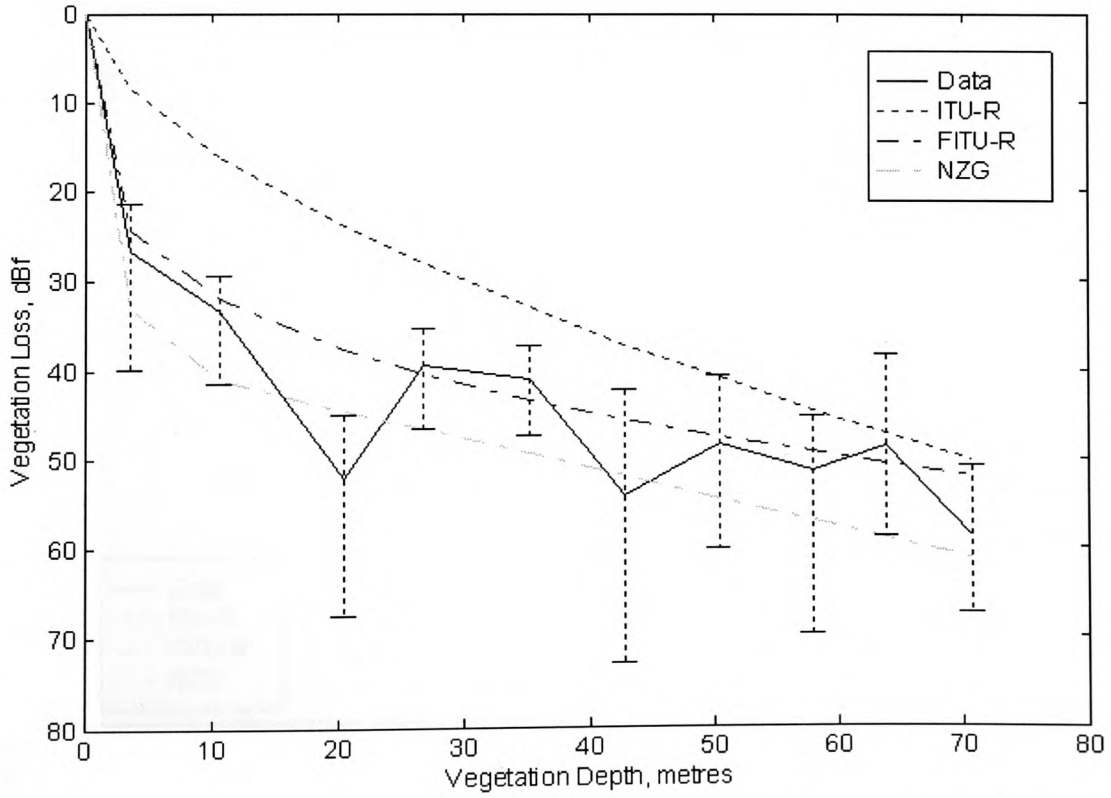

Figure 5-3 Comparison of Modelled and Measured Attenuation in-leaf at 20 GHz for Fermi Avenue.

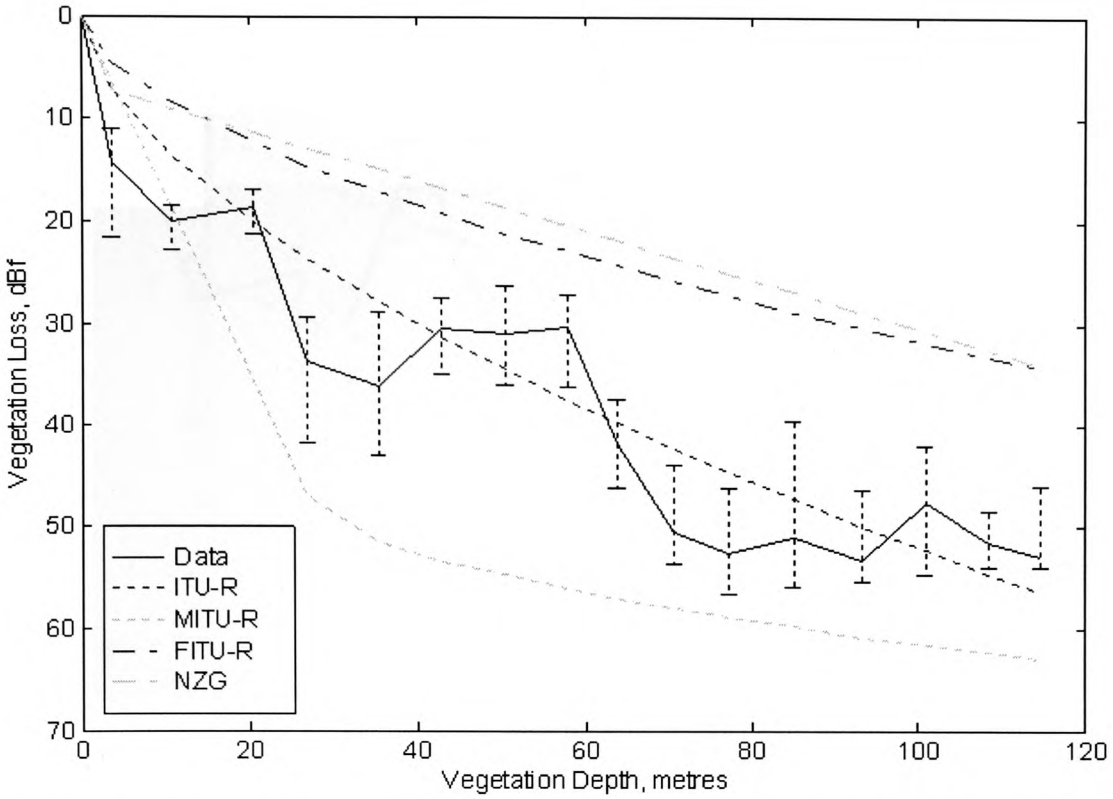

Figure 5-4 Comparison of Modelled and Measured Attenuation Out-of-leaf at 11.2 GHz for Fermi Avenue.

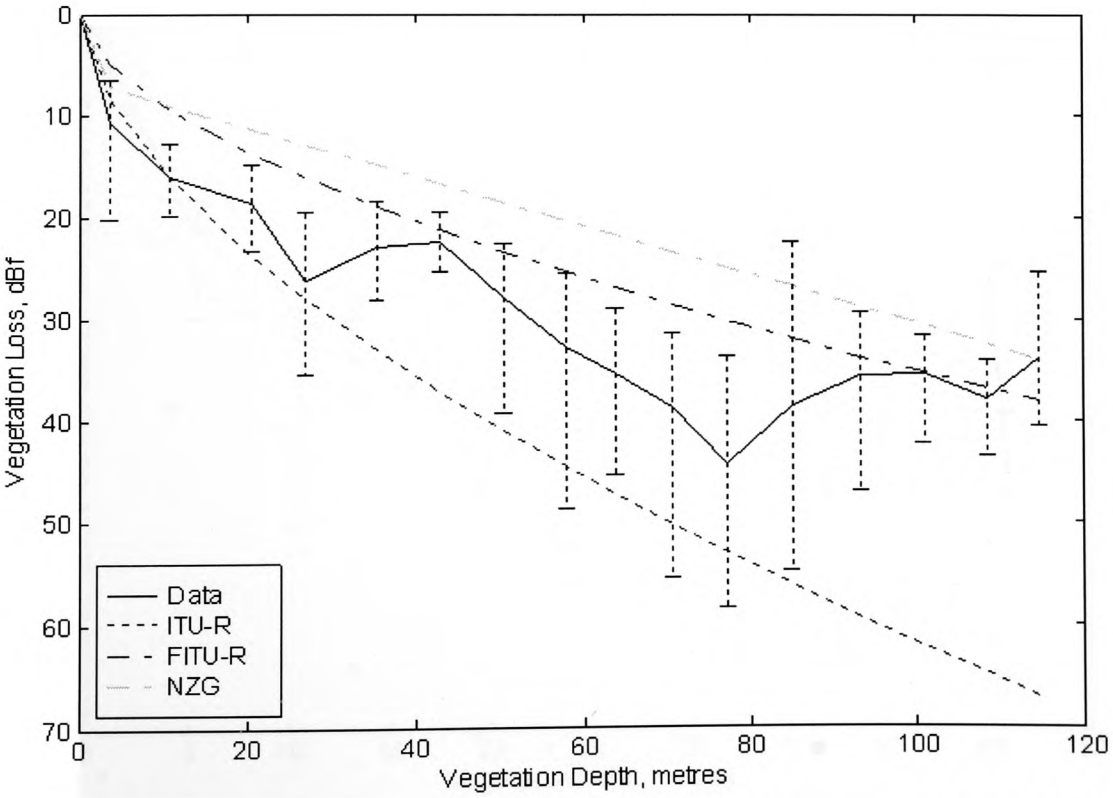

Figure 5-5 Comparison of Modelled and Measured Attenuation Out-of-leaf at 20 GHz for Fermi Avenue.

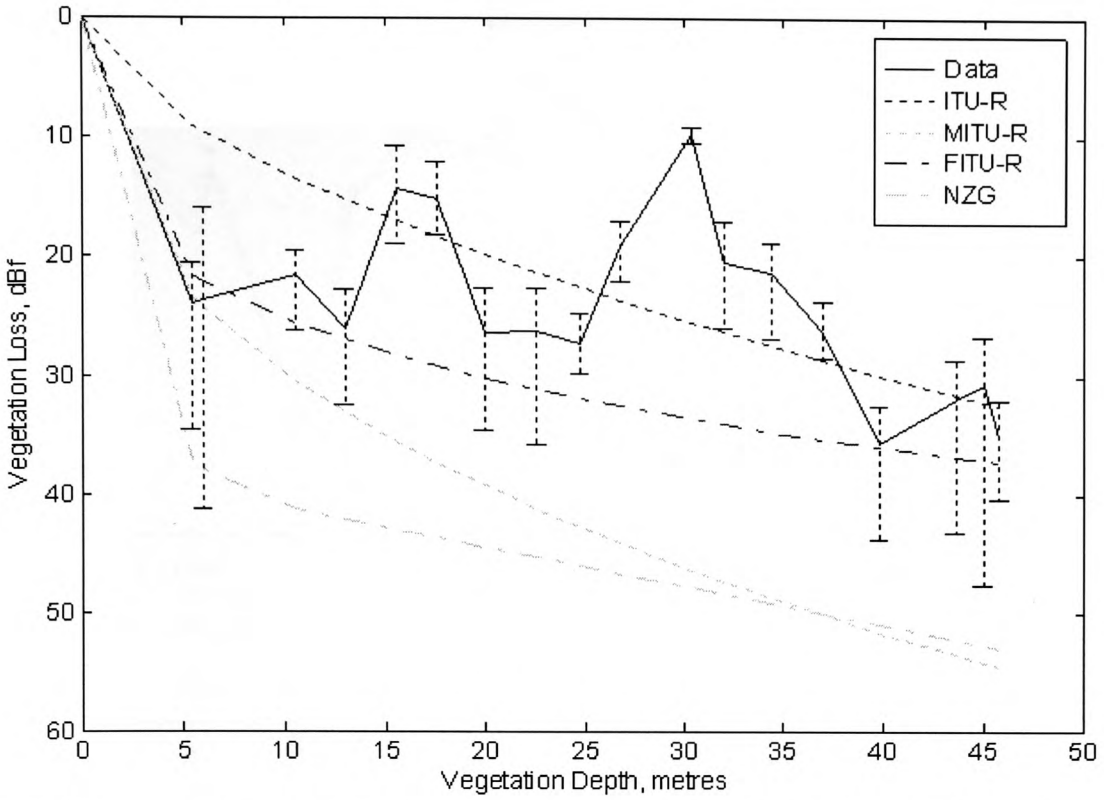

Figure 5-6 Comparison of Modelled and Measured Attenuation in-leaf at 11.2 GHz for the Mound with Receiver at 3m.

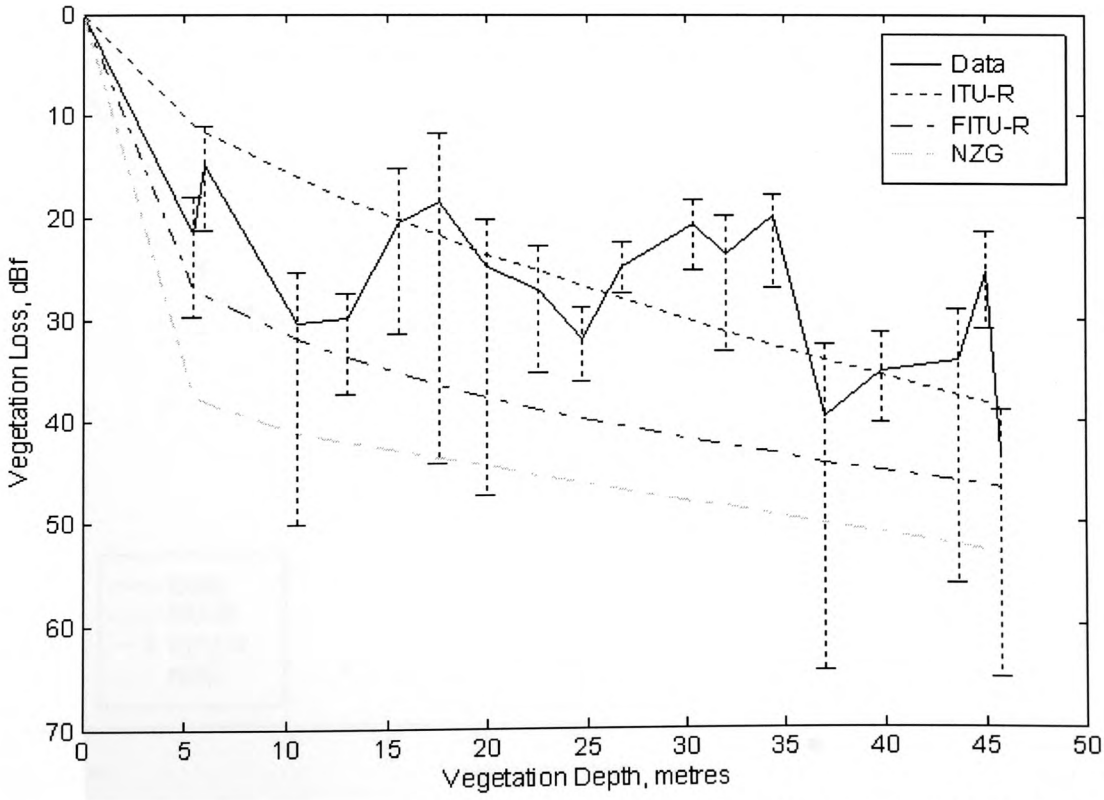

Figure 5-7 Comparison of Modelled and Measured Attenuation in-leaf at 20 GHz for the Mound with Receiver at 3m.

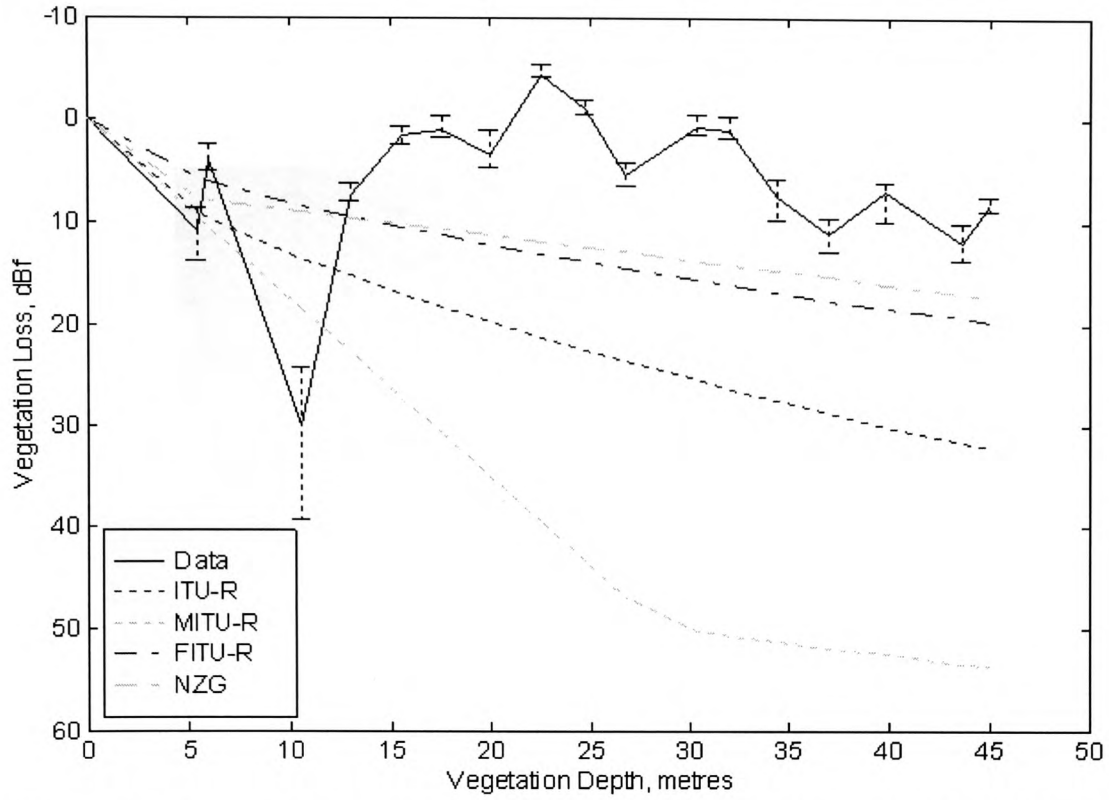

Figure 5-8 Comparison of Modelled and Measured Attenuation Out-of-leaf at 11.2 GHz for the Mound with Receiver at 3m.

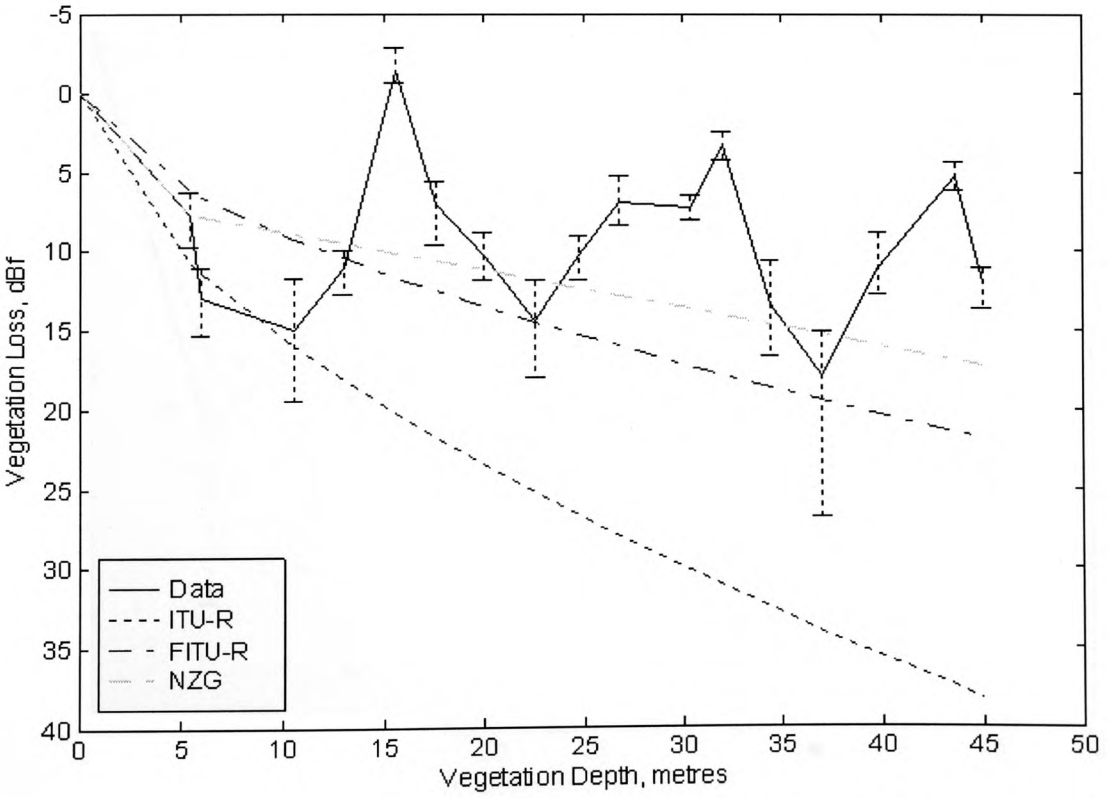

Figure 5-9 Comparison of Modelled and Measured Attenuation Out-of-leaf at 20 GHz for the Mound with Receiver at 3m.

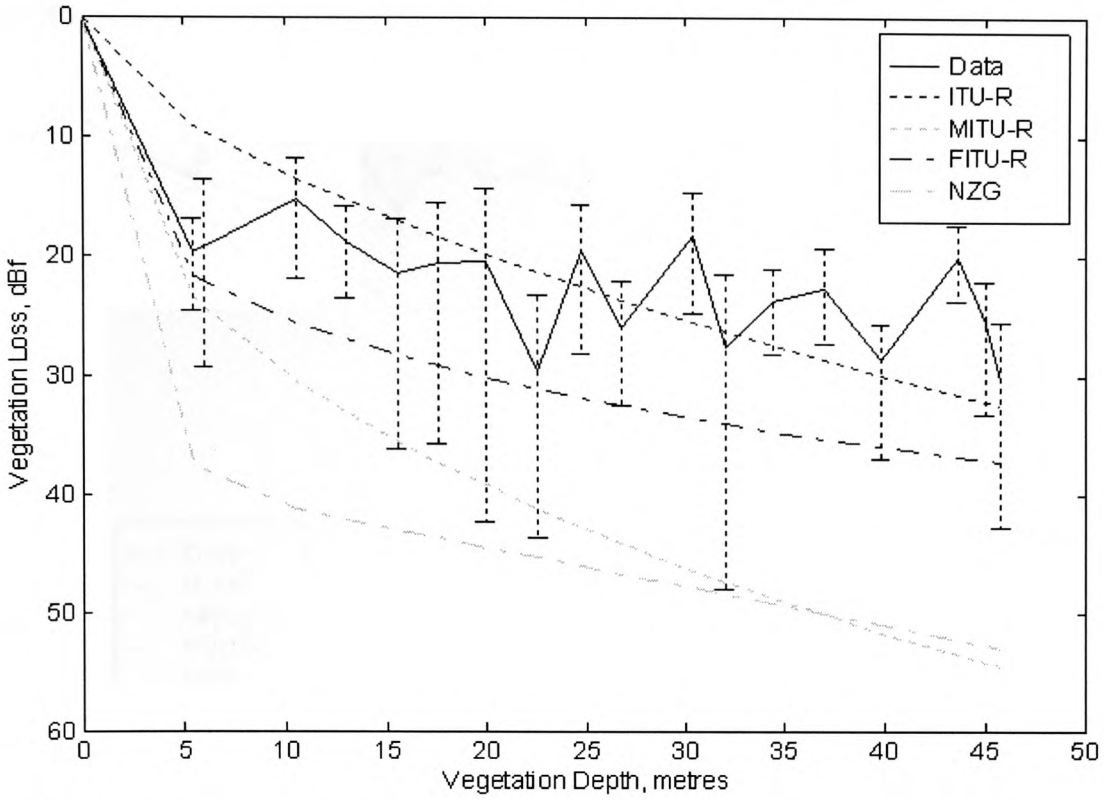

Figure 5-10 Comparison of Modelled and Measured Attenuation in-leaf at 11.2 GHz for the Mound with Receiver at 5m.

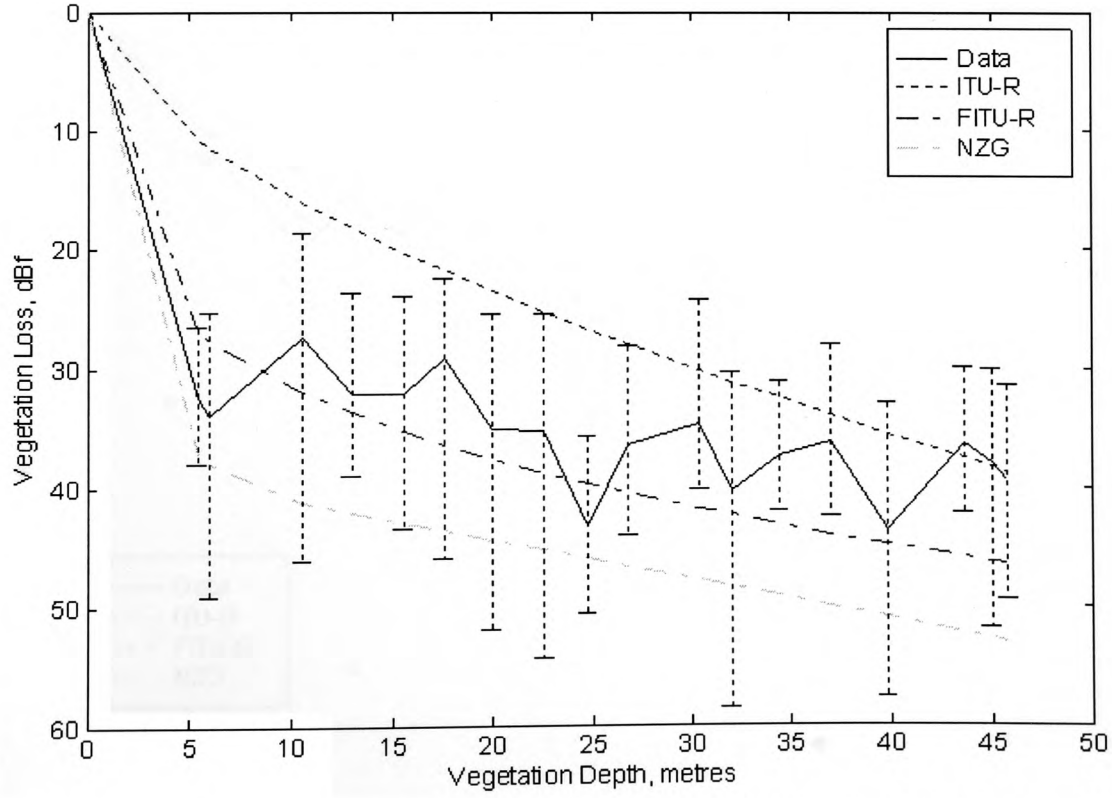

Figure 5-11 Comparison of Modelled and Measured Attenuation in-leaf at 20 GHz for the Mound with Receiver at 5m.

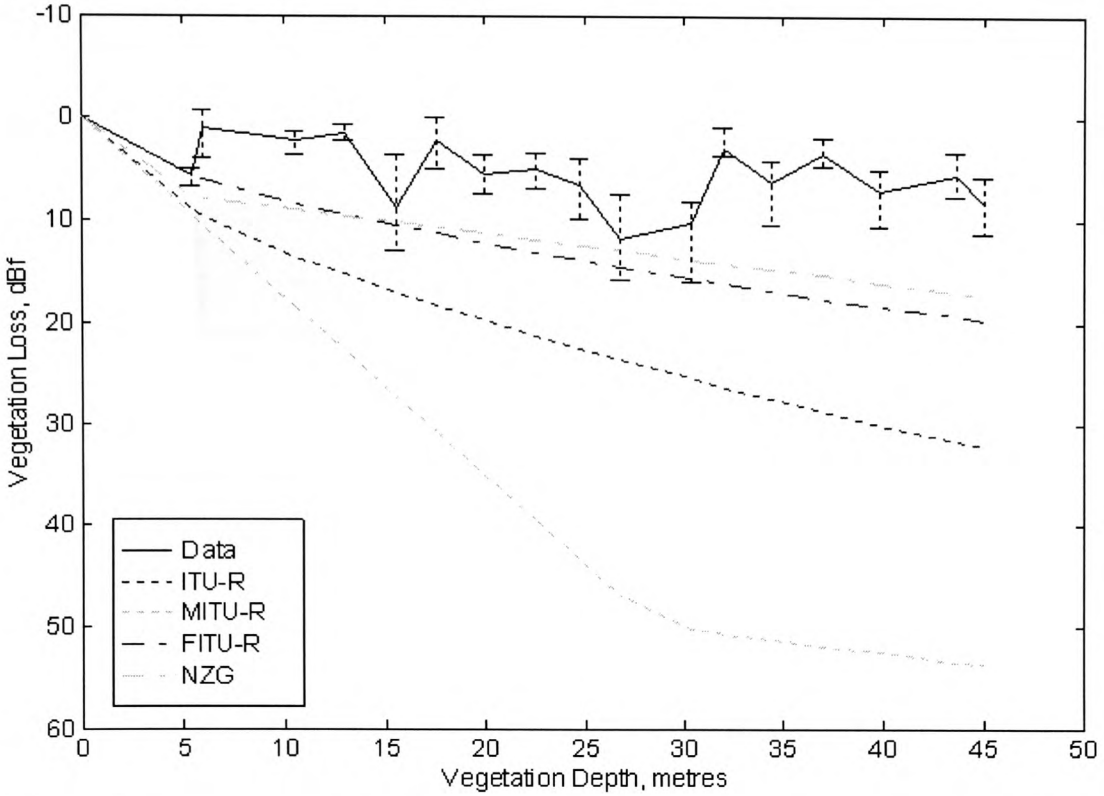

Figure 5-12 Comparison of Modelled and Measured Attenuation Out-of-leaf at 11.2 GHz for the Mound with Receiver at 5m.

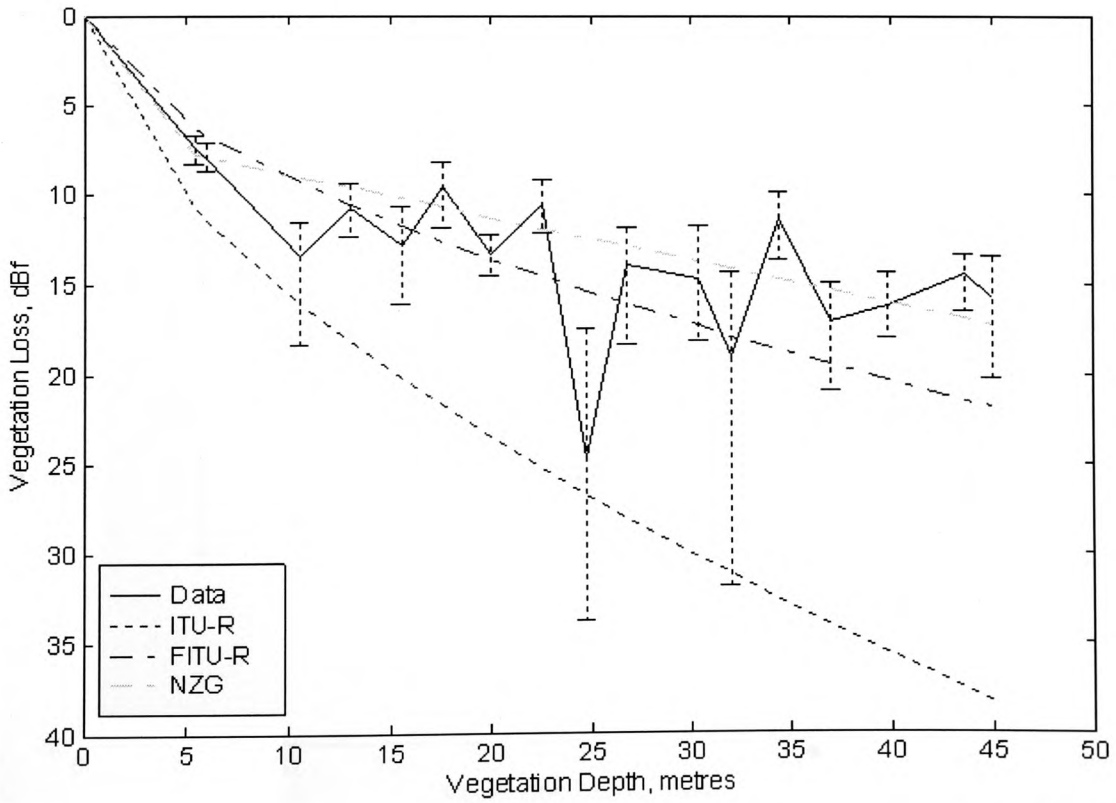

Figure 5-13 Comparison of Modelled and Measured Attenuation Out-of-leaf at 20 GHz for the Mound with Receiver at 5m.

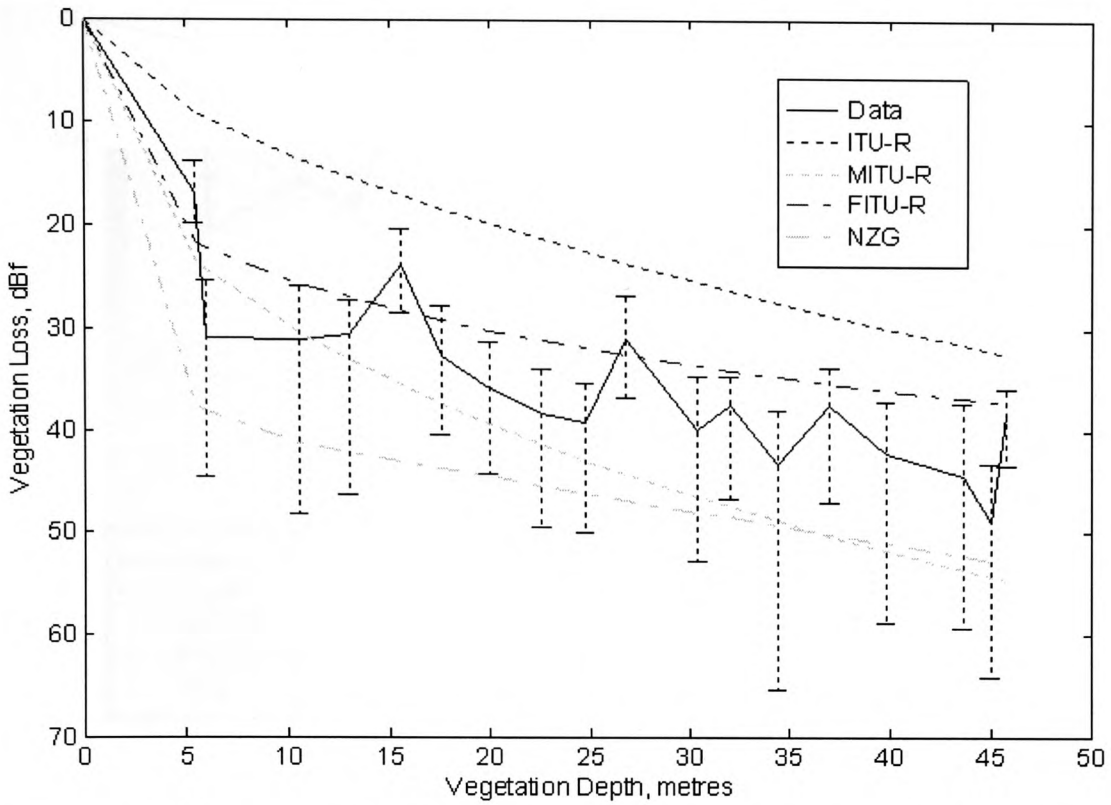

Figure 5-14 Comparison of Modelled and Measured Attenuation in-leaf at 11.2 GHz for the Mound with Receiver at 7m.

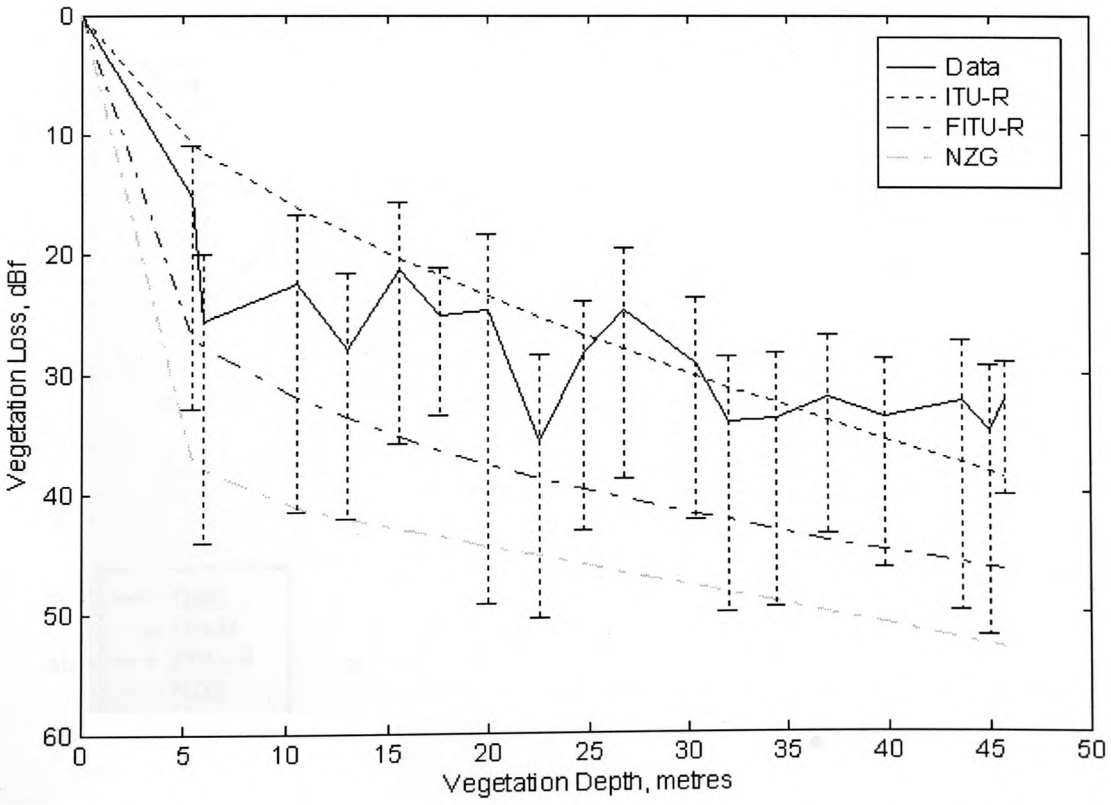

Figure 5-15 Comparison of Modelled and Measured Attenuation in-leaf at 20 GHz for the Mound with Receiver at 7m.

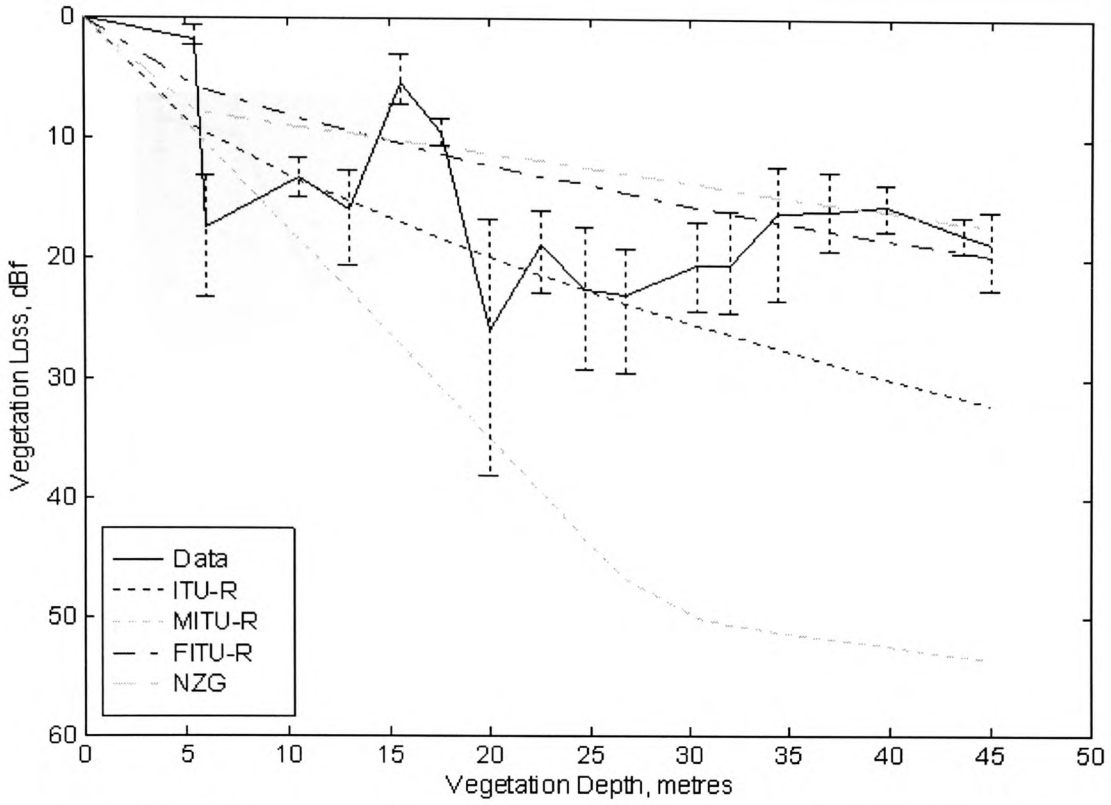

Figure 5-16 Comparison of Modelled and Measured Attenuation Out-of-leaf at 11.2 GHz for the Mound with Receiver at 7m.

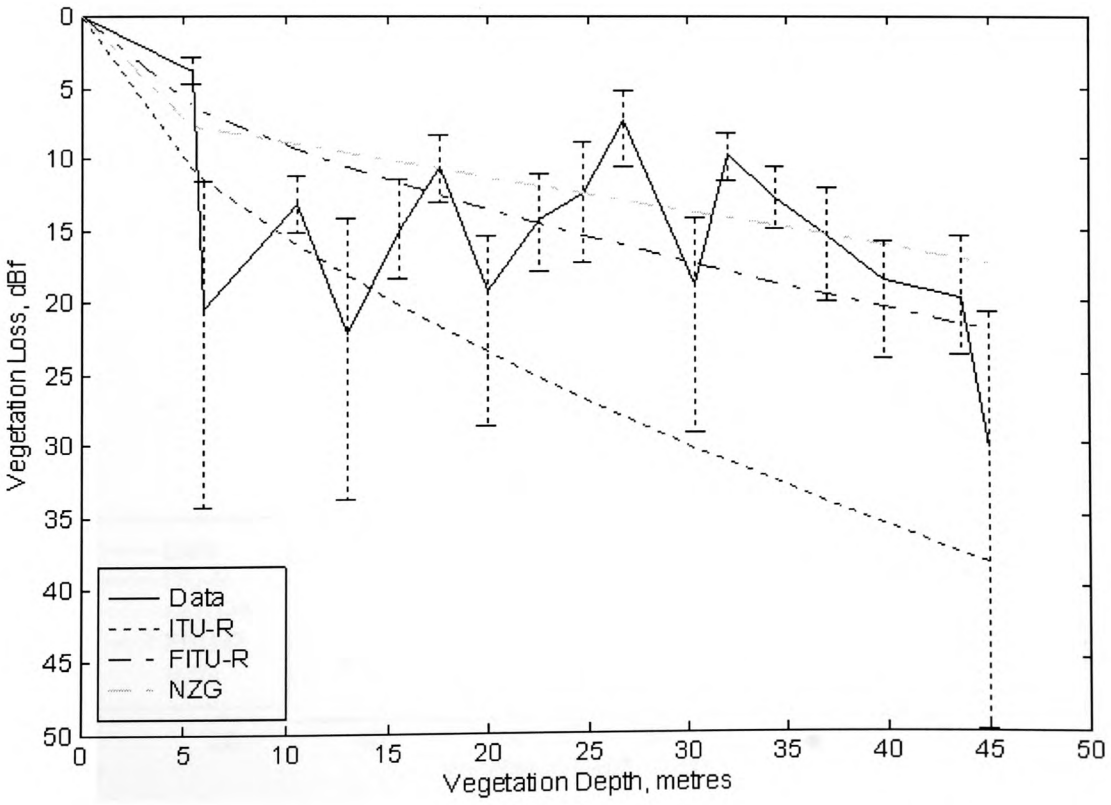

Figure 5-17 Comparison of Modelled and Measured Attenuation Out-of-leaf at 20 GHz for the Mound with Receiver at 7m.

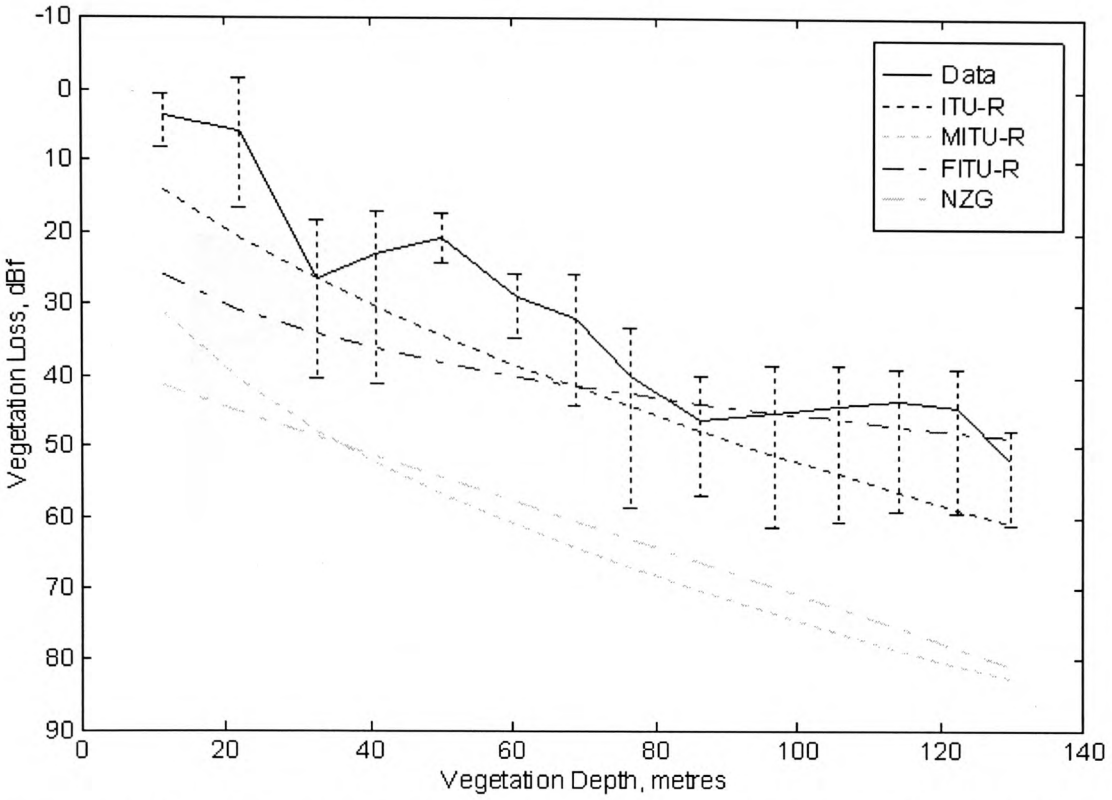

Figure 5-18 Comparison of Modelled and Measured Attenuation in-leaf at 11.2 GHz for the Ridgeway.

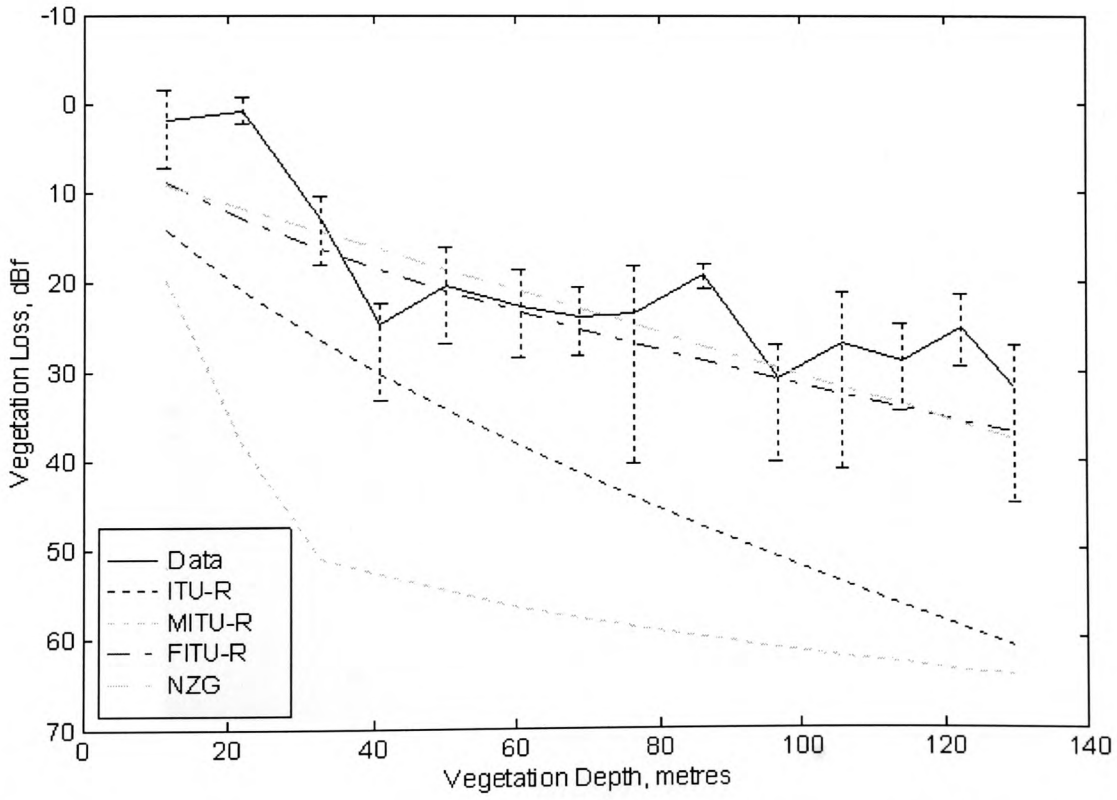

Figure 5-19 Comparison of Modelled and Measured Attenuation Out-of-leaf at 11.2 GHz for the Ridgeway.

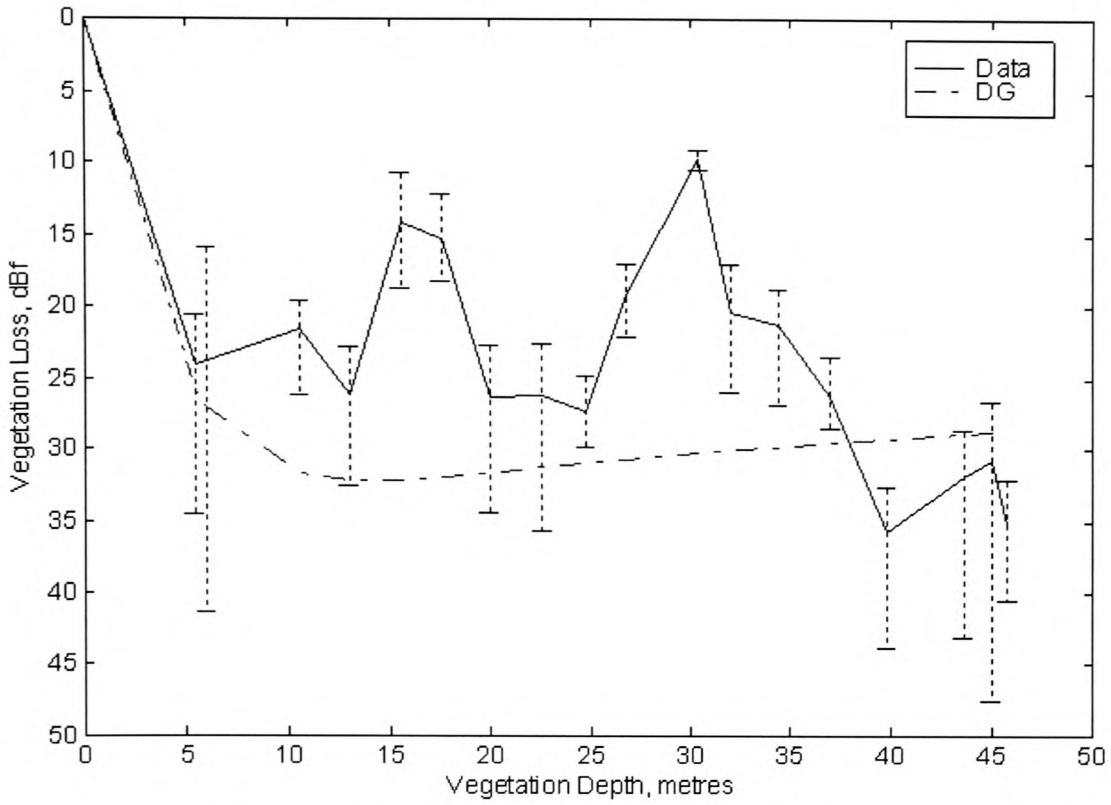

Figure 5-20 Performance of DG Model against Attenuation obtained at the Mound at 11.2 GHz and a height of 3m.

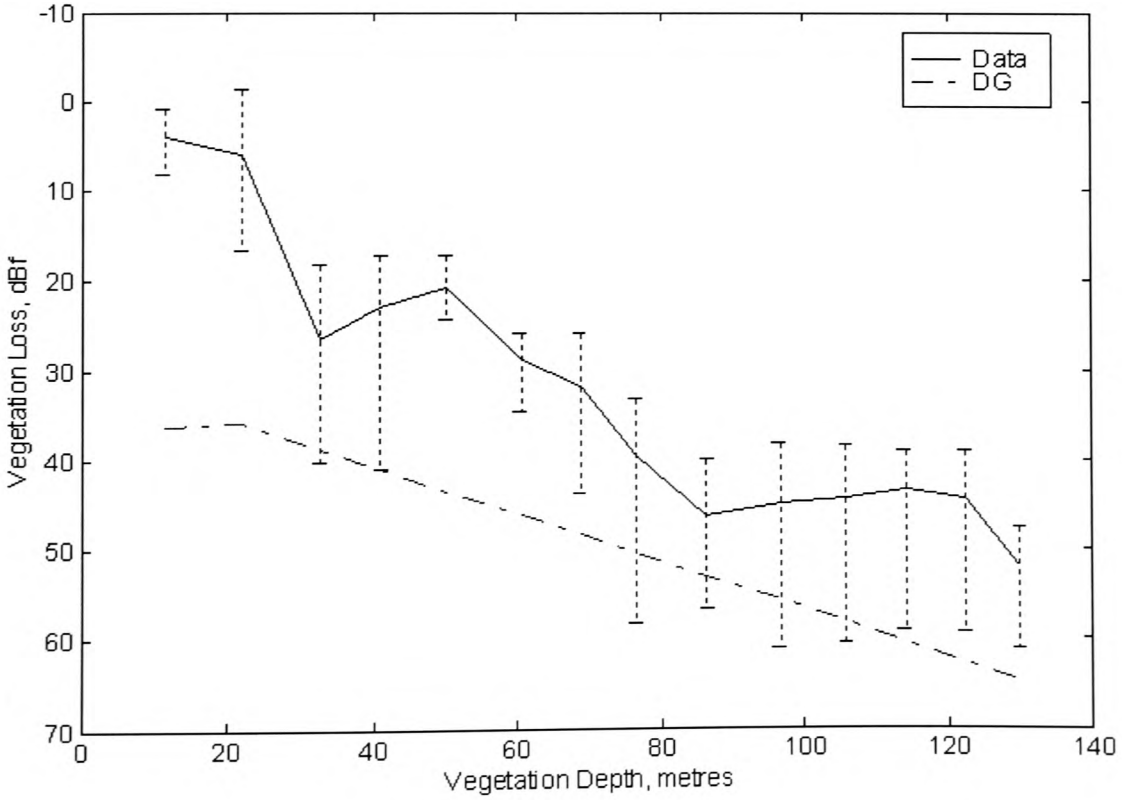

Figure 5-21 Performance of DG Model against Attenuation obtained at the Ridgeway at 11.2 GHz.

6. Depolarisation Studies

6.1 Introduction

In this chapter the representation of the polarisation of a radio wave is discussed for linear and elliptical polarisations. The investigation performed on the depolarisation of microwave signals by vegetation will be presented and discussed. The depolarisation measurements shown in this chapter evolved from the angular attenuation pattern of a single tree presented in Chapter 4. The depolarisation of a signal has been taken to mean; the change of the polarisation of the transmitted wave to another state [Beckmann, 1968]. In this case caused by the vegetation medium. The purpose of the investigation into the depolarisation of microwaves by vegetation was initially to ascertain the cause of the deep nulls seen in the 360° attenuation patterns and to determine where the lost power was being transferred to. More importantly, such an investigation provides a fuller characterisation of the effects of vegetation on the propagation of radio signals.

There are a number of techniques for measuring the polarisation of a propagating microwave signal and these will be discussed in this chapter, together with the reasons for choosing a particular method to measure the polarisation of a radiowave.

All of the depolarisation measurements have been performed at a single frequency of 20 GHz using vertical polarisation of the transmitter. The work presented within this chapter will enable an improved understanding of how and what happens to a microwave signal as it propagates through a body of vegetation. The information available in this chapter, will provide a better insight into the effect vegetation has on the propagating signal which in turn can lead to more accurate prediction models being developed compared to those presently available.

6.2 Representation of the Polarisation of a Radiowave

Polarisation is defined as the orientation of the electric field strength vector, **E**, of an electromagnetic wave at a given point in space during one period of oscillation.

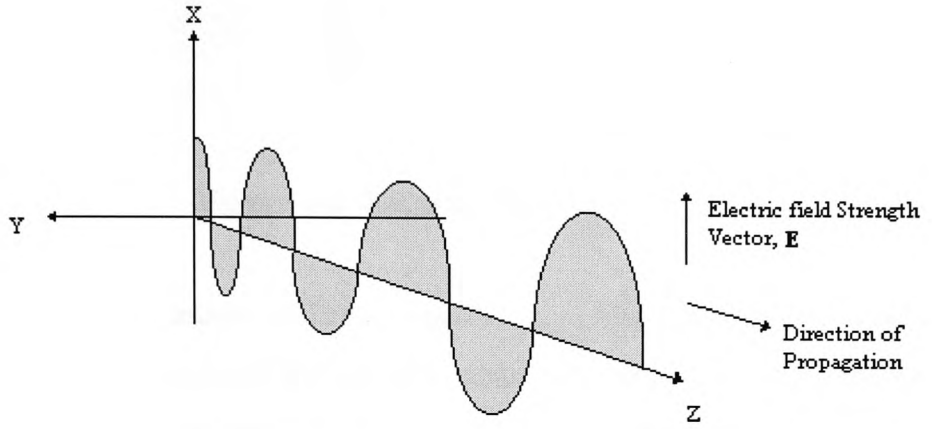

Figure 6-1 Electric Field Strength Vector Propagating with Time.

Figure 6-1 shows the electric field strength of a vertically polarised radio wave as it propagates with time through space. It can be seen that if the vector **E** is viewed from the end on, that the vector **E** would scribe a vertical line. If **E** was parallel to the xz plane then a horizontal line would be scribed and the wave would be horizontally polarised. These two linear polarisations are not the only forms of polarisation. The other forms of polarisation come under the name of elliptical polarisations as the vector **E** when viewed from the direction of propagation will be seen to scribe an ellipse or a circle.

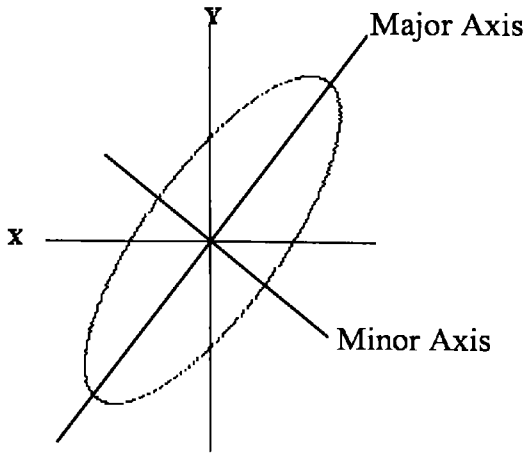

Figure 6-2 Elliptical Polarisation.

The shape of this polarisation ellipse, Figure 6-2, is determined by the ratio of the magnitudes of the horizontal and vertical components as well as their difference in phase. There are a number of ways to mathematically represent an elliptical polarisation. In this study the polarisation of a radio wave, be it linear, elliptical or circular has been represented by two values. These two values are the tilt angle, τ, and the axial ratio, AR, which also provides the sense of polarisation (left or right handed) [Hollis *et al*, 1970], [Kraus, 1985].

The tilt angle, τ, is defined as being the angle between the horizontal plane and the major axis of the polarisation ellipse, Figure 6-4. The tilt angle lies within the range of -90° to +90°. Thus the tilt angle for a horizontally linearly polarised wave would be 0° and 90° for a vertically linearly polarised wave.

The axial ratio, AR, is the ratio between the magnitudes of the minor and major axis of the polarisation ellipse as shown in Equation 6.1, it also provides the sense of polarisation.

$$AR = \frac{\text{Minor Axis}}{\text{Major Axis}} \qquad 6.1$$

The value of the axial ratio lies in the range -1 to +1. Where the sign determines the sense of rotation, negative for right and positive for left hand sense. An AR value of 0 represents a linearly polarised wave and a value of +1 or -1 represents a circularly polarised wave.

With the above two parameters defined, the polarisation of the propagating wave can be defined by a point on the Poincaré sphere [Hollis *et al*, 1970], [Kraus, 1985], Figure 6-3. Each individual point on the sphere uniquely defines a particular polarisation state. The equator of the sphere represents all the linear polarisation states. The position of this unique polarisation state can be described by two angles, α and β. Which are related to the axial ratio and the tilt angle respectively. The tilt angle and β are related by the expression :

$$\tau = \frac{\beta}{2} \qquad 6.2$$

where β is the angle of longitude measured around the equatorial plane from the axis that runs from the centre of the sphere to the point on the equator that represents horizontal linear polarisation. β is in the range $-180° \leq \beta \geq +180°$.

A tilt angle of 0° represents horizontal polarisation and is also 0° around the equator, a 90° tilt angle (β is 180°) represents vertical polarisation.

The axial ratio and the angle α are related by the following formula.

$$AR = \tan\left(\frac{\alpha}{2}\right) \qquad 6.3$$

where α is the angle of latitude between the equatorial plane and the point on the sphere. α lies in the range of $-90° \leq \alpha \geq +90°$.

The hemisphere that the point lies on is determined by the sign of the axial ratio. The northern hemisphere represents left hand sense and the southern right hand sense of polarisation, Figure 6-3.

6.3 Depolarisation Investigation

Depolarisation has been taken to mean that there has been a change from the transmitted polarisation state to another polarisation state caused by some medium [Beckmann, 1968].

Depolarisation was investigated to determine the cause of the nulls seen in the 360° angular attenuation patterns presented in Chapter 4. Also, to determine how the individual components of the vegetation media contribute to the overall effect on the propagating radio wave. To be able to accurately predict the magnitude of depolarisation a signal will suffer from a particular specimen of vegetation is a difficult if not impossible task. This being due to the rather complex nature of vegetation. There are a number of factors that contribute to the overall amount of depolarisation. These factors are the shape and structural attributes of the tree, the polarisation of the incident signal in relation to the orientation of the branches, twigs and leaves. Another factor is the size of these components of the vegetation in relation to the wavelength of the incident signal. External influences, such as the presence and strength of wind are additional factors which may change the relational orientation of the various components of the tree and hence the magnitude of the depolarisation. Beckmann [1968], among others, says that it is possible to predict the amount of depolarisation caused by a given shape and it is for this reason, that the shape of a tree was mentioned as a prime contributory factor. However, a wave is not just scattered from the surface of a tree but propagates through a tree where currents are induced into the various components of the tree which cause a collective depolarisation of the incident wave when the currents are re-radiated. It would also be impossible to catalogue the shape and orientation of all the components of a tree and to compute the overall effect, as the orientation and to a lesser extent the general shape, do not stay constant with time.

6.4 Polarisation Measurement Methods

There are a number of possible methods available for measuring the polarisation of a propagating wave. The methods [IEEE Std Test Proc. for Ant., 1979] [Wolfgang, 1978] presented here are usually associated with measuring the polarisation properties of antennas. In this case, the vegetation is effectively being treated as an antenna as it is re-radiating the wave that was incident upon it. Each of the four methods available allow various amounts of information about the polarisation of the propagating wave to be obtained. These four methods along with the information they provide are described in the following sections and is followed in section 6.2.2 by an assessment of these different methods.

6.4.1 Polarisation Pattern Method

The polarisation pattern method [IEEE, 1979] involves rotating a linearly polarised receive antenna about its central axis in a plane normal to the propagating direction of the incident field. Whilst the receive antenna is rotated through 360° the voltage induced in the antenna is recorded. This recorded information may then be plotted against the rotation angle of the receive antenna, the resulting graph shown in Figure 6-4, being referred to as the polarisation pattern. From the polarisation pattern, the polarisation ellipse can be extrapolated as shown in Figure 6-4 by the dashed ellipse. As can be seen in the aforementioned figure the polarisation pattern is tangent with the polarisation ellipse at the ends of the major and minor axes.

The tilt angle and the axial ratio of the incident wave on the receive antenna may then be determined from the polarisation ellipse. This method does not provide the sense of polarisation so if the polarisation of the measured wave was to be plotted on the Poincaré sphere, two conjugate points would exist, one in each of the two hemispheres.

6.4.2 Rotating Source Method

The rotating source method, as the name suggests, consists of continuously rotating a linearly polarised antenna which is radiating the transmitted signal, whilst the direction of the antenna under test, mounted at the receiver, is changed. The received signal is recorded at each position of the receiver. The rate at which the source is rotated needs to be much greater than the rate at which the test antenna is being moved. This method provides only the axial ratio information and is of most use when testing near circularly polarised antennas. [IEEE, 1979]

6.4.3 Multiple-Amplitude-Component Method

This method provides the complete polarisation information about the antenna under test without the need to measure the phase. This is accomplished by measuring the magnitude responses of four differently polarised, but known antennas, [Knittel, 1967], [Clayton and Hollis, 1965]. At least one of the four antennas needs to be left-hand or right-hand circularly polarised. The remaining three antennas can be of any known polarisation. The most commonly used states are horizontal or vertical linear, diagonally linear at 45° or 135° or the circular polarisation that has not already been used. The gains of the antennas shall be known and any differences between the antennas need to be accounted for in the calibration stage. From the four magnitude responses of the antennas three polarisation ratios can be obtained. With these three ratios the precise polarisation state of the wave can be determined without ambiguity. The angles that define the loci of all possible polarisations on the Poincaré sphere can be determined from the three polarisation ratios.

6.4.4 Phase-Amplitude Method

This method provides complete information about the wave polarisation. In this method all of the data required to determine the polarisation can be measured simultaneously. The antenna under investigation is used at the source as the transmit antenna whilst at the receiver, a dual polarised antenna is

employed. The receive antenna provides magnitudes and relative phases for each of the two polarisations. From this data, the complete polarisation information of the wave can be determined [Hollis, 1970].

6.5 Assessment of Measurement Methods

The four methods discussed above provide varying amounts of information about the polarisation state of the propagating wave and involve varying levels of difficulty in their implementation.

The multiple amplitude component and phase amplitude methods provide all of the necessary information to be able to fully define the polarisation state. The first of the two methods requires a circularly polarised antenna of either or both senses. If, as in this case, more than one antenna is required each antenna may not necessarily be illuminating the same area of vegetation. The latter method requires some means of being able to measure the phases of the two orthogonally polarised waves to determine the sense of the polarisation.

The polarisation pattern method provides the tilt angle and the axial ratio but not the sense. The rotating source method only allows the axial ratio to be determined. Both of these methods therefore produce some ambiguity about the sense of polarisation. They also require either the receiver or source to be rotated about their central axis.

6.5.1 Method Utilised

All of the methods described above can be useful, but the one selected for use in this research is clearly determined by the amount of information required and practical constraints, such as equipment availability for carrying out the necessary measurements.

After examining the above four methods, the following methods were rejected for a variety of reasons:

1. The multiple amplitude component method would have been ideal as there is no complexity involved in trying to measure the phase when no vector network analyser is available. However, the problem encountered with this method was that a left or right-hand circularly polarised antennas was not commercially readily available, making it impossible to conduct the measurements.

2. The phase amplitude method was not chosen as it was not possible to measure the relative phases to any great degree of accuracy without the use of a vector network analyser. To obtain the required accuracy, a calibrated phase changer would be required along with knowledge of the exact lengths of waveguide used in the measurements. The precise amount of phase shift that the receive system introduces would also be required. Owing to the configuration of the receiver, it is not possible to know the amount of phase shift induced or to accurately measure the lengths of the waveguide used.

3. The rotating source method was not utilised primarily because only the axial ratio parameter would be determined. Neither does this method provide sufficient information about the polarisation of the wave.

Having rejected the above three methods, the polarisation pattern method remained and this method was decided upon. This method has been used due to the hardware being readily available after minor modifications. It provides the tilt angle and axial ratio, with the only drawback being that the sense of polarisation is unknown.

6.6 Depolarisation Measurements

After deciding upon the method to be used in providing measurement data, the polarisation pattern method was implemented by taking one of the axes of the

turntable which has a hole directly through the centre. This hole happens to be of sufficient diameter allowing the 20 GHz waveguide to pass through completely unhindered. The waveguide coupled with a 20 dBi standard gain horn antenna was centrally mounted to the front of the rotating platform of this axis of the turntable. Great care was taken in positioning the central axis of the antenna in the centre of the turntable. Mounting the receiver in this manner allows the linearly polarised receive antenna to be rotated about its central axis as required by the polarisation pattern method. The turntable was mounted vertically atop of a tripod equipped with a swivel platform, with the tripod allowing the height of the receiver to be varied from approximately 1 metre to 1.8 metres. Once the height of the receiver had been set, the swivel platform was adjusted to obtain an absolutely level antenna.

The transmitter was mounted at the same height as the receiver and was made level with respect to the receiver. The general measurement geometry used is as shown in Figure 6-5. The distances and heights used changed according to the width and height of the different specimens of vegetation used in the experiments. The transmitter was always placed so that the specimen was in the far field region of the transmit antenna. The distance between the receiver and the specimen of vegetation was set so that the 3 dB beamwidth of the 20 dBi receive antenna was within the width of the tree under investigation. The heights of the transmitter and receiver were aligned at the central height of the foliated part of the tree. Vertical polarisation was used throughout these measurements.

Initially, a freespace measurement was performed by rotating the receiver from its home position, vertically polarised, through 360° in 0.1° increments. This measurement also served as a means of checking the alignment of the receiver. Figure 6-6 shows the polarisation pattern for the freespace measurement. The tilt angle as can be seen is 90° as the transmitted wave was vertically polarised. The axial ratio, being calculated from the magnitude of the minor and major axis, is 0.001, meaning the transmitted wave was linearly polarised.

Each of the initial measurements of the polarisation of the wave emanating from the vegetation would take in the region of one hour to complete. This is due to the rate at which the receive antenna was being rotated at by the turntable to which it was attached. The speed of rotation of the turntable was increased to a point at which the measurement results would not fluctuate for each successive polarisation pattern measurement. This resulted in the duration of one measurement being reduced to fifteen minutes.

Knittel [1967] describes a method similar to the multiple amplitude component method which would allow the tilt angle and axial ratio to be determined from three measurements with a linearly polarised antenna at three different but known tilt angles. This method had the potential to reduce the measurement time to less than five minutes, considerably less time than was required to rotate the receive antenna through 360° as required by the polarisation pattern method. The practicality and implementation of this method are described in the following section.

6.7 Knittel's Measurement Method

Knittel's measurement method [Knittel, 1967] as it will be referred to here, involves measuring the amplitude of the propagating wave with the receive antenna in three linear polarisation states. By generating the relative polarisation efficiency (power ratio) quantities from the amplitude measured from the three states of the linearly polarised antenna, one obtains values which can be used to generate two contours on the Poincaré sphere. The point at which these two contours cross is the polarisation of the wave received. Using just three linearly polarised states means that the two contours will cross at two points on the polarisation sphere, one in each of the hemispheres, thereby giving ambiguity as to the sense of polarisation. With an additional fourth non linearly polarised but known antenna polarisation, this ambiguity would be removed, as the sense of polarisation can be determined. The following paragraphs explain the approach adopted in using this method, its validation and usefulness.

With the values obtained from the three polarisation states of the receive antenna, two relative polarisation efficiency quantities (power ratios) are calculated, e.g.

$$R_1 = \left(\frac{l_1}{l_2}\right)^2 \qquad 6.4$$

$$R_2 = \left(\frac{l_1}{l_3}\right)^2 \qquad 6.5$$

where: R_1 and R_2 are the relative power ratios,

l_1, l_2 and l_3 are the magnitudes of the three different tilt angles of a linearly polarised antenna.

With these two values the two relative polarisation efficiency contours to be drawn on the sphere can be generated. Instead of drawing the contours on the sphere it is easier to produce a stereographic projection [Thomas, 1952] of one of the hemispheres and plot the sections of the contours on this projection. The hemisphere that is projected is determined by the non-linearly polarised antenna measurement which resolves the sense of polarisation. If this measurement is not performed then either hemisphere may be chosen. Generally, the left circular, northern hemisphere is used for this set of measurements.

The contours on a sphere can be represented by circles on the stereographic projection of a hemisphere. The position and radius of these circles may be determined from Equation 6.6 and Equation 6.7 [Knittel, 1967].

$$\left.\begin{aligned} x &= -\frac{R\cos\theta - 1}{R - 1} \\ y &= -\frac{R\sin\theta}{R - 1} \end{aligned}\right\} \qquad 6.6$$

$$r = \sqrt{x^2 + y^2 - 1} \qquad 6.7$$

where :

x and y are the co-ordinates for the centre of the circle.

r is the radius of the circle to be drawn on the projection of the hemisphere. θ is the angular difference between the polarisation states of the antenna at which amplitudes were obtained and used to obtain the value for R.

The process of generating the circles was implemented in Matlab by providing the program written with values for the two power ratios. The program, presented in Appendix C, would then generate the two circles and plot the sections of these circles that fall within the stereographic projection of one of the hemispheres. A unit circle was used to represent the projection of the hemisphere. This section of the program was initially validated by drawing contours of different relative polarisation efficiency and checking their position. It was also validated by drawing two contours that were known to cross at a particular point within the unit circle. Figure 6-7 shows two such contours drawn on the unit circle which were expected to cross on the circumference of the unit circle at a point that corresponds to vertical linear polarisation. The circumference of the unit circle represents the equator of the Poincaré sphere. As can be seen, the contours meet at the expected point on the equator at the particular point that represents vertical linear polarisation.

The Matlab program finds the point at which the two lines intersect and calculates the parameters α and β using simple trigonometry and from this, the axial ratio and tilt angle. From these two values using the previously stated relationships, Equation 6.2 and 6.3, the axial ratio and tilt angle are computed. For the above test the axial ratio computed was 0.002 and the tilt angle 90°. This corresponds to vertical linear polarisation. Linear as the axial ratio is $\cong 0$ and vertical as the tilt angle is 90°.

After having validated the Knittel measurement method defined above, the method was applied to data measured with the receive antenna in three different, but known states. The three antenna polarisations used were vertical polarisation and $\pm 60°$ from the vertical polarisation. In other words the antenna was

positioned at tilt angles of 30°, 90° and -30° with horizontal linear polarisation being the 0° reference.

The tilt angles of 30°, 90° and -30° were chosen so that when contours corresponding to the measured power ratios are drawn on the stereographic projection of a hemisphere they cross in the most precise manner possible. From this, it is meant that the intersection of the two contours occupies the smallest area possible. If angles other than those stated are used then the intersection of the contours becomes spread over an area rather than a point and therefore errors are introduced as the precise polarisation state cannot be pinpointed accurately.

The first measurement performed was a freespace measurement. The above tilt angles of the receive antenna were physically obtained by having the same set-up as described in Section 6.6. Using the Knittel method gave an axial ratio and tilt angle of 0.02 and 90° respectively. Measuring the parameters straight from the polarisation pattern gave an axial ratio of 0.005 and a tilt angle of 90.1°. As can be seen there is some difference between the two sets of values. The results proved interesting, as the difference between the two methods was considered to be of an acceptable level.

The next step was to introduce a specimen of vegetation into the path between the transmitter and receiver. The first plant to be introduced was a Ficus plant of the type shown in Figure 4-17 and described in Section 4.4.1. As for the freespace measurement, the receive antenna was rotated through 360° and the polarisation pattern was measured and is shown in Figure 6-8. The magnitude response of the receive antenna at the previously mentioned angles of 30°, 90° and -30° was available from the polarisation pattern measurement. This also allowed comparison of the two methods to be made. The axial ratio and tilt angle derived from the polarisation pattern is 0.26 and 81.9° respectively. After calculating the power ratios and executing the programs in Matlab, the contours and unit circle were produced as shown in Figure 6-9. The values for the axial ratio and tilt angle using the Knittel method were obtained as 0.44 and 82° respectively. As can be

seen, the two values for the tilt angle are very close, especially as the polarisation pattern was measured in 0.5° increments. Unfortunately, the same cannot be said for the axial ratios, where there are a number of possibilities for the discrepancy between the measured and calculated axial ratio, such as the positioning and linearity of the receive antenna.

The central positioning of the antenna was checked and adjusted as accurately as possible with little improvement being achieved. If the antenna was not rotating about its central axis, different magnitude responses would be obtained for tilt angles that are 180° different. If the antenna was centrally mounted and the antenna was linearly polarised, then equal magnitude responses would be obtained for tilt angles that are 180° different.

After extensive testing of the Knittel measurement method, it was found that the accuracy of the magnitude responses from the receiver system with different tilt angles was not precise enough. This induced errors into the measurements as can be seen in Figure 6-10. For the wave being measured, the tilt angle could lie between 80.6° and 82.4° and the axial ratio may lie between 0.35 and 0.49. This possible range of values does not provide an accurate enough representation of the polarisation of the wave being received. Errors may be introduced into the measurements by the various parts of the receiver system such as the logarithmic amplifier and the data acquisition board. Owing to the complexity involved in accounting and calibrating for sources of error, it was decided to revert to the polarisation pattern measurement method which was found to offer a more accurate and repeatable determination of the polarisation state of the received wave.

6.8 Coniferous Measurements

In this section the results of the depolarisation study conducted using a coniferous tree will be presented along with the method employed in obtaining these measurements.

6.8.1 The Measurement Method

The measurement procedure employed consisted of placing the test subject, a conifer tree, in the direct path between the transmitter and receiver as in Figure 4-16. With both the transmit and receive antennas vertically polarised, the tree was rotated through 360° in 0.1° steps at a rate which would not result in any movement of the tree. This made up a 360° attenuation pattern of the type shown in

Figure 6-11, - 0° being the home position of the turntable on which the tree was placed. To allow for repetition of the experiments, the containers of the tree and the turntable were marked to permit realignment of the two. From the information shown in the 360° attenuation pattern, it was decided to note the angles of rotation to be used in subsequent measurements of the polarisation pattern of the wave emanating from the tree. The angles of tree rotation at which polarisation pattern measurements have, for the most part, been conducted around the measured nulls. The reason for this being, as discussed in Chapter 4, to determine if the cause of the deep nulls in the 360° attenuation patterns were as a result of the incident wave suffering considerable depolarisation which results in neither vertical or horizontal polarisation. The polarisation patterns were measured using the polarisation pattern method as presented in Section 6.4.1.

6.8.2 Coniferous Measurement Results

In total, six conifer trees were used in this investigation, but only a portion of this data will be presented, namely that of three conifers of the Cypress species numbered one through to three and a Spruce conifer. The leaves of the Cypress conifer are shown in Figure 6-14, with the average dimensions of these three trees being at a height of 140 cm and a maximum foliage width of 60 cm. The other species presented, the Spruce conifer, shown in Figure 6-15 - the traditional Christmas tree - has needles with an average length of 1 centimetre.

Figure 6-11 to Figure 6-13 shows the 360° attenuation pattern for the Cypress conifers 1 to 3 respectively. It is considered that these nulls seen in the 360° attenuation patterns are equivalent to the fluctuations experienced when performing the attenuation measurements presented in Chapter 4. After examining the attenuation pattern, angles of rotation of the trees were chosen. These angles encompassed peak values and as well as those around and at null values.

Polarisation patterns measurements were performed at these and other rotation angles on the different tree samples. Owing to the large volume of data obtained in the study, only a sample of data will be presented for each of the trees experimented upon.

6.8.2.1 Cypress Conifer 1

As can be seen in Figure 6-11, there is one exceptionally deep null which occurs at 190.3°. The polarisation pattern of the signal emerging from the vegetation was measured at the rotation angles of this and other nulls and at angles immediately before and after these nulls. The polarisation of the wave from the coniferous specimen was also measured at angles at which peaks in the received signal level were seen, such as at 151.5°.

A freespace measurement was performed and gave a tilt angle of 0.1° and an axial ratio of 0.009. For the polarisation pattern measured at a peak value at 151.5° rotation angle (Figure 6-19), the tilt angle and axial ratio were found to be of values shown in Table 6-1. Polarisation patterns are shown in Figure 6-16 to Figure 6-18 which are for the rotation angles of 189°, 190.3° and 192° respectively. These represent an angle prior to the position of the null, the angle of the deep null and an angle after the null. The tilt angles and axial ratios for these three polarisations are presented in Table 6-1.

Table 6-1 Polarisation States for Cypress Conifer 1.

Rotation Angle	Tilt Angle	Axial Ratio
151.5°	74.4°	0.01
189°	-32.3°	0.19
190.3°	0.2°	0.16
192°	34.7°	0.16

6.8.2.2 Cypress Conifer 2

The 360° polarisation pattern for this tree is shown in Figure 6-12. This conifer was not as densely leafed as conifer 1 and was less homogenous. Several interesting features emerge from the polarisation patterns measured and it is these features that will be presented. These being at the null just after 0° and the null at approximately 325° when viewed from Figure 6-12. For conifer 2, the polarisation patterns that were measured and are presented are rotation angles of 60° and 61° either side of a null. These patterns can be seen in Figure 6-20 and Figure 6-21 respectively, with angles of 321°, 323 ° and 324° being shown in Figure 6-22 to Figure 6-24. The angle of 324° being the angle at which the null was present. Table 6-2 presents the tilt angles and axial ratios for these polarisation patterns.

Table 6-2 Polarisation States for Cypress Conifer 2.

Rotation Angle	Tilt Angle	Axial Ratio
60°	-18.3°	0.17
61°	38.2°	0.45
321°	-86.5°	0.27
323°	87°	0.20
324°	60°	0.20

6.8.2.3 Cypress Conifer 3

Figure 6-13 shows the 360° attenuation pattern for this conifer. This tree was slightly more homogenous than conifer 2. There is a significantly deep null at approximately 50° and 80°. For the first null, polarisation patterns for rotation

angles of 50.5°, 51.1° and 52° are presented in Figure 6-25 to Figure 6-27. Polarisation patterns for the second null are shown in Figure 6-28 to Figure 6-30 for angles of 79°, 80.5° and 81°. The tilt angles and axial ratios are shown in Table 6-3 for the polarisation states at each rotation angle of this particular tree.

Table 6-3 Polarisation States for Cypress Conifer 3.

Rotation Angle	Tilt Angle	Axial Ratio
50.5°	26°	0.37
51.1°	-5.4°	0.28
52°	-29.7°	0.29
79°	-6.1°	0.29
80.5°	2.3°	0.15
81°	17.9°	0.08

6.8.2.4 Spruce Conifer

The measured attenuation pattern for this species of conifer can be seen in Figure 6-31. As can be seen, there are two nulls of particular interest at approximately 175° and 190°. The greater of the two being in the region of -52 dBm. A photograph of the spruce conifer within the anechoic chamber is presented in Figure 6-15. The polarisation patterns for these two nulls and points either side of the nulls are shown in Figure 6-32 to Figure 6-37. Table 6-4 shows the tilt angle and axial ratio for each of these rotation angles of the specimen along with values for a peak values from the attenuation pattern at 185°.

Table 6-4 Polarisation States for Spruce Conifer.

Rotation Angle	Tilt Angle	Axial Ratio
175°	26.2°	0.07
176°	4.2°	0.20
177°	82.2°	0.31
191.5°	76°	0.64
192.2°	69.6°	0.45
193°	73.2°	0.38
185°	81.2°	0.07

6.9 Deciduous Measurements

Presented in this section will be the results from the depolarisation studies performed on deciduous plants, namely the Ficus plant. The measurement method utilised is the same as for the coniferous measurements explained previously.

6.9.1 Deciduous Measurement Results

Three Ficus plants have been used and the structure of these trees is shown in Figure 4-17 along with a full size image of a leaf. The mean dimensions of these three trees was 160 cm in height and a foliage width of 75 cm.

The following sections present the data measured with each of the three Ficus trees in the path between the transmitter and receiver. Initially, a freespace measurement of the transmitted wave was performed and this gave values for the tilt angle of 90.1° and for the axial ratio 0.02 showing that the transmitted wave was a vertical linearly polarised wave.

For the most part, the polarisation patterns measured for the Ficus trees have not been included as they only show a small change in the tilt angle and axial ratio.

6.9.1.1 Ficus 1

Figure 6-38 presents the 360° attenuation pattern for this tree. As can be seen, there is only one null of any significance which is relatively small in comparison to the nulls viewed on other attenuation patterns. Figure 6-41 shows there is a relatively small amount of depolarisation. The tilt angle and axial ratio are in fact -85.6° and 0.10 respectively, indicating a relatively small change in the polarisation of the wave.

6.9.1.2 Ficus 2

The attenuation pattern for this tree is shown in Figure 6-39 and there are two nulls which are at 150.5° and 166.3° and have a signal strength in the region of -43 dBm. Table 6-5 shows the polarisation properties of the waves received at the specified rotation angles. From this information it can be seen that there has been a significant change in the tilt angle of the transmitted wave but a relatively small change in the axial ratio especially for the polarisation state measured at the rotation angle of 166.3°.

Table 6-5 Polarisation States for Ficus 2.

Rotation Angle	Tilt Angle	Axial Ratio
150.5°	9.7°	0.19
166.3°	2.6°	0.06

6.9.1.3 Ficus 3

The attenuation pattern measured when this tree was positioned in the Line-Of-Sight path between the transmitter and receiver is illustrated in Figure 6-40 where two deep nulls can be seen. The tilt angle and axial ratio of the wave received at this rotation angle and at angles about this point are displayed in Table 6-6. This was the most densely populated and homogenous of the three Ficus trees utilised in the experiment programme.

Table 6-6 Polarisation States for Ficus 3.

Rotation Angle	Tilt Angle	Axial Ratio
100°	72.1°	0.21
100.8°	1.75°	0.42
104°	81.2°	0.05
250°	93.9°	0.15
258°	-12.8°	0.38
258.8°	-5.4°	0.17
260°	97.1°	0.10

6.10 Interim Conclusion

The representation of a polarisation state by two parameters has been described together with how these values can be determined from the measured polarisation pattern. Also shown was how these two values relate to the position of a unique point on the surface of the Poincaré sphere. A number of methods for measuring the polarisation of a wave have been presented and discussed as well as the reasons for selecting the polarisation pattern method as a means of measuring the polarisation of the wave emanating from a body of vegetation.

An alternative method, the Knittel measurement method, which provides the same information as the polarisation pattern method was investigated and its applicability discussed. This method was found to be unable to provide results to the required degree of accuracy about the state of the wave received by the antenna. The accuracy not being obtained was due in part to the components of the receive system introducing errors into the measured signal.

Measurements investigating how vegetation depolarises a propagating signal have been performed and the results presented for a number of different trees, coniferous and broad leaf. From the measurements it can be seen that significant depolarisation takes place at the rotation angles which coincide with the measured nulls of the 360° attenuation patterns especially for the conifer trees. In some cases, it has been seen that the transmitted vertical linearly polarised wave has been depolarised to such an extent by the vegetation, that essentially a horizontally polarised wave has been received.

The depolarisation measurements on the broadleaf Ficus trees at the rotation angles which coincide with the attenuation nulls, generally show a smaller depolarisation in comparison to that seen in the measured depolarisation at the nulls of the conifer samples. This may be due to the relatively sparse distribution of the leaves in the plants used. In Ficus 3, a more homogenous specimen, more significant depolarisation appears to occur as a result of the increased number of components of the tree having currents induced. The various components are then

re-radiating the waves at different polarisations resulting in an overall depolarisation of the originally transmitted wave. Ficus 2 also showed a significant change in the incident wave in terms of the tilt angle but not the axial ratio.

The following chapter will discuss and assess the results presented in this chapter.

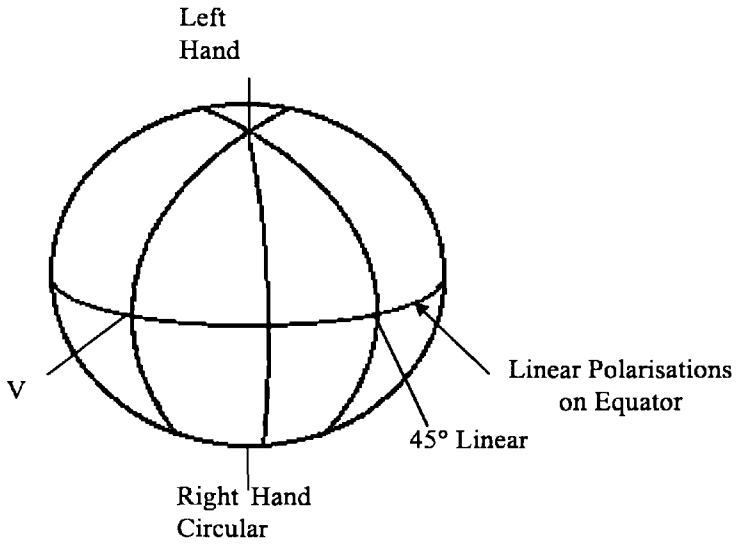

Figure 6-3 The Poincaré Sphere.

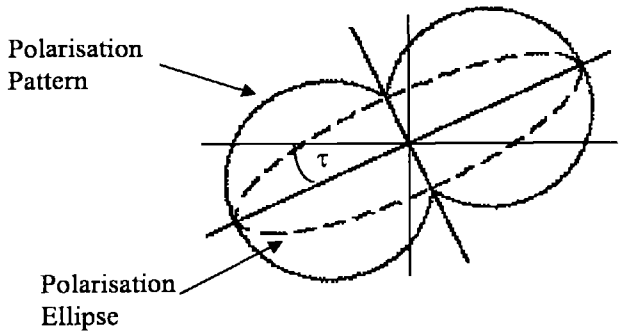

Figure 6-4 Polarisation Pattern.

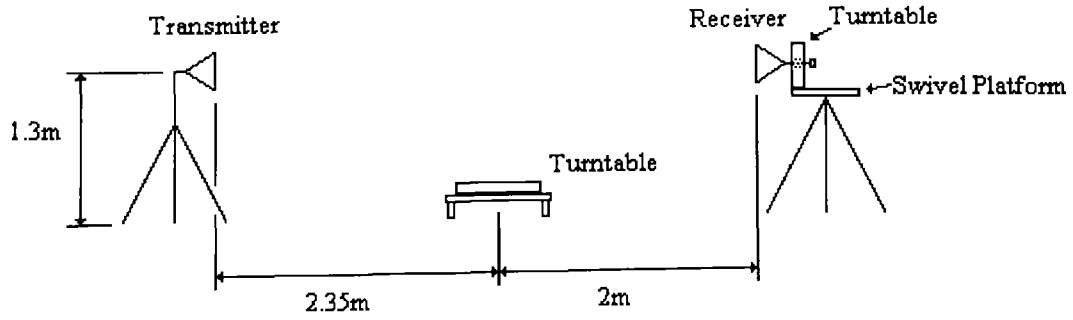

Figure 6-5 Depolarisation Measurement Geometry.

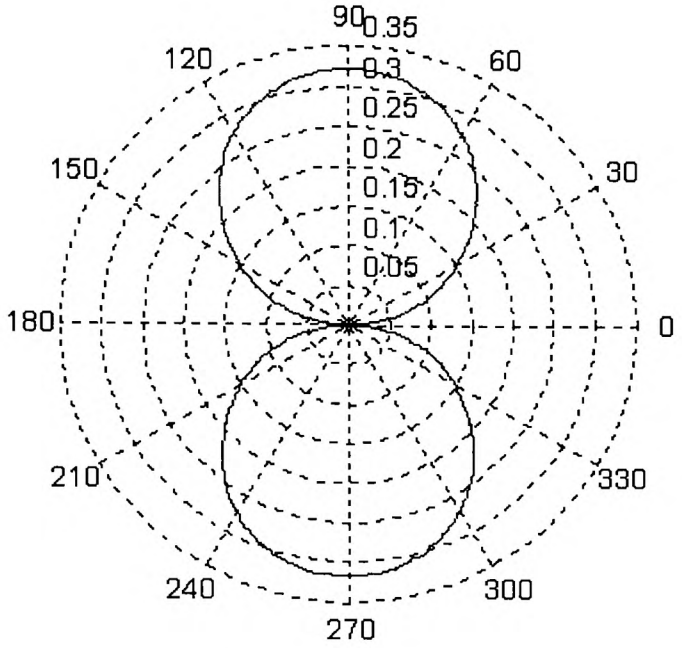

Figure 6-6 Freespace Polarisation Pattern.

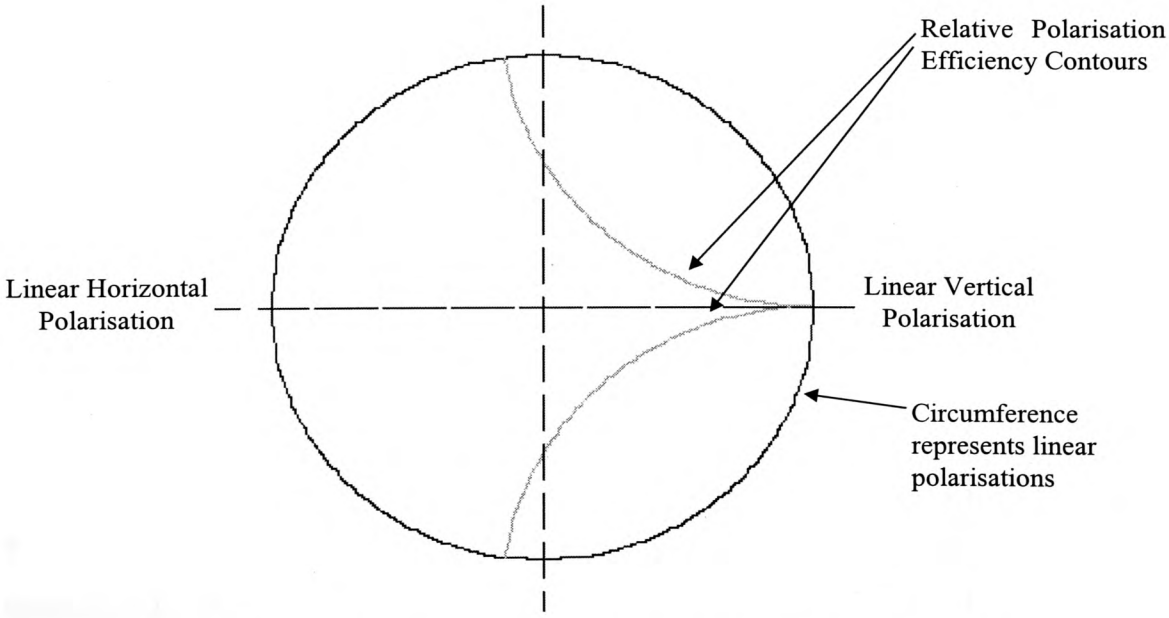

Figure 6-7 Stereographic Projection of Northern Hemisphere with two Contours.

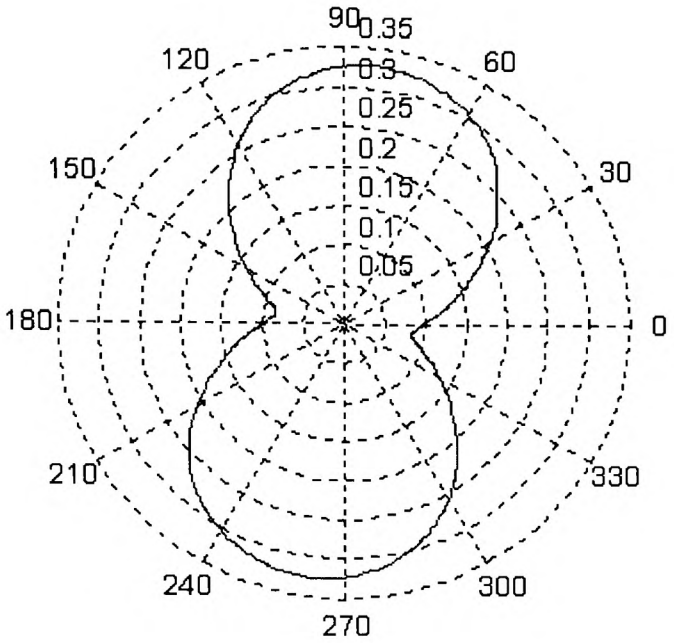

Figure 6-8 Polarisation Pattern with a Ficus Tree in the Path.

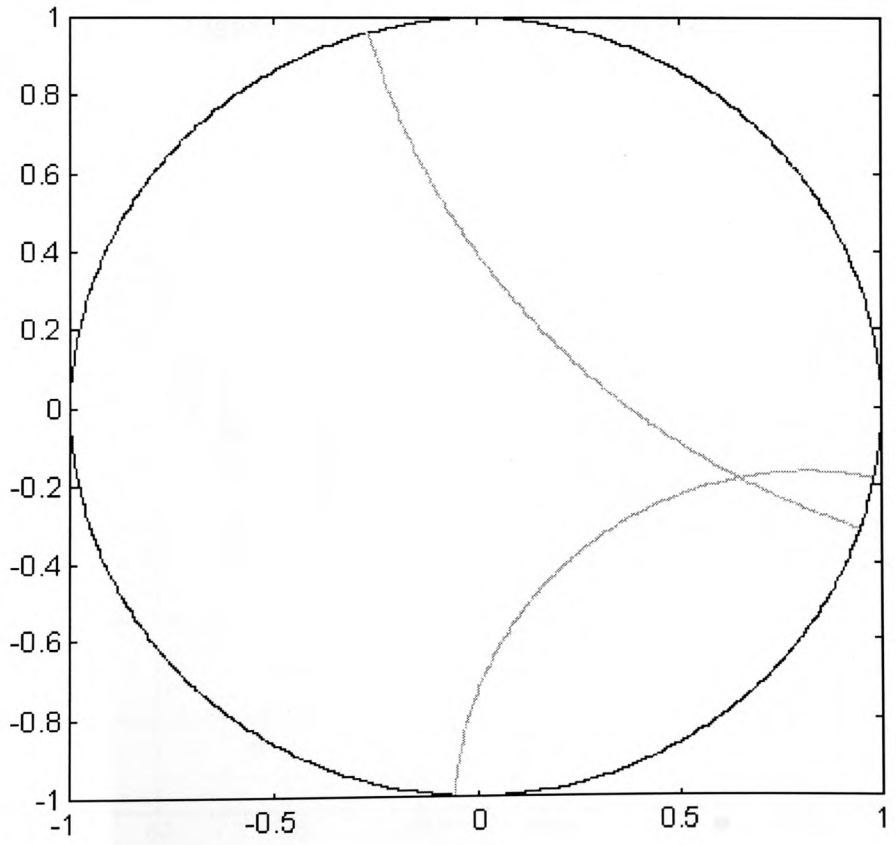

Figure 6-9 Knittel method applied to Data from Ficus Tree in the Path.

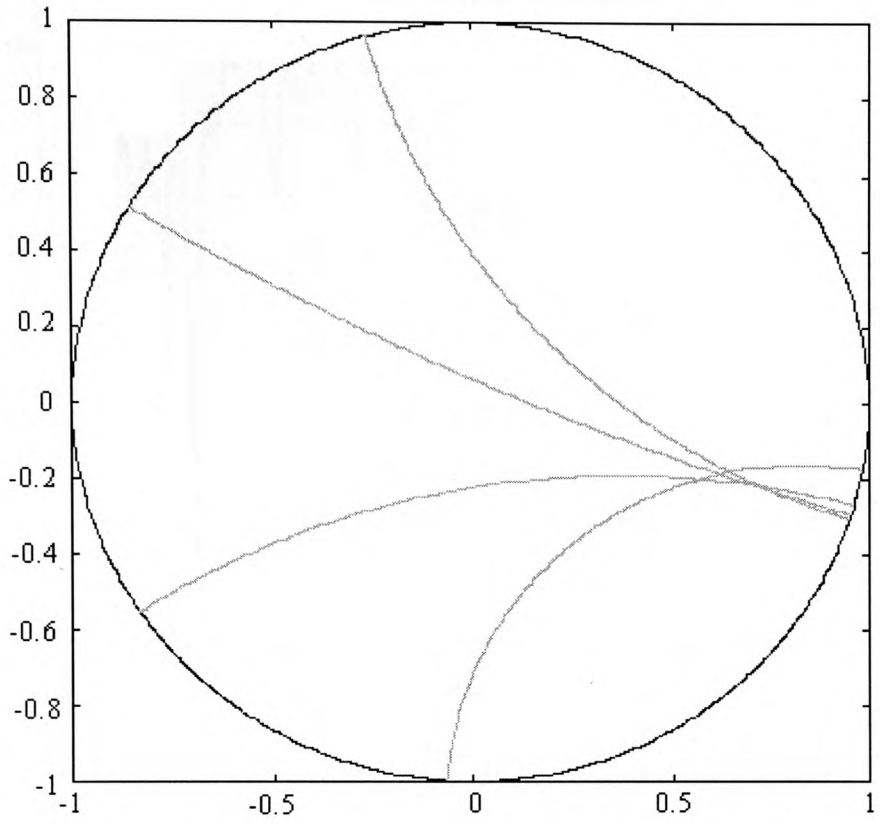

Figure 6-10 Errors in Knittel Method.

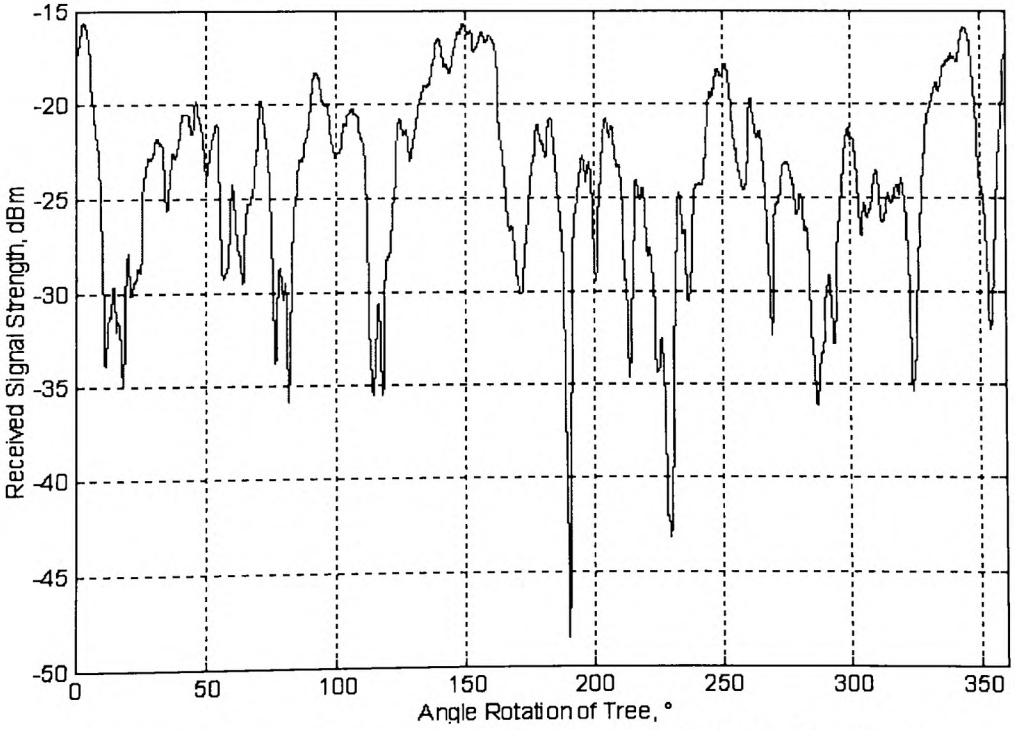

Figure 6-11 360° Attenuation Pattern of Cypress Conifer 1.

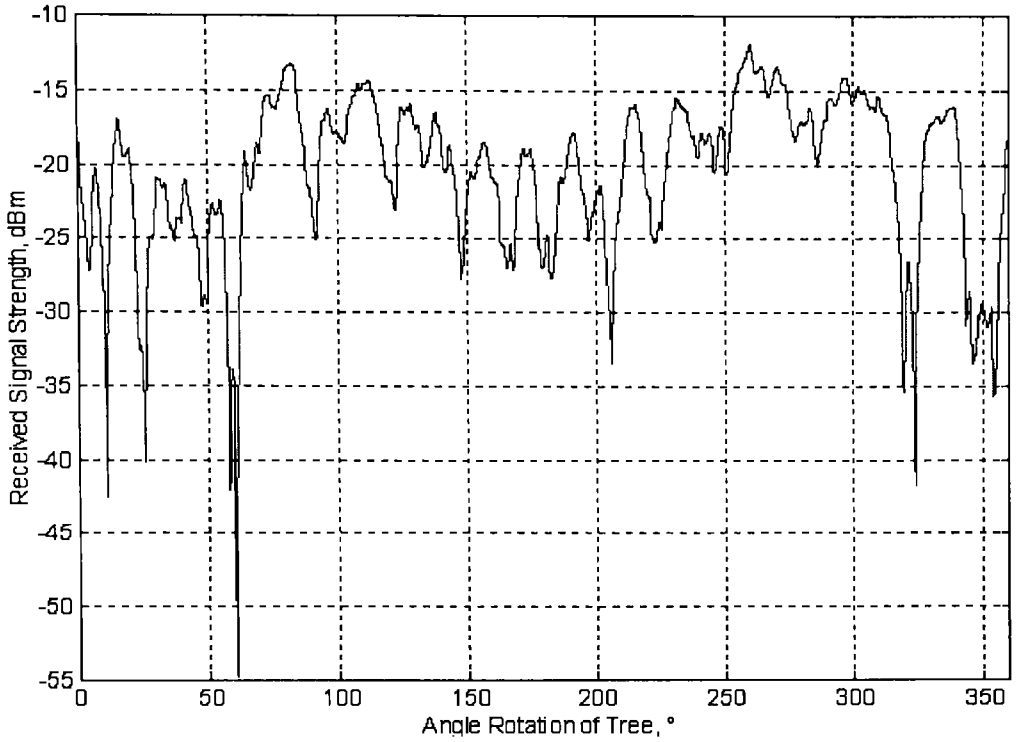

Figure 6-12 360° Attenuation Pattern of Cypress Conifer 2.

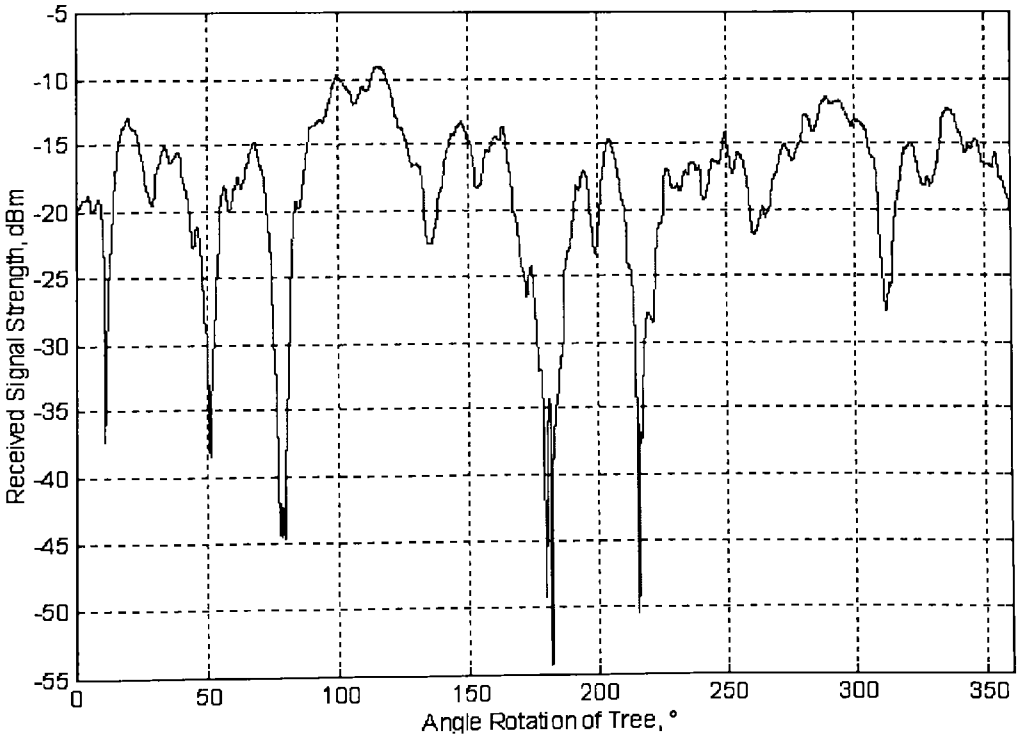

Figure 6-13 360° Attenuation Pattern of Cypress Conifer 3.

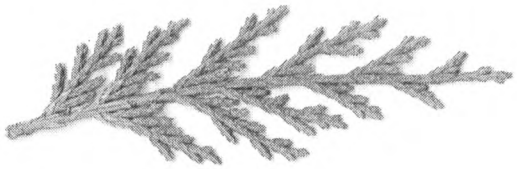

Figure 6-14 Leaves of the Cypress Conifer .

Figure 6-15 Spruce Conifer Inside the Anechoic Chamber.

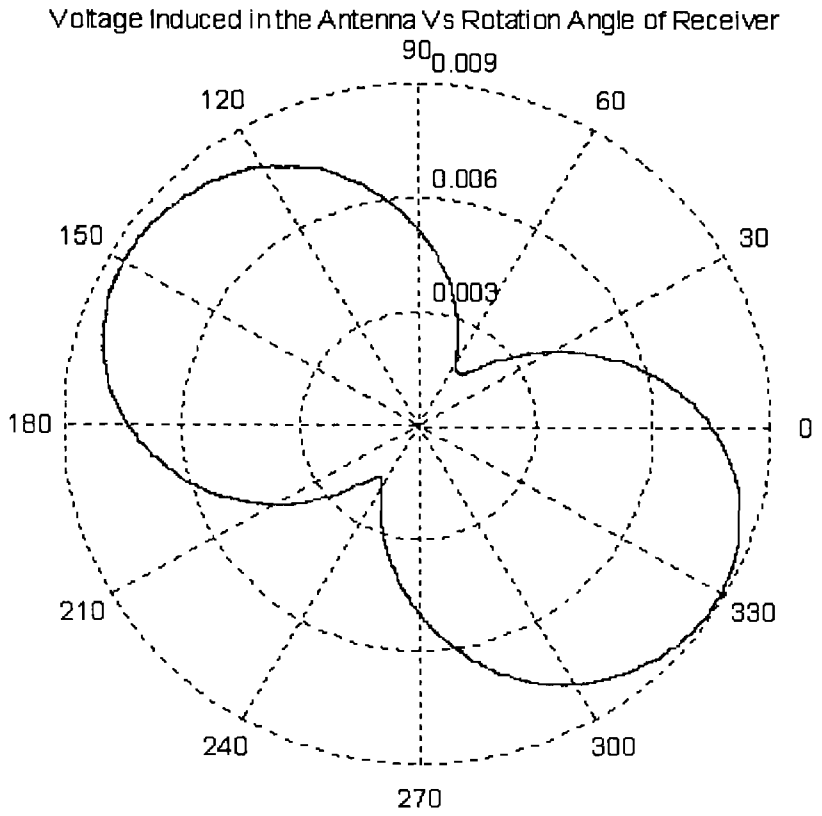

Figure 6-16 Polarisation Pattern at Rotation Angle of 189°.

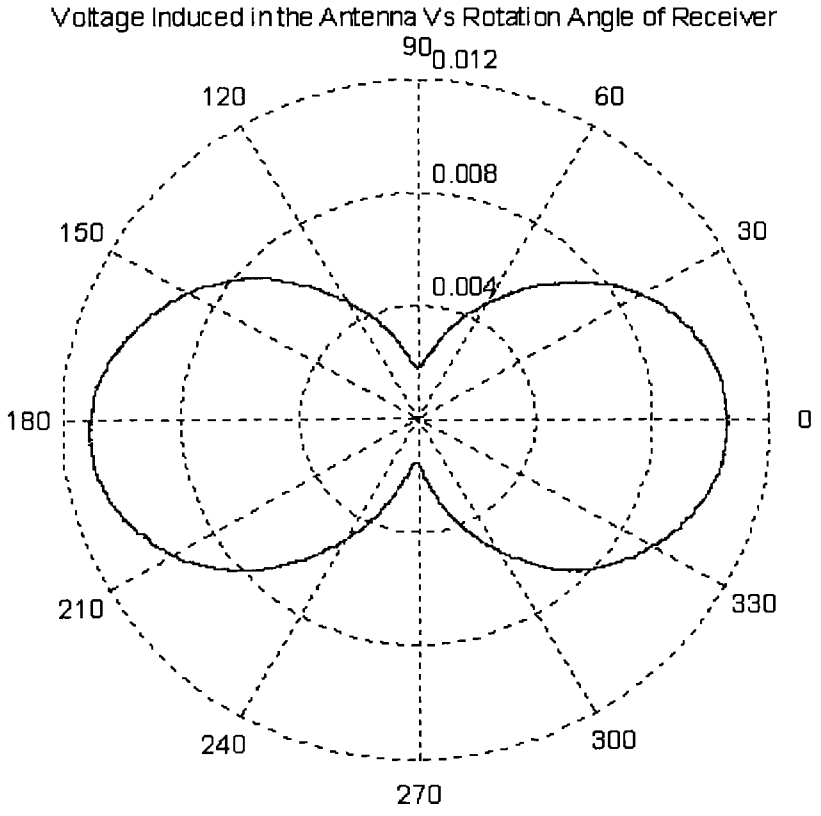

Figure 6-17 Polarisation Pattern at Rotation Angle of Null at 190.3°.

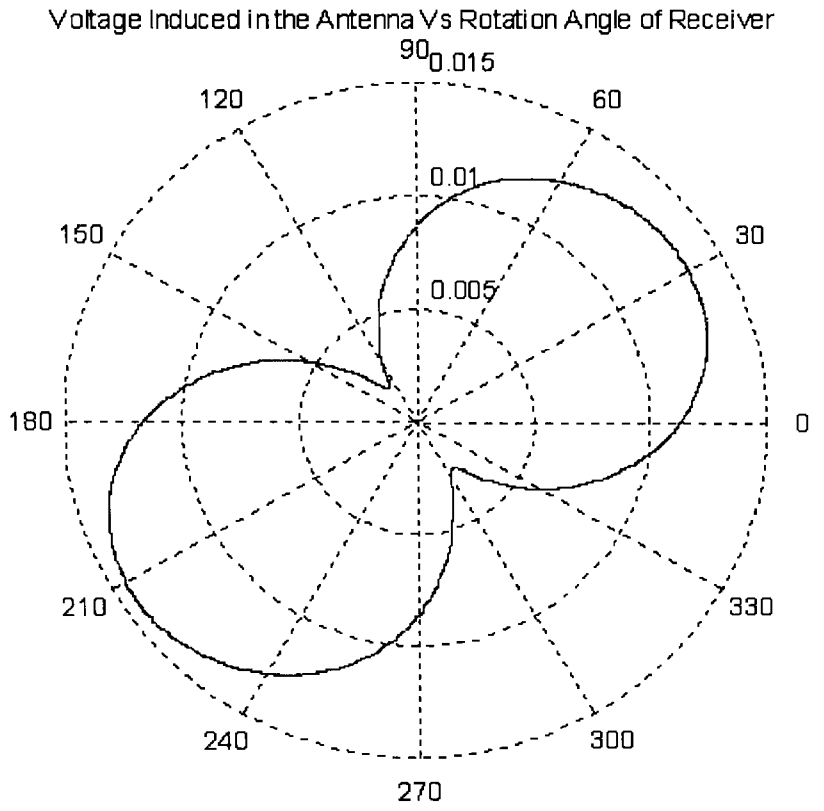

Figure 6-18 Polarisation Pattern at Rotation Angle of 192°.

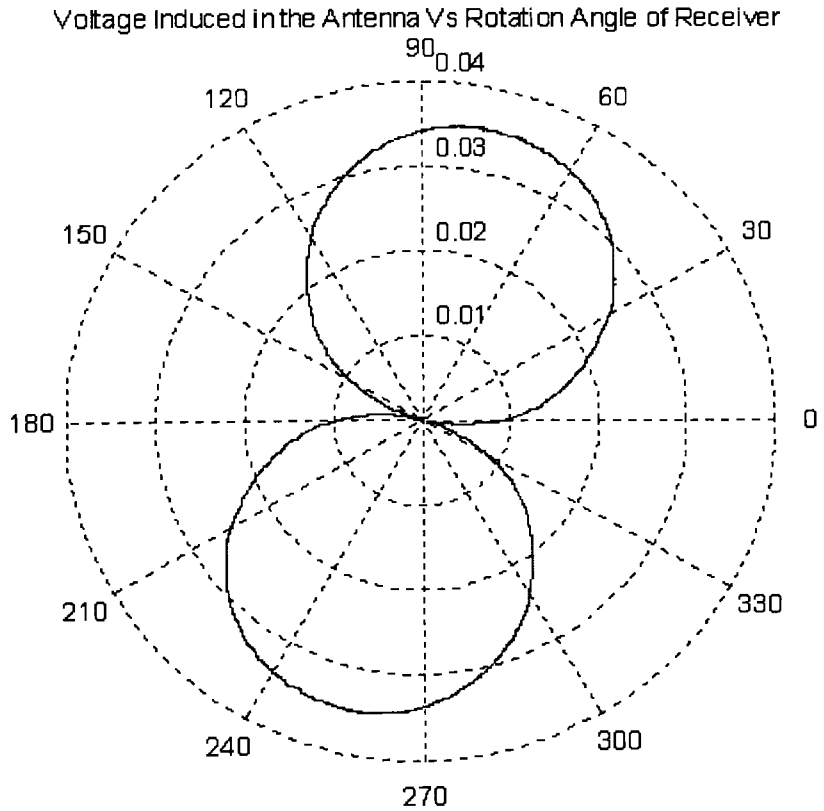

Figure 6-19 Polarisation Pattern at 151.5°, a Peak Value.

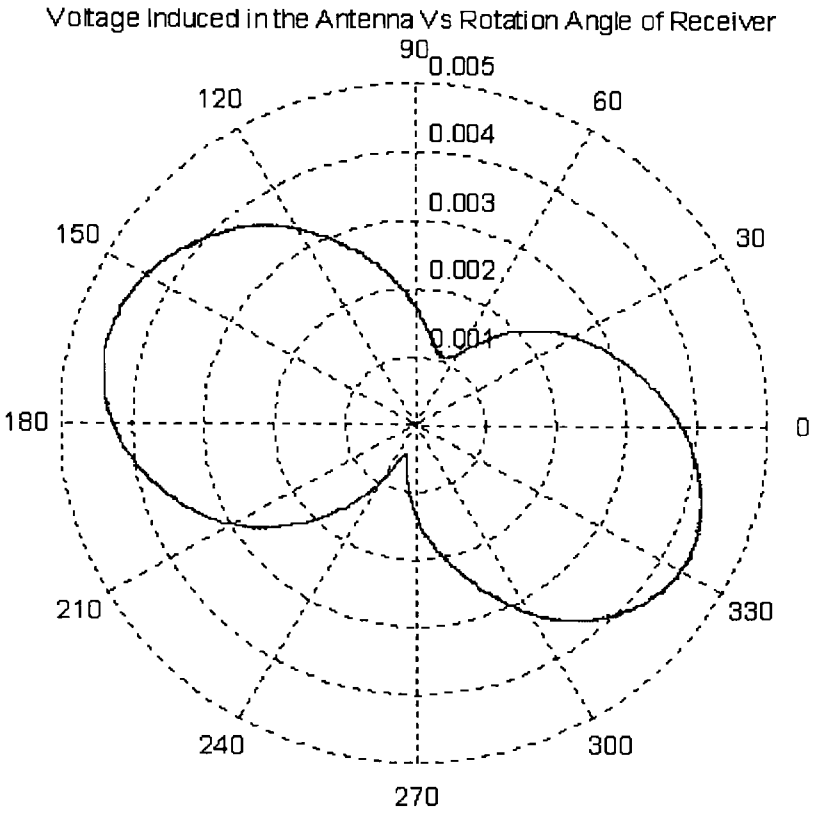

Figure 6-20 Polarisation Pattern at Rotation Angle of 60°.

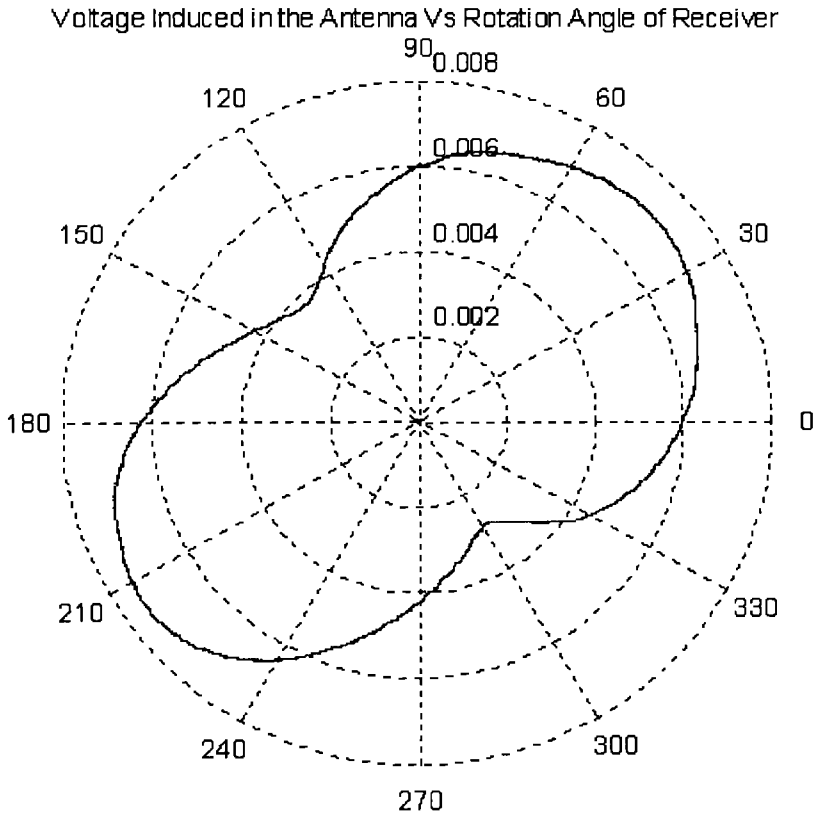

Figure 6-21 Polarisation Pattern at Rotation Angle of 61°.

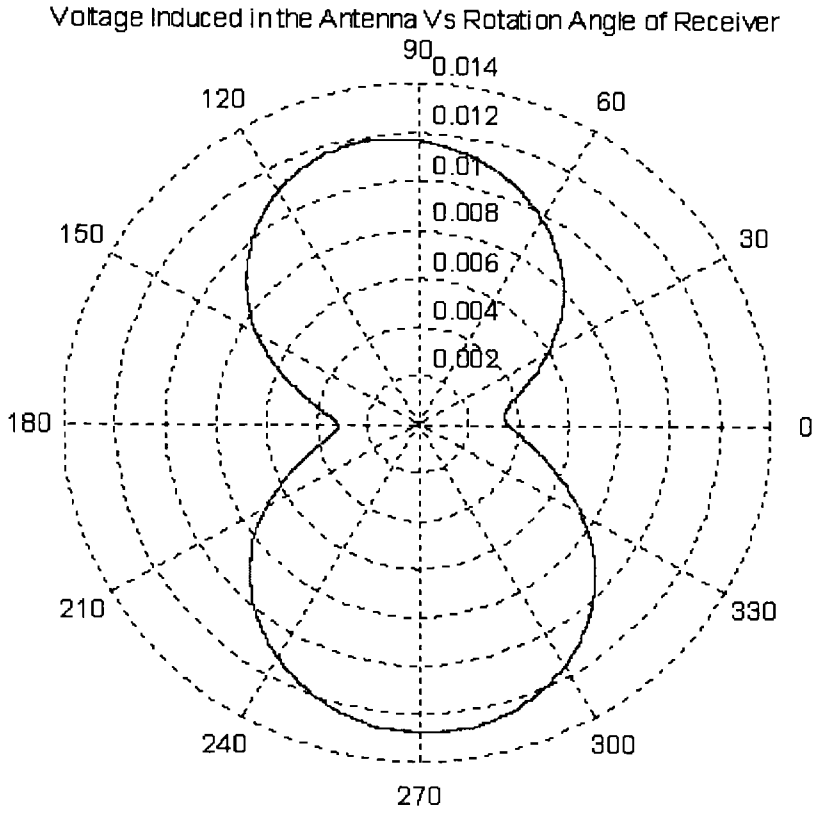

Figure 6-22 Polarisation Pattern at Rotation Angle of 321°.

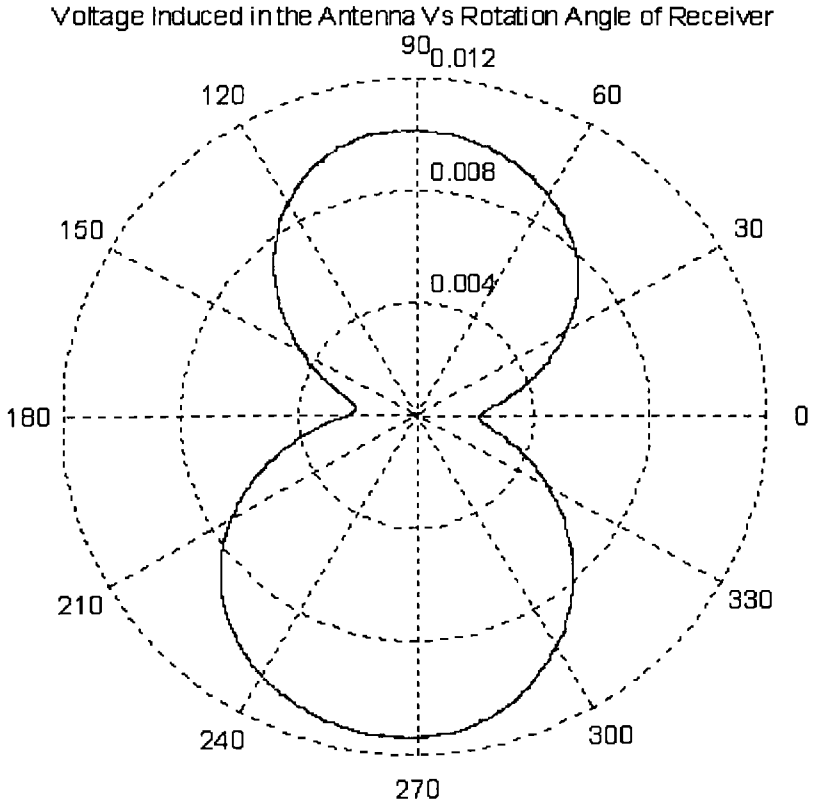

Figure 6-23 Polarisation Pattern at Rotation Angle of 323°.

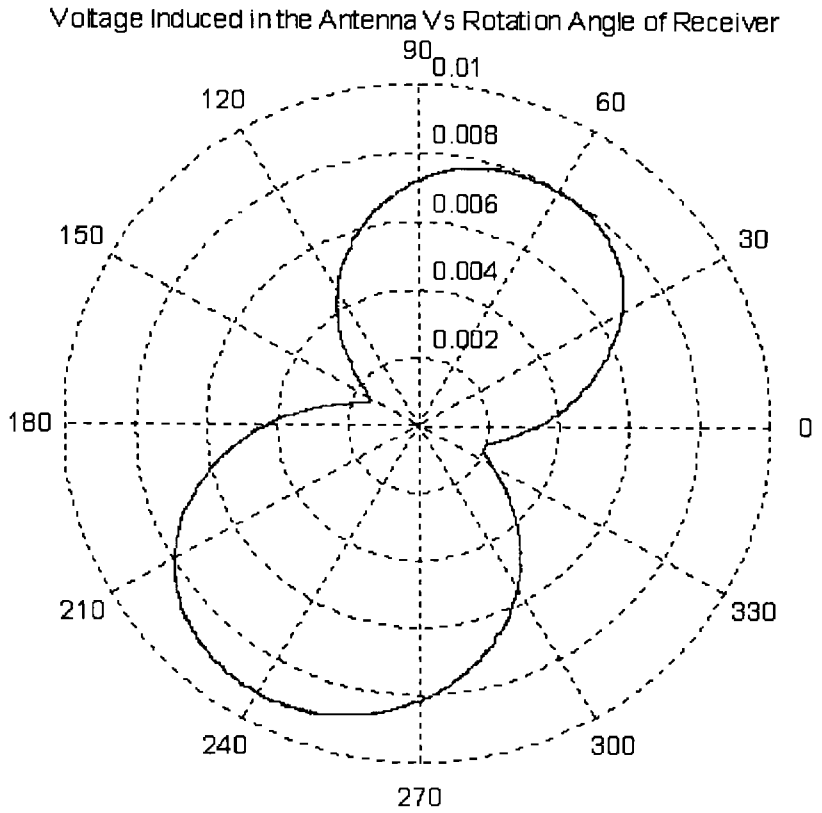

Figure 6-24 Polarisation Pattern at Rotation Angle of 324°.

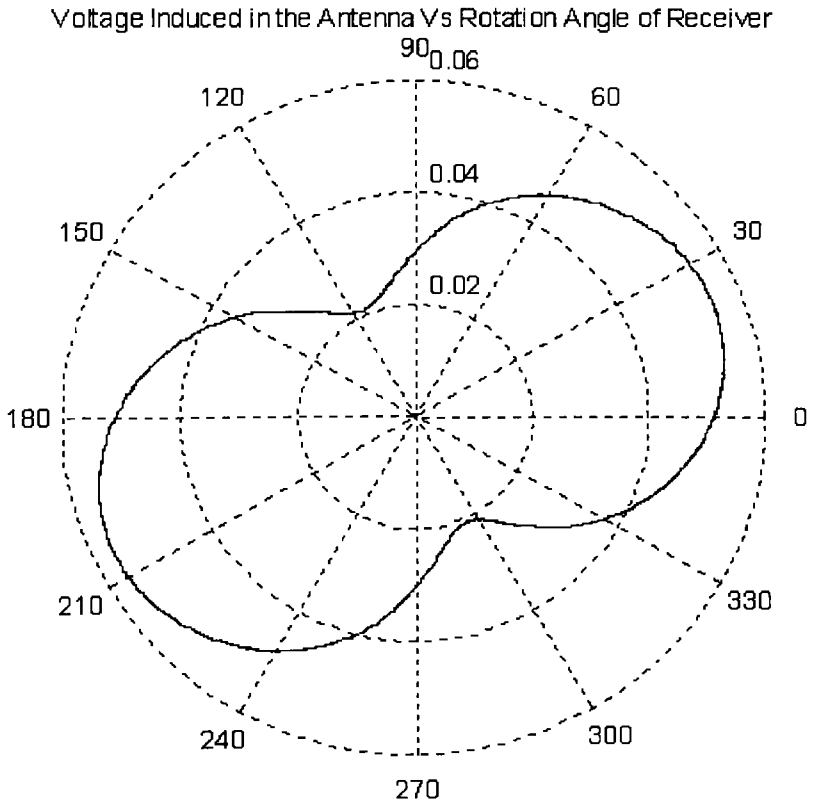

Figure 6-25 Polarisation Pattern at Rotation Angle of 50.5°.

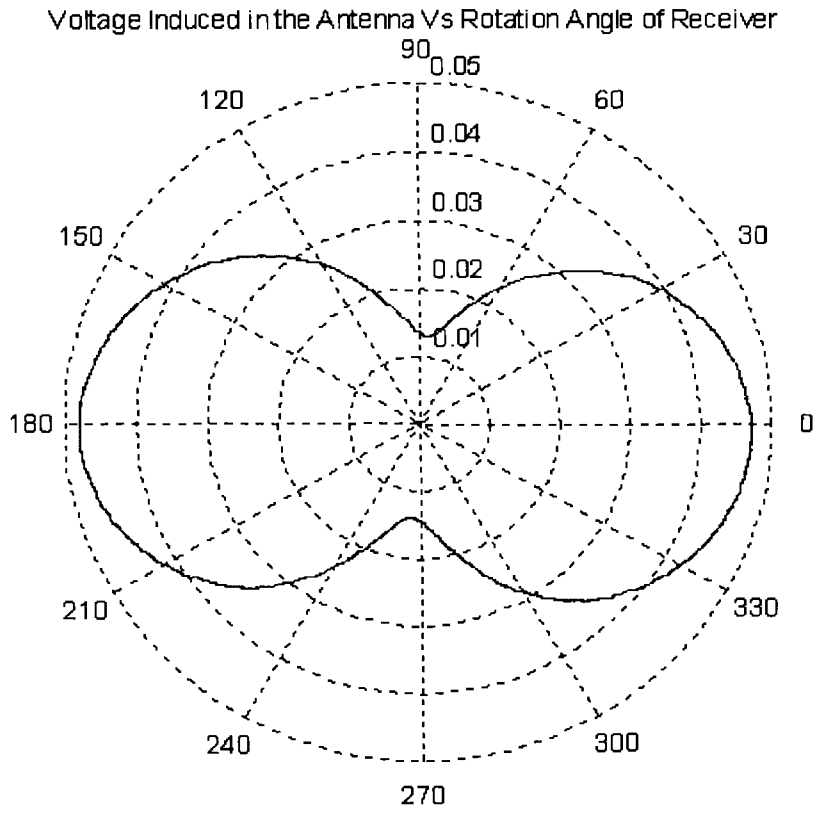

Figure 6-26 Polarisation Pattern at Rotation Angle of 51.1°.

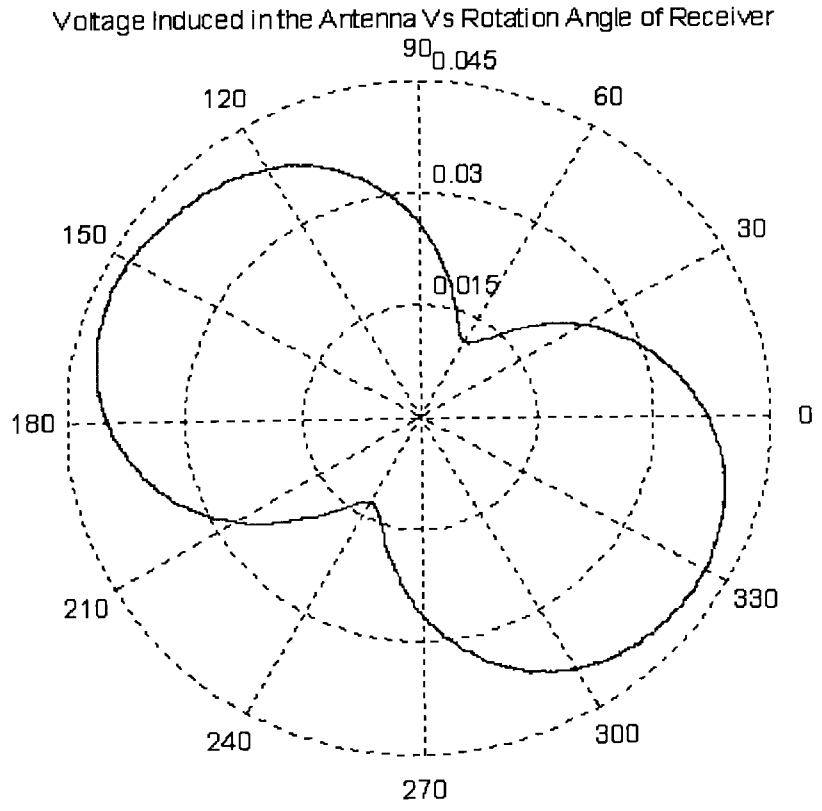

Figure 6-27 Polarisation Pattern at Rotation Angle of 52°.

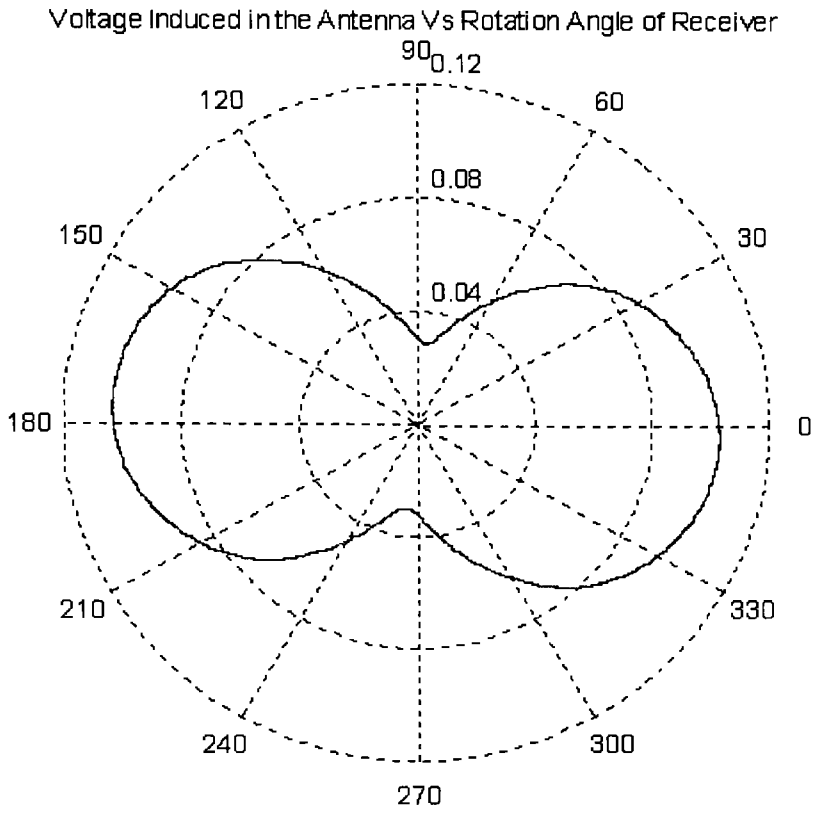

Figure 6-28 Polarisation Pattern at Rotation Angle of 79°.

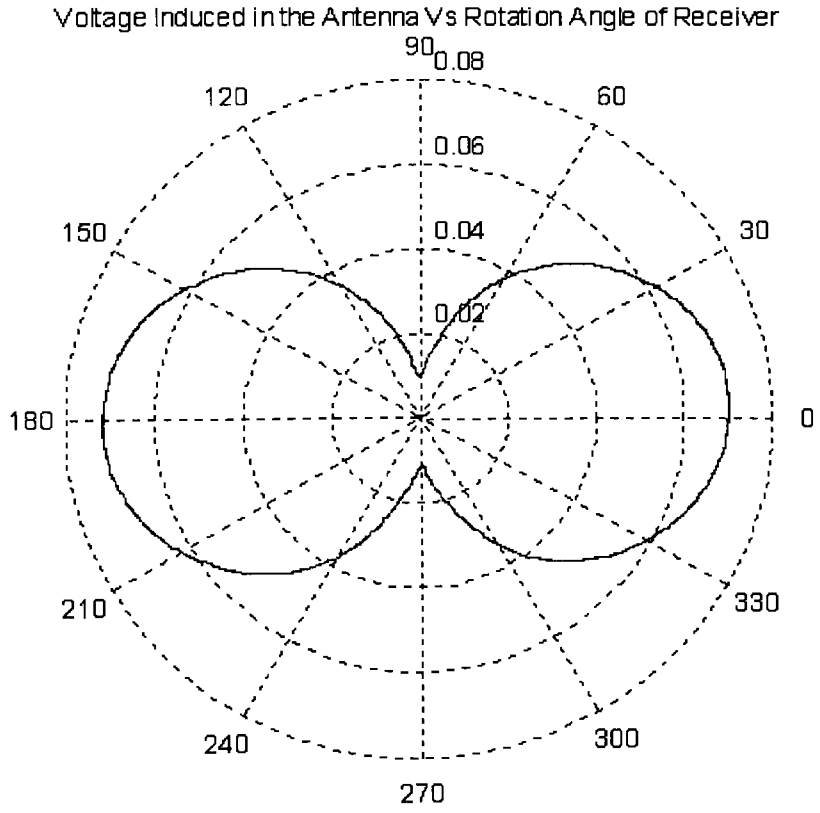

Figure 6-29 Polarisation Pattern at Rotation Angle of 80.5°.

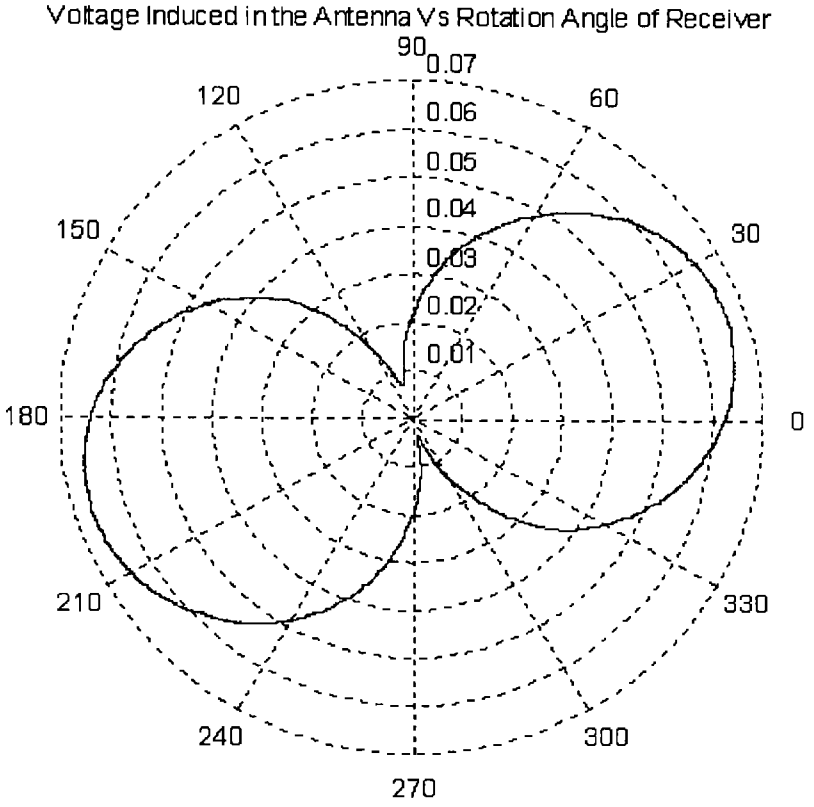

Figure 6-30 Polarisation Pattern at Rotation Angle of 81°.

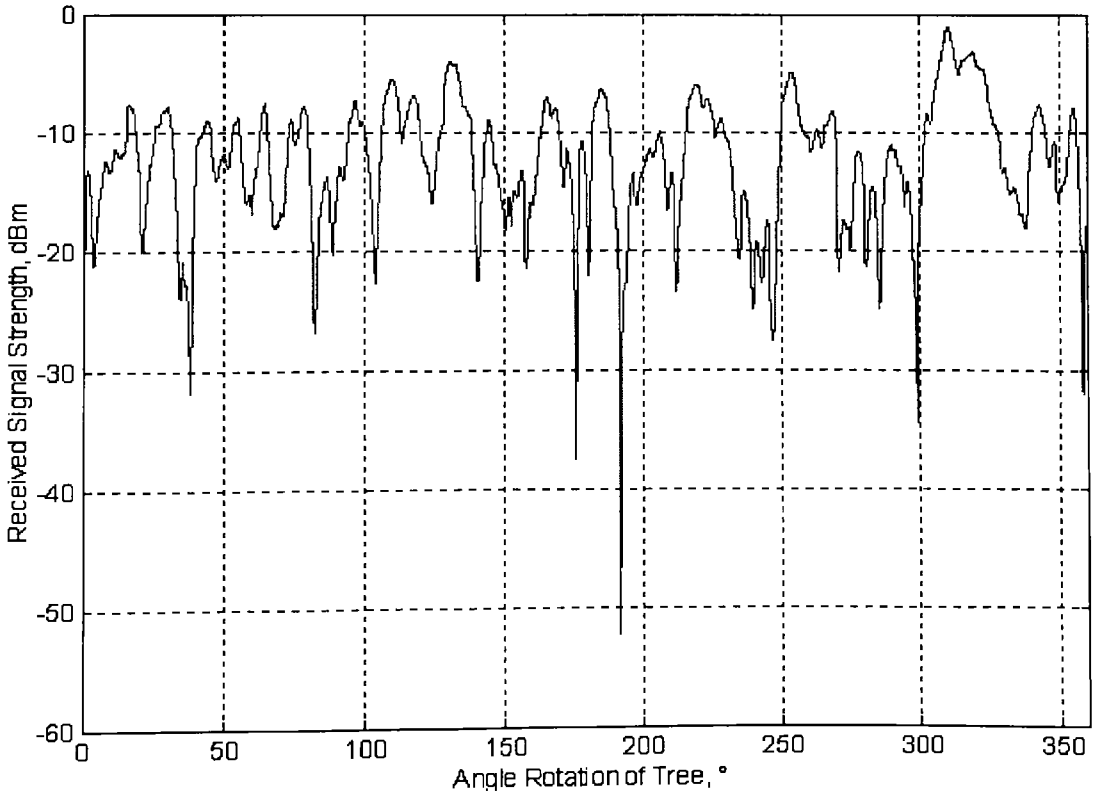

Figure 6-31 360° Attenuation Pattern of Spruce Conifer.

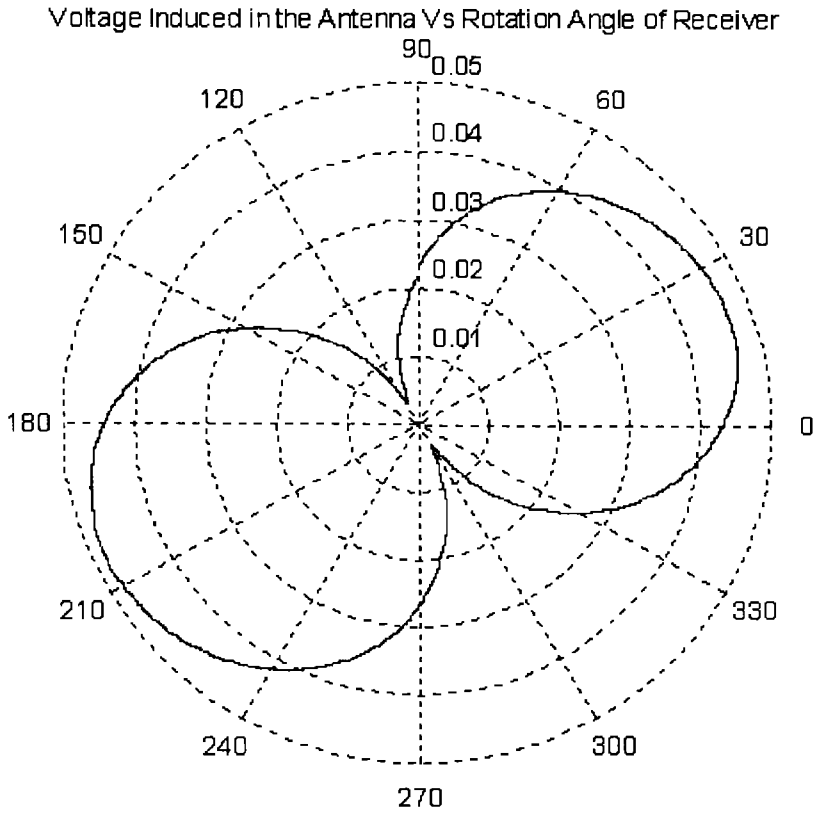

Figure 6-32 Polarisation Pattern at Rotation Angle 175°.

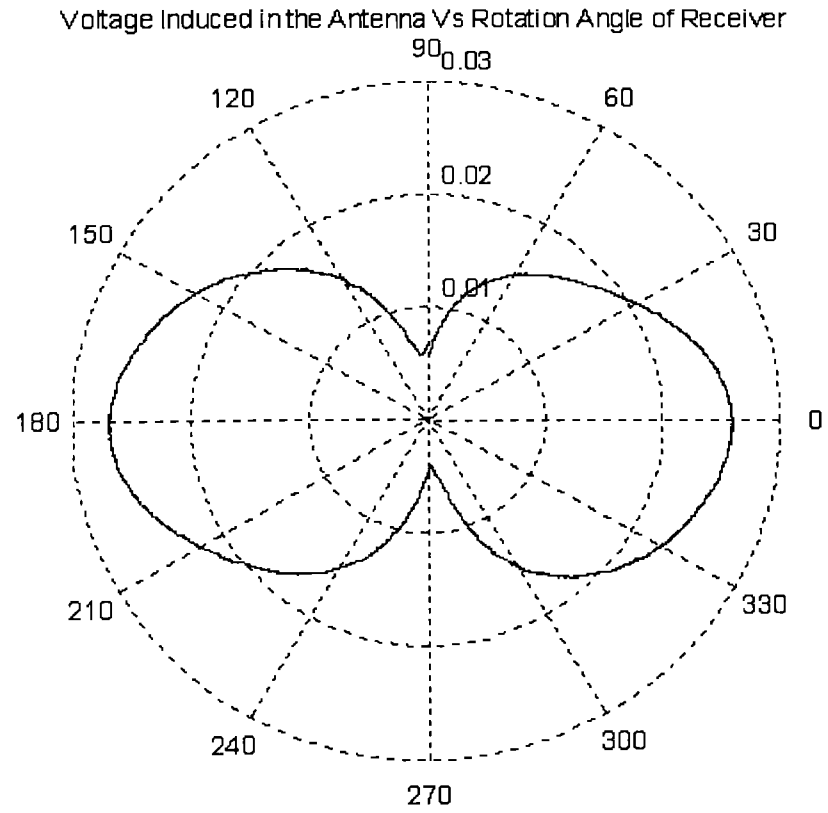

Figure 6-33 Polarisation Pattern at Rotation Angle of 176°.

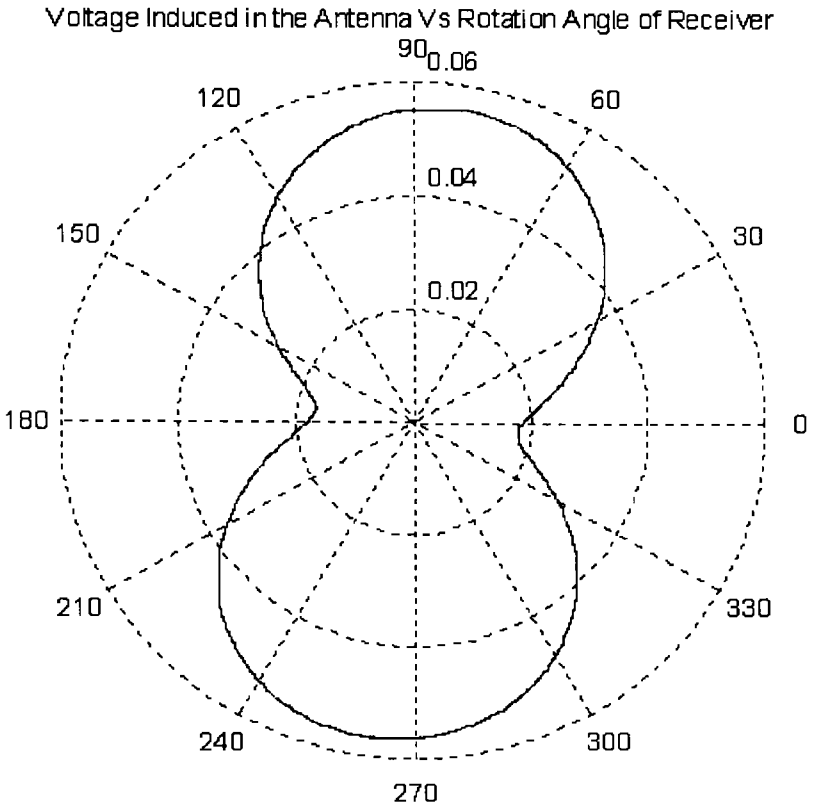

Figure 6-34 Polarisation Pattern at Rotation Angle of 177°.

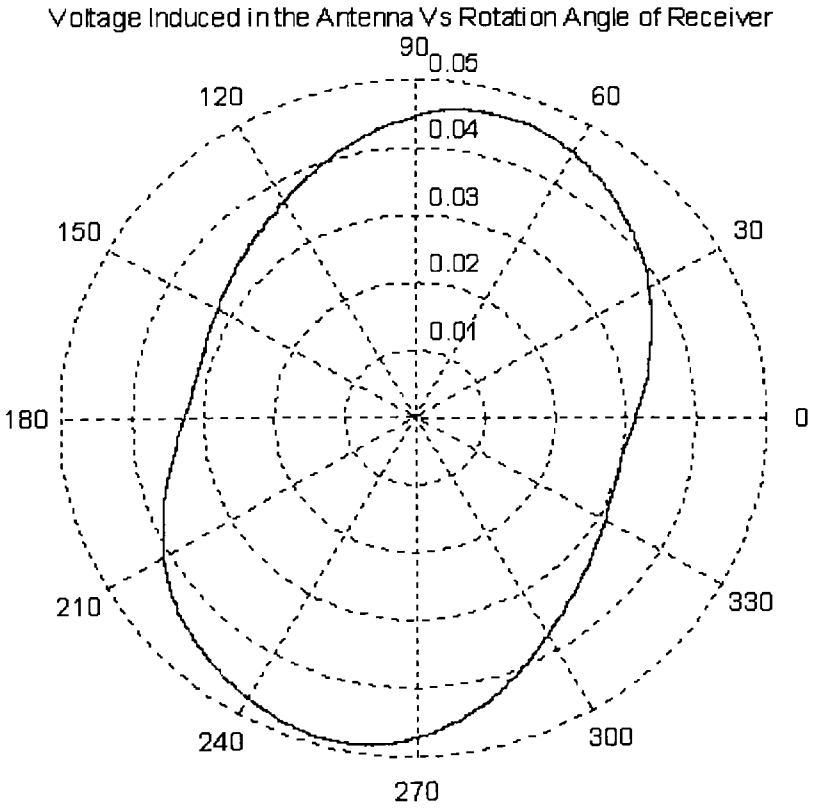

Figure 6-35 Polarisation Pattern at Rotation Angle of 191.5°.

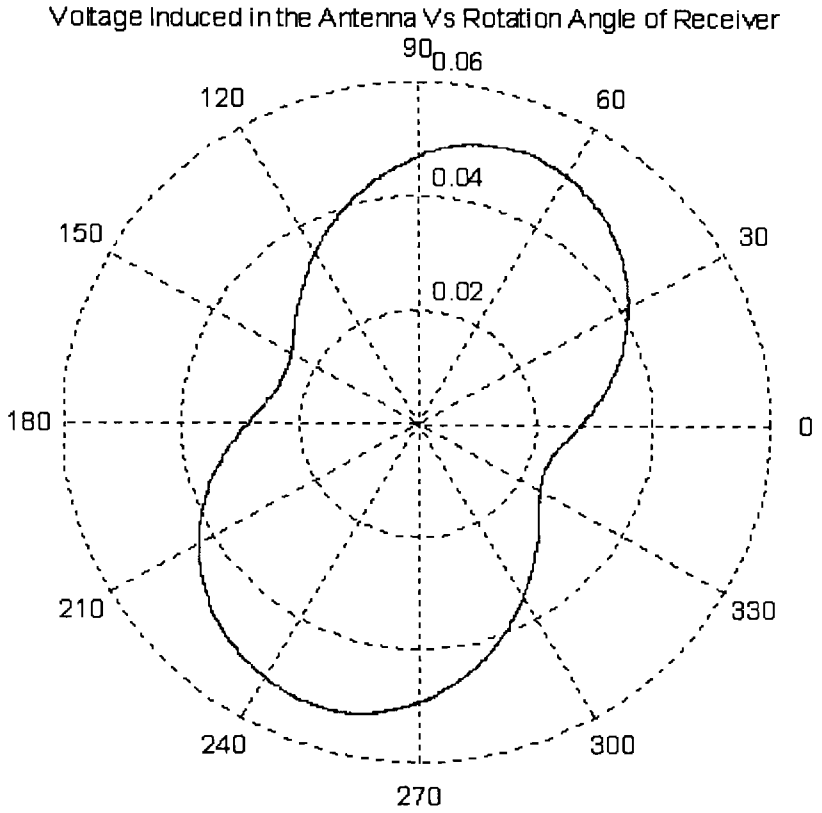

Figure 6-36 Polarisation Pattern at Rotation Angle of 192.2°.

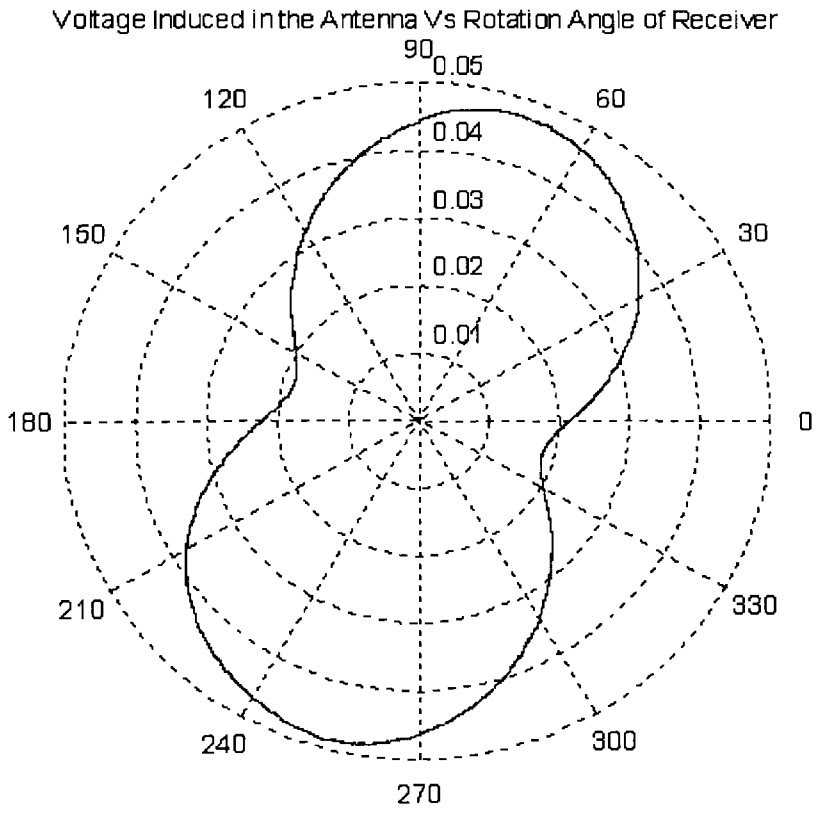

Figure 6-37 Polarisation Pattern at Rotation Angle of 193°.

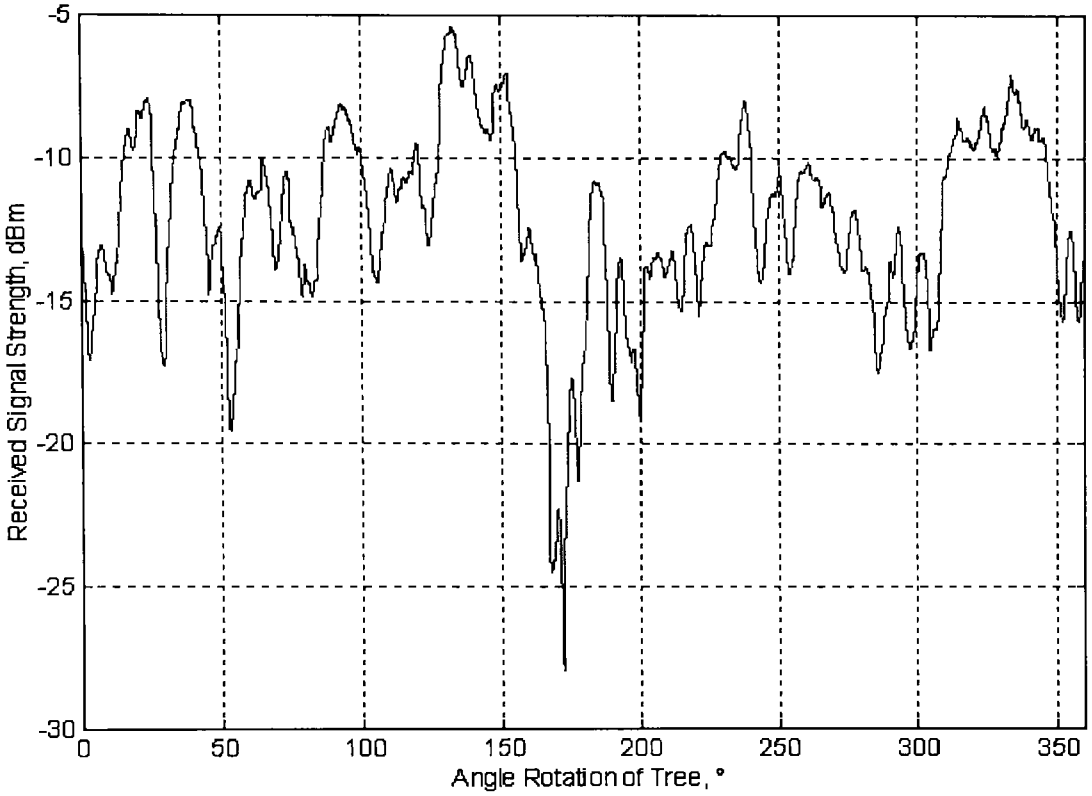

Figure 6-38 360° Attenuation Pattern of Ficus 1.

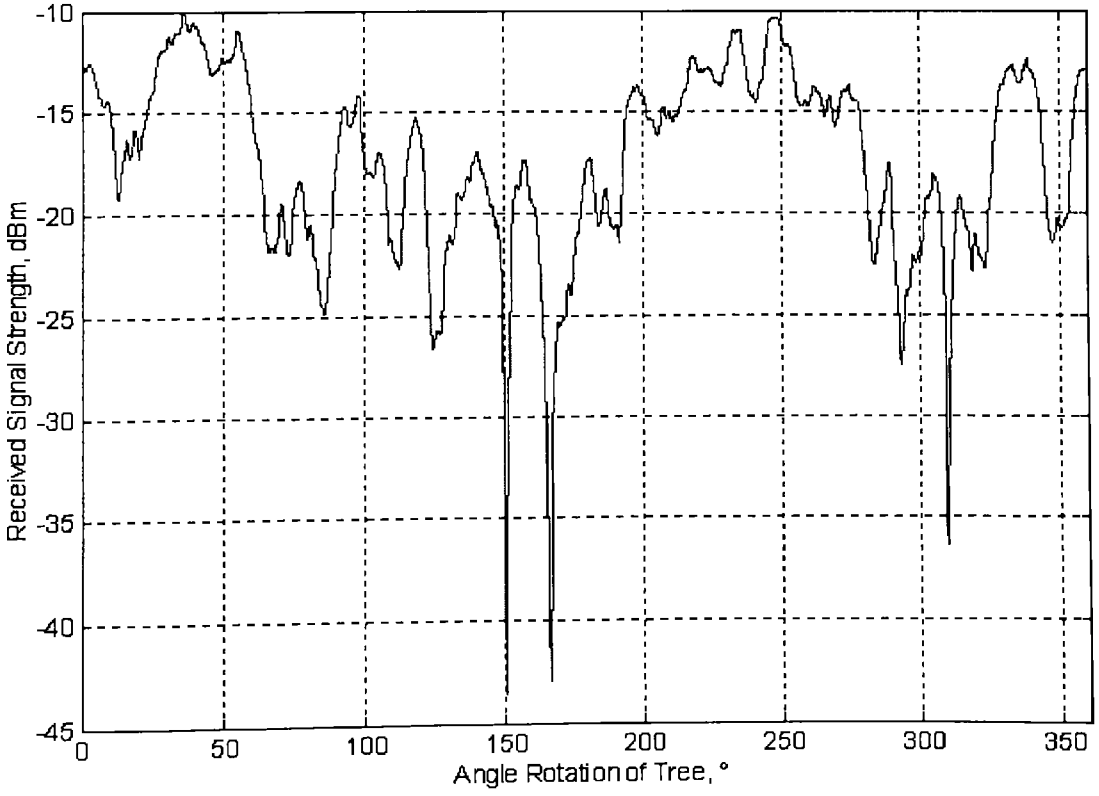

Figure 6-39 360° Attenuation Pattern of Ficus 2.

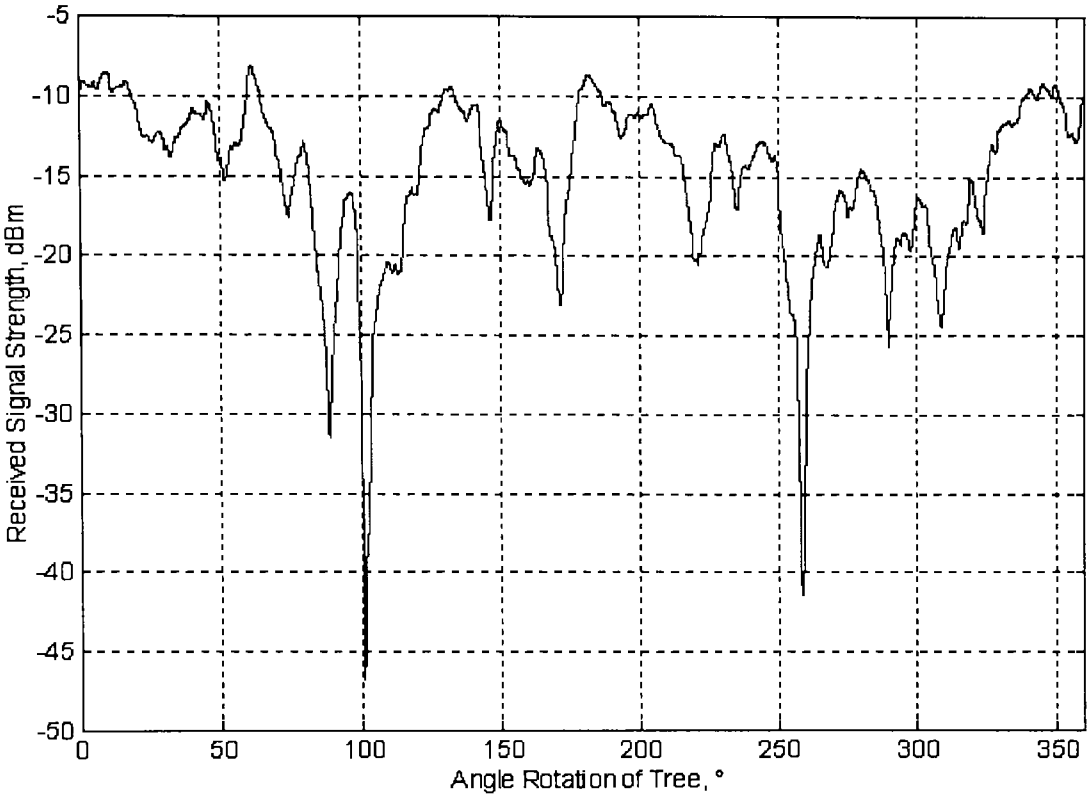

Figure 6-40 360° Attenuation Pattern of Ficus 3.

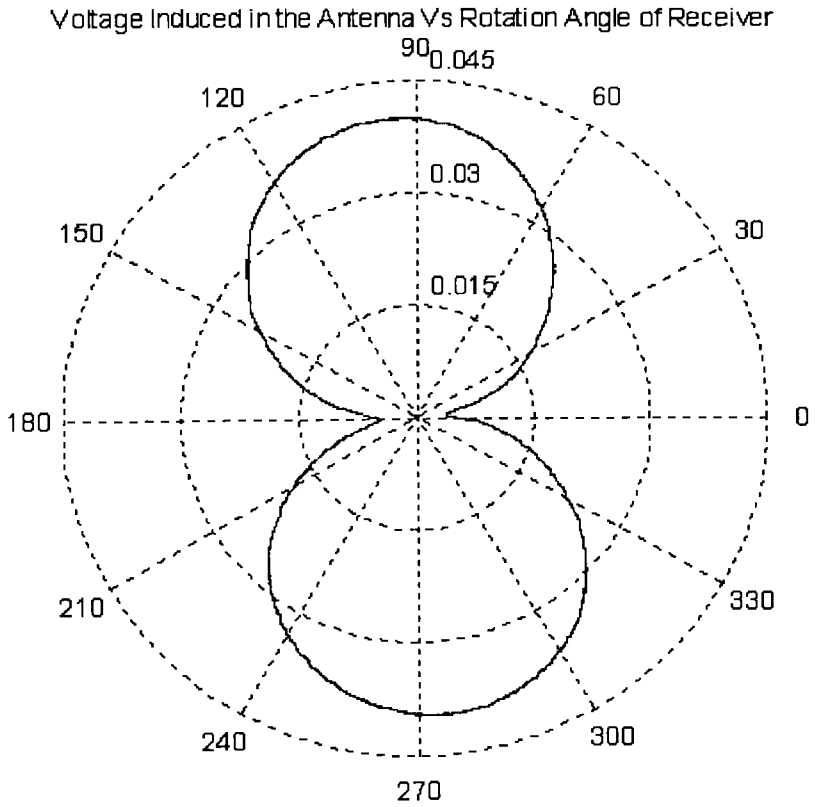

Figure 6-41 Polarisation Pattern at Rotation Angle of 172°.

7. Discussion of Depolarisation Results

7.1 Introduction

In this chapter the results from the depolarisation measurements using the different species of trees presented in Chapter 6 will be discussed and assessed. The discussion will involve examining how the vegetation media affects radiowave propagation, together with an investigation and discussion of the relationship between the depth of vegetation and the degree of depolarisation experienced by the transmitted signal. The issue of natural media converting a polarised field into a partially polarised field has been investigated and the results will be discussed. Partially polarised waves were investigated as during the initial polarisation measurements some of the measured waves did not exhibit a definite polarisation.

A depolarised wave has been taken to mean a change has taken place in the polarisation state of the signal from its original polarisation. Partial polarisation means that the received signal could not be said to have a definite polarisation state, this is explained within this chapter.

7.2 Discussion of Coniferous and Ficus Depolarisation Measurements

Initially in this measurement programme, a 360° attenuation pattern was generated for each tree specimen by measuring the received power at predetermined rotational steps of the tree being rotated through 360°. In this data, as can be seen in the relevant figures of Chapter 6, there are deep nulls in the co-polar signal which were not initially expected. Indeed, what was expected was a relatively small fluctuation of the received signal strength about a mean value. To investigate the cause of the deep nulls the state of polarisation of the field re-radiated by the tree was studied resulting in the measurement of the polarisation pattern in the vicinity of these nulls.

The nulls seen in the attenuation pattern measurements are believed to be the same as the smaller received signal levels seen when acquiring samples at some of the receiver positions when performing the vegetation attenuation measurements introduced in Chapter 4. This is reinforced by the fact that it is the collective and relative positions of the components which comprise the trees structure that cause the depolarisation of the incident field. With the outdoor measurements, the small signals levels are due to the components of the tree which because of wind, are moving in such a way as to cause an increase in absorption but also it is now believed, an increase in the amount of depolarisation generated by the random distribution of the scattering branches and leaves.

To measure the polarisation of the field falling upon the receiving antenna the polarisation pattern method was utilised as discussed in Chapter 6. Three different species of tree were used in this measurement programme and, as previously discussed, these were the Cypress conifer, a Spruce conifer and Ficus trees.

The main result of this programme, as can be seen from the data presented in Chapter 6, is that the greatest amount of depolarisation as indicated by the tilt angle corresponds to the angle in the attenuation pattern measurements where the large nulls in the measured data occur.

To investigate the possibility that at the angles of the nulls, the received power was attenuated in comparison to the power received at an angle where a null did not occur, the power in both the vertical and horizontal planes were extracted from the polarisation patterns along with the peak power detected. This information was taken from the polarisation patterns for the rotation angles of the trees in the tables of Chapter 6. The power in the vertical and horizontal planes as well as the peak power are shown in the following tables. Table 7-1, Table 7-2 and Table 7-3 show the power values described above for the cypress conifers 1, 2 and 3 respectively. The received power levels for the spruce conifer are presented in

Table 7-4, with Table 7-5 showing the values for the Ficus number 3 tree presented in Chapter 6.

Table 7-1 Signal Levels in Cypress Conifer 1 Polarisation States.

Description	Rotation Angle	Vertical Polarisation Power, dBm	Horizontal Polarisation Power, dBm	Peak Power, dBm
Peak	151.5°	-16.40	-27.27	-16.05
Pre-null	189°	-32.90	-29.57	-27.96
null	190.3°	-42.35	-26.31	-26.06
Post-null	192°	-28.26	-25.77	-23.81

Table 7-2 Signal Levels in Cypress Conifer 2 Polarisation States.

Description	Rotation Angle	Vertical Polarisation Power, dBm	Horizontal Polarisation Power, dBm	Peak Power, dBm
Pre-null	60°	-42.12	-34.92	-34.06
Post-null	61°	-32.95	-31.25	-29.33
Pre-null	321°	-25.25	-36.37	-24.84
Pre-null	323°	-26.35	-39.73	-25.84
null	324°	-29.31	-35.28	-27.74

Table 7-3 Signal Levels of Cypress Conifer 3 Polarisation States.

Description	Rotation Angle	Vertical Polarisation Power, dBm	Horizontal Polarisation Power, dBm	Peak Power, dBm
Pre-null	50.5°	-17.50	-12.79	-11.93
null	51.1°	-24.58	-13.47	-13.37
Post-null	52°	-18.59	-15.30	-14.34
Pre-null	79°	-17.01	-6.74	-6.67
null	80.5°	-26.29	-9.98	-9.87
Post-null	81°	-20.72	-10.98	-10.50

For conifer 1, the null in the attenuation pattern occurred at an angle of 190.3°. It is this which is presented along with values for angles either side of the null together with a peak value at an angle of 151.5°. As can be seen from the data presented in Table 7-1, the angle at which the null occurred (190.3°) is the rotation angle at which the vertically polarised transmitted wave has been depolarised to a

horizontally polarised wave. This depolarised wave is not completely linearly polarised as the measured axial ratio was 0.16 (Chapter 6, Table 6-1) indicating that the conifer tree has caused a significant change in both the tilt angle and axial ratio of the transmitted wave. It can be seen by comparing the peak power of the peak and null measurement that there has been a further loss of 10dB due to attenuation of the incident signal but in the vertical plane that there is an additional loss of 16dB due to the signal becoming depolarised. Resulting in an overall loss of 26dB of which the majority is due to the incident signal becoming depolarised. This can also been seen in the rest of the tables where there is a peak or mean to compare with a null.

For conifer 2 in Table 7-2, the angles of 60° and 61° are from either side of a null that is at a angle of 60.3°. The angle of 321° represents the peak between the two nulls seen at either side of this angle (see also Figure 6-10), the last angle (324°) being the one at which the null occurs. It can be seen, especially at the rotation angle of 61° and with reference to Table 6-2 in Chapter 6, that as the vertical and horizontal polarisation powers approach the same value that the tilt angle approaches 45°. The angles which are closest to or are at a null (60° and 324°) exhibit the greatest of energy that has been depolarised into the orthogonal plane, i.e. from the vertical to horizontal polarisation.

Table 7-3 shows the signal levels for the polarisation states of conifer 3. The nulls are at angles of 51.1° and 80.5°, with angles around these nulls being presented to allow for comparison. It can also be seen from the data presented in Table 7-3 that the rotation angles that represent the angles at which nulls were measured, show the greatest transformation of energy from vertical to horizontal polarised states.

For the spruce conifer presented in Table 7-4, the significant nulls occurred at angles of 175° and 192.2°, with angles relating to the rotation of the tree being presented around these nulls, together with the polarisation information at 185° which is a peak on the attenuation pattern shown in Figure 6-29. The peak

measured at the rotation angle of 185° exhibits the least amount of depolarisation and attenuation of the incident signal. This is as a result of the tree at this rotation angle presenting the least amount of vegetation, thus allowing the signal to propagate almost unhindered.

Table 7-4 Signal Levels of Spruce Conifer Polarisation States.

Description	Rotation Angle	Vertical Polarisation Power, dBm	Horizontal Polarisation Power, dBm	Peak Power, dBm
Null	175°	-19.35	-14.18	-13.30
Post-Null	176°	-32.13	-18.57	-18.39
Post-Null	177°	-12.06	-21.67	-11.93
Peak	185°	-6.45	-21.60	-6.19
Pre-Null	191.5°	-13.74	-16.88	-13.19
Null	192.2°	-13.34	-17.94	-12.51
Post-Null	193°	-13.87	-20.17	-13.22

The signal levels for Ficus 3 tree are shown in Table 7-5. The angles at which nulls were found in the attenuation pattern are 100.8° and 258.8°. Angles of rotation of the tree around the null are also shown. The measurement made at the rotation angle of 250° corresponds to a rotation angle that corresponds to the mean signal level measured during the attenuation pattern measurement. At this angle of 250° there is very little depolarisation of the incident signal. At a rotation angle that corresponds to a peak or the mean signal level the incident signal suffers the least amount of depolarisation.

Table 7-5 Signal Levels of Ficus 3 Polarisation States.

Description	Rotation Angle	Vertical Polarisation Power, dBm	Horizontal Polarisation Power, dBm	Peak Power, dBm
Pre-Null	100°	-27.7	-34.87	-26.10
Null	100.8°	-37.52	-34.73	-33.34
Post-Null	104°	-25.64	-40.80	-25.14
Mean	250°	-15.18	-30.69	-15.08
Pre-Null	258°	-32.73	-26.01	-25.64
Null	258.8°	-38.74	-27.20	-26.94
Post-Null	260°	-18.69	-35.15	-18.53

It can be seen from the data for the conifer trees presented in the above tables that the rotation angle of the null does not coincide with the weakest peak power. This indicates that at these rotation angles that the reduction in the signal strength measured is not solely due to absorption and scatter of the incident wave. In fact that a significant portion of the signal loss is due to the incident wave becoming depolarised. For the Ficus tree the rotation angle of the null does present the weakest power as well as the greatest amount of depolarisation in terms of the tilt angle. This contrast between these species is due to the difference in their physical structures. The Ficus tree is not as homogenous as the conifer trees and therefore, at certain rotation angles a greater density of foliage is presented, thus resulting in greater absorption and scattering of the incident field. The Ficus tree also has leaves which are larger than the wavelength at certain orientations, whereas the conifer leaves are all smaller in comparison to the wavelength of 1.5 cm. The nulls in the attenuation pattern of the Ficus tree correspond to a point where the leaves of the Ficus tree are orientated so that a greater number of them are seen to be larger than the wavelength, thereby creating an increase in the amount of absorption and scattering of the wave incident upon the tree. Thus resulting in greater signal loss and depolarisation of the incident signal. The conifer trees leaves in comparison do not create much absorption and scatter but at certain rotation angles fields are re-radiated due to the orientation of the various components of the tree which results in a change in the polarisation state of the signal.

A greater portion of the reduction in the received vertically polarised power for the conifers is due to the energy being randomly depolarised to other states. This occurs as a result of the orientation of the branches and twigs through which currents are induced, resulting in an overall depolarisation of the incident field.

7.3 Relation Between Increase Depth Attenuation Measurements and Depolarisation

It can be seen in the depth attenuation measurements presented in the figures of Chapter 4 that at various depths large variations were measured in the received signal strength, as represented by the vertical lines. At some depths, such as in Figure 4-5 at a depth of 20 metres for the in-leaf curve, it can be seen that there is greater variation below the mean measured value. This is believed to be due to the incident signal becoming depolarised, resulting in a small number of the sixty measurements being recorded at a much reduced signal strength. This depolarisation is caused by the various components of the tree re-radiating the currents induced in them such that an overall depolarised field results. The extent of this depolarisation is altered by the wind which causes movement of the trees' components resulting in a differing amount of depolarisation for each position of the various parts of the tree.

It can be seen in the figures of Chapter 4 that at some depths there is a greater than expected attenuation, such as at 20metres and just after 40 metres for the in-leaf data of Figure 4-5. This is believed to be due to the propagating wave being depolarised in one direction, say towards a tilt angle of -90°, by the vegetation at that depth of vegetation. Whilst the next section of vegetation depolarises the wave in the opposite direction (towards a tilt angle of +90°) resulting in the decrease in the amount of attenuation in the vertical plane (measurements made with vertically polarised antennas) that the vegetation loss curve presents.

7.4 Vegetation Depth Dependence

In this section the investigation into examining a possible relationship between an increasing depth of vegetation and an increase in the amount of depolarisation suffered by a propagating signal is presented and evaluated. The depth dependence has been investigated using both the Cypress conifers and the Ficus trees.

A varying number of trees were used in the study and for these measurements all of the trees were placed at an equal height, one behind each other in the direct path between the transmitter and the receiver. The measurements were performed within the confines of the anechoic chamber to eliminate external influences. The method employed in performing these measurements is explained in the following paragraphs.

For the two tree measurements, one tree was placed in the path between the transmitter and receiver and the polarisation pattern of the wave emitted from the foliage was measured. The second tree was placed behind the first tree and in line with the antennas. The polarisation pattern of the radiowave after it had propagated through the two trees was also measured. The first tree was removed from the chamber and once again, the polarisation pattern of the wave being emitted from the second tree was measured. This method enabled the individual and the cumulative effects of the trees on the transmitted wave to be investigated.

The three tree measurements consisted of the same first two stages of the two tree method, followed by placing the third tree behind the second so that all of the trees were in a line orientated along the direct path between the transmit and receive antennas. With the third tree in place, the polarisation pattern was measured. The first tree measured was removed and the combined effects of the second and third trees on the propagating wave was measured. After this, the second tree was removed and the effect of the third tree was measured. Before removing the second tree, its position within the chamber was recorded. The third tree was removed and the second tree was replaced in its original position and the effect of this tree on the transmitted wave was measured. The three tree measurements were only performed on the conifer trees as only two Ficus plants were available.

The above procedures were repeated a number of times and some of the results are presented in Table 7-6 and Table 7-7 for the two and three conifer tree

measurements respectfully. Table 7-8 shows the measurement results for the two Ficus tree measurements.

Table 7-6 Polarisation Information for Two Conifer Trees.

Conifer 1		Conifer 2		Both Conifers	
Tilt Angle	Axial Ratio	Tilt Angle	Axial Ratio	Tilt Angle	Axial Ratio
-72.9°	0.21	-76.7°	0.13	-71.4°	0.07
-79.6°	0.09	-79.1°	0.22	-74°	0.13
86.4°	0.08	57.5°	0.13	-84.3°	0.36
73.1°	0.17	66.8°	0.08	-84.9°	0.38
-30.8°	0.52	-78.8°	0.07	12.9°	0.70

Table 7-7 Polarisation Information for Three Conifer Trees.

Conifer 1		Conifer 2		Conifer 3		All Conifers	
Tilt Angle	Axial Ratio	Tilt Angle	Axial Ratio	Tilt Angle	Axial Ratio	Tilt Angle	Axial Ratio
-88.8°	0.15	83.2°	0.19	84.6°	0.20	43.9°	0.46
82.9°	0.15	83.2°	0.19	76.4°	0.19	26.9°	0.46
-63°	0.07	72.3°	0.49	76.4°	0.19	30.8°	0.09

Table 7-8 Polarisation Information for Two Ficus Trees.

Ficus 2		Ficus 3		Both Ficus	
Tilt Angle	Axial Ratio	Tilt Angle	Axial Ratio	Tilt Angle	Axial Ratio
-58.2°	0.38	66.1°	0.44	39.2°	0.09
-58.2°	0.38	88.5°	0.02	-69.4°	0.09
-78°	0.11	88.5°	0.02	-73.5°	0.08

For the measurements made for a depth of two conifers the amount of depolarisation has increased in terms of either the tilt angle or the axial ratio for each of the measurements presented in Table 7-6. As can be seen in Table 7-7, where three conifer trees were in the path, there is a definite increase in the amount of depolarisation in terms of the tilt angle and also in two of the three measurements in terms of the axial ratio in comparison to the effect of the individual trees. This general trend indicates a possible correlation between an

increasing depth of vegetation and increasing depolarisation for the conifer species.

The Ficus measurements do not show the same general trend as the conifer measurements. The reason for this difference is due to the physical attributes of each species where the Ficus trees are not as dense or homogenous as the conifer trees.

Therefore, it would seem that there is a correlation between an increasing depth of vegetation and an increase in the degree of depolarisation of the transmitted wave for the conifer trees. This would appear to hold true for vegetation media that is homogenous and fairly dense when seen from the wavelength of the transmitted wave. This situation is less conclusive in the case of the Ficus trees which are not dense or homogenous.

As well as the density and homogeneity of the medium being a factor in determining the amount of depolarisation, the orientation of the branches, twigs and leaves also need to be considered when determining the amount of depolarisation [Beckmann, 1968].

Of course, with an increase in depth of vegetation comes an increase in the attenuation of the propagating signal so, if a large volume of densely vegetated media was being used as a shield between two transmissions of orthogonally polarised signals at the same frequency, there is a high probability that there would not be a problem of interference between the two channels. If the depth of vegetation was not sufficient to cause a large enough attenuation of either signal then there could be enough signal strength depolarised into the orthogonal plane resulting in interference of the other channel.

Initially, at the beginning of the depolarisation studies it was thought that the amount of depolarisation in terms of tilt angle and axial ratio caused by a given body of vegetation could be predicted. Unfortunately as can be seen from the

various measurement data, this is not possible as there is a large amount of variability in the depolarisation for any given depth of vegetation. This variability being due to the number of previously mentioned factors, such as the orientation of the branches and leaves as well as the size of the leaves, which need to be considered in trying to determine the amount of depolarisation. The general trend of this data does however point towards a correlation between an increasing depth of homogenous vegetation and an increase in the amount of depolarisation of the incident vertically polarised field.

7.5 Partial Polarisation

Whilst investigating how vegetation depolarises the transmitted signal, the results from some measurements showed a partially polarised wave, Figure 7-1. This is due to vegetation being a natural medium which causes random scattering. The conductivity of the media allows currents to be induced that are orientated in the generally random direction of the leaves, branches and twigs. This produces an overall depolarisation of the propagating wave which may result in a partially polarised wave. As can be seen in the polarisation pattern presented in Figure 7-1, the polarisation pattern is not clearly defined and the polarisation ellipse can not be uniquely constructed. This is termed a partially polarised wave. The vegetation in this case has caused the incident signal to be depolarised into a partially polarised wave, though only slightly as the polarisation pattern is recognisable as being very close to that expected for a definite polarisation state.

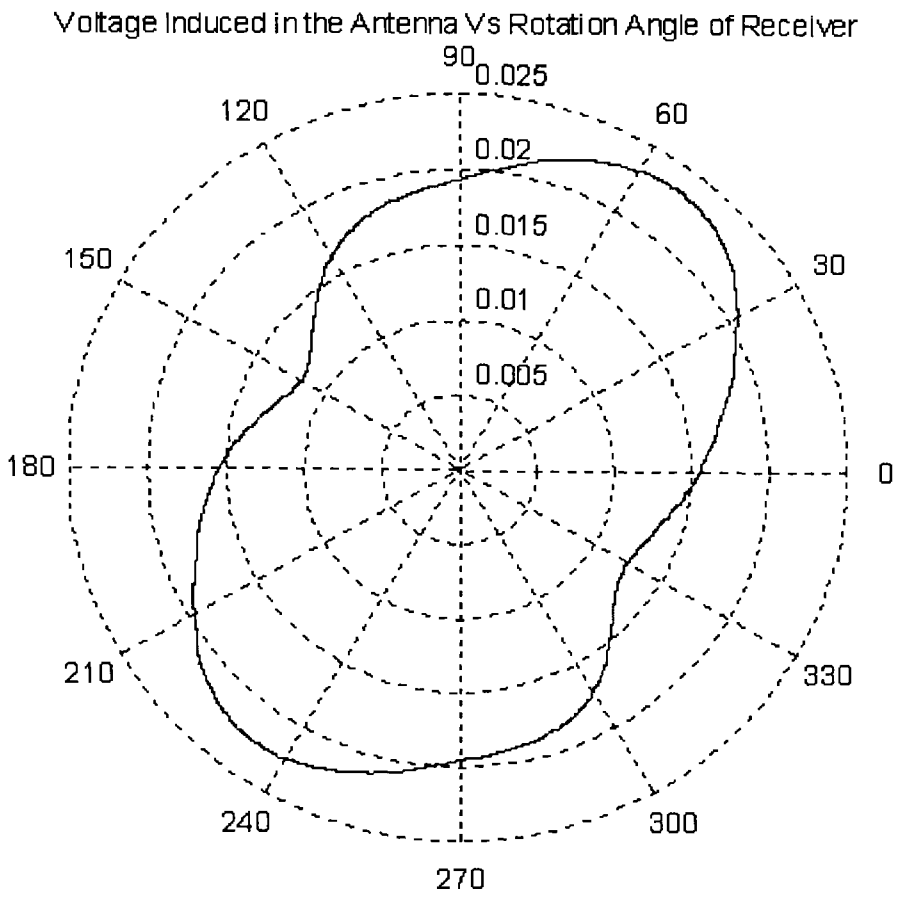

Figure 7-1 A Partially Polarised State of Polarisation.

It has been stated that most, if not all surfaces of natural objects cause the polarised transmitted signal to be degenerated to a partially polarised wave [van Zyl, 1986]. For the vegetation that has been investigated, this does not seem to be the case even for the highly depolarised waves. It is possible, and indeed likely, that at greater depths of vegetation, the wave emanating from the opposite side to which a polarised wave entered will be partially polarised. This is due to the fact (as demonstrated in the vegetation depth measurements) that as the depth of vegetation increases, the received signal becomes mainly dominated by the scattered (incoherent) component. It was not possible to perform measurements of a greater depth than three trees as the workable dimensions of the anechoic chamber would not permit this.

To investigate this theory further without having a large body of vegetation, owing to practical constraints, the receiver was positioned so that it was in the null

of the radiation pattern of the transmit antenna. Thereby, ensuring the scattered component from the vegetation was predominately received. This meant that the coherent signal received directly from the vertically polarised transmitted signal was in the order of -40 dBm. The minimum signal level recorded was in the region of -40 dBm and this was seen in the null of only one of the polarisation patterns measured. This therefore means that the signal level received from the transmitter can be ignored as it is of negligible strength in comparison to the signal received from the scatter caused by the vegetation.

In all the measurements made, the polarisation pattern measured showed that the field propagating from the vegetation was becoming partially polarised. This indicates that at greater depths of vegetation, where there is no longer a coherent component and the incoherent component is propagating through the vegetation, the signal will become more partially polarised. In other words, of no definite polarisation state. If a polarisation pattern were to be measured at a large depth of vegetation the pattern would be different to that corresponding to a definite state of polarisation, such a pattern is shown in Figure 7-2.

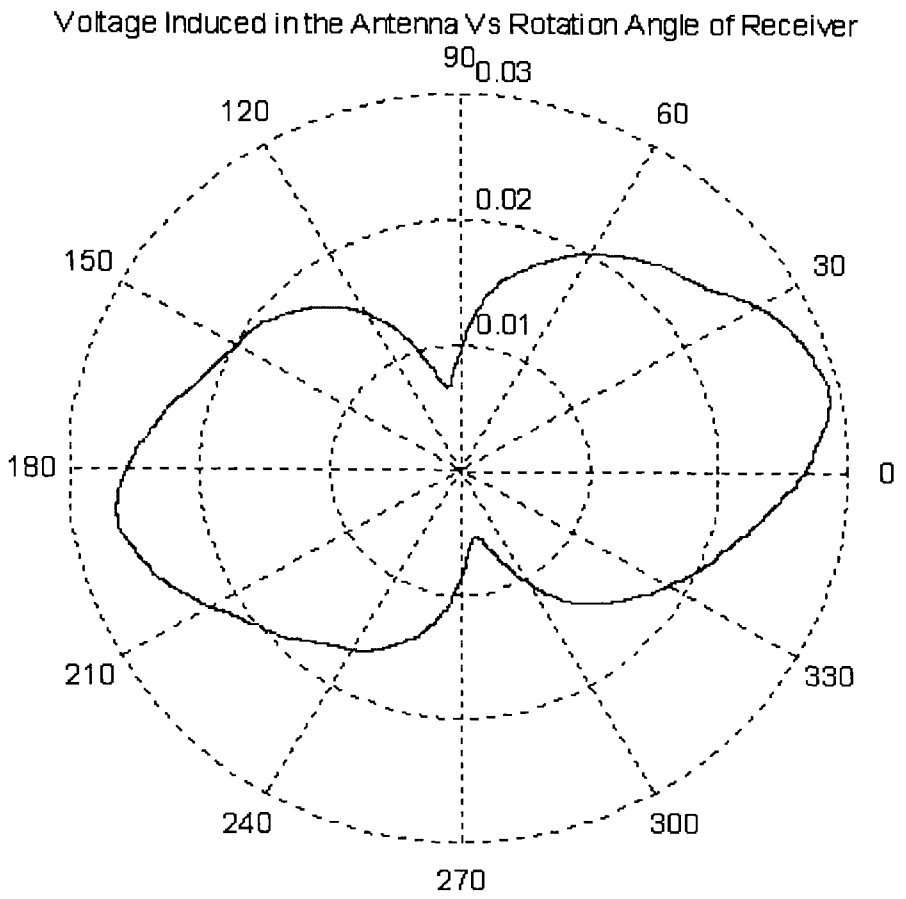

Figure 7-2 A Partially Polarised Field Measured in the Null of the Transmitter.

7.6 Metal Tree Investigation

An examination into how the individual components of a tree affect the propagating wave has been performed by the use of a tree made from metal rods.

The process of this examination was to first of all measure the polarisation of a freespace signal, primarily to check upon the alignment of the antennas and the polarisation state being transmitted. The metal tree was built in stages and at each stage the polarisation pattern was measured.

The first stage was to insert an upright metal rod (to represent the trunk of a tree) of 45 mm diameter into the LOS between the transmitter and receiver. The second stage was to add rods of 20 mm diameter and 30 cm in length to the top of the trunk, with 20 mm diameter rods of 50 cm in length as middle branches. A

third stage comprised the addition of bottom branches of the same length and diameter as the middle branches, as can be seen in Figure 7-3.

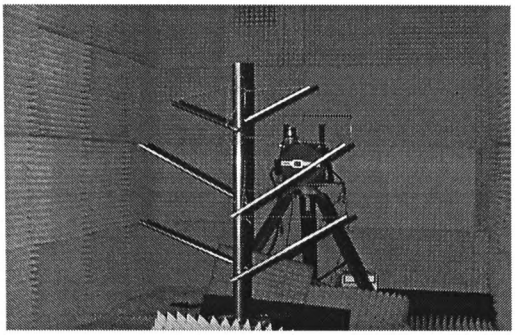

Figure 7-3 Trunk and Main Branches of Metal Tree.

A further stage in the process was to add twelve branches of 17 mm diameter and 15 cm in length to the middle branches, positioned at an angle of 60° relative to the middle branches, with six branches to either side of the trunk. The next stage involved adding an equal number of secondary branches to the bottom branches, followed by attaching four secondary branches to the top branches.

A further six stages involved adding branches of 17 mm diameter and length of 7.5 cm to the outer side of the secondary branches introduced above. After these six stages, the next six were implemented by attaching branches of 17 mm diameter and 7.5 cm in length to the inner side of the secondary branches.

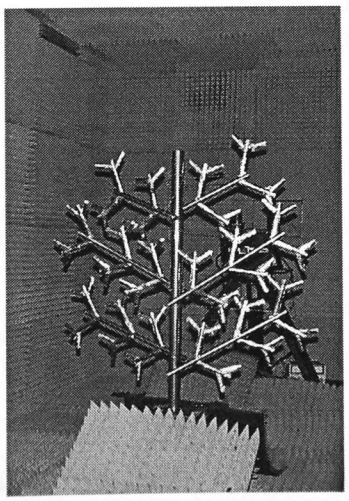

Figure 7-4 The Complete Metal Tree.

After performing all of the above stages a two dimensional tree was obtained as can be seen in Figure 7-4.

Some of the polarisation patterns for the various stages of the metal tree are shown in Figure 7-5 to Figure 7-8. The first of these figures represent the polarisation measured with the trunk in the path. As can be seen, the trunk has a minimal effect on the vertically polarised transmitted wave The trunk basically caused a signal loss of 2.3 dB. Figure 7-6 shows the polarisation pattern for the tree with all the main branches attached as shown in Figure 7-3. Figure 7-7 shows the pattern with all the secondary branches attached to the main branches. The polarisation state of the wave after propagating through the completed metal tree, Figure 7-4, is presented in Figure 7-8.

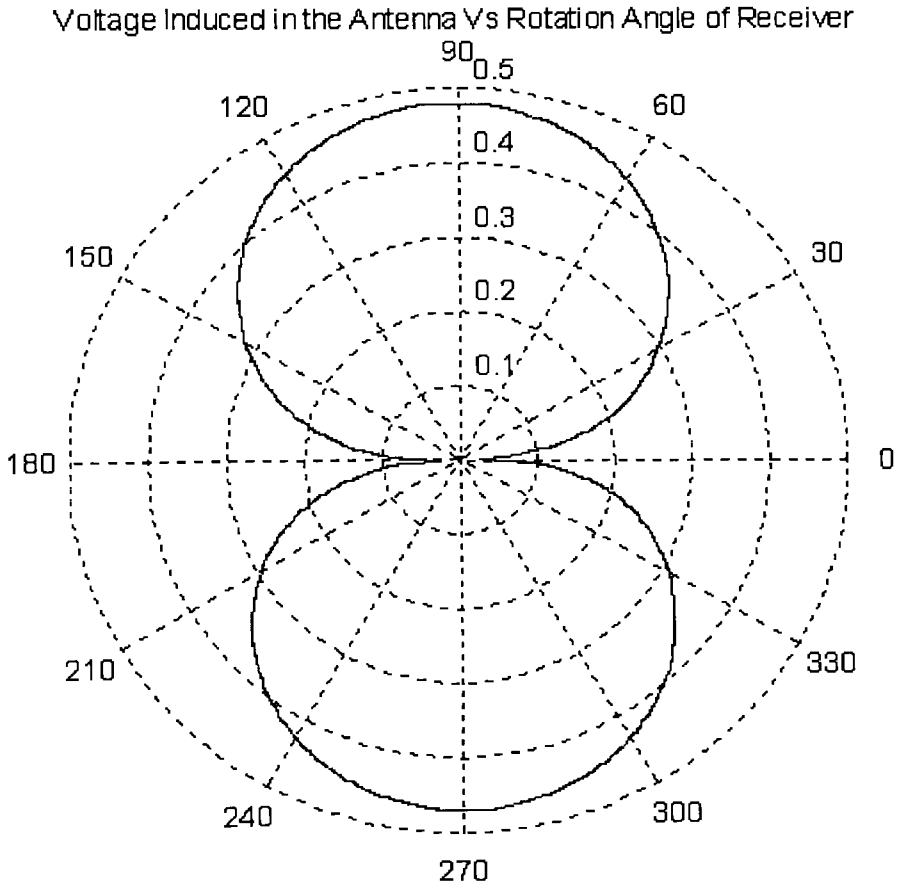

Figure 7-5 Polarisation Pattern From the Metal Trunk.

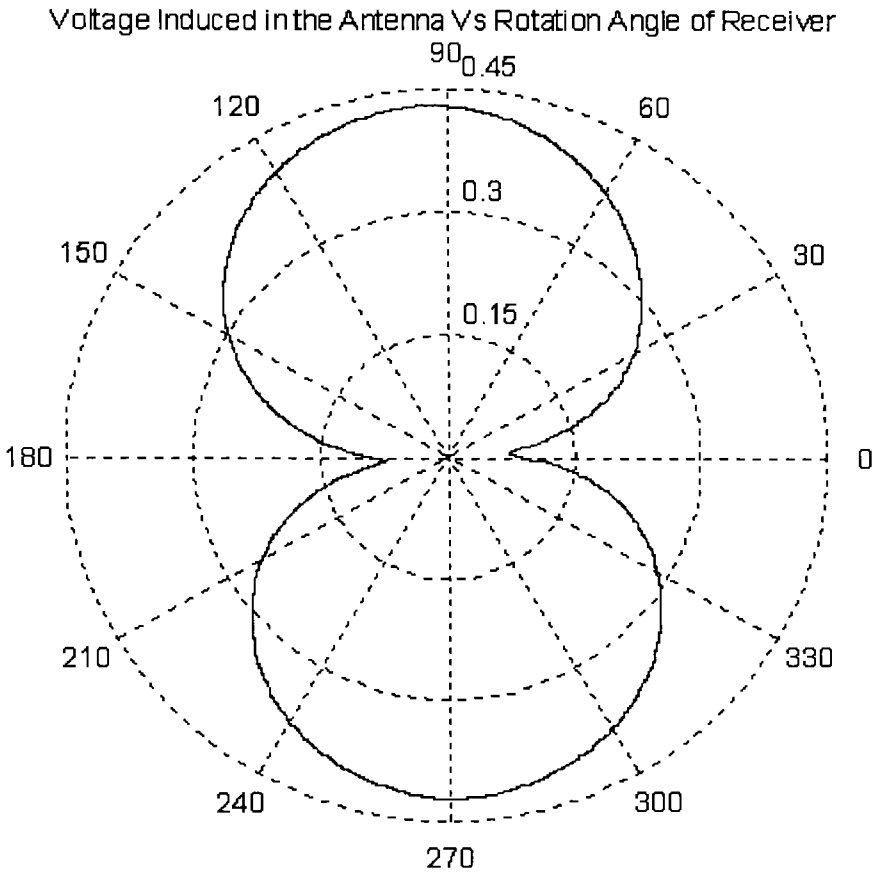

Figure 7-6 Polarisation Pattern with all Main Branches.

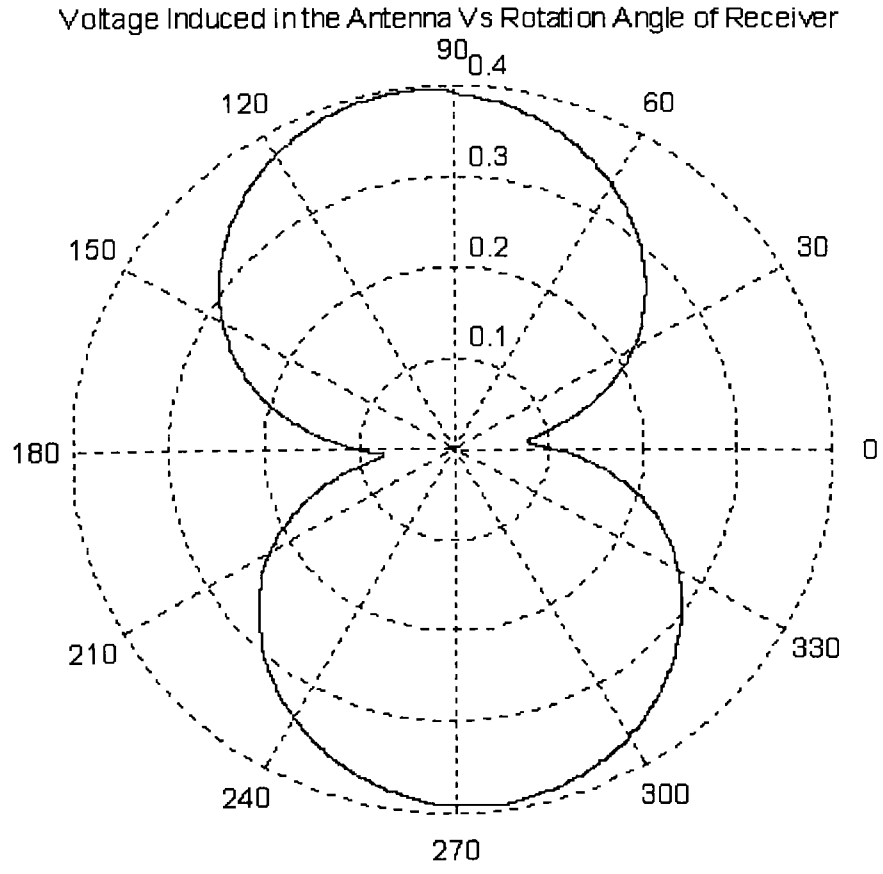

Figure 7-7 Polarisation Pattern with all Secondary Branches.

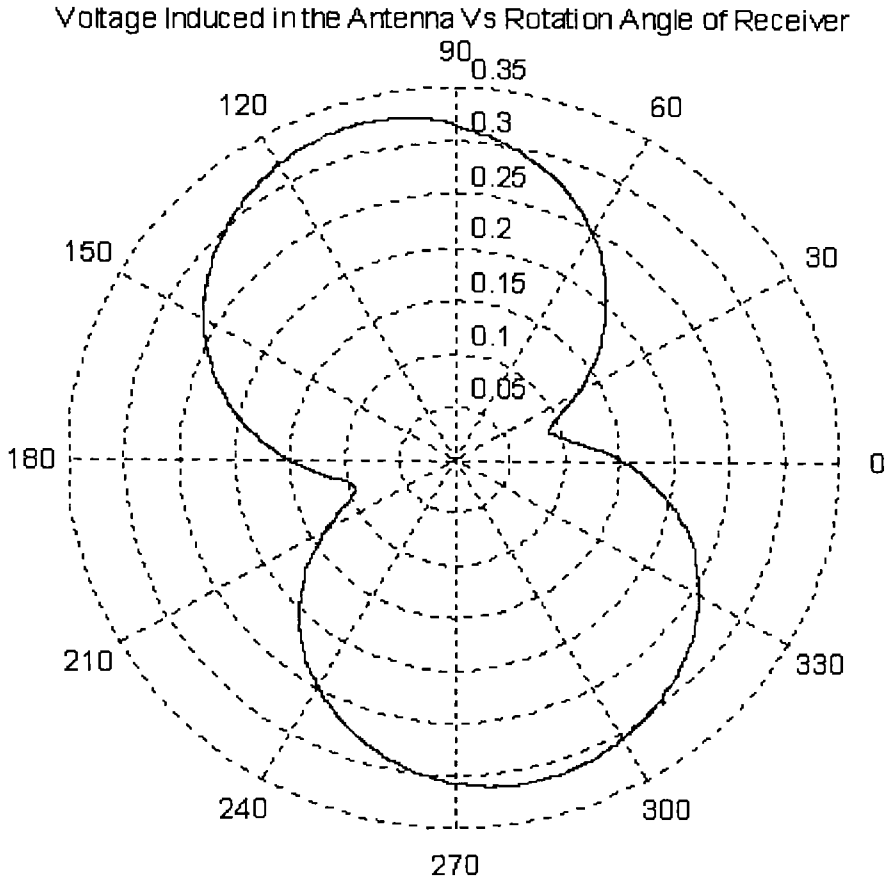

Figure 7-8 Polarisation Pattern of Complete Metal Tree.

Table 7-9 Polarisation State for various Stages of the Metal Tree.

State of Metal Tree	Tilt Angle	Axial ratio
Freespace	-89.4°	0.04
Trunk	-88.5°	0.04
Main Branches	-86.1°	0.16
All Secondary Branches	-69.7°	0.24
Complete Tree	-73.1°	0.28

Presented in Table 7-9 are the individual states of polarisation for the above described stages of the tree.

As can be seen in the figures of the polarisation patterns, the maximum received signal strength decreases as more of the metal tree is built up. This is as expected, as the incident wave is being increasingly scattered in many directions as it strikes

the various components of the tree. The change in the polarisation of the received signal as the structure of the tree was built up (as seen in Table 7-9) is indicated by the increase in the axial ratio and the change in the tilt angle. These parameters have progressively altered as the structure has become more complex. This may be explained by the fields re-radiated by the metal rods (branches) orientated at various angles altering the linear vertical polarisation of the incident field on the metal tree, thereby providing a changed polarisation state.

7.7 Interim Conclusion

The measurement results presented in the previous chapter have been discussed and the cause of the higher than expected signal loss at certain angles of rotation of the tree resulting in deep nulls has been explained. The depolarisation of the incident signal as it propagates through the vegetation media appears to be in the main responsible for the considerable attenuation of the linearly polarised incident signal. This occurs at the angles at which the nulls are observed.

Depolarisation as a function of the depth of vegetation has also been investigated. It has been found generally that an increasing amount of vegetation in the path can lead to a greater amount of depolarisation in addition to the attenuation arising from absorption and scatter. This seems to be particularly the case for the more uniformly structured vegetation bodies such as conifers.

The statement [Van Zyl, 1986] that most, if not all natural mediums cause a partially polarised state has been found not to hold true for the depths of vegetation experimented upon in the anechoic chamber. This can be seen from the polarisations patterns that have been presented in Chapter 6 and in this Chapter. It maybe true that as the depth of vegetation is increased and the incoherent component, which is as a result of scattered waves, becomes the dominant wave that vegetation will cause partially polarised waves. This can be seen in the polarisation pattern, Figure 7-2, that shows no precise polarisation

where the receiver was placed in the null of the transmitters radiation pattern so that no coherent component was received.

Literature states [Johnson *et al*, 1985] that at small depths of vegetation that the incident signal is not depolarised whereas it can be seen from the research that significant depolarisation does occur.

A more controlled investigation was performed on a tree constructed of metal rods to examine the individual effects of branches on the propagating wave. This showed that as the trees' complexity was increased, the amount of depolarisation of the incident signal was observed to increase with the increasing number of components added to the metal tree. The polarisation patterns obtained demonstrated that depolarisation has resulted in the received signals having both vertical and horizontal polarised components. The results obtained from the metal tree investigation have shown that it is an approach which is quite useful in explaining the process of depolarisation by natural media. Allowing for the different complex permittivity between metallic and natural tree structures, this process could be used in developing a relationship between the structure of a tree and the polarisation state of the signal emanating from the tree.

8. Review and Conclusion

8.1 Review of the Thesis

With the increase in the quantity of mobile communications across a wide range of frequencies, the radio system planners require accurate models to be able to predict the field strength of the transmitted signal at any given distance from the transmitter. As well as radio system planners requiring accurate prediction models, they also require the models to be more easily and universally applied.

Models can only be optimised by performing measurements at sites which relate to the topology of the area where predictions are required. Vegetation is regarded as one of the major sources that may cause a significant reduction in the strength of the propagating wave. The work set out in this thesis will provide radio planners with an appropriate method for calculating the signal loss as a function of vegetation depth and frequency. The results also show that signal loss is not just as a result of attenuation and scatter but also due to the depolarisation of the propagating signal.

Measurements to investigate the relation between an increasing depth of vegetation and signal loss were performed at two frequencies of 11.2 GHz and 20 GHz. A number of measurement configurations, sites and types of trees were utilised. The measurements were performed upon real bodies of vegetation as the complexity of a tree cannot be simulated to a high degree of accuracy. The selected sites were chosen as representing typical types of vegetation that are found in temperate areas such as those found in Europe. The vegetation sites chosen represent a compromise between many constraints such that models could be optimised and generalised in a manner which is not predominately affected by site specific geometries and other considerations.

From the measurements made on the various bodies of vegetation, the ITU-R model [CCIR, 1986] was adapted so that accurate attenuation predictions could be

produced for a specific body of vegetation at microwave frequencies. Other models have also been compared to the measured data and the prediction from the adapted ITU-R model.

Whilst investigating the effect of an increasing depth of vegetation on a propagating signal, large fluctuations in the received signal were observed. These fluctuations were caused by the movement of the various components of the trees. As the trees moved, changes were made as to the volume of vegetation in the path of the signal, this resulting in changes in :

1. the attenuation caused by absorption and scattering,
2. the multipath effects,
3. the extent of depolarisation of the incident signal.

To investigate this further, experiments were conducted to examine the depolarisation caused by vegetation as a signal propagates through the said vegetation. The polarisation of a propagating wave was measured using the 'polarisation pattern' method discussed in Chapter 6. A tree was rotated about its central axis on a high precision turntable to provide a 360° attenuation pattern of the tree under examination. The results had many interesting features, one of which being that instead of a small variation in the received signal level as would be expected, large fluctuations about a mean value were seen. The fluctuations seen in these measurements are believed to be the same as the fluctuations seen in the increasing depth of vegetation measurements described in Chapter 4. The reason for this belief is that in both the vegetation depth and 360° attenuation measurements the fluctuations in the received signal level are due to the relative positions of the components of the tree(s). In the case of the vegetation depth measurements the position of the trees components are changed by external influences such as wind resulting periodically in a reduction of the received signal strength. For the 360° attenuation measurements, at certain rotation angles the various components of the tree cause a significant decrease in the received signal strength. To investigate the possible cause of the decreases in the received signal strength further, the polarisation pattern of the wave emanating from the

vegetation sample was measured. A correlation was noted between the sharp decrease in the received signal (nulls) and the amount of depolarisation of the wave incident upon the vegetation sample as indicated by the measured polarisation pattern. The null in the 360° attenuation pattern corresponds to the angle at which the greatest amount of depolarisation takes place. Owing to the complex nature of vegetation, it is not possible to easily predict with any great accuracy the amount of depolarisation that may be expected from a given body of vegetation. As can be seen in the figures presented in Chapter 6 there is considerable variation in the amount of depolarisation caused by the given body of vegetation.

To understand and assess how the signal incident upon a body of vegetation was becoming depolarised, measurements on a specially constructed metal tree were conducted, the results of which are presented and discussed in Chapter 7. The components of this tree had currents induced in them by the incident wave which result in turn in the re-radiation of fields at their own particular angles causing an overall depolarisation of the incident wave. The extent of this depolarisation being governed by the number of components of the tree that were at angles other than the polarisation angle of the incident wave.

8.2 Contributions

The contributions of the work presented within this thesis is summarised in the following sections.

8.2.1 Contribution to Theoretical Models

The contribution to theoretical models has been by the adaptation of the ITU-R model (Chapter 5) which models the attenuation caused by vegetation as a function of vegetation depth. The original ITU-R model [CCIR, 1986] has been adapted to be applicable at microwave frequencies. This model in its original form was said to be applicable up to a frequency of 95 GHz, but has been found to

offer a poor fit to measurement data collected at microwave frequencies. This model was chosen for its simplicity and ease of use making it ideal to provide quick predictions and has been compared with a number of other models in this thesis. The comparison has been carried out against the ITU-R model in its original form and a semi-empirical model referred to as the non-zero gradient model. A newly published model (which is still currently under development) the Dual Gradient model, [COST235, 1996] has also been investigated and shortcomings have been discovered in this model as presented in Chapter 5. The development of the original ITU-R model provides an improved fit to all of the measured data acquired at both the 11.2 GHz and 20 GHz frequencies.

Due to the complex nature of vegetation it has not been possible to derive a model that will easily and accurately predict the amount of depolarisation a specified body of vegetation will created. As can be seen from the data presented in Chapter 6, the amount of depolarisation that a tree can cause varies considerably.

A measurement method has been developed so that accurate and repeatable measurement data can be obtained about the polarisation state of a propagating signal. Results from this measurement method were compared to another measurement method, known as the Knittel method (a multiple amplitude component measurement method). This comparison showed that although the Knittel method permitted faster measurements to be conducted errors were noted and were discussed in Chapter 6. The depolarisation measurements have explained the cause of the large nulls seen in the measured 360° attenuation patterns, so that it can be seen that the signal loss is not solely due to the absorption and scatter of the incident signal.

The variability seen in the 360° attenuation patterns can be associated with the variability seen in the received signal strength at each depth of vegetation in the outdoor measurements. It can therefore be proposed that the variability in the outdoor measurements is not entirely due to absorption and scatter of the incident signal but also due to depolarisation of the signal occurring.

8.2.2 Contribution to Measurement Data

As previously stated, the work presented in this thesis has primarily been of a measurement nature, as it is believed that signal loss caused by vegetation cannot be accurately modelled until all the individual effects caused by vegetation have been quantified in some manner. To this end, a number of the reasons for a microwave suffering signal loss as it propagates through vegetation have been investigated through the acquisition of measurement data for both depth of vegetation and the depolarisation of microwave signals.

The attenuation as a function of vegetation depth and frequency has been investigated and the analysis of the measurement data has been presented for various types of vegetation. Different types of vegetation were used in the investigation as each individual species of tree will cause slight changes in the way the propagating signal is effected as a result of the size, shape and orientation of the various parts which constitute the tree. The frequencies utilised in this study have been 11.2 GHz and 20 GHz and from the available literature it would appear that no previous investigation into the effect of vegetation at 20 GHz has been carried out. The measured data at a frequency of 20 GHz has been shown in comparison to the data measured at 11.2 GHz and it can be seen in the data presented that the higher frequency signal experiences a greater loss than the lower frequency signal. This is due to the smaller wavelength of the higher frequency being smaller than the size of the components of the trees and therefore more absorption and scattering occurs.

Measurements to quantify the amount of depolarisation experienced by a signal as it propagates through a body of vegetation have been performed on various species of vegetation, with the different species (various conifer and Ficus) being employed to examine any dependency between the amount of depolarisation and the type of tree. These measurements were carried out at a frequency of 20 GHz employing the available equipment.

To facilitate the acquisition of the measurement data a number of software programs (Appendix A and B) were written. These programs also allowed the automated control of the measurement hardware as discussed in Chapter 3. In conjunction with the software, the measurement methods were developed so that accurate and repeatable measurement results could be obtained.

8.2.3 Contribution to the Published Literature

During the course of the research a contribution has been made to the published literature which are now listed.

1. Stephens, R.B.L. and Al-Nuaimi, M.O., "Attenuation Measurement and Modelling in Vegetation Media at 11.2 GHz and 20 GHz", Electronics Letters, Vol 31, No. 20, 1995.
2. Hammoudeh, A., Stephens, R.B.L. and Al-Nuaimi, M., "Characterisation and Modelling of Scatter, Attenuation and Depolarisation of Millimetre Waves due to Foliage", 26th EuMC, Prague, Czech Republic, September 1996.
3. D'amato, L., Al-Nuaimi, M. and Stephens, R.B.L, "Modelling Slant Path Attenuation in Vegetation Media Using Measurements at 11.2 GHz and 20 GHz", PIERS '96.
4. Al-Nuaimi, M. and Stephens, R.B.L., "Estimation of the Effects of Hilltop, Singly Distributed, Trees on the Path Loss of Microwave Signals", IEE Electronics Letters, Vol. 33, No. 10, May 1997.
5. Stephens, R.B.L., Al-Nuaimi, M. and Caldeirinha, R., "Characterisation of Depolarisation of Radio Signals by Single Trees at 20 GHz", Fifteenth National Radio Science Conference, Egypt, February 1998.
6. Al-Nuaimi, M. and Stephens, R.B.L., "Prediction Models for the Excess Propagation Attenuation in Vegetation Media and their Optimisation for Microwave Signals", IEE Proceedings, 1998.

Throughout the course of this research, data collected from the vegetation attenuation measurements described in Chapter 4 were presented at COST 235 meetings with the DTI and Rutherford Appleton Laboratory. This data was utilised in the development process of the Dual Gradient model in COST 235 [1996]. Various scenarios of microwaves propagating through vegetation were discussed and measurements were also conducted to evaluate these scenarios. One such scenario being the effect of having trees on the crest of a hill over which a signal would be propagated. The purpose of the measurement was to determine if the vegetation would add to the forward propagating signal which would have been received if the vegetation had not been on the hilltop.

8.3 Attenuation caused by Vegetation

Radio system planners will be able to make accurate predictions of the amount of signal loss due to vegetation at microwave frequencies with the methods and results presented in this thesis. The planning of coverage by cellular planners for wooded areas would also benefit from the use of the information reported in this thesis.

Apart from signal loss by attenuation, it has also been shown that there can be significant signal loss due to depolarisation of the propagating wave, the maximum loss due to depolarisation arising when the polarisation of the signal has been altered by 90°.

8.4 Further Studies

Although the fitted ITU-R (FITU-R) vegetation depth model developed and described in the previous chapters provides a very good prediction of the attenuation to be expected from deciduous trees, the model has not been tested against an increasing depth of coniferous trees. Different parameters are expected for the coniferous vegetation due to the entirely different structure of the coniferous species in comparison to the deciduous trees. In comparison to the

original ITU-R model, the fitted model is still expected to provide the better prediction.

With regards to the depolarisation created by vegetation, the accuracy of the measurements could be greatly improved by the use of a vector network analyser (VNA). The use of a VNA would also substantially reduce the time of measurements permitting more time for analysis of the collected data. The vegetation depth and depolarisation measurements could be performed concurrently with the use of a VNA allowing for any correlations to be more easily investigated. The depolarisation measurements could also then be carried out at sites, allowing comparisons to be made with the measurements performed in the anechoic chamber, thus permitting more 'realistic' measurements (in the sense of the measurements being conducted in an outdoor environment) to be reproduced in the anechoic chamber.

Having more 'realistic' measurements in the anechoic chamber would allow the individual effects that affect the propagating signal to be isolated and categorised. With the separate effects determined, a more accurate and widely applicable prediction model could be developed. To account for any seasonal variation in the reduction in the signal as it passes through vegetation, measurement data could be correlated with data obtained from a weather station local to the site of the measurements. The model would therefore be able to predict the reduction in the received signal level due to absorption, scatter, depolarisation and any seasonal dependant reduction.

The work carried out from the discussions with the DTI on the effect of having trees on the crest of a hill could be carried forward by conducting further investigations, as the measurements conducted were inconclusive and further investigations were not possible owing to a lack of resources.

. Appendix A

.A.1 Anechoic Chamber Measurement Software

This program is used when measurements are being performed in the anechoic chamber. The software allows for the automated control of the high precision turntable that is housed inside the anechoic chamber and control of the data acquisition board.

```
(*****************************************************************
**                                                              **
**      Program to control both the turntable and the data acquisition board    **
**                              via menus                       **
**                                                              **
*****************************************************************)

Program turntable (input,output);
Uses Dos,Crt,PC30;

Const
    COM1 = $03F8;
    max_samp = 13000;

Var
    Filename : Text;
    err,samp_step : Integer;
    c_list : array [0..31] of Integer;
    f_sample : array [0..max_samp] of Integer;
    default : String;

(*****************************************************************
**                                                              **
**      Following procedures are for controlling the turntable  **
**                                                              **
*****************************************************************)

Procedure Clear;
{clears the screen and moves cursor point to 5,5}

begin
    ClrScr;
    GotoXY (5,5);
end;

Procedure Set_Com;
```

```
{Sets up the com port to desired parameters}

begin
{$M $1000,$1000,$1000} {adjusts the stack and heap values}
    SwapVectors;
    Exec ('C:\command.com','/c mode com1 baud=9600,parity=N,data=8,stop=1');
    SwapVectors;
    Writeln ('Switch on the Indexers');
end;    {Set_Com}

Procedure Send_port (lett:Char);
{o/p's to the port the character and delays}
Var
    check : Integer;
begin
    Repeat
        Port[COM1] := Ord(lett);
        Delay(20);
        check := Port[COM1];
    Until (check = Ord(lett)) or (check = 10);
end;

Procedure Set_limits(rese:boolean);
{resets indexers and sets axis 1 to have limits on}
{and axis 2 to have limts off}
Var
    check : Integer;

begin  {Set_limits}
    If rese then begin
        Send_port ('Z');              {reset the indexers}
        Send_port (#13);
    end;
    Send_port ('1');
    Send_port ('L');
    Send_port ('D');
    Send_port ('3');                  {the 3 needs to be a zero to enable limits}
    Send_port (#13);
    Send_port ('2');
    Send_port ('L');
    Send_port ('D');
    Send_port ('3');
    Send_port (#13);
end;    {Set_limits}

Procedure axis_change (Var axis:Char);
{Finds out what axis is to be changed}
```

```
begin  {Axis_change}
    Repeat
        Clear;
        Writeln ('Enter the axis to operate on.');
        GotoXY (7,6);
        Writeln ('0. For both axis.');
        GotoXY (7,7);
        Writeln ('1. For vertical axis.');
        GotoXY (7,8);
        Writeln ('2. For horizontal axis.');
        GotoXY (35,5);
        Readln (axis);
    Until ((axis >='0') and (axis <'3'));
end;   {Axis_change}

Procedure data_out (command,axis:Char;keys:String);
{o/p's the command to the controllers}

Var
    i,j :integer;

begin
    If axis > '0' then
        Send_port (axis);          {o/p axis number}
    Send_port (command);           {followed by the command required}
    j := Length (keys);
    For i := 1 to j do
        Send_port (keys[i]);       {send characters one at a time}
    Send_port (#13);               {send a carriage return}
end;   {data_out}

Procedure Motor_move (direc:Char);
{to tell requested axis to move}

begin
    If direc > '0' then
        Send_port (direc);         {o/p axis number}
    Send_port ('G');               {send Go command}
    Send_port (#13);               {send carriage return}
end;   {Motor_move}

Procedure In_pos (way:Char);
{waits until table is in position}

begin
    GotoXY (5,5);
    Writeln ('Please wait moving                    ');
    Send_port (way);
```

```
    Send_port ('L');                    {send LF and wait till receive it back}
    Send_port ('F');
    Send_port (#13);
    Repeat Until (Port[COM1]=10);
end;    {In_pos}

Procedure Acc;
{Allows the acceleration rate to be modified}

Var
    acc_keys : String;
    axis : Char;

begin
    Axis_change(axis);
    Clear;
    Write ('Enter the new Acceleration rate (0.01 - 999.00) ');
    Readln (acc_keys);
    Data_out ('A',axis,acc_keys);
end;    {Acc}

Procedure Vel;
{allows the velocity setting to be changed}

Var
    vel_keys : String;
    axis : Char;

begin
    Axis_change(axis); {see what axis is to be operated on}
    Clear;
    Write ('Enter the new Velocity rate (0.01 - 50.00) ');
    Readln (vel_keys);
    Data_out ('V',axis,vel_keys);
end;    {Vel}

Procedure Calculate_steps(Var dis_keys : String);
{calculates the steps from the degrees requested}

Var
    numb : Real;
    len : Integer;

begin
    If dis_keys<> '0' then begin
        Val (dis_keys,numb,err);
        numb := numb * 1000;
        Str (Trunc(numb),dis_keys);
```

```
    end
end;    {Calculate_steps}

Procedure Dis;
{allows the distance setting to be changed}

Var
    dis_keys : String;
    axis : Char;

begin
    Axis_change(axis); {see what axis to operate on}
    Clear;
    Write ('Enter the direction and the number of Degrees to move ');
    GotoXY (5,6);
    Write ('Directions are:- + for clockwise, - for anti-clockwise ');
    Readln (dis_keys);
    Calculate_steps (dis_keys);
    Data_out('D',axis,dis_keys);
end;    {Dis}

Procedure positioning (hor_ver:Integer;sta_fin:string;Var var_keys:String);

begin
    Clear;
    Write ('Please enter the ',sta_fin,' position for axis ',hor_ver,' in degrees ');
    Readln (var_keys);
    Calculate_steps (var_keys);
end;    {positioning}

Procedure Case_chk;
{used for testing purposes}

begin
    Case err of
        ok_30 : Writeln ('Operation completed.');
        par_30 : Writeln ('Invalid parameter.');
        err_30 : Writeln ('Data overrun. Check clock rate.');
        mem_30 : Writeln ('Not enough memory.');
        task_30 : Writeln ('Too many task accessing the data acquisition hardware');
        n_comp_30 : Writeln ('Operation being carried out.');
    end; {case}
end;    {Case_chk}

Procedure read_data;

Var
    i,j,num_chan : Integer;
```

```
    d,r : Real;

begin
    j := 0;
    num_chan := 0;
    If samp_step > 0 then begin
        Append (Filename);
        GotoXY (5,5);
        Writeln ('Please wait acquiring data.');
        {rtc_off;}
        err := m_chan(c_list, samp_step, f_sample[0]);
        {rtc_on;}
        {case_chk;}                 {used to display errors when testing}
        Repeat                      {find number of channels sampled}
            Inc (num_chan);
        Until c_list[num_chan] > 15;
        d:=0;
        for i:=0 to (samp_step-1) do
            d:=d+f_sample[i];
        d:=d / samp_step;
        Write(filename,d:8:6);
        Writeln (Filename);             {blank line at end of each block}
        Close (Filename);               {of samples to seperate them}
    end; {if}
end;    {Read_data}

Procedure Sequen (turn_or_data : String);
{Allows user to enter a start, end position and incremental steps}

Var
    axis1_start,axis1_fin,axis2_start,axis2_fin,lone_start,lone_fin : String;
    axis1_snum,axis2_snum,axis1_fnum,axis2_fnum,axis1_inum,axis2_inum,
    lone_snum,lone_fnum,lone_inum,axis1_sint,axis2_sint,lone_sint,deg : Real;
    axis,a : Char;
    err,len : Integer;
    maxis1,maxis2,lone_axis : Longint;
    h,hi,m,mi,s,si,sei,se,h2,m2,s2,se2 : Word;

begin
    Send_port ('M');                {send the Move Position Absolute command}
    Send_port ('P');
    Send_port ('A');
    Send_port (#13);
    Axis_change(axis);              {determine which axis to use}
    If axis='0' then begin
        Positioning (1,'start',axis1_start);
        Positioning (2,'start',axis2_start);
        Data_out ('D','1',axis1_start);
```

```
Motor_move ('1');
Data_out ('D','2',axis2_start);
Motor_move ('2');
In_pos ('1');
In_pos ('2');
Val (axis1_start,axis1_snum,err);
Val (axis2_start,axis2_snum,err);
axis1_sint := axis1_snum;              {save the initial start}
axis2_sint := axis2_snum;              {positions}
Positioning (1,'finish',axis1_fin);
Positioning (2,'finish',axis2_fin);
Val (axis1_fin,axis1_fnum,err);
Val (axis2_fin,axis2_fnum,err);
Clear;
Write ('Enter the incremental step for axis 1 in degrees ');
Readln (axis1_inum);
axis1_inum := axis1_inum*1000;         {convert to steps}
If (axis1_fnum < axis1_snum) then
axis1_inum := axis1_inum-(axis1_inum*2);
GotoXY (5,8);
Write ('Enter the incremental step for axis 2 in degrees ');
Readln (axis2_inum);
ClrScr;
axis2_inum := axis2_inum*1000;
If (axis2_fnum < axis2_snum) then
axis2_inum := axis2_inum-(axis2_inum*2);
If axis1_snum = axis1_fnum then
axis1_inum := 0;
If axis2_snum = axis2_fnum then
axis2_inum := 0;
Repeat
    axis1_snum := axis1_snum+axis1_inum; {incrementing position of counter}
    axis2_snum := axis2_snum+axis2_inum;
    If (axis1_sint < axis1_fnum) and (axis1_snum > axis1_fnum) then
        axis1_snum := axis1_fnum
    else If (axis1_sint > axis1_fnum) and (axis1_snum < axis1_fnum) then
        axis1_snum := axis1_fnum;
    If (axis2_sint < axis2_fnum) and (axis2_snum > axis2_fnum) then
        axis2_snum := axis2_fnum
    else If (axis2_sint > axis2_fnum) and (axis2_snum < axis2_fnum) then
        axis2_snum := axis2_fnum;
    maxis1 := Trunc (axis1_snum);
    maxis2 := Trunc (axis2_snum);
    Str (maxis1,axis1_start);
    Str (maxis2,axis2_start);
    Data_out ('D','1',axis1_start);
    Data_out ('D','2',axis2_start);
    Motor_move ('1');
```

```
        Motor_move ('2');
        In_pos ('1');
        In_pos ('2');
        If turn_or_data = 'Data' then
            Read_data
        else begin
            GotoXY (5,5);
            Writeln ('Press a key for next move');
            Repeat Until keypressed;
            a := readkey;                    {dispose of character}
        end; {else}
    Until (axis1_snum=axis1_fnum) and (axis2_snum=axis2_fnum)
end {if}
else begin
    If axis='1' then
        Positioning (1,'start',lone_start)
    else
        Positioning (2,'start',lone_start);
Data_out ('D',axis,lone_start);
Motor_move (axis);
In_pos (axis);
Val (lone_start,lone_snum,err);
lone_sint := lone_snum;
If axis='1' then
    Positioning (1,'finish',lone_fin)
else
    Positioning (2,'finish',lone_fin);
Val (lone_fin,lone_fnum,err);
GotoXY (5,10);
Write ('Enter the incremental step for axis ',axis,' in degrees ');
Readln (lone_inum);
ClrScr;
lone_inum := lone_inum*1000;          {convert to steps}
If lone_fnum < lone_snum then
    lone_inum := lone_inum-(lone_inum*2);
If lone_snum = lone_fnum then
    lone_inum := 0;
If turn_or_data  = 'Data' then        {read data prior to moving so get}
    read_data;
gettime(h,m,s,se);
Repeat
    lone_snum := lone_snum+lone_inum; {inc position}
    deg:=lone_snum / 1000;
    GotoXY (25,2);
    Writeln ('position = ',deg:3:2,' degrees  ');
    If (lone_sint < lone_fnum) and (lone_snum > lone_fnum) then
        lone_snum := lone_fnum
    else If (lone_sint > lone_fnum) and (lone_snum < lone_fnum) then
```

```
            lone_snum := lone_fnum;
        lone_axis := Trunc (lone_snum);
        Str (lone_axis,lone_start);
        Data_out ('D',axis,lone_start);
        Motor_move (axis);
        In_pos (axis);
        If turn_or_data = 'Data' then
            read_data
        else begin
            GotoXY (5,5);
            Writeln ('Press a key for next move');
            Repeat Until keypressed;
            a := readkey                    {dispose of character from keyboard buffer}
        end;    {else}
    Until (lone_snum = lone_fnum);
    end; {else}
    gettime(hi,mi,si,sei);
    Clrscr;
    Writeln (' Start time ',h,':',m,':',s,'.',se);
    Writeln (' Finish time ',hi,':',mi,':',si,'.',sei);
    Writeln ('Press a key to continue.');
    Repeat Until Keypressed;
    a:=readkey;
    Delay (20);
    Send_port ('M');                    {send the Move }
    Send_port ('P');                    { Position }
    Send_port ('I');                    { Incremental }
    Send_port (#13);                    { command }
end;    {sequen}

Procedure Motor_go;
{send the axis and a G command}

Var
    axis : Char;

begin
    Axis_change(axis);                  {see what axis to go on}
    Motor_move(axis);
    ClrScr;
    If axis > '0' then
        In_pos(axis)
    else begin
        In_pos ('1');
        In_pos ('2');
    end;
end;    {motor_go}
```

```
Procedure Position_report (vert_hoz:Char;Var way:Integer);
{gets a position report}

begin
    Send_port (vert_hoz);              {o/p axis number}
    Send_port ('P');                   {get a postion report to see }
    Send_port ('R');                   {in  which direction home is}
    Port[COM1] := 13;
    Delay(30);
    way := Port[COM1];                 {get a + or - to determine the direction}
end;

Procedure Activate_axis (direction:Integer;ver_ho:Char);
{activates axis to move towards its home position}
Var
    si : Char;

begin
    Delay (50);
    If direction = 43 then         {if it's a + then o/p - to move in opposite direction}
        si := '-'
    else
        si := '+';
    Send_port (ver_ho);
    Send_port ('G');
    Send_port ('H');
    Send_port (si);
    Send_port ('1');           {o/p a 1 for the speed}
    Send_port (#13);           {o/p a carriage return}
end; {activat_axis}

Procedure Go_home;
{returns the selected axis to its home position}

Var
    axis : Char;
    ch : Integer;

begin
    Axis_change (axis);
    If axis > '0' then begin
        Position_report (axis,ch);
        Activate_axis (ch,axis);
        ClrScr;
        In_pos (axis);
        Send_port (axis);
        Send_port ('H');               {send a H to return direction travel to}
        Send_port (#13);               {direction before GH command}
```

```
    end
    else begin
        Position_report ('1',ch);
        Activate_axis (ch,'1');
        Position_report ('2',ch);
        Activate_axis (ch,'2');
        In_pos ('1');
        In_pos ('2');
        Send_port ('H');            {send a H to return direction travel to}
        Send_port (#13);            {direction before GH command}
    end;
end; {Go_home}


(*****************************************************************
**                                                              **
**          Following procedures are for the data acquisition board          **
**                                                              **
*****************************************************************)

Function Init_board : Integer;
{calls all the daq functions necessary to initialise the daq}

Var
    i : Integer;

begin
    samp_step := 0;
    Set_base (1792);            {sets the base address to 700H}
    i := Diag;                  {runs diagnostic tests on DAQ}
    If i <> ok_30 then begin
        If i = task_30 then
            Writeln ('Too many tasks accessing the data acquisition hardware')
        else
            Writeln ('Board faulty or not found');
    end;
    Init_board := i;
    Init;                                   {intialises the DAQ board}
    for i:= 0 to 15 do set_gain(i,0);
    Config_bd (5,5,6,0,0,1,0,0,0,0);        {configure the DAQ board}
    set_osc(100);
    ad_prescaler(2);
    ad_clock(50);                           {sets 100 KHz data acquisition rate}
end; {Init_daq}

Function Chang_conf (one_chang : Integer; chang_text : String) : Integer;

Var
```

```
    value : Integer;
    incorrect : boolean;

begin
    Clear;
    Repeat
        incorrect := false;
        GotoXY (5,5);
        Writeln ('Please enter the new value for the ',chang_text,'          ');
        GotoXY (5,7);
        Case one_chang of
            1 : Write ('Possible levels are :- 0,3,5,7,10,11,12,14,15');
            2..3 : Write ('Possible levels are :- 0,5,6,7');
            4 : Write ('0 for A/D done, 2 for Smart cache.');
            5 : Write ('0 for external, 1 for internal.');
            6 : Write ('0 for -5 to +5V, 1 for 0 to 5V');
        end; {case of}
        GotoXY (60,5);
        Readln (value);
        Case one_chang of
            1 : begin
                If (value < 0) or (value > 15) or (value = 1) or (value = 2)
                or (value = 4) or (value = 6) or (value = 8) or (value = 9)
                or (value = 13) then incorrect := true;
            end;
            2..3  : begin
                If (value < 0) or (value > 7) or (value = 1) or (value = 2)
                or (value = 4)  then incorrect := true;
            end;
            4 : begin
                If (value <> 0) and (value <> 2) then incorrect := true;
            end;
            5..6 : begin
                If (value < 0) or (value > 1) then incorrect := true;
            end;
        end; {case}
        If incorrect then begin
            GotoXY (5,20);
            Writeln ('Invalid entry. Please re-enter.');
        end;
    Until not incorrect;
    Chang_conf := value;
end;    {Chang_conf}

Procedure Bd_con;
{Allows user to configure the daq}

Var
```

```
    choice : Char;
    changed : boolean;
    int_lev, pri_dma, sec_dma, int_sou, clk_sou, inp_ran, i : Integer;

begin
    int_lev := 5; pri_dma := 5; sec_dma := 6; int_sou := 0;
    clk_sou := 1; inp_ran := 0; changed := False;    {setup default values}
    Repeat
        Clear;
        Writeln ('Default settings are as follows:-');
        GotoXY (5,6);
        Writeln ('1. Interrupt level - 5');
        GotoXY (5,7);
        Writeln ('2. Primary DMA level - 5');
        GotoXY (5,8);
        Writeln ('3. Secondary DMA level - 6');
        GotoXY (5,9);
        Writeln ('4. Interrupt Source - A/D done');
        GotoXY (5,10);
        Writeln ('5. A/D clock source - internal');
        GotoXY (5,11);
        Writeln ('6. A/D input range - -5 to +5V');
        GotoXY (5,13);
        Writeln ('Choose one of the above numbers to change ');
        GotoXY (5,14);
        Write ('Press any other key when completed.');
        choice := readkey;
        Case choice of
            '1' : begin int_lev := chang_conf (1,'interrupt level'); changed := true; end;
            '2' : begin pri_dma := chang_conf (2,'primary DMA level'); changed := true;
        end;
            '3' : begin sec_dma := chang_conf (3,'secondary DMA level'); changed :=
        true; end;
            '4' : begin int_sou := chang_conf (4,'interrupt source'); changed := true; end;
            '5' : begin clk_sou := chang_conf (5,'A/D clock source'); changed := true;
        end;
            '6' : begin inp_ran := chang_conf (6,'A/D input range'); changed := true; end;
        end; {case of}
        If (choice < '1') or (choice > '6') and changed then
            err := config_bd (int_lev,pri_dma,sec_dma,int_sou,0,clk_sou,inp_ran,0,0,0)
    Until (choice < '1') or (choice > '6');
end; {Bd_con}

Procedure Set_own_srat;
{allows user to set their own clk,prescaler and osc freq.}

Var
    osc,pres,clk_div,act_samp : LongInt;
```

```
    a : Char;

begin
    Clear;
    Writeln ('The sample rate is calculated as follows:- ');
    GotoXY (10,6);
    Writeln ('Osc. Freq./ ( Prescaler * clock divisor )');
    GotoXY (5,8);
    Write ('Enter your oscillator frequency (10 or 2 MHz) ');
    Readln (osc);
    While (osc <> 10) and (osc <> 2) do begin
        GotoXY (5,10);
        Write ('Invalid. Re-enter. ');
        Readln (osc)
    end;
    GotoXY (5,10);
    Write ('Enter prescaler value.  (2-65535) ');
    Readln (pres);
    While (pres < 2) or (pres > 65535) do begin
        GotoXY (5,12);
        Write ('Invalid. Re-enter. ');
        Readln (pres)
    end;
    GotoXY (5,12);
    Write ('Enter clock divisor value.  (2-65535) ');
    Readln (clk_div);
    While (pres < 2) or (pres > 65535) do begin
        GotoXY (5,14);
        Write ('Invalid. Re-enter. ');
        Readln (clk_div)
    end;
    act_samp := (osc*1000000) div (pres*clk_div);
    GotoXY (5,14);
    Writeln ('The sample rate is ',act_samp, ' Hz');
    GotoXY (5,15);
    Write ('Press Y to use this value.');
    a := Readkey;
    If (a = 'y') or (a = 'Y') then begin
        err := Set_osc (osc*10);
        If err <> ok_30 then
            writeln ('Unable to perform operation.')
        else begin
            Ad_clock (clk_div);
            Ad_prescaler (pres);
        end; {else}
    end; {if}
end;    {set_own_srat}
```

```
Procedure Set_samp;
{Sets the sample rate of the channels}

Var
    samp_rat : Real;
    prescal,clk,act_rate : LongInt;
    a : Char;

begin {set_samp}
    Clear;
    prescal := 5;                    {set the default for the prescaler}
    err := Set_osc (100);            {set the oscillator frequency to 10MHz}
    If err = ok_30 then  begin
        Writeln ('Available sample rates are :-');
        GotoXY (15,6);
        Writeln ('1MHz, 500KHz, 400KHz, 250KHz, 200KHz, 100KHz, etc.');
        GotoXY (5,7);
        Writeln ('Other sample rates may not be accurately obtainable.');
        GotoXY (5,9);
        Writeln ('Enter the sample rate in Hz ');
        GotoXY (5,10);
        Writeln ('or enter 0 to set your own clock and prescaler.');
        Repeat
            GotoXY (33,9);
            Readln (samp_rat);
            GotoXY (33,9);
            Writeln ('                              ');
        Until ((samp_rat<=1000000) and (samp_rat>-1));
        If samp_rat = 0 then
            Set_own_srat
        else begin
            If samp_rat <= 100 then
            prescal := 50000;
            samp_rat := 10000000/samp_rat;          {gets value == prescaler*clock}
            clk := Trunc(samp_rat) Div prescal;
            Ad_clock (clk);
            Ad_prescaler (prescal);
            act_rate := 10000000 div (prescal*clk);
            GotoXY (5,15);
            Writeln ('Actual sample rate used was ',act_rate);
        end;
    end {if}
    else begin
        GotoXY (5,15);
        Writeln ('Too many tasks accessing board.');
    end;
    GotoXY (5,20);
    Write ('Press a key when ready');
```

```
    Repeat Until Keypressed;
    a := readkey;                          {discard key pressed}
end; {set_samp}

Procedure Set_chan;
{sets the number of channels to use}

Var
    i,j,k,l : Integer;
    in_there : Boolean;

begin {set_chan}
    i := -1; k := 26;
    For j := 0 to 31 do
        c_list[j] := 0;
    Clear;
    Writeln ('Enter the number of the channels you wish to use. (0-15)');
    GotoXY (5,6);
    Writeln ('Enter a number >15 to end.');
    GotoXY (5,20);
    Writeln ('Channels selected :-');
    Repeat
        in_there := false;
        GotoXY (62,5);
        Write (' ');
        GotoXY (62,5);
        If i < 32 then begin
            Inc (i);
            Readln (c_list[i]);
            For j := 0 to i-1 do begin
                If c_list[j] = c_list[i] then
                    in_there := true;
            end; {for}
            If not in_there then begin
                GotoXY (k,20);
                Write (c_list[i],',');
            end
            else
                Dec (i);
        end;
        If (c_list[i] > 9) and (not in_there) then
            k := k+3
        else begin
        If not in_there then
            k := k+2;
        end;
    Until (c_list[i] > 15);
end;    {set_chan}
```

```
Procedure Set_num;

begin
    Repeat
        Clear;
        Writeln ('Enter the number of samples per step of the turntable ');
        Writeln ('    Maximum number is ',max_samp);
        GotoXY (60,5);
        Readln (samp_step);
    Until samp_step <= max_samp;
end;

Procedure turn_dat;
{sequences the turntable and records data at each step}

begin {turn_dat}
    Clean;                  {clears the A/D subsystem}
    Sequen ('Data');
end; {turn_dat}

Procedure Change_name;
{Allows user to change the name of the file data will be written to}

Var
    user_file : string;

begin
    Clear;
    Writeln ('Please enter drive and name of file.');
    GotoXY (5,6);
    Writeln ('Default is ',default);
    GotoXY (5,7);
    Readln (user_file);
    If user_file <> #13 then begin
        If user_file ='' then
            Assign (Filename,default)
        else begin
            Assign (Filename,user_file);
            Rewrite (Filename);
            Close (Filename);
            default := user_file
        end
    end;
end;    {Change_name}

Procedure Jurg;
```

```
Var
    a : Char;
    I: Integer;

begin {jurg}
    Clear;
    I := 0;
    Writeln ('Press any key to record data.');
    GotoXY (5,6);
    Writeln ('or Escape to end.');
    Repeat Until Keypressed;
    Repeat
        a := readkey;
        Writeln ('reading keypress');
    Until (not keypressed);
    Delay (2000);
    While a <> #27 do begin
        ClrScr;
        Read_data;
        I := i+1;
        Write(#7);
        While keypressed do
            a := readkey;
        Clear;
        Writeln ('Press any key to record data.');
        GotoXY (5,6);
        Writeln ('or Escape to end.');
        GotoXY (15,15);
        Writeln (i,' pieces of data acquired');
        Repeat
            a := readkey;
        Until (not keypressed);
    end;
end;    {jurg}

Procedure Acq_menu;

Var
    acq_func : char;

begin
    Repeat
        Clear;
        Writeln ('          Data Acquisition Menu');
        Writeln ('      Please choose one of the following :-');
        Writeln ('        1. Configure board');
        Writeln ('        2. Set Sampling rate');
        Writeln ('        3. Set channels to sample');
```

```
        Writeln ('       4. Set number of samples');
        Writeln ('       5. Change filename to store data in');
        Writeln ('       6. ');
        Writeln ('       7. J',#129,'rgen',#39,'s Procedure');
        Writeln ('       8. Record data');
        Writeln ('       9. Sequence turntable and record data');
        Writeln ('       0. Turntable menu');
        Write ('         ');
        Readln (acq_func);
        Case acq_func of
            '1' : bd_con;
            '2' : set_samp;
            '3' : set_chan;
            '4' : set_num;
            '5' : Change_name;
            '6' : ;
            '7' : Jurg;
            '8' : begin
                Clear;
                Read_data;
            end;
            '9' : turn_dat;
        end; {case of}
    Until acq_func = '0';
end;    {Acq_menu}

Procedure Menu;

Var
    set_func : Char;

begin
    Repeat
        Clear;
        Writeln ('          Turntable Menu');
        Writeln ('      Please choose one of the following :-');
        Writeln ('       1. Acceleration');
        Writeln ('       2. Velocity');
        Writeln ('       3. Degrees to move');
        Writeln ('       4. Run setup (if power has been removed)');
        Writeln ('       5. ');
        Writeln ('       6. Sequence');
        Writeln ('       7. Go to the home position');
        Writeln ('       8. Move the turntable');
        Writeln ('       9. Data Acquisition Menu');
        Writeln ('       0. Exit');
        Write ('         ');
        Readln (set_func);
```

```
        Case set_func of
            '1' : Acc;
            '2' : Vel;
            '3' : Dis;
            '4' : Set_limits(True);
            '5' : ;
            '6' : Sequen ('Turn');
            '7' : Go_home;
            '8' : Motor_go;
            '9' : Acq_menu;
        end; {case of}
    Until set_func = '0';
end;    {menu}

begin  {main}
    default := 'c:\data.txt';
    Set_Com;
    Set_limits (False);
    err := Init_board;
    If err = ok_30 then begin
        Assign (Filename,default);
        Rewrite (Filename);
        Close (Filename);
        Textbackground (blue);
        Menu;
        Textbackground (black);
        ClrScr;
    end;
    Daq_close;                  {closes the driver system}
end.    {main}
```

. Appendix B

.B.1 Outdoor Measurement Software

Shown below is the program listing for the software used when performing measurements in the field. The program interfaces with a spectrum analyser via an IEEE to RS232 converter and permits remote control of the analyser by the computer user. Data acquired from the analyser can be stored into the file of the user's choice.

```
Program IEEE_TO_RS (input,output);
Uses Crt,Dos;

Const
    hdr=#27+'%GPIB ';
    send=hdr+'OUTPUT 18% ';

Type
    Storage = array [1..5000] of Real;

Var
    TAS016TX:text;
    TAS016Rx:text;
    Filename,Filename1:text;
    Default,Default1:string;
    marker:boolean;

Procedure Set_Com;
{Sets up the com port to desired parameters}

begin
{$M $F000,$1000,$1000}
    SwapVectors;
    Exec('C:\command.com','/c mode com1 baud=9600,parity=e,data=7,stop=1');
    SwapVectors;
end;

Procedure Clear;
{procedure clears the screen and sets the cursor to co-ordinates 5,5}

begin
    ClrScr;
    GotoXY (5,5)
end;
```

```
Procedure File_store (num:Integer;dat_arr:Storage;aver,max,min,sta_dev:Real);
{stores all data in the specified file}

Var
    times : integer;

begin
    Append (Filename);
    For times := 1 to num do
        Writeln (Filename,dat_arr[times]:5:2);
    Writeln (Filename,'Average = ',aver:5:2);
    Writeln (Filename,'Maximum = ',max:5:2);
    Writeln (Filename,'Minimum = ',min:5:2);
    Writeln (Filename,'Standard deviation = ',sta_dev:5:2);
    Writeln (Filename);
    Close (Filename);
    Append (Filename1);
    Writeln (Filename1,aver:5:2,'  ',max:5:2,'  ',min:5:2,'  ',sta_dev:5:2);
    Close (Filename1)
end;

Procedure Display_data (num_of : integer; data_store : Storage; aver, max, min, sta_dev
: Real);
{Allows data to be displayed if required}

Var
    Ch : Char;
    Start, Stop, middle, i, x, y : Integer;

begin
    Clear;
    Start := 1; middle :=20; Stop := num_of; x := 0; y := 0; {initialise values}
    Write ('Do you wish to view this data  (Y/N) ');
    Readln (Ch);
    If (Ch = 'y') or (Ch= 'Y') then begin
        ClrScr;
        Writeln;
        For i := 1 to num_of do begin
            GotoXY (1+x,2+y);
            Writeln (data_store[i]:5:2);
            Inc (y);                          {increment y position by one}
            If i mod 20 = 0 then begin
                x:=x+10;
                y:=0;
            end;
            If x = 80 then begin
                x := 0; y := 0;
                GotoXY (1,22);
```

```
            Write ('Press return for next screen');
            Repeat
                Read (Ch);
            Until Ch = #13;
        end;
    end;
    GotoXY (1,22);
    Write ('Press return for Average, Maximum, Minimum and standard deviation
values');
    Repeat
        Read (Ch);
    Until Ch = #13;
    Writeln ('Average :  ',aver:5:2);
    Writeln ('Maximum :  ',max:5:2);
    Writeln ('Minimum :  ',min:5:2);
    Writeln ('Standard deviation :  ',sta_dev:5:2);
    Write ('Press return when ready');
    Repeat
        Read (Ch);
    Until Ch = #13;
end; {if}
end;    {Display_data}

Procedure Trace_samp;
{reads the data from a single sweep}

Var
    trace : Storage;
    i : integer;

begin
    Clear;
    Writeln ('Please wait. Sampling');
    Append (filename);
    i := 1;                                    {initialise i}
    Writeln (TAS016Tx, send+'SNGLS; TS;');     {take a single sweep}
    Writeln (TAS016Tx, send+'TA?;');           {request trace data}
    Repeat
        Writeln (TAS016Tx, hdr+'ENTER 18%');
        Read (TAS016Rx, trace[i]);             {get and store trace data}
        i := i + 1;
    Until i = 402;
    i := 1;                                    {re-initialise i}
    Repeat
        Writeln (filename, trace[i]:5:2);      {write data to file}
        Inc (i);
    Until i = 402;
    Writeln (Filename);                        {insert blank line in data file}
```

```
    Close (filename);
    Writeln (TAS016Tx, send+'CONTS;');
end;    {trace_samp}

Procedure Ave_max_min (tot_samp : integer; samp_stor : storage;
                Var aver, maxi, mini, sta_dev : real);

Var
    i : integer;

begin
    aver := 0;
    sta_dev := 0;
    maxi := samp_stor[1];
    mini := maxi;                          {initialise to first value in array}
    For i := 1 to tot_samp do begin
        aver := aver + samp_stor[i];
        If maxi < samp_stor[i] then
            maxi := samp_stor[i];
        If mini > samp_stor[i] then
            mini := samp_stor[i]
    end;
    aver := aver / tot_samp;
    For i := 1 to tot_samp do
        sta_dev := sta_dev + (sqr(samp_stor[i] - aver));
    sta_dev  := sqrt (sta_dev / tot_samp);
end;    {Ave_max_min}

Procedure Add_Text;
{Allows the user to add text to the file where the data will be saved}

Var
    user_text : String;
    i : Char;
    j : Integer;

begin
    Clear;
    j := 0;
    Append (Filename);
    Writeln ('Please enter the text you wish to place in the data file');
    GotoXY (5,6);
    Writeln ('Type exit on a new line when completed.');
    GotoXY (5,8);
    Repeat
        Inc (j);
        Readln (user_text);
        If user_text <> 'exit' then begin
```

```
            Writeln (Filename, user_text);
            GotoXY (5,8+j);
        end;
    Until user_text = 'exit';
    Close (Filename);
end;    {Add_text}

Procedure Change_name;
{Allows user to change the name of the file data will be written to}

Var
    user_file : string;
    len, i : Integer;
    found : Boolean;

begin
    Clear;
    found := False;
    Writeln ('Please enter drive and name of file.');
    GotoXY (5,6);
    Writeln ('Default is ',default);
    GotoXY (5,7);
    Readln (user_file);
    If user_file <> #13 then begin
        If user_file ='' then begin
            Assign (Filename, default);
            Assign (Filename1, default1)
        end
    else begin
        len := length(user_file);
        For i := 1 to len do
            If user_file[i] = '.' then
                found := True;
            If not found then
                user_file := user_file+'.TXT';
            Assign (Filename, user_file);
            default := user_file;
            len := length(user_file);
            user_file[len-4]:='1';
            Assign (Filename1, user_file);
            Rewrite (Filename);
            Close (Filename);
            Rewrite (Filename1);
            Close (Filename1);
        end
    end
end;    {Change_name}
```

```
Procedure Marker_peak;
{Will find if marker is on or off and then do opposite to the markers status}

begin
    If not marker then begin
        marker := True;
        Writeln (TAS016Tx, send+'MKPK; MT1;');
    end
    else begin
        marker := False;
        Writeln (TAS016Tx, send+'MKOFF;')
    end;
end;    {marker_peak}

Procedure Sweep_rate;
{Allows the sweep rate to be changed on the spectrum analyser}

Var
    swe_rat: string;

begin
    Clear;
    Write ('Please enter sweep rate in milliseconds (20mS-100S) :- ');
    Readln (swe_rat);
    Writeln (TAS016Tx,send+'ST '+swe_rat)
end;    {sweep_rate}

Procedure Sample (Var sample_mins, sample_sec : word);
{Sets up the amount of timeto take a sample for}
Var
    chec : string;

begin
    Repeat
        ClrScr;
        Repeat
            GotoXY (10,10);
            Write ('Please enter number of minutes :- ');
            Readln (sample_mins);
        Until (sample_mins < 60);

        Repeat
            GotoXY (10,11);
            Write ('Please enter number of seconds :- ');
            Readln (sample_sec);
        Until (sample_sec < 60);

        GotoXY (10,20);
```

```
        Writeln (sample_mins,' Minutes, ',sample_sec,' Seconds');
        Repeat
            GotoXY (10,21);
            Write ('Is this correct (Y/N)? ');
            Readln (chec);
        Until (chec='y') or (chec='n') or (chec='Y') or (chec='N');
    Until (chec = 'Y') or (chec='y')
end;    {Sample}

Procedure Get_sample (smin, ssec : word);
{procedure to read a set of data from the spectrum analyser for the duration
specified}

Var
    thour,act_hour,tmin,act_min,tsec,act_sec,tsec100,act_sec100 : Word;
    i,loop : Integer;
    Store : Storage;
    aver,maxi,mini,sta_dev : Real;

begin
    If marker then begin
        If (smin > 0) or (ssec > 0) then begin
            i := 1;
            Clear;
            Writeln ('Please Wait. Sampling.');
            GetTime (act_hour, tmin, tsec, act_sec100); {get the present time}
            act_sec := tsec+ssec;
            If act_sec > 59 then begin
                act_sec := act_sec-60;
                act_min := 1+tmin+smin;
            end
            else
                act_min := tmin+smin;
            If act_min > 59 then begin
                act_min := act_min-60;
                Inc (act_hour);
            end;
            Repeat
                Writeln (TAS016Tx, send+'MA');
                Writeln (TAS016Tx, hdr+'ENTER 18%');
                Read (TAS016Rx, Store[i]);
                Inc (i);
                GetTime (thour, tmin, tsec, tsec100);
            Until ((thour >= act_hour) and (tmin >= act_min) and (tsec >= act_sec) and
        (tsec100 >= act_sec100));
            Ave_max_min (i-1, Store, aver, maxi, mini, sta_dev);
            File_store (i-1, Store, aver, maxi, mini, sta_dev);
            Display_data (i-1, Store, aver, maxi, mini, sta_dev);
```

```
            Writeln (TAS016Tx, send+'MKPK;');
        end;
    end
    else begin
        Clear;
        Writeln ('Please turn on the marker.');
        Delay (5000);
    end;
end;    {get_sample}

Procedure Centre_frequency;

Var
    cen_frq : String;

begin
    Clear;
    Write ('Enter required centre frequency (MHz) ');
    Readln (cen_frq);
    Writeln (TAS016Tx, send+'CF '+cen_frq+'MZ;')
end;    {centre_frequency}

Procedure Span_size;

Var
    span : string;

begin
    Clear;
    Write ('Enter required Span (MHz) ');
    Readln (span);
    Writeln (TAS016Tx, send+'SP '+span+'MZ;')
end;    {span_size}

Procedure Res_band;
{Allows the resolution bandwidth to be altered}

Var
    bandw : string[5];

begin
    Clear;
    Writeln ('Available  resolutions are:-');
    GotoXY (5,6);
    Writeln ('1KZ, 3KZ, 10KZ, 30KZ, 100KZ, 300KZ, 1MZ, 3MZ');
    GotoXY (5,8);
    Write ('Please enter the new resolution bandwidth ');
    Readln (bandw);
```

```
    Writeln (TAS016Tx, send+'RB '+bandw+';');
end;    {Res_band}

Procedure Num_samp (Var num_of: integer);
{set up the number of samples to be taken}

begin
    Clear;
    Writeln ('Please enter the number of samples');
    Repeat
        GotoXY (5,6);
        Write ('you wish to take, (Max 5000) ');
        Readln (num_of);
    Until num_of < 5001;
end; {Num_samp}

Procedure Get_num_samp (num_of : integer);
{Gets the number of samples requested}

Var
    Ch : Char;
    i : integer;
    samp_store : storage;
    Aver, maxi, mini, sta_dev : Real;

begin
    If marker then begin
        Clear;
        Writeln ('Please wait sampling ');
        If num_of >= 1 then begin
            For i := 1 to num_of do begin              {obtain the number of samples}
                Writeln (TAS016Tx, send+'MA;');
                Writeln (TAS016Tx, hdr+'ENTER 18%');
                Read (TAS016Rx, samp_store[i]);
            end;
            Ave_max_min (num_of, samp_store, aver, maxi, mini, sta_dev);
                                                {Obtain Average, maximum &
        minimum}
            File_store (num_of, samp_store, aver, maxi, mini, sta_dev);
            Display_data (num_of, samp_store, aver, maxi, mini, sta_dev);
            Writeln (TAS016Tx, send+'MKPK;');
        end;
    end
    else begin
        Clear;
        Writeln ('Please turn marker on.');
        Delay (5000);
    end;
```

```
end;    {Get_num_samp}

Procedure Atten;
{allows the attenuation to be changed on the spectrum analyser}

Var
    att_rate : String;

begin
    Clear;
    Writeln ('Please enter the new attenuation value you wish to use.');
    GotoXY (10,6);
    Write ('Valid values 0 to 60 dB in 10 dB steps. ');
    Readln (att_rate);
    Writeln (TAS016Tx, send+'AT '+att_rate+';');
end;

Procedure Ref_lev;
{Allows the reference level to be altered}

Var
    ref_l : String;

begin
    Clear;
    Writeln ('Please enter the new reference level.');
    GotoXY (10,6);
    Write ('Valid values are in the range -139.9 to 50 dB. ');
    Readln (ref_l);
    Writeln (TAS016Tx, send+'RL '+ref_l+';');
end;

Procedure Menu_2;
{displays the second menu, containing all sampling choices}

Var
    func, num_of : integer;
    mins, secs, sec100 : word;

begin
    num_of := 0;                    {initialise variables}
    mins := 0000;
    secs := 0000;

    Repeat
        Clear;
        Writeln ('              Menu 2');
        Writeln ('    Please choose one of the following :-');
```

```
        Writeln ('       1. Set time of sample');
        Writeln ('       2. Take sample for set time');
        Writeln ('       3. Set number of samples');
        Writeln ('       4. Take samples for set number');
        Writeln ('       5. Take a single sweep and store data');
        Writeln ('       6. ');
        Writeln ('       7. ');
        Writeln ('       8. Change filename');
        Writeln ('       9. Add text to file');
        Writeln ('       0. Menu 1');
        Write ('         ');
        Readln (func);
        Case func of
            1 : Sample (mins,secs);
            2 : Get_sample (mins,secs);
            3 : Num_samp (num_of);
            4 : Get_num_samp (num_of);
            5 : Trace_samp;
            6..7 : ;
            8 : Change_name;
            9 : Add_text;
        end;
    Until func = 0;
end; {menu_2}

Procedure Menu;
{procedure to allow setting up of the spectrum analyser to the requirements
of the user and reading of data from the same}

Var
    set_func : integer;

begin
    marker := False;                {iniatlise boolean variable marker to false}
    Repeat
        Clear;
        Writeln ('              MENU 1');
        Writeln ('     Please choose one of the following :-');
        Writeln ('       1. Centre Frequency');
        Writeln ('       2. Span');
        Writeln ('       3. Turn marker on/off at peak value');
        Writeln ('       4. Sweep rate');
        Writeln ('       5. Resolution bandwidth');
        Writeln ('       6. Input Attenuation');
        Writeln ('       7. Reference level');
        Writeln ('       8. Reset spectrum analyser');
        Writeln ('       9. Menu 2');
        Writeln ('       0. Exit');
```

```
        Write ('          ');
        readln (set_func);
        Case set_func of
            1 : Centre_frequency;
            2 : Span_size;
            3 : Marker_peak;
            4 : Sweep_rate;
            5 : Res_band;
            6 : Atten;
            7 : Ref_lev;
            8 : begin
                Writeln (TAS016Tx, send+'IP;');
                marker := False;
            end;
            9 : Menu_2;
        end; {case of}
    Until set_func = 0;
end; {menu}

begin {main}
    Set_Com;
    default := 'C:\Sample.txt';
    default1 := 'C:\Sample1.txt';
    Assign (TAS016Tx,'AUX');                {serial I/O on COM1}
    Assign (TAS016Rx,'AUX');
    Assign (Filename,default);
    Assign (Filename1,default1);
    Reset (TAS016Rx);                       {prepare to read}
    Rewrite (TAS016Tx);                     {and write to COM1}
    Rewrite (Filename);
    Rewrite (Filename1);
    Close (Filename);
    Close (Filename1);
    ClrScr;
    textbackground(blue);
    Writeln (TAS016Tx,send+'IP;');          {reset spectrum analyser}
    Writeln (TAS016Tx,send+'TDF P;');       {set data format}
    Menu;
    Textbackground(black);                  {reset the background to black}
    ClrScr;
end.    {main}
```

. Appendix C

.C.1 Program for Knittel Method

Shown below is the Matlab program for implementing the Knittel method. The program calls a function CONT (see C.2) to calculate and draw the two contours within a unit circle. The point at which the two contours cross is determined and the tilt angle and axial ratio are calculated.

```
clear all;
format long e;
x=[-1:0.001:1];                    %x co-ordinates for unit circle
R=[3 2];
ang = [60 120];
[ly lyy] = cont(R,ang);            %call function CONT to calculate and draw
                                   %contours
set(1,'name','Knittel Theory');    %change the name on the figure window
cy1 = ly(:,1); cy2 = ly(:,2);      %separate out variables returned by CONT
cyy1 = lyy(:,1); cyy2 = lyy(:,2);

a = -(cy1) + (cy2);                %the two top halves of the contours cross
b = -(cy1) + (cyy2);               %the top of contour 1  and the bottom of contour 2 cross
c = -(cyy1) + (cy2);               %the bottom of contour 1 and the top of contour 2 cross
d = -(cyy1) - (cyy2);              %the bottom of contour 1 and 3 cross

fa = find(a)          ;            %find which quarters have numbers in
fb = find(b);
fc = find(c);
fd = find(d);

dif = 100;          %initalise difference value
if fa ~= []
    ea = size(fa);
    for k = fa(1):fa(ea(1)),
        val1 = cy1(k); val2 = cy2(k);
        difval = val1 - val2;
        if difval < 0
            difval = difval - 2 * difval;   %make value positive;
        end;
        if difval < dif
            dif = difval;        %record new minimum value;
            x_co = x(k); y_co = mean ([cy2(k) cy1(k)]);
            par = 1;
        end;
```

```
    end;
end;

if fb ~= []
    ea = size(fb);
    for k = fb(1):fb(ea(1)),
        val1 = cy1(k); val2 = cyy2(k);
        difval = val1 - val2;
        if difval < 0
            difval = difval - 2 * difval;   %make value positive;
        end;
        if difval < dif
            dif = difval;        %record new minimum value;
            x_co = x(k); y_co = mean([cyy2(k) cy1(k)]);
            par = 2;
        end;
    end;
end;

if fc ~= []
    ea = size(fc);
    for k = fc(1):fc(ea(1)),
        val1 = cyy1(k); val2 = cy2(k);
        difval = val1 - val2;
        if difval < 0
            difval = difval - 2 * difval;   %make value positive;
        end;
        if difval < dif
            dif = difval;        %record new minimum value;
            x_co = x(k); y_co = mean([cy2(k) cyy1(k)]);
            par = 3;
        end;
    end;
end;

if fd ~= []
    ea = size(fd);
    for k = fd(1):fd(ea(1)),
        val1 = cyy1(k); val2 = cyy2(k);
        difval = val1 - val2;
        if difval < 0
            difval = difval - 2 * difval;   %make value positive;
        end;
        if difval < dif
            dif = difval;        %record new minimum value;
            x_co = x(k); y_co = mean([cyy2(k) cyy1(k)]);
            par = 4;
        end;
```

```
    end;
end;


if x_co > 0
    longit = ((atan(y_co / x_co)) / pi * 180);
elseif y_co > 0                    %x_co negative and y_co positive
    longit = ((atan(y_co / x_co)) / pi*180) + 180;
else                               %x_co negative and y_co negative
    longit = 180 - ((atan(y_co / x_co)) / pi * 180);
    longit = -longit;
end;

tilt = longit / 2;                          %calculate the tilt angle
rlatit = acos(sqrt(x_co^2 + y_co^2));
latit = rlatit / pi * 180;
ar = tan(rlatit / 2);                       %calculate the axial ratio
hold off;
figure(gcf)                    %bring the figure to the foreground
```

.C.2 Contour Function

The following program listing is for a function the above main program calls to calculate the contours and to draw them on the stereographic projection of one of the two hemispheres.

```
function [ly,lyy]=cont(R,ang);
%where R is the power ratio, ang is the angle between the two antennas
%returns the x, y values for the contours

r = 1;
b = 0;                  %offset from the origin in the y axis
a = 0;                  %offset from the origin in the x axis
x = [-r+a:0.001:r+a];          %obtain x axis values so have no complex values

y = b + sqrt(r^2 - (x - a).^2);          %positive half of circle;
yy = (-sqrt(r^2 - (x - a).^2))+b;        %negative half of circle;
plot(x,y,'b',x,yy,'b')
hold on;

%Contours for any two antennas
for i=1:size(R');
    if ang(i) ~= 180
        centx = -((R(i) * cos(ang(i) / 180 * pi) - 1) / (R(i) - 1))
        centy = -((R(i) * sin(ang(i) / 180 * pi)) / (R(i) - 1))
```

```
    else
        centx = (R(i) + 1) / (R(i) - 1);
        centy = 0;
    end;
    radR = sqrt(centx^2 + centy^2-1)        %radius of constant circle

    if radR == Inf;
        if ang(i) ~= 180
            slan = (90 - (ang(i) - 90)) / 180 * pi;
            if ang(i)<0 | ang(i) > 180
                va = -1;
                ind = 1;
            else
                va = 1;
                ind = 2001;
            end;
            y0 = tan(slan) * va;
            while y0 > y(ind)
                if ang(i) < 0 | ang(i) > 180
                    va = va + 0.001;
                    ind = ind + 1;
                else
                    va = va - 0.001;
                    ind = ind - 1;
                end;
                y0 = tan(slan) * va;
            end
        else
            y0 = 0;
        end;
        plot([-x(ind) x(ind)],[-y0 y0],'b');
    else

%Calculating the points of the circle
        cy = (centy + sqrt(radR^2 - (x - centx).^2));        %top half of circle
        cyy = -((sqrt(radR^2 - (x - centx).^2)) + centy);        %bottom half of circle
        cyy = cyy + 2 * centy;

%Remove the complex part
        imcy = imag(cy);
        imcyy = imag(cyy);

        for k = 1:size(cy')
            if imcy(k) ~= 0
                cy(k) = NaN;
            end
            if imcyy(k) ~= 0
                cyy(k) = NaN;
```

```
        end
    end;


%removing values outside the unit circle
    for j = 1:(size(x')),
        if cy(j) > y(j)
            cy(j) = NaN;
        elseif centy < 0 & cy(j) < yy(j);
            cy(j) = NaN;
        end;
        if cyy(j) < yy(j);
            cyy(j) = NaN;
        elseif centy > 0 & cyy(j) > y(j);
            cyy(j) = NaN;
        end;
    end;

% putting the one and only required zero in
    top = find(cy);
    bot = find(cyy);
    tt = size(top');
    bb = size(bot');

    if tt(1) >= 1 | bb(1) >= 1
        if centx < 0 & centy > -1 & centy < 1
            if tt(1) > 1
                d = top(tt(1)) + 1;
                cy(d(1)) = centy;
            end
            if bb(1) >= 1
                e = bot(bb(1)) + 1;
                cyy(e(1)) = centy;
            end
        elseif centx > 0 & centy > -1 & centy < 1
            if tt(1) >= 1
                cy(top(1) - 1) = centy;
            end
            if bb(1) >= 1
                cyy(bot(1) - 1) = centy;
            end
        elseif centx == 0 & centy == 0
            if tt(1) >= 1
                cy(top(1) - 1) = centy;
                f = top(tt(1)) + 1;
                cy(f(1)) = centy;
            end
            if bb(1) >= 1
```

```
                    cyy(bot(1) - 1) = centy;
                    g = bot(bb(1)) + 1;
                    cyy(g(1)) = centy;
                end
            end
        end

        plot(x,cy,'g',x,cyy,'g');
    end;
    ly(:,i) = cy';
    lyy(:,i) = cyy';
end;    %of for i=
```

References

Al-Nuaimi, M.O. and Hammoudeh, A.M., "Attenuation Functions of Microwave Signals Propagated Through Trees", Electronic Letters, Vol. 29, No. 4, 1993a.

Al-Nuaimi, M.O. and Hammoudeh, A.M., "Influence of Vegetation on Attenuation of Radiowave Signals in the X-Band Frequency Region", COST 235 TD, CP 149, June 1993b.

Al-Nuaimi, M.O. and Hammoudeh, A.M., "Measurements and Predictions of Attenuation and Scatter of Microwave Signals by Trees", IEE proceeding on Antennas and Propagation, Part H, Vol. 141, No. 2, 1994.

Beckmann, P., "The Depolarization of Electromagnetic Waves", The Golem Press, 1968.

CCIR study programme 1A/5, "Influence of Terrain Irregularities and Vegetation on Tropospheric Propagation", Report 236-6, 1986.

Clayton, L. and Hollis, J. S., "Antenna Polarisation Analysis by Amplitude Measurement of Multiple Components", Microwave Journal, Vol. 8, Jan 1965

COST 235, "Radiowave Propagation Effects on Next-Generation Fixed-Services Terrestrial Telecommunications Systems", Final Report, 1996, ISBN 92-827-8023-6.

Ding, M. S., "Modelling and Measurement of the Scatter of Microwaves by Buildings", PhD Thesis, University of Glamorgan, 1994.

Gates, D. M., "Water Relations of Forest Trees", IEEE Transactions on Geoscience and Remote Sensing, Vol. 29, No. 6, November 1991.

Hammoudeh, A., Stephens, R. and Al-Nuaimi, M., "Characterisation and Modelling of Scatter, Attenuation and Depolarisation of Millimetre Waves due to Foliage", 26th EuMC, Prague, Czech Republic, September 1996.

Haslett, C. J., "Modelling and Measurement of the Diffraction of Microwaves by Buildings", PhD Thesis, University of Glamorgan, 1993.

Hollis, J. S., Lyon, T. J. and Clayton, L., "Microwave Antenna Measurements", Scientific-Atlanta Inc., 1970.

IEEE Standard Test Procedures for Antennas, The Institute of Electrical and Electronic Engineers Inc., Wiley - Interscience, 1979.

Ishimaru, A., "Wave Propagation and Scattering in Random Media", Vol. 1, Academic Press, 1978.

Johnson, R. A. And Schwering, F., "A Transport Theory of Millimeter Wave Propagation in Woods and Forests", CECOM-TR-85-1, Fort Monnouth, New Jersey, February 1985.

Jull, E. V., "Aperture Antennas and Diffraction Theory", Peregrinus on behalf of the Institute of Electrical Engineers, (IEE Electromagnetic waves series, 10),1981.

Knittel, G. H., "The Polarisation Sphere as a Graphical Aid in Determining the Polarisation of an Antenna by Amplitude Measurements Only", IEEE Transactions on Antennas and Propagation, Vol AP-15, Mar 1967.

Kraus, J. D., "Electromagnetics", McGraw-Hill, 1985.

Lian, H. and Lewin, L., "UHF RadioLoss in Forest Modeled by Four Layered Media with Two Anisotropic Slabs", IEEE AP-S Int. Symp. Digest Antennas and Propagation, Vol. 1, 1986

Macario, R. C. V., "Personal and Mobile Radio Systems", Peregrinus on behalf of the Institute of Electrical Engineers, (IEE telecommunications series; 25), 1991.

Mo, T., Choudhury, B. J., Schmugge, T. J., Wang, J. R. and Jackson, T. J., "A Model for Microwave Emission From Vegetation-Covered Fields", Journal of Geophysical Research, Vol. 87, No.C13, 1982.

Riegger, S. and Wiesbeck, W., "Coherent Polarimetric RCS Measurements on Trees", Proceedings of IGRASS 1986, 1986.

Sachs, D. L. and Wyatt, P. J., "A Conducting-Slab Model for Electromagnetic Propagation Within a Jungle Medium", Radio Science, Vol. 3, No. 2, February 1968.

Schwering, F. K., Violette, E. J. and Espeland, R. H. :"Millimeter-Wave Propagation in Vegetation: Experiments and Theory", IEEE Transactions on Geoscience and Remote Sensing, Vol. 26, No. 3, May 1988.

Seker, S. S., "VHF/UHF Radiowave Propagation Through Forests: Modelling and Experimental Observations", IEE Proceedings-H, Vol. 139, No. 1, February 1992.

Seville, A. and Craig, K.H., "A Semi-Emphirical Model for Millimetrewave Vegetation Attenuation Rates", Electronic Letters, Vol. 31, No. 17, 1995.

Stephens, R.B.L. and Al-Nuaimi, M.O., "Attenuation Measurement and Modelling in Vegetation Media at 11.2 GHz and 20 GHz", Electronics Letters, Vol 31, No. 20, 1995.

Thomas, P. D., "Conformal projections in geodesy and cartography", Special publication 251, U. S. Dept. Of Commerce, Coast and Geodetic Survey, U. S. Gov't Printing Office, 1952.

Toups, M. F., Ayasli, S. and Fleischman, J. G., "Part II: Analysis of Foliage-Induced Synthetic Pattern Distortions", IEEE Transactions on Aerospace and Electronics Systems, Vol. 32, No. 1, January 1996.

Ulaby, F. T., Van Deventer, T. E., East, J. R., Haddock, T. F. and Coluzzi, M. E., "Millimeter-Wave Bistatic Scattering From Ground and Vegetation Targets", IEEE Trans. On Geosc. and Remote Sens., Vol. 26, No. 3, May 1988.

Weissberger, M. A., "An initial Critical Summary of Models for Predictiong th e Attenuation of Radio Waves by Foliage", ECAC-TR-81-101, Electromagnetic Compatiblity Analysis Center, Annapolis, USA, August 1981.

Van Zyl, J. J., "On the importance of Polarization in Radar Scattering Problems", PhD Thesis, California Institute of Technology, Pasadena, California, 1986.

Wolfgang, H. K., and Gillespie, E. S., "Antenna Measurements - 1978", Proceedings of the IEEE, Vol. 66, No. 4, April 1978